Coupling process / mechanical characterization of sandwich materials Metal / Hybrid composite based on jute fabrics

Muzzamal Hussain

No d'ordre : 109928

UNIVERSITÉ DE LILLE

UNITÉ DE MÉCANIQUE DE LILLE

ÉCOLE DOCTORALE SCIENCES POUR L'INGÉNIEUR (SPI)

Rapport de thèse pour l'obtention du grade de

Docteur de l'Université de Lille

Spécialité : Mécanique, énergétique, génie des procédés, génie civil

Présentée par : **Muzzamal HUSSAIN**

Couplage procédé / propriétés mécaniques des matériaux sandwiches Métal / Composite hybride à base de tissus en jute

Coupling process / mechanical characterization of sandwich materials Metal / Hybrid composite based on jute fabrics

Thèse soutenue publiquement le jeudi 19 février 2021

Devant le jury composé de :

M. B. Castanié	Professeur, INSA de Toulouse	Président du Jury
Mme K. Charlet	MCF HDR, SIGMA Clermont Ferrand	Rapporteure
M. Y. Nawab	Assoc. Prof. NTU, Pakistan	Examinateur
M. T. Kanit	MCF-HDR, Université de Lille	Examinateur
M. A. Saouab	Professeur, Université du Havre	Co-Directeur de thèse
M. A. Imad	Professeur, Université de Lille	Directeur de thèse

Acknowledgment

First of all I would like to thank Almighty, who made me able to accomplish this thesis. Then I would like to express my deep and sincere gratitude to my thesis director Prof. Abdellatif Imad and co-director Prof. Abdelghani Saouab and Dr. Toufik Kanit for their valuable guidance, suggestions, inspiration and encouragement to complete this work. I am also extremely indebted to Dr. Yasir Nawab for his unconditional support throughout my PhD and before. I am also thankful to Shahood uz Zaman, Muhammad Ayub Asghar, Muhammad Kashif, Dr. Khubab Shaker, Dr. Christophe Herbelot, Dr. Shafiq Sukiman, Habib Awais and all the laboratory staff. I would like to extend my acknowledgements to National Center for Composite Materials (NC2M),National Textile University, Pakistan and CISIT, University of Lille, France for providing me their services whenever I needed.

I would like to offer special gratitude to Muhammad Zeeshan and Dr. Muhammad Umair for their valuable help in doing the experiments and being with me even off days.

I also pay special thanks to my lab mates Quoc Hoan Pham, Hamza Lamini, Essonam Arfa and Nada Ben Lteif for their wonderful company through this journey.

Last but not the least I would like to thank my beloved parents, my siblings and colleagues who enabled and motivated me to perform and successfully complete this research work. I also want to pay special thanks to my wife and son who kept me motivated throughout this journey.

I am thankful to National Textile University, Pakistan for their financial support for this PhD work.

Dedication

To my parents and teachers

Table of Contents

List of Figures

List of Tables

Abbreviations

FMLs	:	Fibre Metal Laminates
ARALL	:	Aramid Reinforced ALuminium Laminate
GLARE	:	Glass Laminate Aluminium Reinforced Epoxy
CARAL	:	Carbon Reinforced Aluminium Laminate
SLC	:	Structural laminate company
FRC	:	Fibre-reinforced composite
NASA	:	National Aeronautics and Space Administration
LaRC	:	NASA Langley Research Center
SRPP	:	Self Reinforced PolyPropylene
TFML	:	Thermoplastic Fibre Metal Laminate
NFML	:	Natural Fibre Metal Laminates
AFM	:	Atomic Force Microscopy
MVF	:	Metal Volume Fraction
MSD	:	Multi Sight Damage
GFRE	:	Glass-Fibre Reinforced Epoxy
BMG	:	Bulk Metallic Glass
CFRP	:	Carbon Fibre Reinforced Plastic
PDA	:	Polydopamine
MWCNT	:	Multiwalled Carbon Nanotubes

NFC	:	Natural Fibre Composites
CAJRALL	:	CArbon-Jute Reinforced ALuminium Laminate
CAJRMAL	:	CArbon-Jute Reinforced MAgnesium Laminate
OPEFB	:	Oil Palm Empty Fruit Bunch
BFRE	:	Basalt Fibre Reinforced Epoxy composites
MGP	:	Micro Glass Powder
FPL-Etching	:	Forest Products Laboratory Etching
SAA	:	Sulfuric Acid Anodizing
LVI	:	Low-velocity impact
FC	:	First Crack
TTT	:	Through the Thickness crack
NIS	:	Non-impacted side
TGA	:	Thermographic Analysis
JFRCs	:	Jute Fibre Reinforced Composites
JuRALs	:	Jute Reinforced Aluminium Laminates
FVC	:	First Visible Crack
SVC	:	Second Visible Crack
PVB	:	PolyVinyl Butyryl
PP	:	PolyPropylene

Indices

Tg	:	Glass Transition Temperature
Av	:	Average
max	:	Maximum
min	:	Minimum

Introduction Générale

Contexte de l'étude

L'allégement des structures mécaniques constitue une préoccupation primordiale dans le domaine de l'ingénierie des matériaux. Dans cette voie, l'utilisation des alliages d'aluminium dans l'industrie aéronautique a été guidée essentiellement par leur faible densité et leurs propriétés mécaniques. Aussi, les matériaux composites à haute performance ont permis d'apporter une solution intéressante pour répondre aux exigences de résistance mécanique tout en diminuant le poids des structures. Ceci a contribué fortement au développement d'une conception légère dans le domaine aéronautique, par exemple. On assiste alors à une concurrence entre l'utilisation des matériaux composites et des alliages d'aluminium dans plusieurs domaines. C'est dans ce cadre que le développement des multi-matériaux, connus sous le vocable « matériaux sandwiches », a permis de combiner leurs propriétés mécaniques ainsi que leur légèreté. Dans cette perspective, plusieurs travaux de recherche ont porté sur l'élaboration de nouveaux matériaux intégrant à la fois du métal et du composite. Ces matériaux sont connus sous le vocable anglophone de FML (Fibre MetalLaminates). Souvent, les alliages d'aluminium et les composites à fibres synthétiques sont utilisés pour la fabrication des FML. Il faut noter qu'un FML présente une structure en sandwich dans laquelle des couches composites et métalliques sont placées en alternance. Les matériaux composites ont généralement d'excellentes propriétés de résistance, de rigidité et de fatigue, mais ils présentent une faible ductilité. En raison de cette fragilité, ils ont de mauvaises propriétés sous impact. En revanche, le métal présente une certaine performance sous une charge d'impact en raison de sa ténacité et de sa déformation plastique avant fissuration. Par conséquent, la combinaison du composite et du métal conduit manifestement à une meilleure solution technologique pour des structures mécaniques pouvant être soumises à un chargement dynamique.

Objectif de la Thèse

Le travail de thèse porte sur l'utilisation des fibres naturelles pour l'élaboration de nouveaux FML à base de tissus en jute 2D et 3D, avec des plaques en aluminium. Un accent est mis sur le couplage entre les précédés d'élaboration et les propriétés mécaniques de ces nouveaux matériaux sandwiches. Plusieurs configurations ont été fabriquées et testées conduisant à une étude paramétrique intégrant à la fois le type de tissage (2D et 3D) et la nature de la matrice polymérique (thermoplastique, thermodurcissable). Nous avons aussi testé des FML hybride en utilisant des tissus à fibres naturelles de jute et des fibres synthétiques à base de verre, d'aramide et de carbone.

Cette étude est basée sur une approche expérimentale en vue de caractériser les différentes configurations des structures sandwiches métal/composite, intégrant des fibres naturelles en jute. Dans ce cadre, la qualité des interfaces a été vérifiée via des tests spécifiques de pelage. Aussi, nous avons effectué des essais monotones de traction et de flexion afin d'évaluer les propriétés mécaniques en corrélation avec les paramètres liés au procédé d'élaboration. Une large partie expérimentale a été consacrée aux essais d'impact à faible vitesse. Les mécanismes et les modes d'endommagement ont été analysés à partir des observations microscopiques. Cette partie constitue une phase importante du travail de la thèse et a conduit à mieux cerner les configurations qui présentent une performance de résistance à l'impact. L'ajout du tissu en jute a permis d'améliorer les propriétés dynamiques des structures sandwiches.

Structuration du rapport

Le présent rapport est structuré en 5 chapitres :

Chapitre 1 :

Ce chapitre porte sur une large revue bibliographique qui est divisée en quatre sections. Dans la première section, un bref historique des FML et de ses différentes applications sont présentées. La deuxième section contient les détails sur les matériaux, la fabrication et les propriétés générales des FML. La troisième section contient les détails du processus de fabrication des FML. Le traitement de surface des métaux est une partie très importante de la fabrication des FML pour obtenir une adhérence uniforme. Les techniques de préparation de surface sont discutées en détail ainsi que leur effet sur les performances mécaniques. Les différentes techniques utilisées pour fabriquer des FML, y compris l'autoclave, le moulage par transfert de résine assisté par vide VARTM et la presse à chaud par compression sont présentées en détail. La dernière section présente la caractérisation mécanique des FML. Il présente une évaluation du collage, des propriétés monotones et des propriétés dynamiques. Le mécanisme de rupture de la liaison adhésive, de la traction, de la flexion et de l'impact à faible vitesse est également présenté. La caractérisation des propriétés mécaniques par rapport aux matériaux constitutifs est également présentée à partir de la littérature.

Chapitre 2 :

Dans ce chapitre, différents types de matériaux et de techniques de fabrication ont été utilisés pour fabriquer les stratifiés de fibres métalliques dans l'étude actuelle. Des évaluations tant qualitatives que quantitatives ont été effectuées pour caractériser les stratifiés de fibres métalliques. Le jute a été utilisé comme fibre principale pour le tissage de renfort tissé 3D. Une fois la structure du tissage optimisée, le jute tissé 3D a été pris en sandwich avec du jute tissé 2D, de l'aramide, du carbone et du verre, respectivement. Les FML avec renforcement hybride ont été développés en utilisant des matrices époxy, PP et PVB. Dans la première étape, une infusion sous vide a été utilisée pour fabriquer des FML en jute tissé 3D. Pour la fabrication de

composites hybrides et de FML, les techniques de compression à chaud ont été utilisées. La qualité de la liaison adhésive entre le composite et l'aluminium a été obtenue à l'aide de tests de pelage en T et de pelage au rouleau flottant. Les propriétés monotones ont été étudiées à l'aide d'essais de traction et de flexion, tandis que la performance d'impact a été examinée à l'aide d'un essai d'impact à faible vitesse de chute.

Chapitre 3 :

Ce chapitre est consacré à une étude expérimentale portant sur l'analyse de la qualité du procédé d'élaboration des FML en se basant sur des tests de pelage pour caractériser les interfaces aluminium/composite. La surface de l'aluminium a été préparée en utilisant une anodisation à l'acide phosphorique avant la fabrication des FML. L'angle de contact avec l'eau de l'aluminium anodisé était inférieur à celui de l'aluminium non ionisé, montrant une énergie libre de surface supérieure de l'aluminium anodisé. Les résultats du test de pelage en T ont montré que les propriétés de liaison des composites aluminium-jute 3D dépendent uniquement du type de matériaux de liaison plutôt que du type de structure de renforcement. Le test de pelage a été utilisé pour explorer l'effet de différentes fibres et matrices sur les propriétés adhésives. Le résultat montre que la matrice PVB globale a les propriétés les plus élevées. Même si le type de rupture n'était pas cohésif, la ductilité de la matrice a joué un rôle essentiel dans les propriétés finales.

Chapitre 4 :

Ce chapitre concerne les propriétés monotones de l'optimisation de la structure tissée 3D pour la fabrication FML, puis l'hybridation ultérieure d'un tissu de jute tissé 3D optimisé avec un tissu tissé 2D. Les tests de traction et de flexion ont été menés à la fois pour l'optimisation et l'hybridation de structures tissées 3D. Le résultat montre que les structures tissées OTT sont meilleures pour la fabrication FML que d'autres types de structures. Alors que les FML

hybrides renforcés ont été fabriqués avec un renforcement 2D / 3D et une matrice époxy, PP et PVB, respectivement. Les FML hybrides avaient des propriétés plus cohérentes que les composites constituants. Les composites à base d'époxy et les FML ont montré des propriétés de traction et de flexion globalement plus élevées, mais les composites à base de PVB et les FML ont également montré des performances très prometteuses en tant que remplacement possible de l'époxy. Les propriétés de flexion des FML à base de PP hybride étaient très médiocres en raison d'une défaillance prématurée.

Chapitre 5 :

Les propriétés d'impact à faible vitesse des FML et des composites correspondants fabriqués avec des armatures hybrides et différentes matrices sont décrites dans ce dernier chapitre. Le but de l'hybridation du jute 3D avec un renforcement synthétique 2D était d'accéder à l'amélioration des propriétés par rapport à l'interface métal-matrice, métal-composite et composite-matrice. Le mécanisme de propagation, d'endommagement et de défaillance des fissures a également été consulté. L'effet des matrices thermoplastiques et thermodurcissables a également été déterminé pour examiner comment la dissipation d'énergie et les caractéristiques de propagation des fissures changent pour différentes matrices. Les composites à base de PVB et les FML ont montré des performances d'impact globalement supérieures à celles des matrices époxy et PP. La plasticité de la matrice et les caractéristiques de dissipation d'énergie des composites à base de PVB et des FML étaient à l'origine de l'amélioration des performances d'impact. Parmi les différents types de renforcement hybride, la combinaison aramide / jute 3D a montré de meilleures performances d'impact en raison de la nature de la fibre aramide.

General Introduction

Context of the study

The reduction of weight of mechanical structures is a primary concern in the field of materials engineering. In this direction, the use of aluminum alloys in the aviation industry has been guided mainly by their low density and better mechanical properties. Also, high-performance composite materials have provided an interesting solution to meet mechanical requirements while reducing the weight of structures. This has contributed greatly to the development of a lightweight design in the aeronautics field, for example. With this in mind, several research studies have focused on the development of new materials incorporating both metal and composite. These materials are known as FML (Fibre Metal Laminates). Aluminium alloys and synthetic fiber composites are often used to make FMLs. It should be noted that an FML has a sandwich structure in which composite and metal layers are placed alternately. Composite materials generally have excellent properties of strength, stiffness and fatigue, but they have low ductility. Because of this fragility, they have bad properties under impact. On the other hand, the metal exhibits a certain performance under an impact load due to its tenacity and plastic deformation before cracking. Therefore, the combination of composite and metal clearly leads to a better technological solution for mechanical structures that can be subjected to dynamic loading.

Objective of Thesis

The thesis work focuses on the use of natural fibres for the development of new FMLs based on 2D and 3D jute fabrics, with aluminum plates. An emphasis is placed on the coupling between the pre-development and the mechanical properties of these new sandwich materials. Several configurations have been manufactured and tested leading to a parametric study incorporating both the type of weaving (2D and 3D) and the polymer matrix (thermoplastic,

thermoset). We also tested hybrid FML using natural jute fiber fabrics and synthetic fibers made from glass, aramid and carbon.

This study is based on an experimental approach to characterize the different configurations of metal/composite sandwich structures, incorporating natural jute fibers. In this context, the quality of the interfaces has been verified through specific peel tests. We also conducted monotonous traction and bending tests to measure the mechanical properties correlated with the parameters associated with the development process. A large amount of experiment has been devoted to low-speed impact tests. The mechanisms and modes of damage were analyzed from microscopic observations. This part is an important phase of the thesis work and has led to a better understanding of the configurations that exhibit an impact resistance performance. The addition of jute fabric has improved the dynamic properties of sandwich structures.

Structuring the report

This report is structured into five chapters:

Chapter 1:

In this chapter, the literature review about Fibre Metal Laminates FMLs is discussed, and it is divided into four sections. In the first section, a brief history of FMLs and different applications are presented. The second section contains the details of materials, manufacturing, and properties of commercially used FMLs present in the literature. The modification in the FMLs w.r.t to the metal, matrix, and reinforcement are also presented in detail. The third section contains the manufacturing process used to make FMLs. The surface treatment of metals is an essential part of FMLs fabrication to achieve even adhesion. The surface preparation techniques are discussed, along with their effect on mechanical performance. The different techniques used to make FMLs, including autoclave, Vacuum Assisted Resin Transfer Moulding VARTM, and compression hot press, are discussed w.r.t their scope. The final

section contains the mechanical characterization of FMLs. It presents an evaluation of adhesive bonding, monotonic properties, and dynamic properties. The failure mechanism of delamination, tensile, flexural, and low-velocity impact is also discussed to elaborate on how properties change for different constituents. The mechanical properties characterization w.r.t constituent materials is also presented from the literature.

Chapter 2:

In this chapter, different types of materials and manufacturing techniques are discussed which were used to make metal fiber laminates. Both qualitative and quantitative assessments were carried out to characterize the FMLs. The jute was used as the primary fibre for the weaving of 3D woven reinforcement. Once the weave structure was optimized, the 3D woven jute fabric was sandwiched with 2D woven jute, aramid, carbon, and glass, respectively, for the development of hybrid reinforced samples. The hybrid reinforced samples were developed using epoxy, PP, and PVB matrix. In the first step, vacuum infusion was used to make 3D woven jute reinforced composites and FMLs with epoxy. For the fabrication of hybrid reinforced composites and FMLs, the compression hot press technique was used. The quality of adhesive bonding between composite and aluminium was accessed using T-peel and floating roller peel tests. The monotonic properties were investigated using tensile and flexural tests, while impact performance was examined using a drop weight low-velocity impact test.

Chapter 3:

The chapter presents the water contact angle results of pre-treated and post-treated aluminium surfaces along with T-peel and floating roller peel test results of the aluminium-composite bonds. The surface of aluminium was prepared using phosphoric acid anodizing before FMLs fabrication. The water contact angle of the anodized aluminium was lower than non-ionized aluminium showing higher surface free energy of anodized aluminium. The T-peel test results

showed that the aluminium-3D jute composites bond properties solely depend upon the type of bonding materials rather structure type of reinforcement. The floating roller peel test was used to explore the effect of different fibres and matrices on the adhesive properties. The result shows that the overall PVB matrix has the highest properties. Even though the failure type was not cohesive, the ductility of the matrix played a vital role in the final properties.

Chapter 4:

This chapter concerns the monotonic properties of optimizing 3D woven structure for FML fabrication and then subsequent hybridization of optimized 3D woven jute fabric with 2D woven fabric. The tensile and flexural tests were conducted for both optimization and hybridization of 3D woven structures. The result shows that the OTT woven structures are better for FML fabrication than other types of structures. While the hybrid reinforced FMLs were made with 2D /3D reinforcement and epoxy, PP, and PVB matrix, respectively. The hybrid FMLs had more consistent properties than constituent composites. The epoxy-based composites and FMLs showed overall higher tensile and flexural properties, but the PVB based composites and FMLs also showed very promising performance as a possible replacement of epoxy. The flexural properties of hybrid-PP-based FMLs were very poor due to premature failure.

Chapter 5:

This chapter concerns the low-velocity impact properties of FMLs and corresponding composites made with hybrid reinforcement and different matrices. The purpose of hybridizing 3D jute with 2D synthetic reinforcement was to access the improvement in the properties w.r.t metal-matrix, metal-composite, and composite-matrix interface. The crack propagation, damage, and failure mechanism were also accessed. The effect of thermoplastic and thermoset matrices was also determined to examine how the energy dissipation and crack propagation

characteristics changes for different matrices. The PVB based composites and FMLs showed overall higher impact performance as compared to both epoxy and PP matrix. The plasticity of matrix and energy dissipation characteristics of PVB based composites and FMLs was the reason behind improved impact performance. Out of different types of hybrid reinforcement, the aramid /3D jute combination showed better impact performance due to nature of aramid fibre.

Chapter 1. Literature Review

In this chapter the literature review is presented, and it is further divided in four sections. In the first section the brief history of fibre metal laminates (FMLs) and different applications are presented. The second section contains the details of materials, manufacturing, and properties of commercially used FMLs present in literature. The modification in the FMLs w.r.t to metal, matrix and reinforcement are also elaborated in detail. The third section contains the details of manufacturing process used to make FMLs. The surface treatment of metals is very important part of FMLs fabrication to achieve even adhesion. The surface preparation techniques are discussed in detail along with their effect on the mechanical performance. The different techniques used to make FMLs including autoclave, Vacuum Assisted Resin Transfer Moulding VARTM and compression hot press are presented in detail. The final section presents the mechanical characterization of FMLs. It presents evaluation of adhesive bonding, monotonic properties, and dynamic properties. The failure mechanism of adhesive bonding, tensile, flexural, and low velocity impact is also presented. The mechanical properties characterization w.r.t constituent materials is also presented from the literature.

1.1 Introduction

The development of Fibre Metal Laminates FMLs started just after 2nd world war. In 1945 when one of engineer named Rob Schliekelmann working on Fokker facilities visited English aircraft manufacturer De Havilland and saw the facility of metal bonding. He applied metal bonding technology on Fokker-27 [1]. In 1978 USA aviation authority implemented new rules *Federal Airworthiness Regulations FAR Part 25.571,* containing the damage tolerance and fatigue evaluation certification requirements for passenger aircraft. The European Union also adopted the same rules, despite these strict rules still the main reason for aeroplane crash was fatigue cracking or incidental damage [2]. Due to these reasons combination of composite and aluminium was the point of interest in the USA and Britain as a possible replacement of composite and aluminium due to its potential low cost compared to composite and high fatigue resistant like aluminium with reduced weight. Schliekelmann at the end of 70s visited USA and saw the trials of metal bonding with composites. His team was already doing bonding of metals without fibres. In 1978 Schijve and Vogelesang started simulations test for flights on Aramid and Carbon laminates. Delft University continues its research to improve the quality of bonding and load bridging, so load can be transformed from metal layer to composite layer. AKZO, ALCOA and 3M joined hands with Delft University for manufacturing of FMLs. The 1st patent of FMLs was filed in the US on January 9, 1981 [1]. The first FML made was aramid based called Aramid Reinforced Aluminium Laminate ARALL in 1978 and AKZO held the commercial rights [3]. The 1st patent about Glass Laminate Aluminium Reinforced Epoxy GLARE was filed in October 1987 by AKZO. AKZO and ALCOA made a partnership in 1991 to commercialize GLARE. In June 1991 AKZO and ALCOA signed formal agreement form a Structural Laminate Company SLC, this agreement ensured that R&D and marketing will be done in Delft University and production will be done in New Kensington, Pennsylvania [1].

These early developments laid the foundation of FML research and use in different applications.

FML due to its coupled effect of metal and composite has been widely used in aerospace applications [4]. ARALL was developed and used in a lower wing panel of Fokker 27 aircraft and the cargo door of C-17. GLARE is used in A380 fuselage and the leading edge of the tailplane of A380 [5], [6]. More than 25% of its body were made of GLARE. GLARE is used in floor panel of Boeing 777 [3]. Blast protection walls can be developed using fibre metal laminates as they have excellent energy dissipation characteristics [7].

The automotive industry is another potential segment where FML can be used, especially Natural Fibre Metal Laminate NFML and natural hybrid FML [8], [9]. The use of FMLs can significantly reduce the mass of parts as compared to currently used materials. The train, cars and truck roofs and the floor are a potential application area for FMLs. The fire-resistant properties can be used to manufacture fire barriers (Figure 1.1) [10].

Figure 1.1. Different applications of Fibre Metal Laminates (a) fuselage of A380 (b) ballistic armor (c) space structures (d) auto-mobile

Despite excellent properties, FMLs are not used in applications other than aerospace. Thermosetting FMLs usually have long processing cycles and high cost of production that's why they are not so frequently used. With the development of low-cost thermoplastic and natural FML, the scope of FMLs will be more global than specific [11].

1.2 Fibre Metal Laminates FMLs

FMLs are multi-layered materials based on the alternative arrangement of aluminium alloys and Fibre-Reinforced Composite FRC materials, as shown in Figure 1.2.

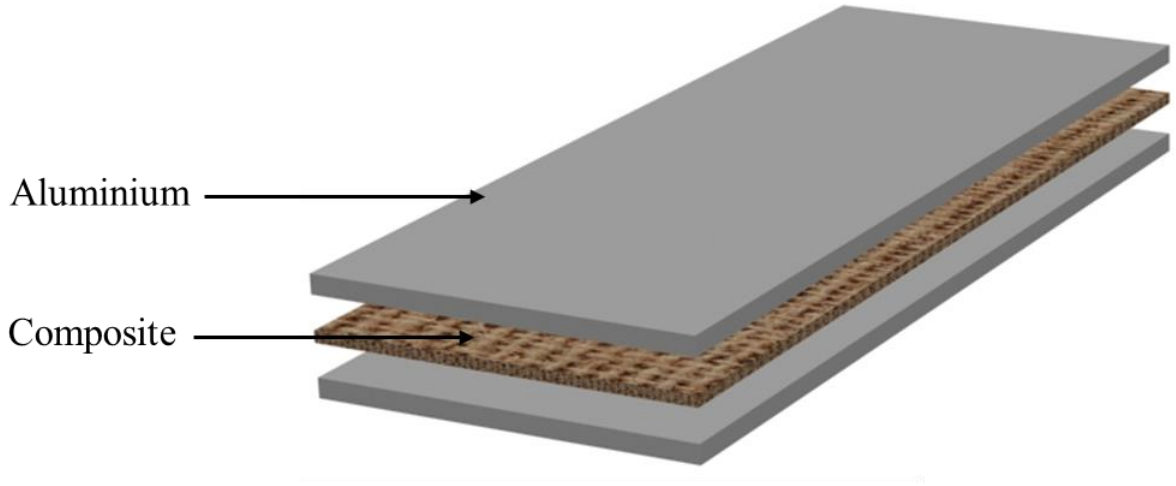

Figure 1.2. Schematic view of plies of fibre metal laminate

FMLs combine the characteristics of both constituents, high impact resistance and easy reparability of metals, high fatigue and strength of composites [11]. Crack propagation of FMLs is better than monolithic aluminium and usually limited to the metal layer. The reason behind much better fatigue crack propagation is a fibre / epoxy layer which hinders the crack growth due to this reason FMLs are future aircraft materials [12].

1.2.1 Configuration of plies in FMLs

Metal and fibre can be placed in several ways; the simplest configuration in FMLs is 2/1, as shown in Figure 1.3.

Figure 1.3. (a) 2/1 orientation of FML (b) 3/2 orientation of FML

The configuration can be 3/2, 4/3 or can be changed as per end requirement. The direction of the fabric plies in composite decide the properties of FMLs, whether they will be isotropic, anisotropic, and quasi-isotropic. The properties required in the aerospace industry are usually anisotropic.

1.2.2 Reinforcement used for FML fabrication

Different types of reinforcement materials are reported in the literature, used for the FML fabrication; synthetic, natural and hybrid. The commercially used FMLs are made with synthetic reinforcement including aramid, carbon and glass [13], [14]. Natural fibre reinforced Fibre Metal Laminates NFMLs are gaining attention and number of researchers are working on its commercially viability. The jute, kenaf, banana, sisal, coir, bamboo, flax, basalt and hemp fibres are used to make NFMLs [15]–[21].

Hybrid composites can be made by the combination of different constituents to combine the properties of each component and to overcome the problem associated with single component. The possible combination of fibres to make hybrid composite can be synthetic-synthetic, synthetic-natural, natural-natural depends upon end properties [22]. One such example of hybrid fibre metal laminate is Al/GFRP/CFRP/GFRP/Al, as glass fibre layer is placed above and below the carbon fibre to avoid galvanic corrosion between carbon and Al and to also get properties of carbon fibre [23].

1.2.3 Types of metals used for FMLs fabrication

2024-T3,7075-T6,7475-T6 and 6061-T6 are the main types of aluminium alloys used to make fibre metal laminates, but now other alloys are also being used. Till now, Aluminium is a signal contender to make FML due to its cost-effectiveness and easy processing [24]. Table 1.1 shows the different type of metals being used to make FMLs.

Table 1.1. Different types of metals used to make FMLS and their properties [24]–[27]

Type of Metal	**Grade**	**Properties**
Aluminium	1000	Used limited, Pure Wrought Alloy
	2000	Ductile & Slightly Stiffer, Aluminium Copper Wrought Alloy
	3000	Aluminium- Manganese Wrought Alloy
	4000	Aluminium-Silicon Wrought Alloy
	5000	Aluminium-Magnesium Wrought Alloy
	6000	Aluminium-Magnesium-Silicon Wrought Alloy
	7000	Stronger, Brittle& Low Fatigue, Aluminium-Zinc Wrought Alloy
Magnesium		Low density, improved electromagnetic shielding and superior corrosion resistance
Titanium		Low ductility & stronger
Steel		Limited use

The tensile strength of pure aluminium is 90MPa which can be increased over 690MPa by heat treatment of some alloys. Different types of treatments are done to aluminium alloys to impart different properties. Different suffix with different grades shows the type of treatment

performed, *e.g.*, T6 means solution heat treated cold worked and naturally aged to a substantially. Suffix like O, T, W and H can be with different grades of Aluminium [25].

1.2.4 Type of polymer matrices

Both thermoset and thermoplastic matrices can be used depending upon end applications, but epoxy is the preferred system in FMLs [5].

Thermosetting composites are usually brittle, strong and require high curing temperature [11]. Epoxy is preferred for the fabrication of FML due to its distinct quality, easy processability and good mechanical properties. Epoxy is used as a resin in ARALL, CARAL and GLARE.

Although thermoset based FMLs are used in high tech applications but with growing environmental concerns, there is more pressure to use recyclable material [28]. Further long production cycle and brittleness of thermoset resin is reason to use thermoplastic resin [24]. Thermoplastic FMLs have high toughness and contain a short processing cycle, with the evident advantage of recyclability [11].

1.2.5 Properties of FMLs

The high flame resistance of FMLs, especially GLARE, is very important keeping in view the current aviation rules. According to Airworthiness Regulations, in case of emergency, an aircraft must be evacuated within 90 seconds. It is quite impossible keeping in view the current sizes of passenger aircraft. With high fire-resistant , it provides more time for emergency exist [2]. Fatigue crack growth in aerospace structures causes catastrophic failure. This catastrophic failure can be avoided by reducing fatigue crack growth, which is possible by bonding thin sheets of material instead using a single sheet. The advantage of using bonded laminates is more evident when cracking initiates in single lamina other layer act as a shield and crack will be resisted until propagate in neighbouring sheet [2]. FMLs have some added functionalities

like high specific bending strength, acoustic absorption, vibration transmissibility and damping [11]. Table 1.2 shows the key properties of FMLs

Table 1.2. Key features of FMLS [3]

Property	**Key Feature**
Material Behaviour	• High Fatigue resistance • High Strength • High Fracture toughness • High Impact resistance • High Energy Absorption
Physical Properties	• Low Density
Durability	• Excellent Moisture Resistance • Excellent Corrosion Resistance • Lower Material Degradation
Safety	• Fire Resistant
Low Cost	• Strength to weight ratio

1.2.6 Types of FMLs

Based on constituents and stacking sequence of metal and composites, FMLs can be classified in four broad categories. FMLs classification is shown in Figure 1.4.

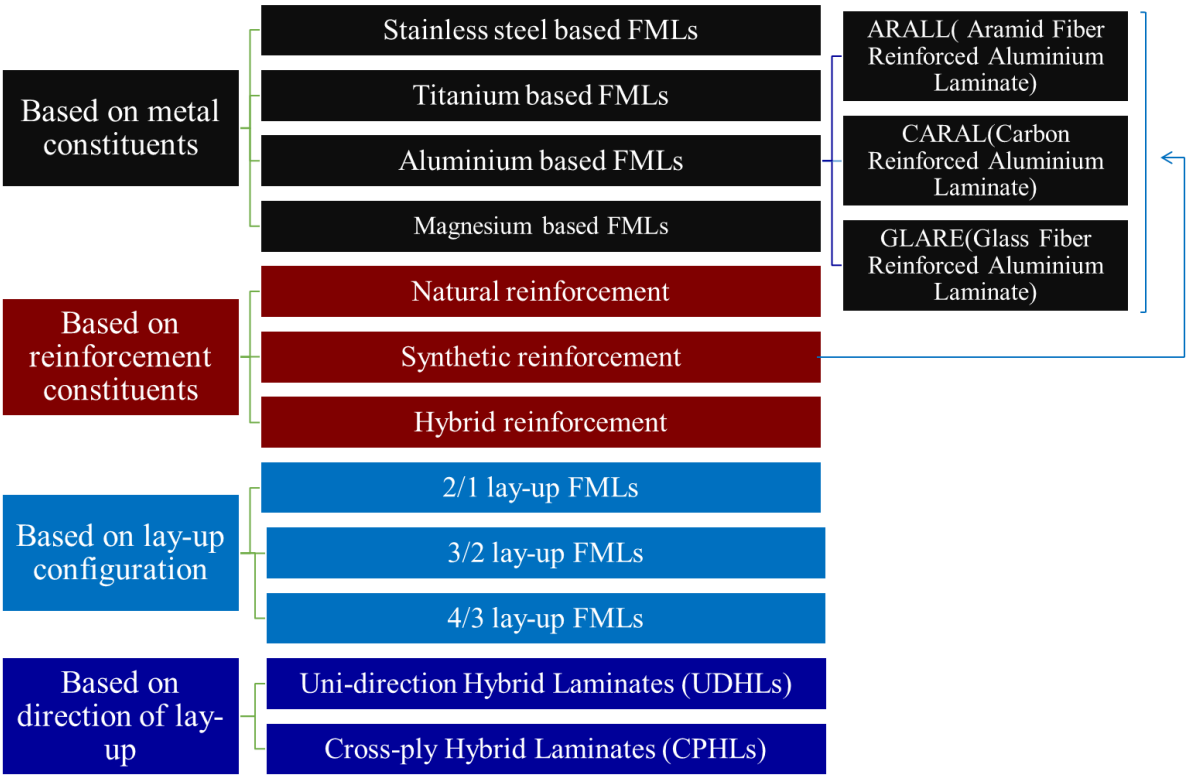

Figure 1.4. Classification of fibre metal laminates [3], [13]

1.2.7 Aramid fibre Reinforced ALuminium Laminate ARALL

ARALL is a first fibre metal laminate that was used commercially. ARALL is made by putting aramid / epoxy prepreg between alternative aluminium sheets. Epoxy and aramid fibre are placed unidirectional with fibre to resin weight ratio 50:50. ARALL panels are cured in hot press or autoclave for an appropriate time. ARALL combines the unique properties of aluminium and aramid in single material [3]. The main feature of ARALL is to reduce the crack growth, propagation by bridging of fibre and metal, due to this fatigue crack growth rendering, the life of ARALL is better than both constituents. Mainly the fibre composite is insensitive to crack growth so that FML render fatigue crack growth propagation (Table 1.3) [29].

Table 1.3. Different types of commercially available ARALLs and their properties [3], [29]

ARALL Type	Aluminium Type	Metal Thickness [mm]	Fibre Layer [mm]	Fibre Direction [°]	Stretched [%]	Characteristics
ARALL 1	7075-T6	0.3	0.22	0/0	0.4 Stretched	Fatigue, strength
ARALL 2	2024-T3	0.3	0.22	0/0	No Stretch	Fatigue, formability
ARALL 3	7475-T76	0.3	0.22	0/0	0.4 Stretched	Fatigue, strength, exfoliation
ARALL 4	2024-T8	0.3	0.22	0/0	No Stretch	Fatigue, elevated temperature

ARALL could not gain much popularity despite extensive attention due to the following reasons:

1) The low interface between fibres and adhesive materials, so it was not possible to produce a material with higher fibre volume fraction and acceptable shear properties.
2) Although ARALL has better fatigue resistant than bare aluminium but fibre failure in crack bridging fibre layer occurs. This problem was soluble with post stretching, but post stretching was not viable due to three reasons (a) Additional high cost of post stretching (b) Not possible to do post stretching of larger parts (c) Unnecessary delay.
3) Due to unidirectional fibres in FMLs, ARALL has more isotropic behaviour, and for biaxial loading, its performance was reduced.
4) ARALL has poor blunt notch strength than monolithic aluminium alloy due to low failure strain (2.4%) compared to Al [2].

1.2.8 Carbon Reinforced Aluminium Laminate CARAL

To improve the limitations of ARALL, a new FML was developed in which aramid fibres were replaced with much stiffer carbon fibres [30]. The production process of CARAL was like ARALL. Al surface was treated to enhance the adhesion with epoxy resin. Table 1.4 shows the different variants of CARAL.

Table 1.4. Different types of commercially available CARAL and their properties [13]

CARAL Type	**Aluminium Type**	**Metal Thickness [mm]**	**Fibre type**	**Fibre Direction [°]**	**Characteristics**
CARAL 1	2024-T3	0.2-0.5	HM/T300	0/0	Stiffness, strength
CARAL 2	2024-T3	0.2-0.5	HM/T300	90/90	Stiffness, strength

Due to superior stiffness, high specific modulus and impact properties than ARALL, it had great potential to be used as impact absorber in helicopter struts and aircrafts seats. The CARAL had excellent crack bridging and compressive strength characteristics due to the high stiffness of carbon fibres [3], [7]. The CARAL also showed low fatigue resistance due to low failure strain (0.5-2%) of carbon fibres [31]. Galvanic corrosion between carbon fibre and aluminium layer in the moist environment was a big problem which rendered its use in the commercial applications. As the for aerospace applications corrosion is a big problem [2].

By solving the problem of galvanic corrosion, the CARAL could be used for commercial applications. By isolating aluminium sheet from carbon fibre, the challenge of galvanic corrosion can be diminished. There are some studies reported in which thermoplastic polyetherimide coatings or extra glass fibre sheet between aluminium and carbon is used to

isolate them [32]. The use of titanium alloy can also reduce the effect of galvanic corrosion significantly.

1.2.9 Glass Laminate Aluminium Reinforced Epoxy GLARE

After limitations of both ARALL and CARAL, a new FML was developed with high strength glass fibre called GLARE. Due to the good adhesion of glass and adhesive, the compressive strength of GLARE was much higher. Other advantages of GLARE over ARALL were its higher tensile and compressive strength, better impact behaviour, higher ultimate strain and higher residual strength [2]. The GLARE family got much acceptance, and different variations are imparted as per requirement. The different GLARE and their properties are shown in Table 1.5.

Table 1.5. Different types of commercially available GLARE and their properties

GLARE Type	**Sub-Type**	**Aluminium Type**	**Metal Thickness [mm]**	**Fibre Layer [mm]**	**Fibre Direction [°]**	**Characteristics**
GLARE 1		7475-T761	0.3-.04	0.266	0/0	Fatigue, strength. Yield stress
GLARE 2	GLARE 2A	2024-T3	0.2–0.5	0.266	0/0	Fatigue, strength
	GLARE 2B	2024-T3	0.2–0.5	0.266	90/90	Fatigue, strength
GLARE 3		2024-T3	0.2-0.5	0.266	0/90	Fatigue, Impact
GLARE 4	GLARE 4A	2024-T3	0.2-0.5	0.266	0/90/0	Fatigue, strength in 0° direction
	GLARE 4B	2024-T3	0.2-0.5	0.266	90/0/90	Fatigue, strength in 90° direction
GLARE 5		2024-T3	0.2-0.5	0.266	0/90/90/0	Impact, shear off axis properties

GLARE 6	GLARE 6A	2024-T3	0.2-0.5	0.266	+45/-45	Shear, off-axis properties
	GLARE 6B	2024-T3	0.2-0.5	0.266	+45/-45	Shear, off axis properties

The GLAREs rarely fail due to excellent adhesion between glass fibre and resin. GLARE has excellent impact resistant Unlike ARALL and CARAL fibre failure during fatigue loading is hardly observed in GLARE. The failure mechanism in GLARE is metal dominated. GLARE has good tensile strength, impact strength, residual strength and compressive strength [2].

There are certain disadvantages of GLARE as they have lower stiffness as compared to aluminium metal and ARALL. It is especially dominant in GLARE with cross-ply of glass fibres. The high production price is also an obstacle to replace Al alloys with GLARE as the production cost is about ten times higher [2].

1.3 Manufacturing process of FMLs

In this section, the manufacturing process of FMLs is discussed in detail, including surface treatment and fabrication techniques. The surface of metal is prepared before fabrication of FMLs to enhance the bonding between metal and composite, which plays a crucial part in the final properties. The fabrication of FMLs is done by different techniques. The autoclave is used currently for commercial preparation of samples as most of current FMLs are used for aerospace application. The VARTM and compression hot press are also reported in literature used to make FMLs; the detail is in the below section.

1.3.1 Surface treatment of metals for FMLs fabrication

The surface of the metal is prepared to increase bonding with resin before using them for FML fabrication. Pores are generated on the surface to improve the adhesion. Table 1.6 shows the

different types of surface treatments done to increase the adhesion of aluminium with composites.

Table 1.6. Type of surface treatments and their nature to modify Aluminium surface [33]

Type of Treatment	**Nature of Treatments**
Mechanical	1. Grit Blasting 2. Excimer Laser Texturing 3. Abrasion with sandpaper
Chemical	1. Chromic-Sulfuric Acid etch 2. Forest Product Laboratory 3. Sulfo-Ferric acid etch 4. Alkaline Etch
Electrochemical Alternating Current AC Direct Current DC	1. Sulphuric Acid Anodizing-SAA (AC&DC) 2. Phosphoric Acid Anodizing-PAA (AC&DC) 3. Chromic Acid Anodizing-CAA (DC) 4. Boric-Sulphuric Acid Anodizing-BSAA
Coupling Agent	1. Silane 2. Sol-Gel
Dry Surface Treatment	1. Ion Beam Enhanced Deposition IBED 2. Plasma-sprayed coating 3. Excimer laser Texturing

Before any treatment, the surface of aluminium is degreased with certain solvents. Solvent decreasing removes dust, dirt, and waxes from the surface of the metal, which reduces its ability of bonding. Solvent degreasing does not make metal acceptable for FML fabrication solely, still need further treatment to make it ready to use for FML fabrication. The degreasing is done either with chlorinated solvents such as trichloroethylene, 1, 1, 1-trichloroethane, perchloroethylene or dichloromethane or with non-chlorinated solvents including methyl ethyl ketone, methanol, isobutanol, toluene or acetone [3].

After degreasing of aluminium, it is mechanically prepared to remove the unfixed oxide layer and prepare for subsequent processes. As mentioned earlier, mechanical preparation is mostly done with grit blasting / sandpaper. Once the unfixed oxide layer is removed, then chemical etching or anodizing is done to create micro-roughness. To avoid corrosion and better bonding, the surface of aluminium is anodized. Even good adhesion can be achieved by solvent degreasing and subsequent chemical etching. However, only chemical etching is not sufficient surface treatment. The aluminium surface is anodized before it is used in all types of aerospace applications. Two kinds of films can grow on the Al surface using anodizing, *i.e*., Porous and Barrier. CAA produce barrier oxide layer and PAA produces porous oxide layer on the surface of the aluminium. A porous oxide layer, however, produces better interfacial bond, which facilitates subsequent bonding. Figure 1.5 shows the difference of anodized and non-anodized surfaces [34].

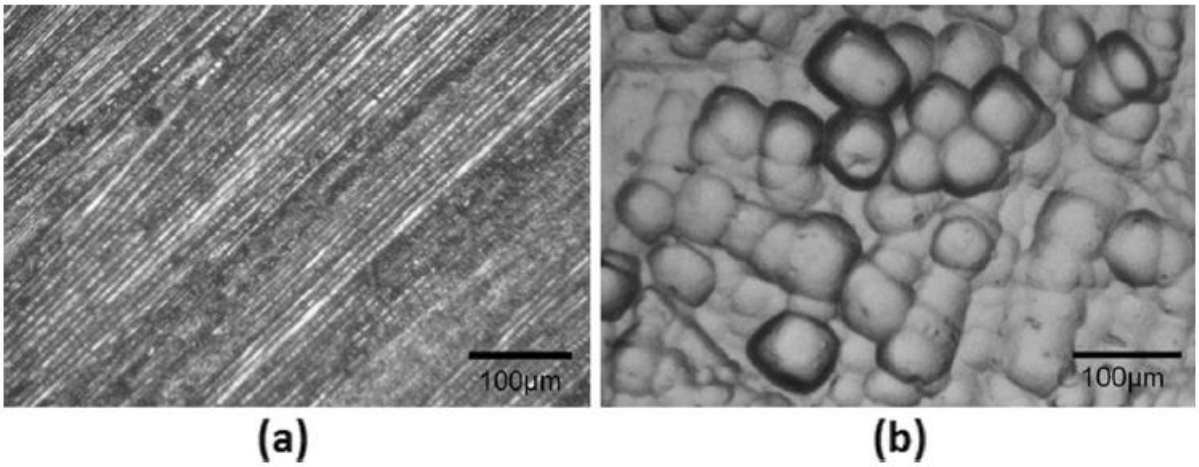

Figure 1.5. (a) Mechanically treated Aluminium surface (b) Anodized aluminium surface showing the porous oxide layer [34]

DC Phosphoric Acid anodizing is the most popular type of anodizing technique and currently used by Boeing as well. The surface oxide is in the range 400-800 nm including ~100 nm of

small protruding fibrils. The oxide is highly porous, with a cell diameter of ~40 nm and with thin walls compared to those on the Chromic Acid Anodizing CAA oxide [35].

Phosphoric Acid Anodizing is carried out in the following steps to get better results [34]:

1. Solvent degreasing
2. Mechanical abrasion
3. Alkaline cleaning
4. Deoxidation
5. Anodizing

ASTM D3933 standard is strictly followed to get repeatable results. Anodizing is an electrochemical process of surface treatment of metals. In this, a thin oxide layer is formed on the surface of the metal, which helps in corrosion resistance and enhances bonding. Usually, the target surface is used as the anode while the cathode is stainless-steel or carbon plate. When the circuit is closed the electrons are withdrawn from the surface of the metal. Due to the movement of electrons, the ions are created on the surface, these ions react with the water in the solution and creating the oxide layer. The surface of the aluminium plate is rubbed with emery paper / sandpaper to remove the foible oxide layer and create an active site for further chemical treatment. The epoxy ring-opening reaction is discussed below with the anodized surface.

The epoxy ring-opening reaction in the presence of amine hardener is presented in step 1 in [29]. Step 2 demonstrates the creation of ion exchange sites on the aluminium surface as a result of acid treatment. In step 3, the ion exchange reaction has been shown, which is responsible for the bonding between aluminium surface and epoxy chain. The extent of cross-linking creates an extended network of bonded polymer chains on the metal surface. Therefore, by increasing the number of cross-linking sites and optimizing ring-opening reactions, one can expect to have better bonding of aluminium with the resin system (Figure 1.6) [36].

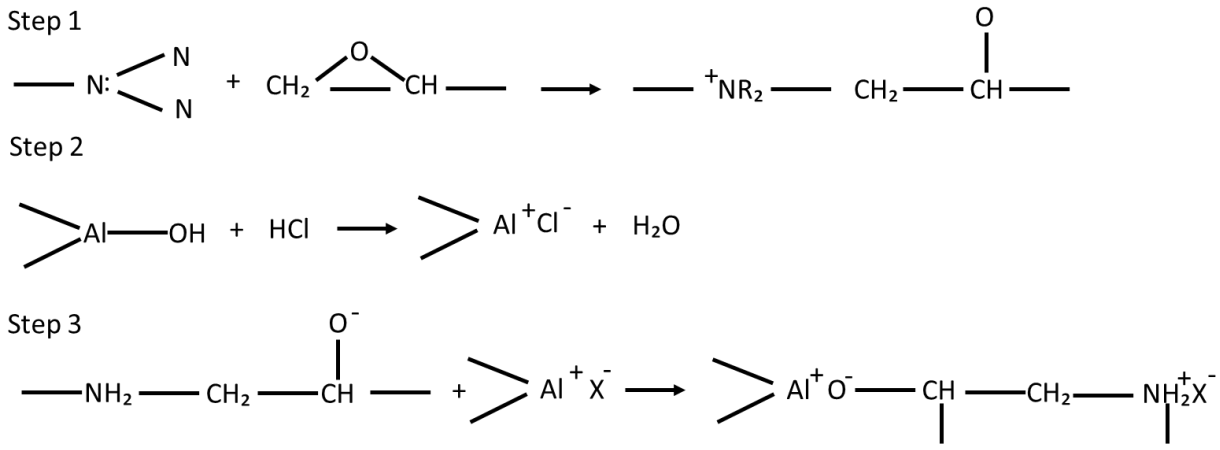

Figure 1.6. Ring-opening, ion exchange site creation and ion exchange reaction between the epoxy resin system and the Aluminium surface [36]

1.3.2 Autoclave process

The most commonly used and effective procedures to manufacture FMLs is an autoclave process in which prepreg material and metal sheets are used (Figure 1.7).

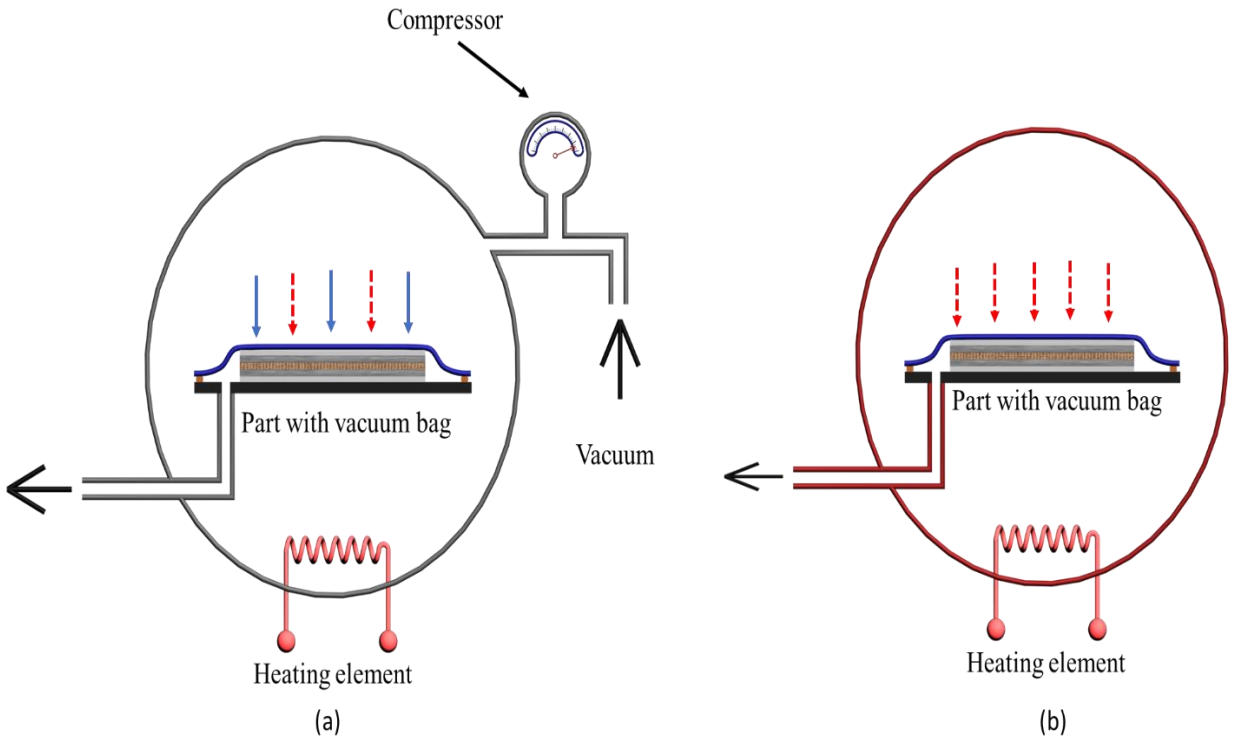

Figure 1.7. Schematic view of (a) autoclave consolidation with (b) oven post-curing, heat (dashed arrow), consolidation pressure (solid arrow) [37]

FMLs (ARALL, CARAL and GLARE) are produced in autoclave usually the temperature is more than 200 °C. Autoclave process is generally carried out in the following steps (Figure 1.8) [10], [38], [39].

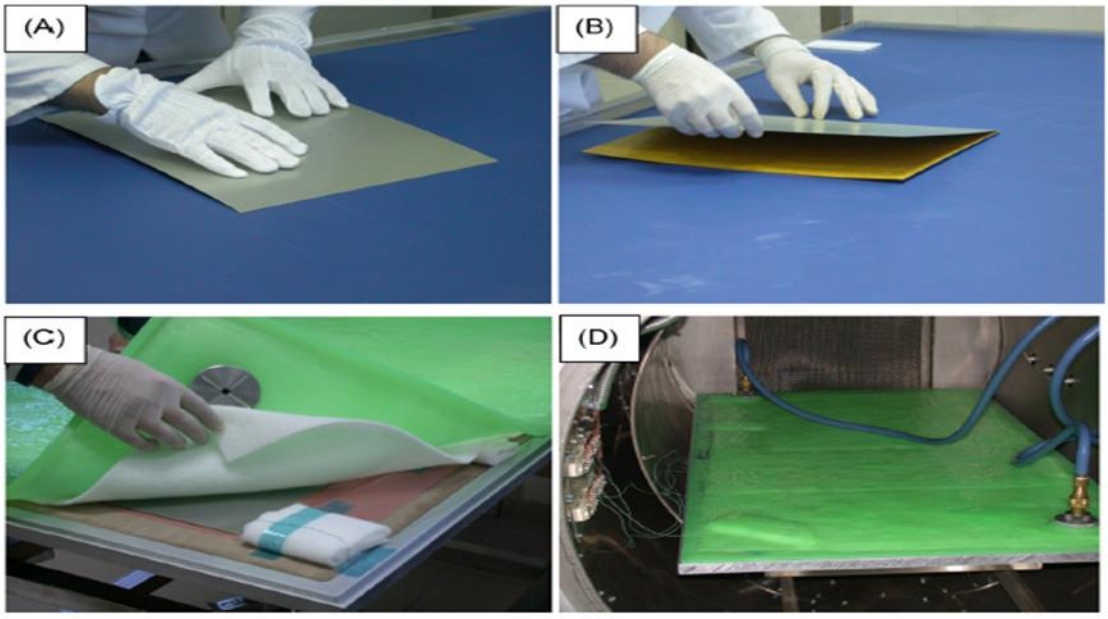

Figure 1.8. FML structure manufacturing: (A) components preparation (B) layer configuration (C) Vacuum bag preparation (D) Loading for autoclave curing [10]

1. Tool and material preparation, which includes pre-treatment of metal layers for adhesion and corrosion resistance
2. Forming of elements which contain cutting of metal and prepreg, lay-up of metal and prepreg layers as per desired stacking sequence, vacuum bag preparation
3. Cure in the autoclave which includes consolidation process
4. The inspection, which contains non-destructive and destructive tests

The autoclave process causes the high thermal residual stresses in the FMLs during fabrication and to solve this problem; different researchers proposed different methods to overcome this problem. Khan *et al.* [29] proposed a technique in which FMLs is stretched up to the plastic region during post-curing to eliminate the tensile residual stresses. Xue *et al.* [40] used the thermal expansion control clamps to control the residual thermal stresses in CARALs. Jarosław

Bieniaś [41] developed titanium-based FMLs using autoclave process, he determined that the titanium / glass fibre reinforced laminates (Ti-G) produced using an autoclave process have uniformity in structure and less void content (<1%). Park *et al.* [37] investigated the physical and thermal properties of GLARE for modified autoclave process. They used autoclaves, oven and consolidated autoclave curing cycle and found that consolidated autoclave and oven post-cured GLARE have a higher fibre volume fraction, fewer voids, and uniform thickness of plies.

The autoclave process has advantages of part of high quality with fewer void contents, but on the other hand, it is quite an expensive process, and the part size is limited due to autoclave size. Distortions and residual stresses are generated during the manufacturing of FML [42], [43].

1.3.3 VARTM process

The FMLs are traditionally developed using an autoclave process, which is quite an expensive process. That is why the FMLs produced with autoclave process are used for high-tech applications. National Aeronautics and Space Administration NASA, Langley Research Center LaRC developed the FMLs using low cost and faster VARTM process for FMLs fabrication for the first time with properties comparable with the conventional FMLs made with autoclave process. The FML produced by VARTM and RTM does not compromise on features. NASA claims that FML produced by this method is successfully used in aircraft and space construction [10]. The VARTM process developed by the NASA LaRC for the fabrication of FMLs needed certain perforation in the metal layers so the resin can flow through the thickness (Figure 1.9).

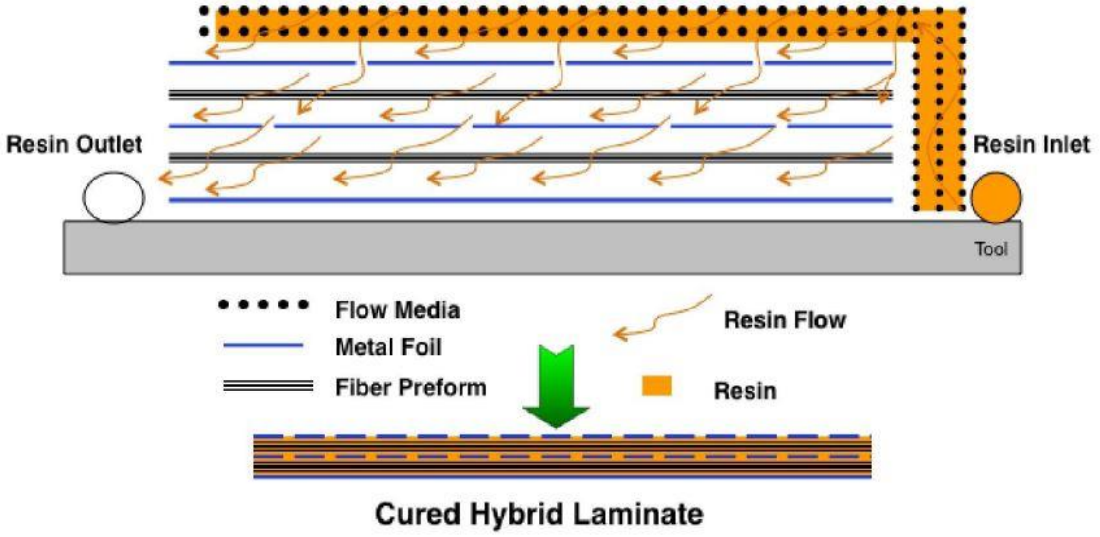

Figure 1.9. Illustration of the resin flow during VARTM of VARTM FMLs [42]

The perforations (pathways) are made using the different types of drilling techniques, *e.g.* Dremel drill, water jet, Nd: Yag laser and precision drill. Out of these different drilling techniques, the precision drilling has lowest effect on the fatigue properties of FMLs. The drilling still has some effect on the fatigue properties of FMLs as compared to non-drilled FMLs [44].

A lot of literature has been reported regarding the resin flow study of the VARTM process for FML fabrication to check the effect of perforations and resin delivery in the transverse direction. They found that the resin flows more rapidly through the length direction and slowly through the thickness direction due to the overall stacking sequence of metal and composite; this significantly affects the infusion times. The VARTM process has shown its effectiveness to replace the other FMLs fabrication processes like autoclave and pressure Moulding [44]–[46]. The static and dynamic properties of FMLs manufactured using VARTM are highly affected by the perforation made for resin flow and usually crack initiates at the tip of the hole. Though the properties are comparable to FMLs manufactured using the autoclave process, the problem of perforations made for resin flow needs to be addressed [47], [48].

Qaiser *et al.* [34] developed the ARALL using VARTM process to check the effect of surface treatment on the interlaminar adhesion of metal and aramid composites.

VARTM has drawbacks like the variable thickness of the part, which cause variable fibre volume fractions and for bigger parts, the filling time increase because of limitations of vacuum and pressure. To cope with this problem, Hergan *et al.* [49] introduced the concept of vacuum infusion with a rigid mould. With that rigid mould, the resin flow was controlled with high injection pressure, as shown in Figure 1.10.

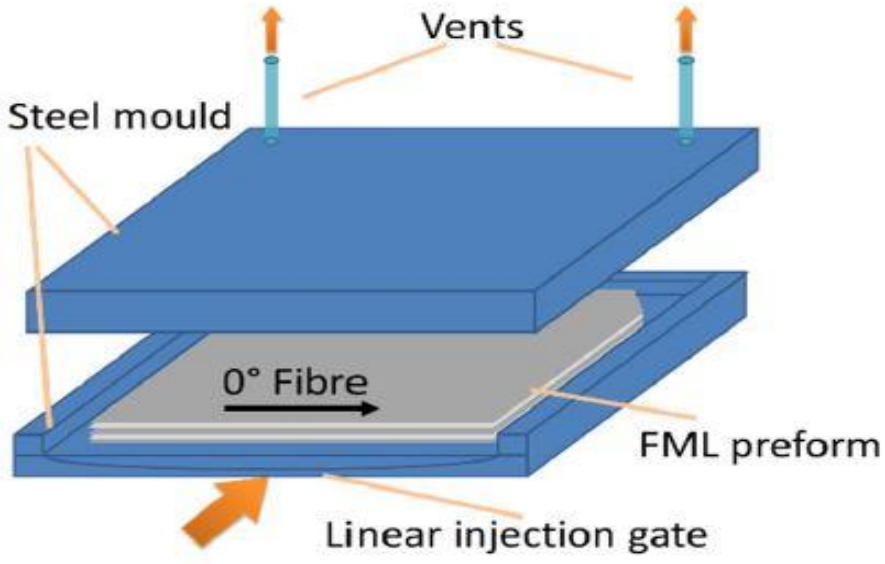

Figure 1.10. Modified VARTM with rigid mould for manufacturing of FMLs [49]

Due to rigid mould the thickness of the final part and fibre volume fraction was controllable. The processing cycle of VARTM is shorter than the autoclave process. The curing time required in VARTM is also less than autoclave process. Table 1.7 shows the comparison of processing time of VARTM and autoclave process for FMLs. The sample preparation path of oven and autoclave is alike except consolidation as discussed earlier. The VARTM is economical process due to short curing cycle.

Table 1.7. Comparison of processing time; breakdown by operation for laboratory-scale processes [37], [49]

Production Steps	**VA (RTM)**	**Autoclave**	**Oven Cure**
Tooling preparation	25	25	25
Prepreg / metal sheet cutting	30	30	30
Surface treatments	390	390	390
Hand lay-up	10	30	30
Vacuum bagging		25	25
Cure cycle	25	260	260
Debagging	5	10	10
Total production time [min]	485	770	770

1.3.4 Compression hot press

Thermoplastic FML is made using a hot compression moulding technique. Sometime FML made by hand lay-up technique is also placed in a hot press to cure appropriately [11]. The compression moulding is one step process and requires fewer arrangements, that is why it is gaining considerable attention as replacement of conventional autoclave process. With the emergence of thermoplastic fibre metal laminates, the more emphasis is being laid on compression hot press. In one such study, Múgica *et al.* [50] developed the FMLs of Al and Mg-based on Self Reinforced Poly Propylene (SRPP) using a hot press at 30bar pressure and 165 ºC temperature. Abdullah and Cantwell [51] investigated the high-velocity impact properties of FML reinforced with polypropylene composite core. They developed FMLs using a compression hot press at a consolidated pressure of 5-6 bar and temperature of 160-165ºC. Santiago *et al.* [52] Implied the similar FMLs fabrication technique to manufacture Thermoplastic Fibre Metal Laminate (TFML) as shown in Figure 1.11.

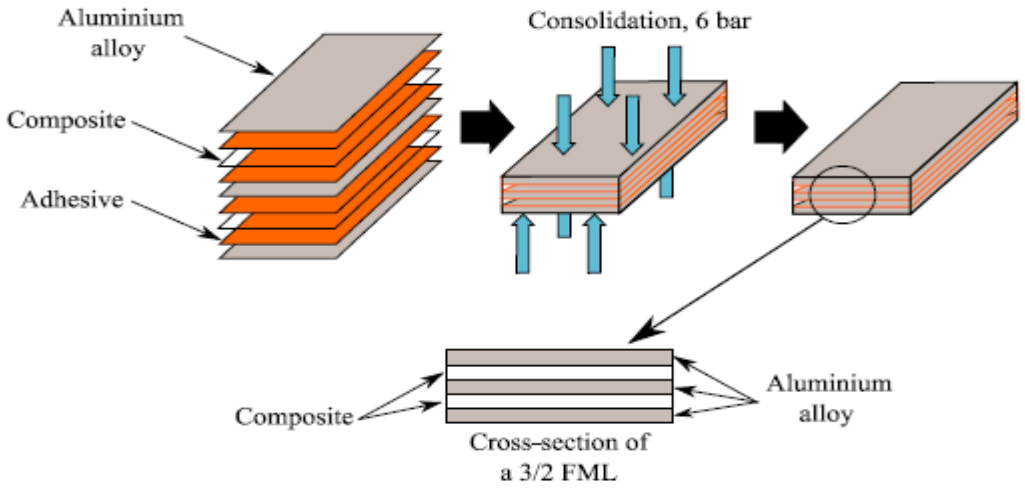

Figure 1.11. Schematic illustration of FML fabrication using compression hot press

The TFML are also manufactured using an air circulating curing oven and cold press. Before moving the sample in the cold press, the plies are stacked in the picture frame as per configuration and put in the oven at 185 ºC [53], [54]. There are issues of part thickness, crystallinity and plies orientation during fabrication of FMLs on compression hot press to address these issues, Chen *et al.*[55] investigated the properties of Al/GF/PP FML made on compression hot press. They developed the samples with normal peel ply, intermittent peel ply and peel ply with holes. The part was cooled with air, water, oil, and mould cooling. The peel ply with holes with air colling of the sample provided better mechanical properties as compared to the rest of the methods. The fast cooling with air helped in maintaining the low degree of crystallization resulting in better tensile properties.

1.4 Mechanical Properties

The composite and metal are joined through adhesive, so the bond between metal and composite is very crucial, and properties of FML are driven by the nature of adhesion between metal and composite. Different test methods are employed to measure the properties of the adhesive layer. The various tests can be categorized in different ways. The first category of the tests is peel tests, including floating roller peel drum and t-peel test. The second category of

the tests is shear tests and done for lap joints. These tests include a different kind of lap shear tests. The third group of tests is tensile and cleavage tests. While the fourth class of tests includes determination of fracture energy of the adhesive layer, these include criteria for determination of mode I, II and mix mode fracture energy. Out of all these tests, the first category of tests gives an assessment of the quality adhesive bonding. The adhesion properties are critical to check the adherence and endurance of the cohesive bond. Interfacial adhesion is also very important before evaluating the subsequent fracture or shear strength determination [56]. The different type of tests conducted to check the quality of interfacial adhesive bonding as shown in Figure 1.12 [57], [58].

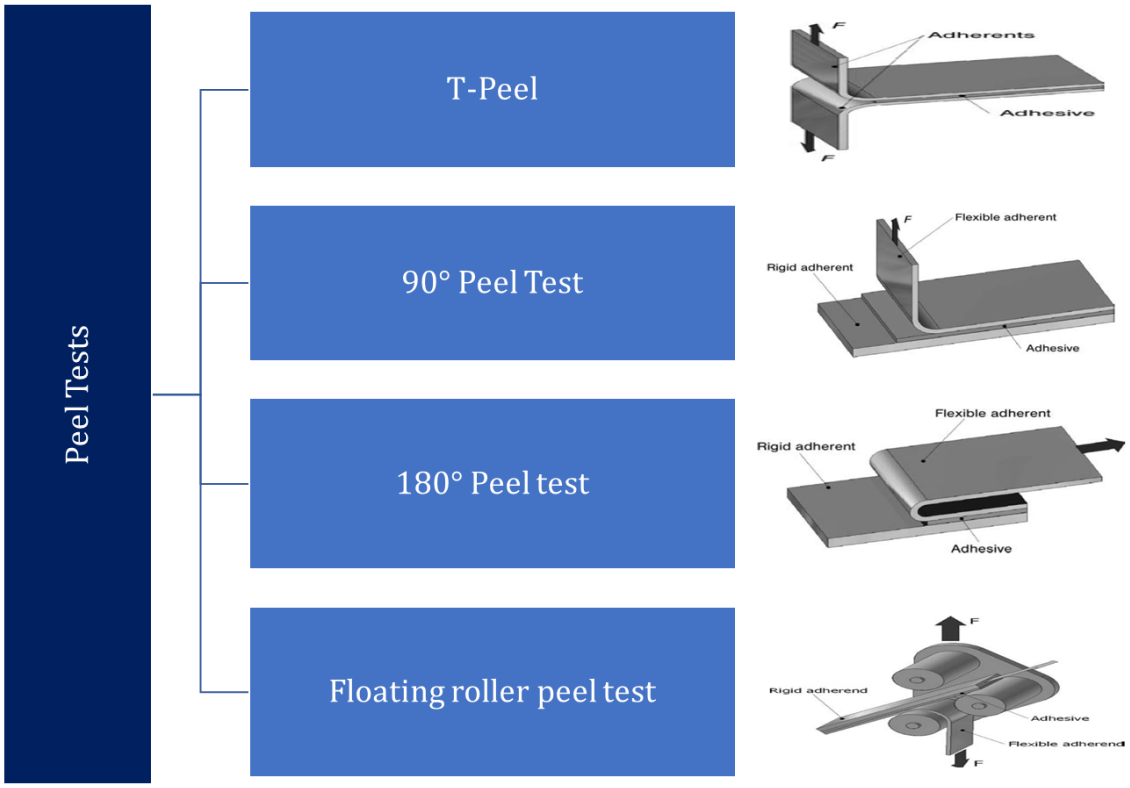

Figure 1.12. Different peel tests done to check the quality of the adhesive bonding layer [57], [58]

Different types of monotonic and dynamic mechanical characterization of FMLs are carried out to analyse their properties. The mechanical characterizations reported in literature for FMLs is shown in Figure 1.13.

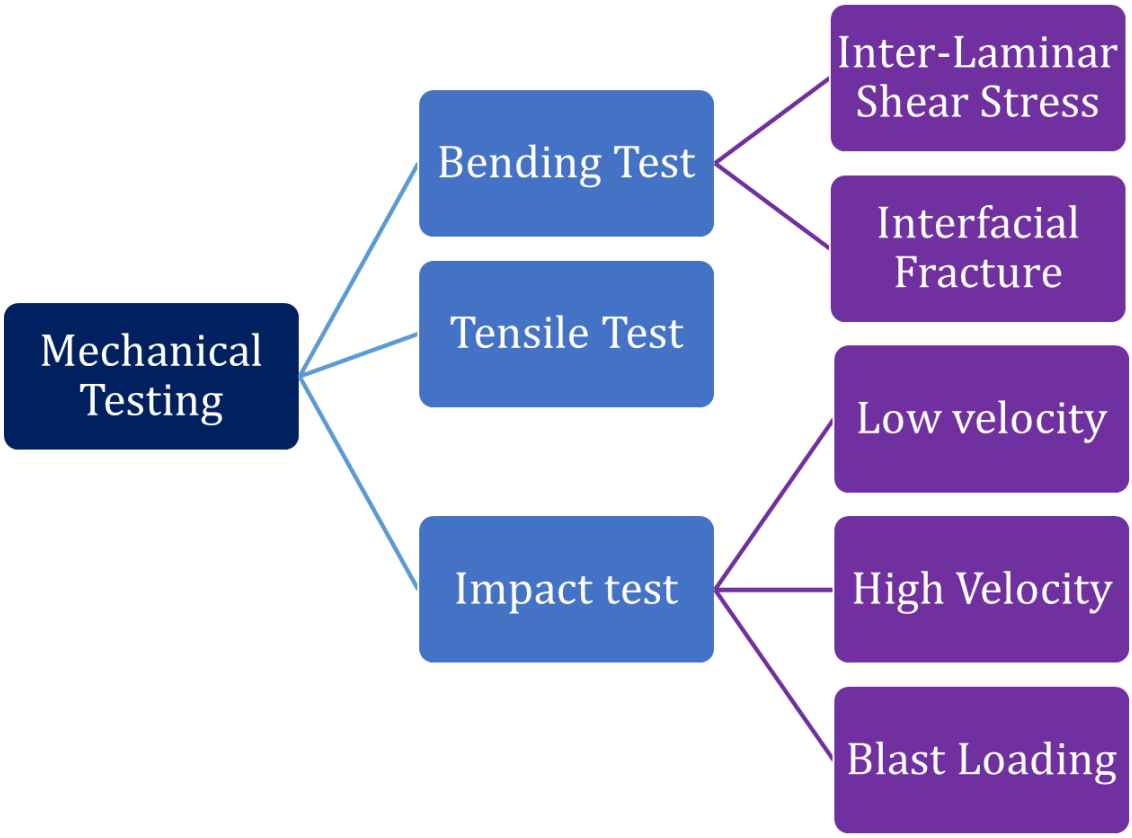

Figure 1.13. Flow chart of mechanical test performed for FML reported in Literature

Tensile test of FMLs can be performed using both rectangular or dog bone shape type specimen. The test can be either on constant crosshead speed or at a continuous strain. The flexural properties of FMLs are checked using three types of tests as reported in the literature:

1. Compression loading
2. Three and four-point bending
3. Short beam shear

FMLs are involved in a different kind of impact loading during their service life, including low-velocity impact, high-velocity impact, and blast loading. The low-velocity impact test is

conducted on a drop weight impact testing machine. The shape of the impactor is usually hemispherical, but diameter can vary. The impact velocity is usually less than 10*m/s* [3]. An air gun consisted of the high-pressure vessel is used to test the high-velocity impact properties of FMLs. A square shape specimen is clamped so that the impactor can hit the centre of the target. The impactor hit with velocities varying from 25 to 100 *m/s*. The distance between gun and target can be measured using light-emitting diode photovoltaic cell pairs [59]. The blast loading test of FMLs is being conducted using a plastic explosive PE4, PE4 is 88% RDX and 12% lithium grease. The detonation velocity is usually in the range of 8800m/s [3].

In this section the adhesive properties, monotonic properties, and low velocity impact properties of FMLs will be presented in detail.

1.4.1 Assessment of quality of metal-composite adhesive bonding

As FMLs are made with a combination of metal and composite, these two components are joined together with adhesive. The adhesive layer makes two kinds of interfaces:

1. The interface between the adhesive and the metal
2. The interface between the adhesive and the composite

In case of failure, the failure occurs; (a) adhesive failure, (b) cohesive failure and (c) intra-laminar failure. The adhesive failure occurs between the interface of two materials, so it is considered a bad failure, indicating poor bonding. The cohesive failure occurs within the adhesive layer, so indicate good adhesion. The intra-laminar failure is in the composite laminate; it also indicates good adhesion since the failure does not occur at the interface of two materials [60].

The different surface treatments cause a different type of failure modes. Agha Mohammadi *et al.* [19] studied four different types of surface treatments effect on the aluminium surface. They employed mechanical, alkaline etching, Forest Products Laboratory Etching FPL-Etching and

Sulphuric Acid Anodizing SAA. They made basalt based FMLs. The flexural test results showed that mechanical and alkaline etching caused poor bonding, and the failure mode was adhesive. The FPL-Etching caused excellent bonding between aluminium and composite and failure mode was cohesive. Since the surface treatment of metal is crucial for even and good interfacial bonding, different researchers have conducted research on the effect of surface treatments. Wu *et al.* [61] worked on the optimization of different surface treatments and their effect on the Inter Laminar Shear Strength ILSS of FMLs. They used solvent degreasing, mechanical abrasion, plasma treatment and alkaline cleaning for surface treatment of aluminium. Out of different types of surface treatments, the sandpaper of 180 grit size and alkaline cleaning with 10% concentration of NaOH showed highest ILSS as shown in Table 1.8.

Table 1.8. Influence of various surface treatment methods on the ILSS of FMLs samples

Surface Treatment Methods	ILSS [N/mm²]	
	The Novel process	The Traditional autoclave process
Reference solvent degreasing	26.98±0.89	-
Acetone	27.26±1.23	-
Ethanol	28.17±1.43	-
Plasma		
O_2	35.24±0.89	-
N_2	39.39±1.55	-
Mechanical abrasion/grinding		
180 grit	42.06±2.13	-
320 grit	38.34±1.21	-
500 grit	33.24±0.94	-
Alkaline degreasing		
2 weight% NaOH	39.02±1.75	-
5 weight% NaOH	39.56±0.60	-
10 weight% NaOH	41.63±0.53	-
15 weight% NaOH	37.19±0.60	-
Combine process		
Grinding (180 grit) /alkaline degreasing (10 weight% NaOH)	42.39±1.21	42.03±1.43

The reason for high ILSS for abrading the metal surface with the sandpaper of lower grit is that the high roughness is achieved as compared to abrade with sandpaper of higher grit. There is an interface layer produce with alkaline cleaning, the thickness of that interface layer increase with increasing the concentration of NaOH. This interface layer causes a bridging effect between aluminium and composite, which cause an increase in adhesion. The ILSS increase for the concentration of NaOH up to 10%, but decrease after that, the reason of decrease in ILSS at a higher concentration than 10% is that the mechanical performance of aluminium is compromised with increasing thickness of interface layer and thinning of aluminium plate with the reaction.

The surface of aluminium is pre-treated to achieve better corrosion resistance and excellent adhesion. Zakria *et al.* [62] compared the effect of different surface treatments on the interfacial fracture toughness of aluminium-carbon laminates by using double cantilever beam test. They employed three kinds of surface treatments, acid etching, alkaline etching and acid-alkaline etching and compared the results with the reference sample only degreased and abraded with sandpaper. The acid-alkaline etched samples showed the highest interfacial properties. The Atomic Force Microscope AFM results also demonstrated that the acid-alkaline etched surface was rougher and more porous as compared to other treated surfaces. The Lee Hamill & Steven Nutt [63] used Al-6061-T6 alloy and Bulk Metallic Glass (BMG) alloy Zr44Ti11Ni10Cu10Be25 to make CARAL and employed three types of surface treatments: 1-Abrasion, 2-Phosphoric Acid Anodizing PAA, 3- Silane treatment. Composite was made using autoclave and Vacuum bagging separately. Shear loading of samples confirmed the effectiveness of BMG as a possible replacement of Al in FMLs. Figure 1.14 shows the lap shear test results of BMG and Al-based FMLs.

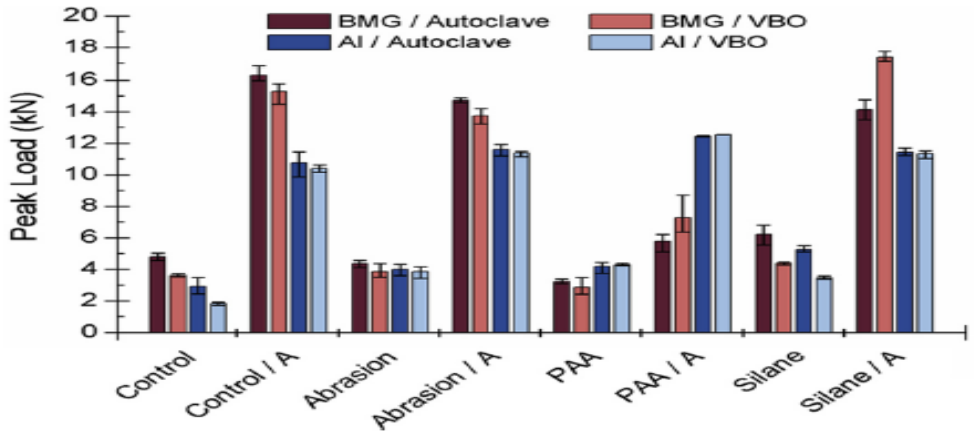

Figure 1.14. Lap shear test results of AL-6061-T6 and BMG alloy FML

The PAA is more effective for aluminium surface treatment than other types of surface modification techniques.

De Freitas and Sinke [64] assessed the bonding properties of different metal-metal, metal-composite and composite-composite adhesive joints using a floating roller peel test. They used two different epoxy resin systems to evaluate the adhesion properties, and the pattern of delamination, The FM 73 and EA 9695 was used as a resin system. The phenomenon of failure was also assessed, and the most prominent failure mechanism with excellent bonding was a cohesive failure rather adhesive failure. Qaiser *et al.* [34] used PAA to increase the surface roughness of aluminium 2024-T3 to improve the adhesion with composite. They compared their results with non-anodized aluminium FMLs. They used the T-peel test ASTM D1876 to examine the interfacial strength of the adhesive layer. The results showed that anodized aluminium FMLs have higher adhesion properties. Khan *et al.* [65] also used T-peel tests to evaluate the interlaminar bond strength of CARAL. The surface of aluminium was prepared using three different kinds of surface treatments, including PAA. The PAA showed excellent bonding properties for the aluminium composite bond. (Figure 1.15).

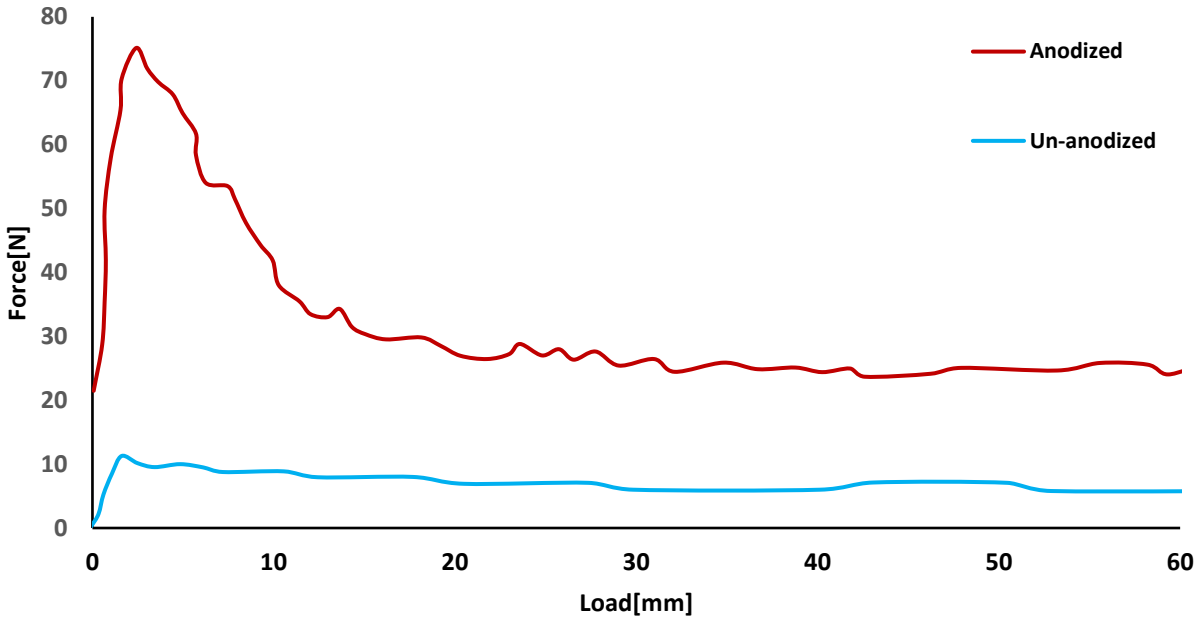

Figure 1.15. Load-extension curve of T-peel test of anodized and un-anodized aluminium-carbon bond [65]

Thermoplastic matrix is extensively used by researchers these days for the FML fabrication. The composite metal bonding of thermoplastic based FMLs is also a point of interest since most thermoplastics are polyolefins. Cache *et al*. [66] investigated the adhesion strength of PP based joints using a single lap joint test. The results showed optimal bonding of aluminium-composite and aluminium-aluminium PP-based bond. They concluded that the PP could be successfully used for FML fabrication. Shanmugum *et al*. [67] compared the Metal Thermoplastic Composite Interface MTCI of titanium thermoplastic FMLs. They made titanium based FMLs in which surfaces of both titanium and reinforcement fibres were treated. The titanium surface was anodized and annealed, while the surface of fibres was functionalized using PolyDopAmine PDA and coated with multiwalled carbon nanotubes MWCNT. The results showed that anodized and annealed titanium surface has a high roughness as compared to the simple titanium surface. The double cantilever results showed the highest force and fracture toughness for the metal-composite bond in which anodized and annealed titanium was

used along with PDA+MWCNT modification of fibres. Hussain *et al.* [68] made Aluminium / Oil Palm Empty Fruit Bunch fibre OPEFB reinforced polypropylene FML, two different types of surface treatment of Al metal were carried out to check interfacial shear strength; 1- degreased with ethanol to remove impurities, 2- Immersion in 0.1% NaOH solution for 10 minutes to remove the weak oxide layer and create roughness. Both type of treatments shown almost similar results.

1.4.2 Monotonic properties of FMLs

The tensile and flexural properties of FMLs are fundamental and sought-after properties found in the literature. Since the FMLs is made with a combination of metal and composites, so the properties of both the constituents contribute to the final properties. That is why the tensile stress strain-strain curve of FMLs GLARE exhibits a highly non-linear response due to the plasticity of the metal part. The high deviation from Hook's law is observed in the case of GLARE FMLs. The higher strain to failure of glass woven fabric (3%) which cause the high metal non-linearity, as a result of this the magnitude of tensile strength and elongation at break of GLARE can be 50-100% higher than the corresponding value at yield strength [48], [49]. The elastic modulus of GLARE is in between the constituents, as can be seen in Figure 1.16.

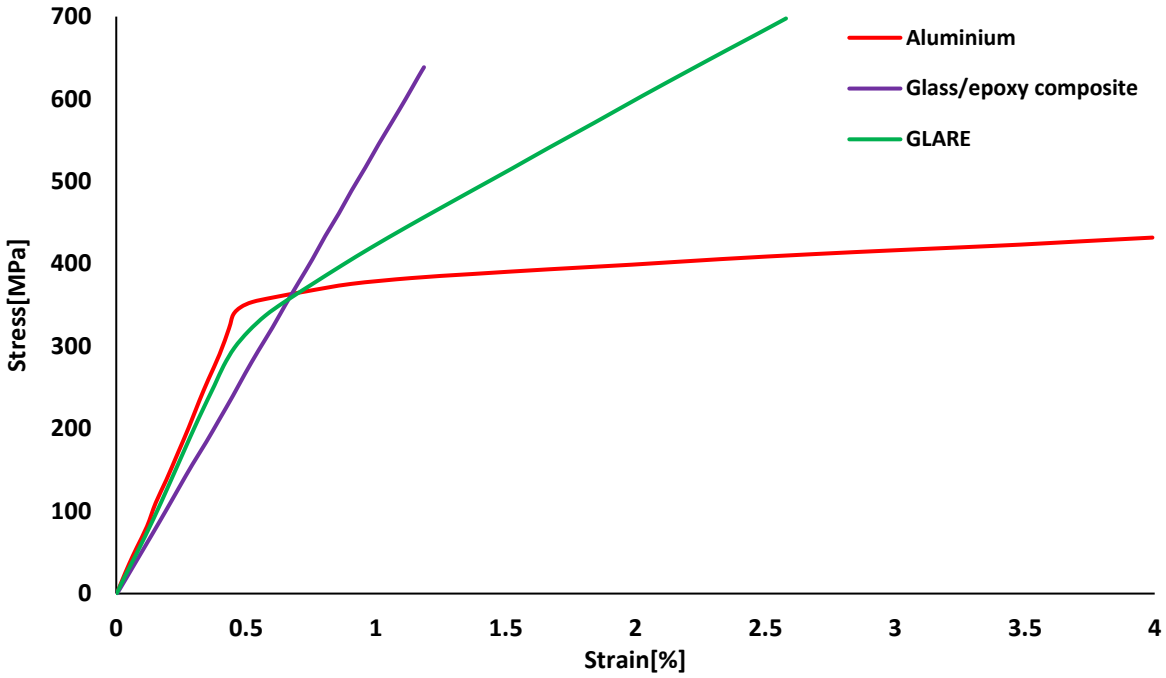

Figure 1.16. Comparison of stress-strain curves of GLARE, aluminium and glass / epoxy composites [71]

The glass / epoxy composite has a slightly low modulus so the final modulus of GLARE is lower than aluminium [69]–[71]. For stress-strain curve in FMLs, initially, both composites and metal are loaded elastically, so the initial part of the curve is elastic. Then the metal starts yielding, and the curve becomes non-linear. The composites still keep reinforcing the metal part until the fracture so the glass fibres can be assumed linear elastic, and the behaviour of the curve becomes linear elastic again (Figure 1.16) [50].

The GLARE exhibit fatigue life around 50-100% higher than the monolithic aluminium. The reason for this prolonged crack life is that the unbroken fibre carries much of the load at the crack tip and slow down the propagation of the crack. There is always the constant crack growth rate due to balance between delamination length, crack opening and crack bridging stress [72].

The delamination at the interface of metal composites is often observed in FMLs. This delamination is usually induced by the shear forces that arise because of fibre bridging Transfer of load from composite to aluminium layer [73].

The metal volume fraction also affects the mechanical properties of fibre metal laminates with the increase of metal volume fraction, the fatigue life of laminates is improved. Further, the delamination will be more in thin laminates as compared to thick laminates. The more significant delamination results in the reduction of bridging stress and consequently, larger crack opening [74]. The Metal Volume Fraction MVF is the ratio of the thickness of the metal and the total thickness of laminate as shown in the equation below:

$$MVF = \frac{\sum_1^n t_{metal}}{t_{lam}} \qquad (1)$$

In equation 1, t_{metal} = thickness of each aluminium layer, n is the number of aluminium layers, and t_{lam} is the thickness of the total laminate.

Precisely, MVF value describes the contribution of the metal layer in FML, and it varies between 0 and 1: MVF 1 means monolithic aluminium, while MVF 0 indicates contribution only of fibre layer [75]. In a characterization study of FMLs, WU *et al.* [76] used MVF approach to predict the tensile and flexural properties of fibre metal laminates. The predicted results showed a good increment with the experimental results.

A. Thermosetting Fibre Metal Laminates

The thermosetting fibre metal laminates are the first set of FMLs and are used widely in different commercial applications. Torshizi *et al.* [77] studied the effect of fibre orientation of FML on tensile properties of Uni-Directional UD Glass / Kevlar reinforced Aluminium epoxy hybrid FML. He used different combinations of Glass / Kevlar at ± 45 and 0 / 90 orientation, The results showed that the 0° plies added the modulus of elasticity, yield stress and ultimate tensile strength considerably (Figure 1.17).

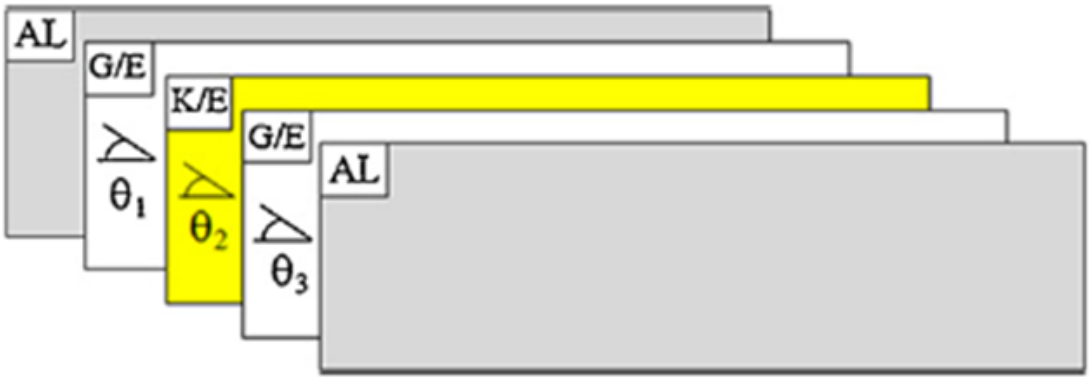

Figure 1.17. Schematic view of Kevlar / Glass hybrid fibre metal laminate

FML is more stable structure than the simple composites. Nam *et al.* [78] studied the effect of stacking sequence on mechanical properties of FMLs and compared it with simple composite under different loading conditions. They used two stacking sequence of FMLs with different plies angles of fibres. FMLs showed excellent performance than composites in point and uniform loading conditions and for unexpected loading. Asghar *et al.* [79] investigated the fatigue crack growth rate experimentally and analytically for ARALL, CARAL and GLARE. They prepared samples using VARTM. CARAL showed the highest ultimate tensile strength and Fatigue crack growth toughness than ARALL and GLARE. The moisture management properties of FMLs will also be better than its constituents. Bothelo *et al.* [80] studied the Hygrothermal effect on damping behaviour of FML, Al and Glass Fibre Reinforced Epoxy GFRE. Viscoelastic properties were analysed during hygrothermal conditioning, and it was established that GLARE FML offer maximum resistance to deterioration by moisture.

B. Thermoplastic Fibre Metal Laminates TFML

In all three basic FMLs (ARALL, CARAL and GLARE) epoxy is used as a resin, which is thermoset in nature. Recently a lot of research has been conducted to study the TFML. Conventional FMLs have the number of issues associated with them, *e.g.* Longer production

cycle and modest interlaminar fracture toughness [81]. TFML has offered improved energy absorption capabilities along with short production cycle, the part can directly be made, and unlike thermoset don't need autoclave [82]. The TFMLs are made through compression moulding technique as discussed in section **1.3.4**. Polypropylene and Self-reinforced SRPP TFMLs are the most common type of TFMLs reported in the literature [81].

Reyes and Kang [28] investigated the static tensile and fatigue properties of PP based TFML and its constituents. One TFML was made with SFRP, and another was made with glass fibre and PP prepreg. The TFML made with SRPP showed ductile behaviour while TFML with glass fibre prepreg showed brittle failure. Cache *et al.* [66] investigated the tensile properties of PP-aramid based FMLs and its constituents. The FML showed a more ductile fracture than its components. The PP based FML also showed more strain to failure, which is very important for engineering applications [66]. Figure 1.18 shows the comparison of TFML and its constituents.

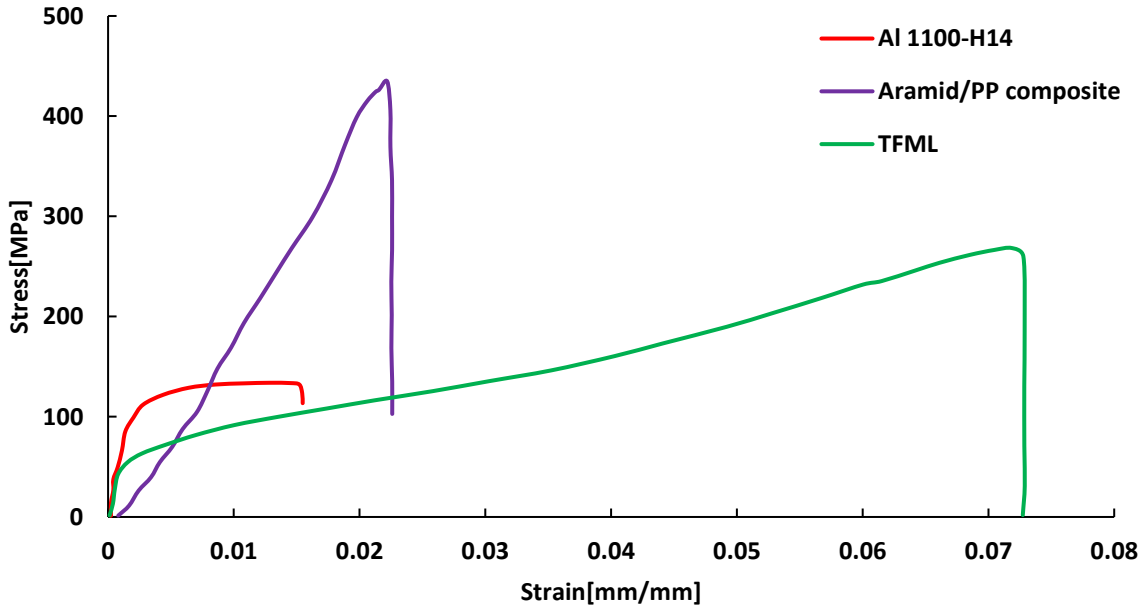

Figure 1.18. Comparison of stress-strain curves for the tensile tests of aluminium, composite material and FML [66]

Carillo and Cantwell *et al.* [82] investigated the flexural and tensile properties of FMLs based on SRPP. They used two orientations of PP plies 0º / 90º and ± 45º. Flexural properties showed that the plies orientation has no effect on determining the final properties. The tensile failure strain of ± 45º plies FMLs was higher than 0º / 90º. The tensile properties of FMLs were in between the constituents, as shown in Figure 1.19.

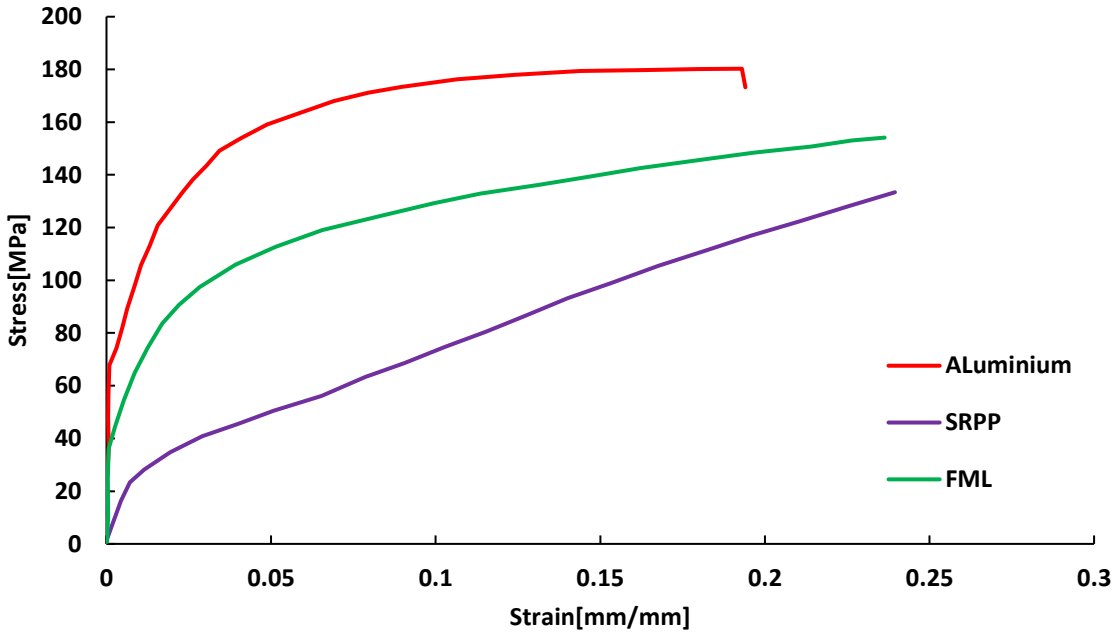

Figure 1.19. Comparison of stress-strain traces following tensile tests on the plain aluminium, the SRPP composite and the FML specimen

The surface treatment of aluminium greatly enhances the mechanical properties of FML. In one such study Cache *et al.* [83] investigated the effect of surface treatment on mechanical properties of PP based TFML. They used three types of surface treatments, including degreasing, sanding, and chemical treatment. The surface characterization and mechanical testing suggested superior properties of FMLs made with chemically treated aluminium. Zopp *et al.* [84] developed carbon and polyamide-based thermoplastic FMLs. The composite core of FML was made using a hybrid configuration, in which four CFRP sheets were sandwiched between GFRP sheets. The purpose of GFRP was to avoid galvanic corrosion and enhanced

adhesion. They studied the static and dynamic flexural properties of FMLs and its constituents. The newly developed hybrid FML performed better than conventional polyamide carbon-based FML due to hybrid configuration of glass / carbon fibre. The fatigue properties of glass fibre based TFMLs were better than SRPP based TFMLs on all levels. Beside polypropylene, other types of thermoplastic adhesive can also be used in FML though not used recently. Poly-Ether-Ether-Ketone PEEK, Poly-Ether-Ketone-Ketone PEKK, Poly-Phenylene-Sulfide PPS, Poly-Ether-Sulphone PES, Poly-Ether-Imide PEI, poly (urethane amido imide) and PA6 (Poly-Amide 6) are also thermoplastic adhesive system [23], [85].

C. Natural Fibre-reinforced Metal Laminates NFML

Raising environmental concern is the reason behind to use recyclable materials in the composite industry. The natural fibres are used to replace the synthetic fibres in FMLs due to their environmental impact. Natural fibres like kenaf, jute, sisal, coir and flax *etc*. are used to make composites, Table 1.9 shows different types of fibres used to make Natural Fibre Composites NFC [86].

Table 1.9. Comparison of properties of natural fibres and synthetic fibres [87],[22]

Fibre	**Density [g/cm^{-3}]**	**Tensile Strength [MPa]**	**Elastic Modulus [GPa]**	**Elongation [%]**	**Specific Tensile Strength [MPa/g/cm^{-3}]**	**Specific Elastic Modulus [GPa/g/cm^{-3}]**
Cotton	1.5-1.6	287-800	5.5-12.6	7.0-8.0	190-530	3.7-8.4
Jute	1.3-1.5	393-800	10.5-55	1.5-1.8	300-610	7.1-39
Flax	1.5	345-1830	27-80	2.7-3.2	230-1220	18-53
Hemp	1.5	550-1110	58-70	2-4	370-740	39-47
Kenaf	1.45	930	53	1.6		
Ramie	1.5	400-938	44-128	3.6-3.8	270-620	29-85
Sisal	1.3-1.5	507-855	9.4-28	2.0-2.5	362-610	6.7-20

Coir	1.2	131-220	4.0-6.0	30	110-180	3.3-5
E-Glass	2.5	2000-3000	70	0.5	800-1400	29
S-Glass	2.5	4570	86	2.8	1800	34.4
Aramid	1.4	3000-3150	63-67	3.3-3.7	2100-2300	45-48
Carbon	1.4	4000	230-240	1.4-1.8	3000	165-172

The advantages of using NFC over polymer composites are their low cost, low density, comparable specific tensile properties, reduced energy consumption, less health risk, renewability, recyclability and biodegradability [87]. NFCs have broad applications in automobiles, aerospace, sports, electronics, and construction industry. Market size growth of NFCs is roughly at a pace of 10 % since 2010 [22].

Natural fibre-based composites can be used to make FMLs. The properties of FMLs can be tailored as per the requirements. Two types of natural fibre metal laminates are reported in the literature: Pure natural fibre based FMLs (only one type of natural fibre) and hybrid natural fibre metal laminates (synthetic-natural, natural-natural). Both thermoset and thermoplastic resin are used to make NFML [88]. Pure natural fibre based FMLs are the point of interest for researchers due to the need to develop FMLs with 100 % natural reinforcement. Li *et al.* [89] studied the mechanical properties of bamboo / Aluminium and reformed bamboo / Aluminium-based NFML and found that reformed bamboo / Aluminium exhibit better mechanical properties. Sui *et al.* [90] extended the work of Li *et al.* [89], they made cross-ply and unidirectional bamboo / Aluminium NFML as shown in Figure 1.20.

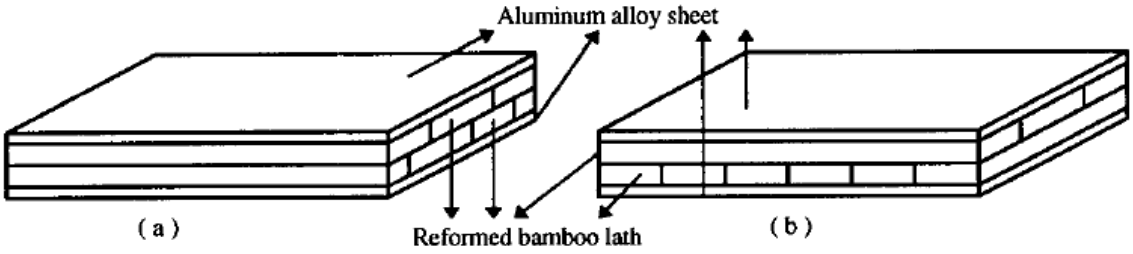

Figure 1.20. Schematic view of bamboo / Aluminium NFML (a) unidirectional (b) Cross-ply bamboo lathes

Tensile, compressive, and bending test was performed to check the failure mechanism, particularly delamination at layer interface. The significant delamination between aluminium and composite cause the failure of FML. Comparison of small and large size parts shown that the large parts have compromised properties due to more defects in the larger parts [90].

Malingam *et al*. [91] studied the fatigue life of Oil Palm Empty Fruit Bunch OPEFB based FML. They used different weight percentages of OPEFB to determine the best combination (10, 20, 30 and 40 %). 30 % OPEFB showed highest fatigue life properties than others, and the FML made with OPEFB was 30 % lighter than monolithic Aluminium which also advantages. Vieira *et al.* [11] used sisal woven fabric to make NFML. They named it Sisal fibre Reinforced Aluminium Laminates SiRALs and prepared using the cold pressing technique. SFRC and SiRALs were compared, and significant improvement of properties was found in SiRALs as compared to SFRC.

The hybridization of natural fibres with natural fibres is also a point of interest for many researchers due to different sources of natural fibres and hence different properties. Zareei *et al.* [17] developed the hybrid NFML in which basalt and jute were sandwiched alternatively. They studied the tensile and ILSS properties of FMLs. The results showed that the FMLs in which jute fibre was sandwiched with basalt fibre showed the highest tensile properties. In contrast, the FML in which the basalt fibre was sandwiched between jute fibres showed high

energy absorption. The reason for higher tensile properties of FML in which basalt used outside was its excellent adhesion with aluminium sheet.

The properties of hybrid NFML were studied extensively by different researchers. The reason for hybridizing natural fibres with synthetic fibre is to minimize the drawbacks associated with the natural fibres, as the natural fibre has high moisture uptake with low mechanical properties. Thirumurugan *et al.* [92] used a novel method to make NFML, they used aluminium as reinforcement in Glass Fibre Reinforced Plastic GFRP both as foils and wire meshes, along with banana fibre-strands to modify standard GLARE. Both GFRP and Glass-Aluminium-Banana-Glass hybrid composite GABGRP were fabricated through the hand-lay-up process. Surprisingly wire mesh type GABGRP show ductility along with high impact and tensile properties. Kenaf fibre is also used in natural fibre composite and has very good mechanical properties. Notching affects the properties of FMLs, a very little work reports on the effect of notching on the mechanical performance of FMLs. Feng *et al.* [8] studied the effect of fibre orientation and notch on the mechanical properties of Al / Kenaf / Glass hybrid FML. FML was made using four different configuration and two angles of plies (0° / 90° and ± 45°) as shown in Figure 1.21.

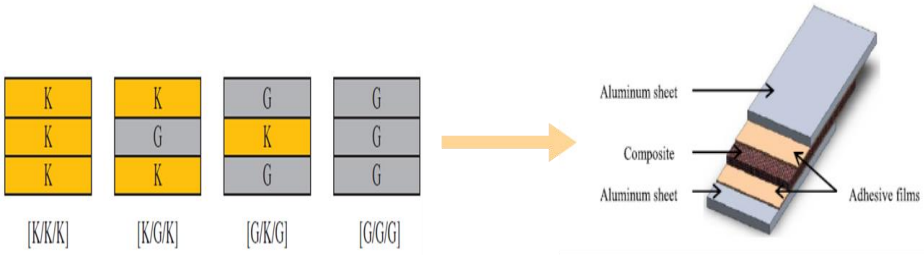

Figure 1.21. Kenaf / Glass hybrid fibre metal laminate ply configuration

Feng *et al.* [93] extended the previous study to determine the effect of fibre orientation and stress ratio on the fatigue performance of thermoplastic hybrid composite reinforced metal laminate with different fibre lay-up. The results showed the poor properties with the reduction

of amount of glass fibre content. The sandwiching kenaf with glass showed better response than sandwiching glass with kenaf fibres.

Subramaniam *et al.* [94] made hybrid thermoplastic fibre metal laminates of Glass / Kenaf with different configuration and studied the tensile and quasi-static penetration using indenter of two different sizes. They found interesting results as the FMLs in which kenaf was sandwiched between glass layers showed improved tensile properties as compared to FMLs in which only glass fibres were used as shown in Figure 1.22.

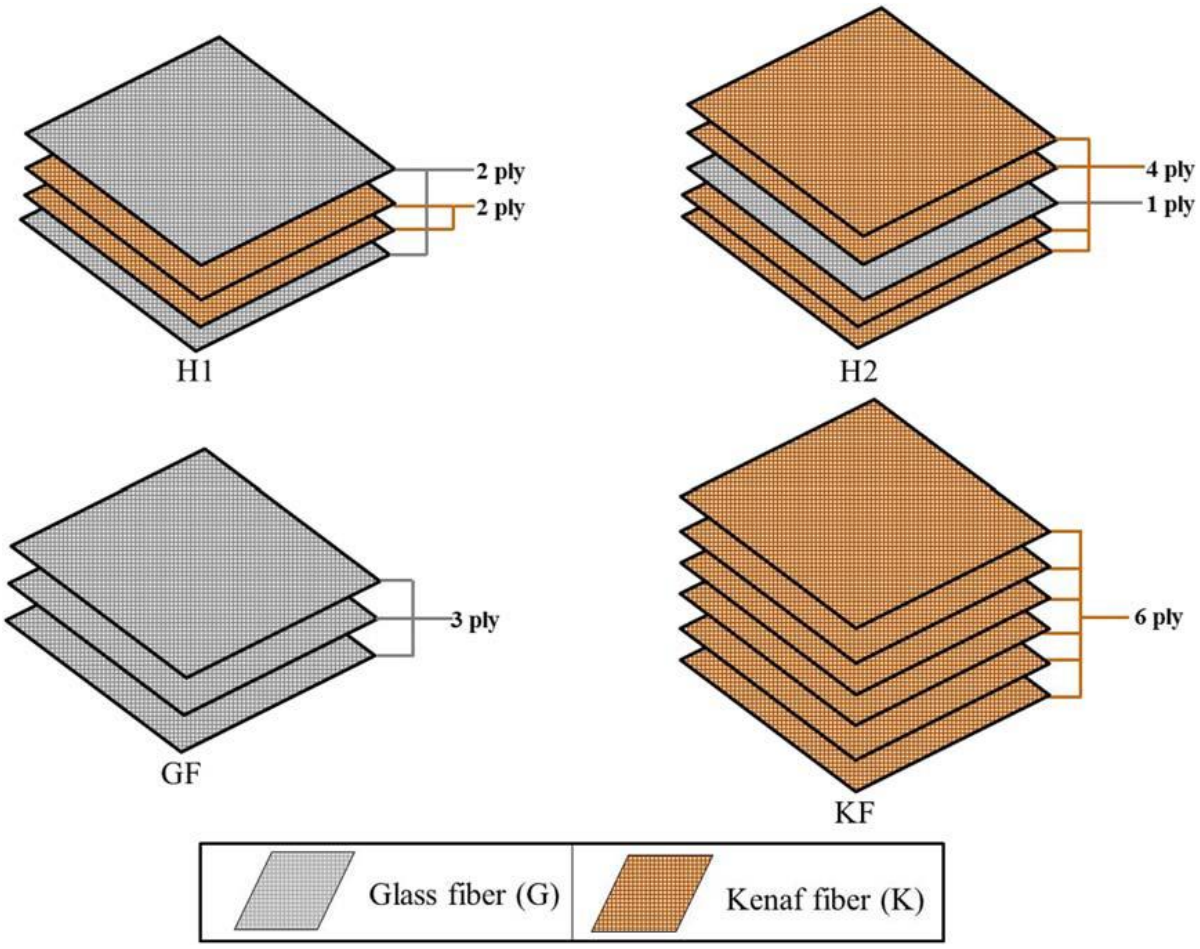

Figure 1.22 Stacking sequence of plies used for glass / kenaf hybrid FMLs [94]

Sivakumar *et al.* [95] investigated the impact and tensile properties of Kenaf / Glass epoxy hybrid fibre metal laminates made with the different configuration of plies placed at different

angles. The incorporation of glass fabric layer in replacement of kenaf fabric significantly improved the mechanical properties of hybrid FML as compared to pure kenaf FML. Mohammed *et al.* [96] made hybrid FML using two different combinations of fibres kenaf / carbon and flax / carbon. Out of these two-former shown better flexural properties, while the latter showed good tensile and impact properties. Sandwiching synthetic with natural fibre or natural fibre has different effect on the properties. Muthukumar *et al.* [97] made hybrid FML with carbon and Flax fibre using two different configurations of fibre layer: Carbon Flax Carbon CFC and Flax Carbon Flax FCF, the CFC configuration showed better tensile and flexural properties as compared to FCF configuration. El-Baky *et al.*[18] developed the glass / jute hybrid FMLs to check the effect of hybridization on the mechanical properties. The results showed that the increased content of glass fibre enhanced the tensile properties, on the other hand, poor flexural properties. The flexural properties were higher for the FMLs in which glass fibre was used in the skin while jute was used inside. As the glass fibre provides better adhesion with aluminium. Kali *et al* [98] studied the vibration damping characteristics of glass / bamboo and carbon / bamboo hybrid FMLs. They used three different configurations to compare the effect of bamboo fibres on vibration damping. Al/GF/B/GF/Al, Al/CF/B/CF/Al and Al/CF/Al/CF/Al configurations were tested. The Al/GF/B/GF/Al configuration showed better damping characteristics with higher flexibility and lightweight-ness. The flax fibre is also a candidate for a lot of applications due to its high strength and stability. Chandrasekar *et al.* [99] investigated the effect of stacking sequence and hybridization of CARAL with flax and sugar palm fibre. They sandwiched flax and sugar palm fibre between carbon-fibre plies. The results showed the excellent mechanical properties of flax / carbon hybrid FML. The failure analysis showed the bridging phenomenon of flax fibres like synthetic fibres which make it an excellent candidate for aerospace applications. Magnesium is also used by some researchers to make FMLs as a possible replacement of aluminium alloy. Vasumathi *et al.* [100] studied two new

aluminium and magnesium-based hybrid FMLs reinforced with carbon and jute fibres named CArbon-Jute Reinforced ALuminium Laminate CAJRALL and CArbon-Jute Reinforced MAgnesium Laminate CAJRMAL. The authors concluded that the addition of jute fibre in CARAL has a greater effect on tensile and flexural properties, and in case of impact properties magnesium has more effect rather than aluminium.

1.4.3 Dynamic Properties of Fibre Metal Laminates

The impact properties of FMLs include high, low and blast impact properties, but the low-velocity impact properties are the most discussed properties of FMLs. As the high-velocity impact and blast impact event cause detectable and significant damage, while low-velocity impact event can cause invisible damage which can lead to some catastrophic failure at some later stage. The low velocity impact event also occur on the day to day basis, so the low-velocity impact properties of FMLs will discussed in detail here [101]–[103].

Normally impact event for composite materials is different from fibre metal laminates. In composite materials the impact damage happens with incomplete penetration, delamination, matrix cracking and fibre failure. Normally there is no sign of plastic deformation [104]. While in the FMLs there are other parameters as well which contribute to the impact performance of FMLs including metal composite bonding and plastic deformation of the metal part. The main reason behind the excellent impact properties of FMLs are that they combine the properties of its constituents' materials, the composites offer better fatigue properties and metal has good plasticity with durability. The crack propagation is also hindered in the FMLs as compared to its constituents thanks to fibre bridging effect [105]. The aluminium alloy add certain features in FMLs after addition with composites. Which are as follow [106]:

- Yielding of the materials at high loads.
- Stable extension before fracture.

- Providing better residual strength.
- Good fatigue performance.
- Excellent blunt notch strength, short crack performance.

The failure phenomenon in FMLs is shown in Figure 1.23.

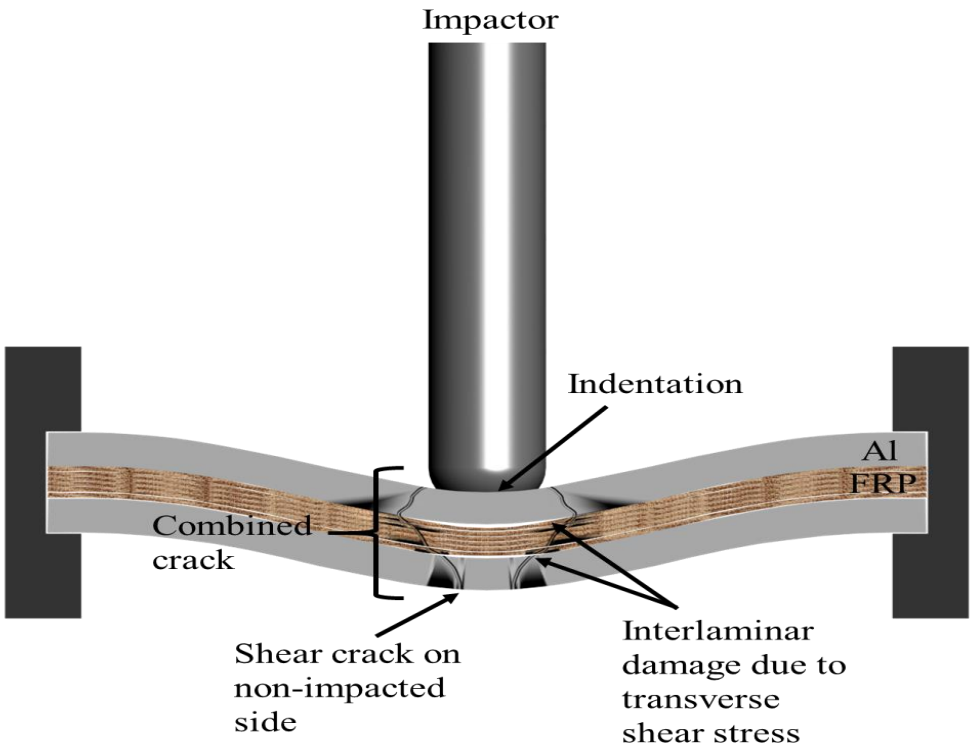

Figure 1.23. Possible failure modes in clamped FML plate during a low-velocity impact event [106]

In the fibre metal laminates the main concern during Low-Velocity Impact LVI is delamination. The delamination within the composites is different materials of plies and plies orientation. The delamination between metal and composite layer is also area of concern as the delamination pave way to crack propagation. Normally the bonding between composite layer and metal is stronger than within the laminates of composites so first the failure starts from composite plies and then propagate. At higher energy level there is denting beyond a limit which cause crack in outer aluminium layer called First Crack FC. Then the crack can also penetrate across the sample that is referred as Through the Thickness crack TTT. Comparing

two different types of grades of aluminium, the grade having higher yield strength will be more tolerant to impact response. The delamination and permanent deformation (Plastic work on metal) are two very important parameters to understand the behaviour of FMLs during the LVI. Usually for different types of metal systems the deformation is different. If the permanent dent and delamination area are compared, the delamination area is usually higher than dented area, as the delamination is normally spread to surrounding areas of dented part of metals, that shows the amount of work done for delamination [107]. When we talk about different types of FMLs made with different type of resin, reinforcement, and metal. A resin system or reinforcement capable of dissipating more energy will be suitable candidate for impact application. The damage is more visible in FMLs during LVI due to plasticity of metals as there is usually a dent. While in the composites there is no dent in composites even though they suffer sufficient internal damages. The visible dent in FMLs shows the occurrence of the impact event [108]. In the FMLs the overall deformation has two parts, one due to plastic work and other due to deformation in structure. The denting in the metal sheet is due to plastic deformation. The structural deformation between the layers cause the lowering of bending stiffness which results in more fragile behaviour of structure towards impact incident [109]. The metal, composite and FMLs behave differently against LVI [Figure 1.24].

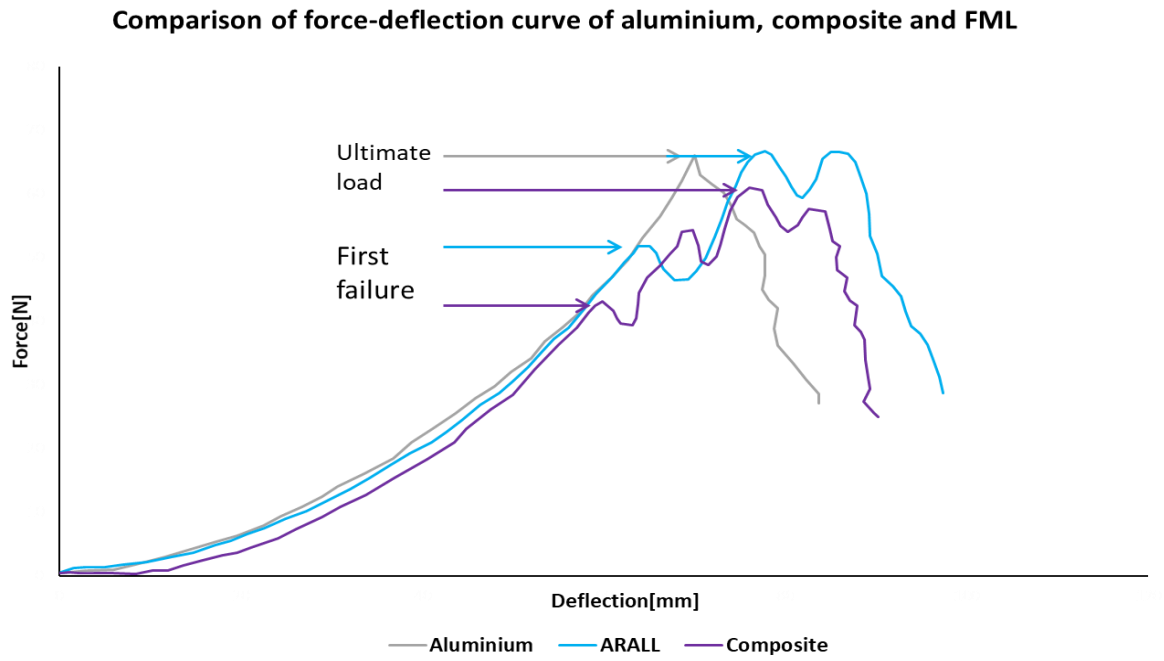

Figure 1.24. Typical load-deflection curves comparison of aluminium, composite and FML [24]

The aluminium shows a steady increase in the force with deflection and then fails at ultimate load. The composites show two peaks one at first failure and second at ultimate load. The first peak relates to the matrix crack and second peak at ultimate load relate to ply failure. In the FMLs the failure is either metal dominant or fibre dominant. If the metal dominant than the first failure will be at ultimate load like monolithic aluminium, while for fibre dominant failure behaviour the curve will look like composite failure curve. The failure in the FML start with cracking and delamination with subsequent crack propagation. In the fibre dominant failure a crack is observed on Non-Impacted Side NIS of metal. While in case of metal dominant failure the crack in the metal layer will run in the rolling direction regardless of fibre direction in the composite. Further if the fibre are also placed in the rolling direction of metal than the crack in metal and composite will run in the same direction while they remain intact [24]. The first failure point in the FMLs relates to damage initiation force, at that point mainly the drop in the peak is observed due to sufficient deep indentor penetration, matrix cracking or significant delamination. The delamination is usually result of matrix cracking [110]. The ultimate load or

F*max* point shows the maximum resistance of a material towards the impact, as after reaching F*max* the rest of impact energy is absorbed in crack opening or perforation. The perforation is very critical point to understand the low velocity impact events, the perforation is mainly due to stress relaxation of fibres as there can be massive pileup of stresses in the fibres after reaching F*max* and the fibre fracture to release excessive stresses [50], [111].

The impact response of composite is different from the FMLs due to the properties of constituents and nature of laminates. During the course of LVI impact, the composite structure behaves differently. There are three possibilities that a structure will behave towards the impact. One is that the impactor strikes the structure and then due to undissipated elastic energy there is rebound, as the structure will transmit that undissipated elastic energy back to the impactor. Second case is that the impactor strikes the structure and there is no rebound rather there is some crack in the composite but no perforation. Then the impactor stops and no elastic energy for rebound. In the third case there is complete perforation as the impactor will perforate the structure, as all the energy will be utilized in the perforation. The force deflection curves for all three cases will be different as shown in Figure 1.25 [112].

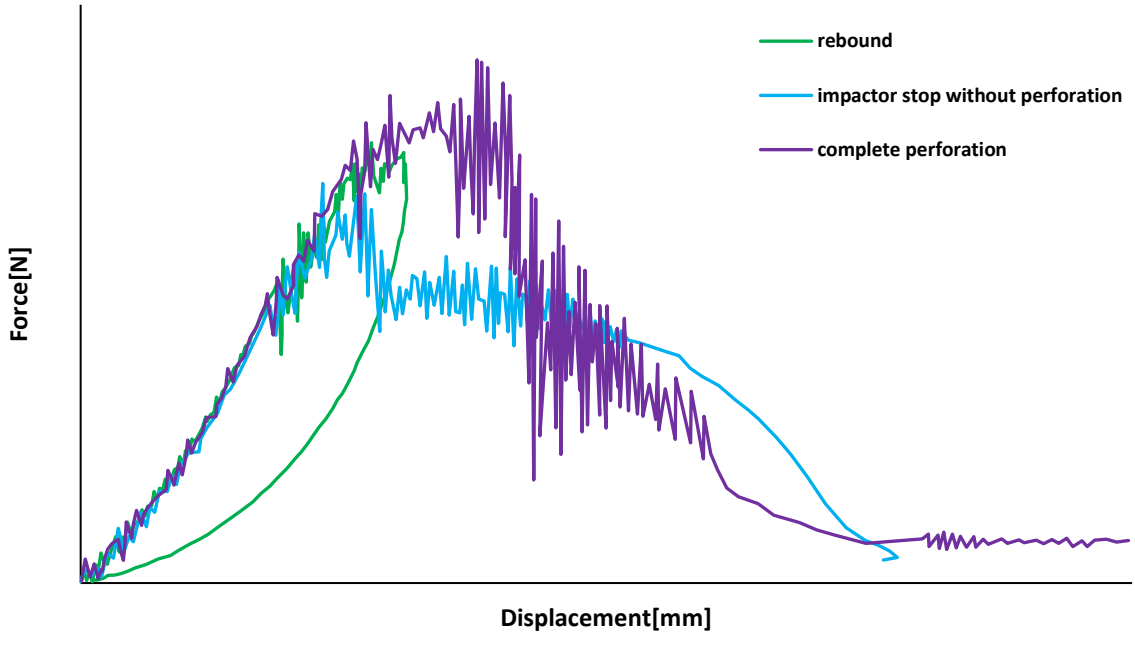

Figure 1.25. Typical force-displacement curves of impact test of composite structure [112]

During LVI test the impactor can penetrate or rebound after hitting the FML specimen. In case of rebound, the absorbed energy is difference of impact energy and rebound energy; whereas for the perforation event, the absorb energy is almost equal to impact energy [104]. During the impact event of an FML, the energy is absorbed for the plastic deformation of metal, metal-composite delamination, matrix cracking, fibre fracture, fibres debonding and plies delamination. The more will be absorbed energy the more will be the damage as the energy indicates the area under the force-displacement curve [

Figure 1.26] [109].

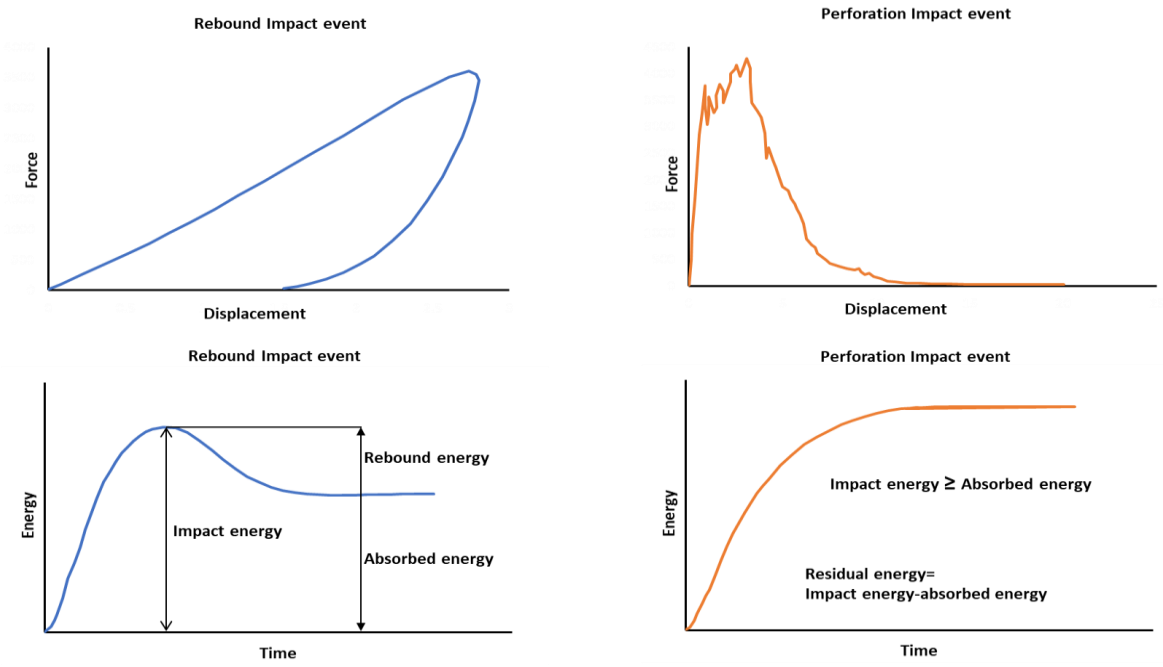

Figure 1.26. The typical force-displacement and energy-time curves of a drop-weight impact test when the impactor rebounds or perforates through the FML impacted panel [104]

Different FMLs behave differently towards impact event at different energy level. The GLARE absorb energy through plastic deformation, delamination, and propagation, while CARAL

absorb energy through penetration and perforation. This is due to the nature of reinforcement [110].

The surface treatment of metal also effects the properties of FMLs during LVI. Li *et al.* [113] used titanium to make FML; they employed three different surface treatments annealing, sandblasting and anodizing. Hand layup technique was used to manufacture FML. He studied the low-velocity impact properties of three different kinds of FMLs, as shown in the Figure 1.27.

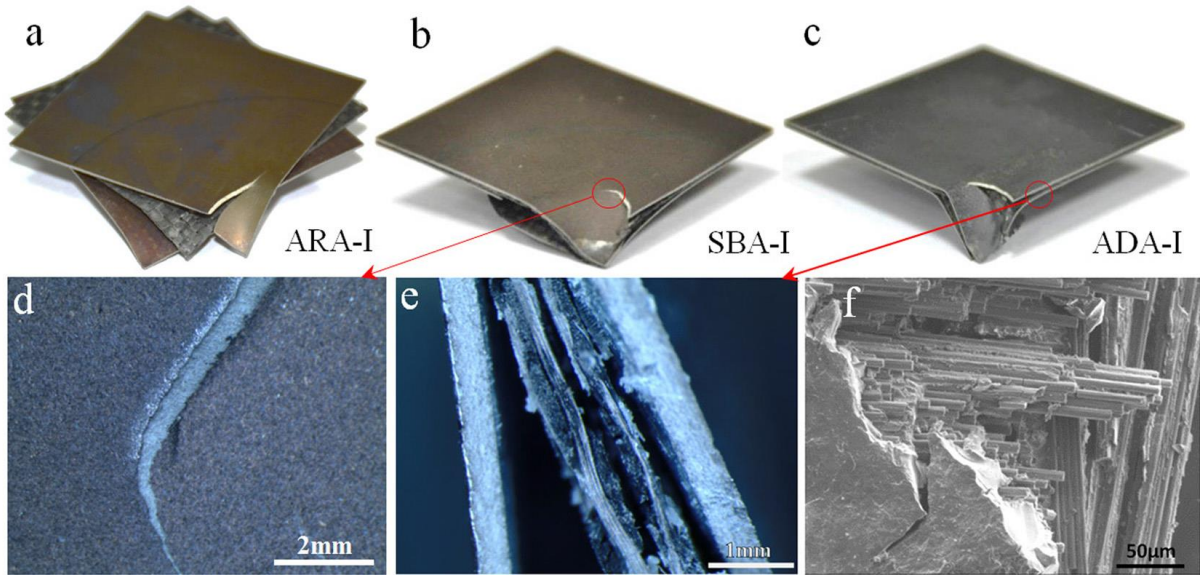

Figure 1.27. Failure mechanisms of FML panels, (a) reference, (b) sandblasting, (c) anodized, (d) crack of titanium sheet, (e) debonding and delamination and (f) micro failure [113]

The results showed that the anodizing significantly improved the LVI of FMLs. As the impact velocity was increased the effect of anodizing became prominent. The structural integrity increased, while caused low resistance to damage and low energy absorption.

A. Modes of Failure in Low-Velocity Impact Damage

As the FMLs are made with a combination of metal and composites, so the damage in the FML has a portion of both, perhaps depends upon each other qualities and proportion. Mode of

failure can be one of the following or combination of these depending upon the properties of constituents (Figure 1.28) [54]:

I. Fibre breakage
II. Matrix cracking
III. Delamination of the composite layer
IV. Plastic deformation
V. Buckling in the metal layer
VI. Debonding between different layers

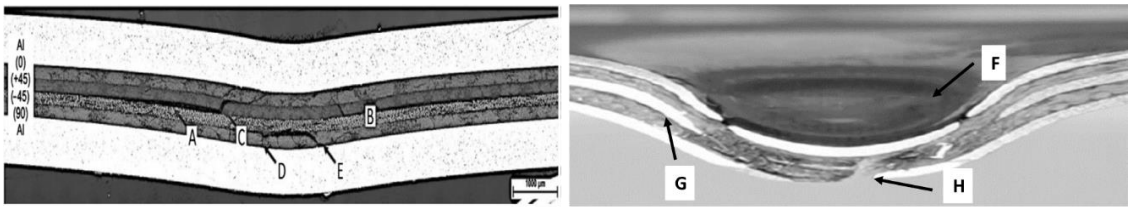

Figure 1.28. Cross-section of FMLs subjected to LVI showing different damage phenomenon (A— delamination, B—ply separations, C, E—transverse cracks, D—flexural cracks, G-metal-composite delamination, H-metal crack, F-plastic deformation) [111], [114]

Under the impact loading, the FMLs experience the debonding due to matrix crack. Then the delamination progress to the successive plies and between metal-composite. This delamination is a source of dissipation of energy; the more will be delamination the less will be perforation [115]. The FMLs use a different mechanism to dissipate the energy after impact, including post stretching, delamination and fibre bridging. The energy needs to be dissipated to avoid its concentration and sudden failure after crack initiation [116].

Another factor which has a very significant influence on the impact performance of FMLs is fibre bridging / crack arresting. This phenomenon is also very crucial in the understanding of the performance of FMLs during cracking and fatigue life. When the metal layer starts to crack due to excessive loads, the adjacent fibre layers provide a path to dissipate the excess energy to the composite layer. This helps in the superior fatigue life of fibre metal laminates as

compared to monolithic aluminium or composites [117], [118]. The adhesive layer between metal-composite and different plies of composites prevent the spreading of crack to a larger area and also catastrophic fibre failure. The adhesive layer has a very important role in the crack / fibre bridging phenomenon of FMLs [119]. Figure 1.29 shows the crack bridging phenomenon of FML.

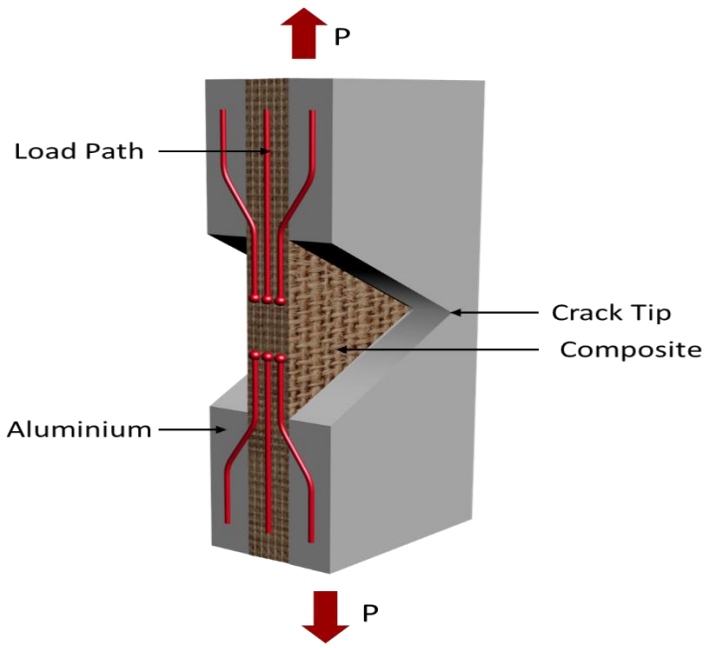

Figure 1.29. The crack-bridging phenomenon in the FMLs [34]

The matrix damage and delamination in FMLs during impact event start side by side. The delamination between the composite layer and metal layer is caused by plastic deformation of the aluminium layer and high shear stresses. Matrix crack is a result of incompatibility of the properties of fibre and matrix. The resin which are brittle show low resistance to crack propagation and delamination e.g. epoxy [120]–[123].

There are two kinds of matrix crack present in the composite structure: Flexural and shear cracks (Figure 1.28). These cracks propagate due to the large number of shear forces and impactor-laminate contact during the LVI. There are three main reasons for excessive delamination in FMLs due to nature of materials which are as follow.

The high brittleness and low strength of a matrix which makes it less resistive towards crack initiation and propagation. The bending stiffness mis-adjustments between different plies of composite and low interfacial adhesion strength between metal-composite is another reason of excessive delamination. The reason for high mis-adjustment of bending stiffness of different composites plies is a large difference of ratio of longitudinal and transversal modulus of the plies [124]–[126]. The quality of interfacial bonding between metal and composite also influence the delamination between metal composites heavily. The damaged area of FMLs with the poor metal-composite bond will be larger than the FMLs having good bonding between metal and composite. The delamination is largely observed at low impact energy than at higher impact energy, as at the lower impact energy the delamination is associated with plastic deformation of the metal. At the higher impact energy, there are other damage phenomenon which contributes, *e.g*. fibre failure, penetration and perforation *etc*. [111].

The fibre and metal damage are also very vital phenomenon when the damage due to LVI is discussed. The FMLs in which composite part is made of high modulus fibre experience high fibre cracking and perforation. While the FMLs with low modulus composite reinforcement experience high delamination [110]. The fibre cracking or perforation is experienced at high impact energy, as discussed earlier. The reason for fibre damage at high impact energy is that at high incident impact energy the value of force is high enough to delaminate the relatively stiff composites. This energy is still high enough that after delamination, it causes the even further destruction by fibre perforation. The fibre cracking in the composite starts due to compressive stresses which are generated due to microfiber buckling. These microcracking make ways to meso and macro fibre cracks in the composites. These microcracking points create the pressure points on the surface of the lower aluminium plate, which cause the cracking of metal [111], [127].

The metal cracking is the indication of the end of resistance of a FMLs towards the LVI and the start of perforation. In the literature, the most emphasis is rather on the other factors like matrix cracking, delamination and fibre cracking etc., the least focus is on the demographics of metal cracking. The cracking in the aluminium mostly start in the rolling direction, but for the high modulus and brittle material like carbon, the cracking in the metal layer mostly depends upon the orientation of adjacent ply to metal layer. In the FMLs the crack appears normally in the layer opposite to impacted side due to already discussed reasons [128]–[130].

B. Effect of Different Parameters on the Impact Properties of FMLs

Impact properties of fibre metal laminates are better than both composites and monolithic metal. As the impact involves the transversal non-linear dynamic load, as there is no through the thickness reinforcement, so the impact damage resistance is poor for composites. There is low strength between plies, interlamination stresses (shear and tension) cause delamination with matrix crack and fibre damage [106]. The configuration of plies in the composite is very important at high impact energy. Normally at lower impact energy, a major part of the energy is used in the plastic deformation of metal part and delamination. At the higher impact energy when the composite part is exposed, then the orientation of plies become more crucial in the LVI. The quasi-isotropic (0/45/-45/90) arrangement of fibre offers better impact resistance than the cross-ply (0/90/90/0) and unidirectional $(0)_4$ arrangement of the plies. The cross-ply arrangement offers better impact properties than UD arrangement but poorer than quasi-isotropic arrangement [104], [131]. The quasi-isotropic laminates have even distribution of energy of the incident impact, so their energy dissipation is better than UD and cross-ply configuration. Further, when the plies are placed at a certain angle, then there is also the effect of buckling, which creates more resistance towards the penetration.

The impact properties of ductile and stiffer 2024-T3 alloy are better than 7475-T76 stronger alloy. The 2024-T3 offer more ductility towards damage [104]. Sharma *et al.* [109] investigated

the effect of through the thickness metal layer distribution with the different thicknesses. He concluded that with the placement of multiple metal layers the maximum force reduces, and deformation increases. The thinner sheet cause early cracking with larger crack size. The metal layer thickness and distribution also effected the degree of damage as for thicker sheet on the face and simple configuration causes lower degree of damage while with thinner sheet on the face and more sheet in the thickness cause the more damage. The effect of bending stiffness was also investigated and it was found that the composites layer with higher bending stiffness caused the premature failure of FML at higher energy level [109]. Out of two grades mainly used in the FMLs fabrication the 2xxx series is preferred due to its damage tolerance characteristics. Different grades of 2xxx are used for FMLs fabrication including 2524, 2195 and 2097 [111]. Magnesium and titanium FMLs are also fabricated but they yet have to find space in the commercial applications [132]–[135]. The titanium / carbon FMLs have shown very impressive performance for high temperature applications up to 300 °C [136]. The metal-composite bonding of titanium is big issue for its application point of view, further the low velocity impact response of titanium based FMLs can also be poor due to its low ductility [137]. The titanium although have high fatigue performance and good static strength but for impact applications it is not suitable due to its lower ductility [137], [138]. The GFRP core expose and experience an inter-laminar delamination because of crack initiation in the titanium layer, the titanium layer is responsible for failure in case of LVI [128], [139]. The magnesium based FMLs though have proven better anti-corrosion properties, low density and high electromagnetic shielding yet have some shortcomings against low velocity impact like energy restitution coefficient, permanent deformation and maximum impact force [116], [140].

The failure during low-velocity impact can be of two types, either fibre dominant or aluminium dominant. ARALL and CARAL due to low strain to failure (2 %) always shows fibre dominant failure while GLARE due to high strain to failure (5 %) sometimes show fibre dominant or

aluminium dominant failure behaviour [24]. The GLARE due to high strain ratio of reinforcing fibres and extensive delamination shows the lower final central deflection, while the CARAL contrarily shows the catastrophic perforation due to excessive bending stresses in the composite layer [108], [141]. When compared the reinforcement materials of currently commercially available grades of FMLs, the glass and aramids show less fibre cracking as compared to carbon fibre. To understand the behaviour of material towards impact, the stress-strain characteristics is very important tool. Which give insight of material response towards LVI [111].

Different types of materials of reinforcement has different effect on the impact response, for the commonly used FMLs normally the synthetic material is used for fabrication, most recently the hybrid reinforcement is also used for the FMLs fabrication along with the traditional reinforcements. Ferrante *et al*. [105] studied the LVI response of basalt fibre reinforced FMLs. They used 2D woven basalt prepreg of 220 g/m² with 2024-T3 aluminium of 0.6mm 3/2 configuration to develop FMLs. They used two types of impactors with hemispherical and ogival shape. They compared the results of basalt FMLs with a monolithic aluminium sheet of comparable thickness. They concluded that the specific impact energy of basalt reinforced FMLs was higher than the monolithic aluminium irrespective of shape of indenter. When compared the dent depth, the FMLs got more profound denting than the aluminium. The ogival shape impactor made deeper dent than the hemispherical shape impactor. The optical assessment indicated that the main reason of damage in basalt FMLs was due to delamination between aluminium and composites layer. The poor delamination properties were because of poor interface between aluminium and composites despite of electrochemical treatment of aluminium [108].

The stacking sequence of reinforcement plies also effect the impact performance of FMLs. Yaghoubi *et al.* [131] conducted an experimental study to check the effect of different stacking sequence configurations on LVI of GLARE 5 (3/2). They used four different kinds of stacking

sequence. Unidirectional, cross-ply, angle-ply and quasi-isotopic. Four different energy level were used to initially access the energy level which gives the complete profile with some penetration and perforation. As the energy level is increased the pattern of damage also changes. At low energy level the predominant failure mechanism is delamination between composite and metal layer, at subsequent higher energy levels the delamination accompanies with the perforation and fracture. They also made observation that with the C-scan only the profile of damage zone can be detected. To reveal the type of damaged, the cross-section view of impacted samples after cutting from center of sample should be done. The unidirectional GLARE exhibited poorest impact properties while the quasi-isotropic showed the best impact properties, with least deflection and higher energy release for quasi-isotropic configuration [131]. The crack shape of unidirectional and woven reinforced fibre metal laminates also different from each other. The square hole is obtained with the woven reinforced FMLs and a straight crack running in the fibre direction is obtained with unidirectional fibre metal laminate [142].

C. Impact properties of Thermoplastic Fibre Metal Laminates TFML

The commercially available FMLs are made with thermoset matrix which is epoxy. These thermoset matrices have higher stiffness, strength, and temperature performance, but there are certain drawbacks of thermoset resin systems, *e.g.* long processing cycle, brittleness, high processing cost and recyclability. The thermoset resin based FMLs also have the same kind of problems. So by replacing a thermoset resin system with the thermoplastic resin systems these problems can be coped with less environmental concerns. Thermoplastic resin systems can be used with relative ease as their fabrication is one-step process. By using thermoplastic resin system, both time and costs can be saved associated with the manufacturing process. The repairing of damaged thermoplastic fibre metal laminates is easier than thermoset counterpart as with the application of heat and pressure can be repaired easily [143]. The TFML also offer

better impact performance than the thermoset resin based FMLs due to improved toughness of the thermoplastic matrices than thermoset counterpart. Thermoplastic resin has also higher energy at first and ultimate failure [5]. High energy absorption at high velocity impact of thermoplastic based FMLs may be the result of the fact that at high velocity impacts, the bond between the interlayer and thermoplastic composite and aluminium layers is weak. There is a considerable buckling of debonded aluminium layer along the interface which may release some amount of tensile residual stress inside of aluminium layer induced during high temperature curing, allowing it to absorb more energy; a phenomenon which was not observed in the low energy impact. The thermoplastic based FML shows better energy absorption at high velocity impact and lower at low velocity. This behaviour is hinderance to replace thermoset FMLs with thermoplastic FMLs [24].

Thermoplastic composite made using self-reinforced composites are also gaining attention. The Self-Reinforced Poly-Propylene SRPP composites are extensively used by different researchers. The thermoplastic FMLs are also being developed using magnesium. In one such study the LVI performance of Mg-FML and Al-FMLs reinforced with SRPP was compared. The Al based FMLs shown excellent impact properties than Mg based FMLs. Even the specific properties were higher for Al based FMLs than Mg. The Al based FMLs also shown better energy dissipation and higher perforation resistance at different impact energies from low to high impact energies [50]. Abdullah *et al.* [144] studied the effect of different configurations of TFML made by PP reinforcement under low and high impact velocity, they concluded that the 4/3 configuration shows better impact performance compared to 3/2 and 2/1 configuration [144]. The comparison of the impact performance of TFML with the already commercially used FML is also very important to check its commercial viability. Santiago *et al.* [52] compared the relative low velocity impact performance of SRPP FML with GLARE. The TFML shown better relative impactive performance than GLARE under impact loading. Some

variation is also made in TFML with respect to resin and reinforcement. In one such study Tan *et al*. [145] investigated the impact response of TFML made with a polypropylene honeycomb core, the TFML absorb all energy till threshold point after that show global failure. Compston conducted study to check the high velocity impact response of Polypropylene based FML. The specific impact energy of PP based FML is 25% higher than thermoset FML [146]. The processing temperature of thermoplastic resin systems are very crucial as it will produce high internal stresses with loss of ductility, both these parameters effect the impact performance of FMLs. Due to the effect of these change in the aluminium ductility and internal stresses the mode of failure also change from fibre dominant to aluminium dominant [24]. So this is very genuine concern for TFML. Different types of thermoplastic resin systems have been used to develop the FMLs. Vlot [147] conducted a study to check the low velocity impact response of Poly-Ether-Imide PEI based thermoplastic FML. At high curing temperature the Al sheet lose its ductility and high internal stresses were generated which caused cause decrease in properties. The failure was even higher in thermoplastic variant than thermosetting [147].

Different types of thermoplastic matrix has been reported in the literature used to make FMLs including PP, PEEK, PEI and PMR polyimide [32], [83], [148], [149]. The TFML yet to prove its commercial applicability, as far now there is no commercial application of TFML unlike thermoset FMLs.

D. Impact properties of Natural Fibre Metal Laminates NFML

Researchers are doing a lot of studies to replace the synthetic materials with natural materials in high performance applications. But due to compromised mechanical properties of natural materials as compared to synthetic, they are not welcomed. By sandwiching the natural fibre with metal can increase its properties to many folds and can be a viable option to use natural materials in high tech applications. To explore this option number of researchers in recent years

are making NFMLs. These NFMLs are made both with thermoset and thermoplastic matrix systems [150].

Zhang *et al.* [151] developed the bamboo / aluminium laminated FMLs and compared the static indentation and impact properties of these FMLs made with different configurations, further the mode of fracture were also studied using C-scan. Sivakumar [152] investigated the NFML made with kenaf bast fibres. He used three variables to make the samples: 1-Length of fibre, 2- Treated and untreated with NaOH, 3-Different % age of fibre by weight to make FML. FML absorbed the highest energy made with the longest fibre, treated, and have the highest % age of fibre. Natural fibre and thermoplastic resin system can be a commercially viable solution in impact applications. Kuan *et al.* [153] compared the impact properties of basalt, hemp, flax and PP composites and FMLs. The composites and FMLs were made with PP matrix for all type of reinforcement. The SRPP showed the better impact properties compared to other type of composite and FMLs. As the SRPP experience complete plastic deformation as compared to other natural fibre reinforced FMLs. The pure natural fibre based FMLs can be point of interest for many technical applications. Pang *et al*. [154] studied static indentation behaviour of Al / Kenaf epoxy NFML at three different rates of loading to check the effect of the rate of loading. With increasing the rate of loading the maximum force and absorb energy increase for 2/1 configuration. In comparison, for 3/2 configuration, the delamination starts at a lower loading rate, so the maximum force was higher at low loading rate as compared to higher loading rate. Oil palm fibres are found in abundance and it can be a low-cost substitute in a lot of applications. By sandwiching oil palm fibres with metal can enhance its mechanical properties. Savikumar *et al*. [155] investigated the effect of Oil Palm Empty Fruit Bunches OPEFB fibre loading on low-velocity impact behaviour of thermoplastic FML based on OPEFB reinforced polypropylene composite and 6061-O aluminium alloy. The properties of FML and Al layer of

the same thickness shown the significant difference of properties. The FML has superior mechanical properties than monolithic Al. The OPEFB based FML are shown in Figure 1.30.

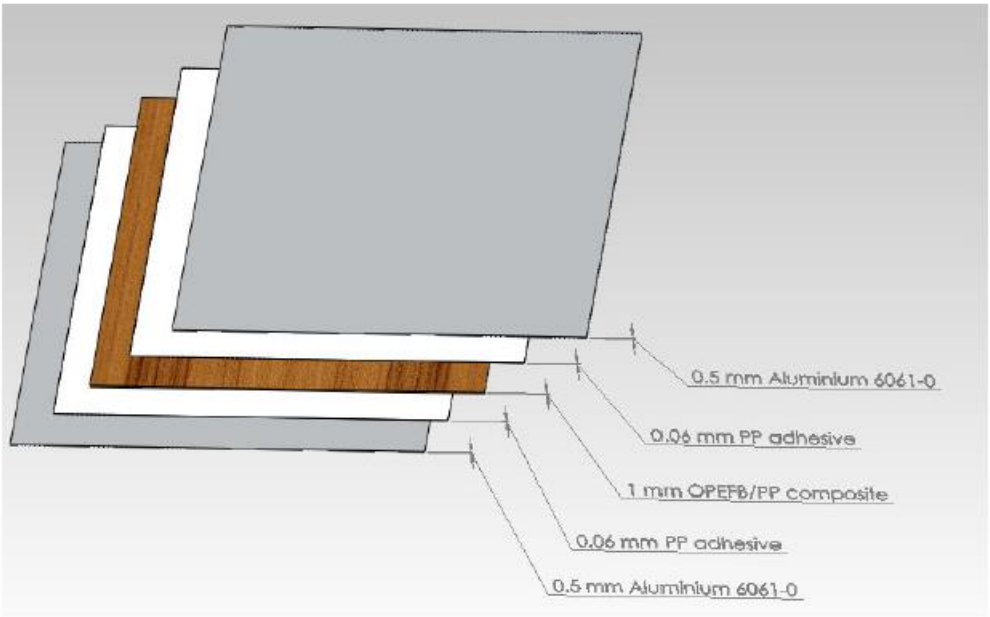

Figure 1.30. Schematic view of stacking sequence of thermoplastic OPEFB based FML

The FMLs made with hybrid reinforcement are also being developed to check the effect of hybridization at composite scale in FMLs. The hybridization of natural fibres with already commercially available FMLs are done by a lot of researchers to find a way for commercial applications, in one such study the Malingam *et al.* [156] developed the FMLs using a different configuration of glass / kenaf composites, further the PP was used as matrix and woven fabric plies were placed at 0/90 and ± 45 degree. The 0/90 orientation shown better tensile performance while ± 45 shown better Charpy impact performance. Most of the researchers have studied the static and Charpy impact performance of NFMLs, the LVI performance of NFML is not explored in detail especially comparison of NFMLs made with a different type of thermosetting and thermoplastic resin system is not done.

1.5 Thesis objectives

FML consist of metal and composite, so it combines the properties of both constituents. The new material is more durable and endured as compared to both the constituents. Some of the key features of FML is that it is lightweight material with high strength, high fracture toughness, high impact resistance and high energy absorption characteristics. The FML also has better fire resistance, corrosion resistance and moisture resistance properties. Keeping in view all these benefits the FMLs has great potential to use in different applications to replace the existing materials.

1.5.1 Research problem

From the above literature review it can be seen that the commercially used FMLs are made with synthetic materials using very expensive autoclave manufacturing process. The high cost of manufacturing is limiting its application to only high-tech applications. The synthetic materials used in FMLs *e.g.* fibre and epoxy are also causing environmental concern as they are not recyclable. Some researchers are investigating the natural fibres as an alternative to synthetic, but they are still not up to mark due to poor mechanical performance and metal composite bonding. The thermoplastic matrix used to make FMLs require very high curing temperature which cause lost in ductility and mechanical properties of metal. Another less explored area is use of 3D woven reinforcement for FMLs fabrication, even though it has better mechanical properties with benefits of cost. It has not been used to make FMLs. The low mechanical performance issue of natural fibres can be improved using 3D woven reinforcement. To address all these issues of alternative of synthetic materials, low mechanical performance of natural fibre, poor bonding of natural fibre with aluminium and high temperature thermoplastic matrix. Following research objective are defined.

1.5.2 Research Objectives

The primary objective of the research is to develop and mechanically characterize the 3D woven jute reinforced Aluminium laminate and 3D woven hybrid (Natural / Synthetic) reinforced Aluminium laminate. In addition the effect of thermoplastic and thermoset matrix is also investigated. To achieve this objective following specific objectives has been set (Figure 1.31):

1. To characterize the quality of adhesive bonding of aluminium-composites bond made with different fibres and matrix
2. Optimization of 3D woven structures for Fibre Metal Laminate FML fabrication
3. To develop and characterize the hybrid 3D woven jute reinforced composites and FMLs to check the effect of different fibres and matrix

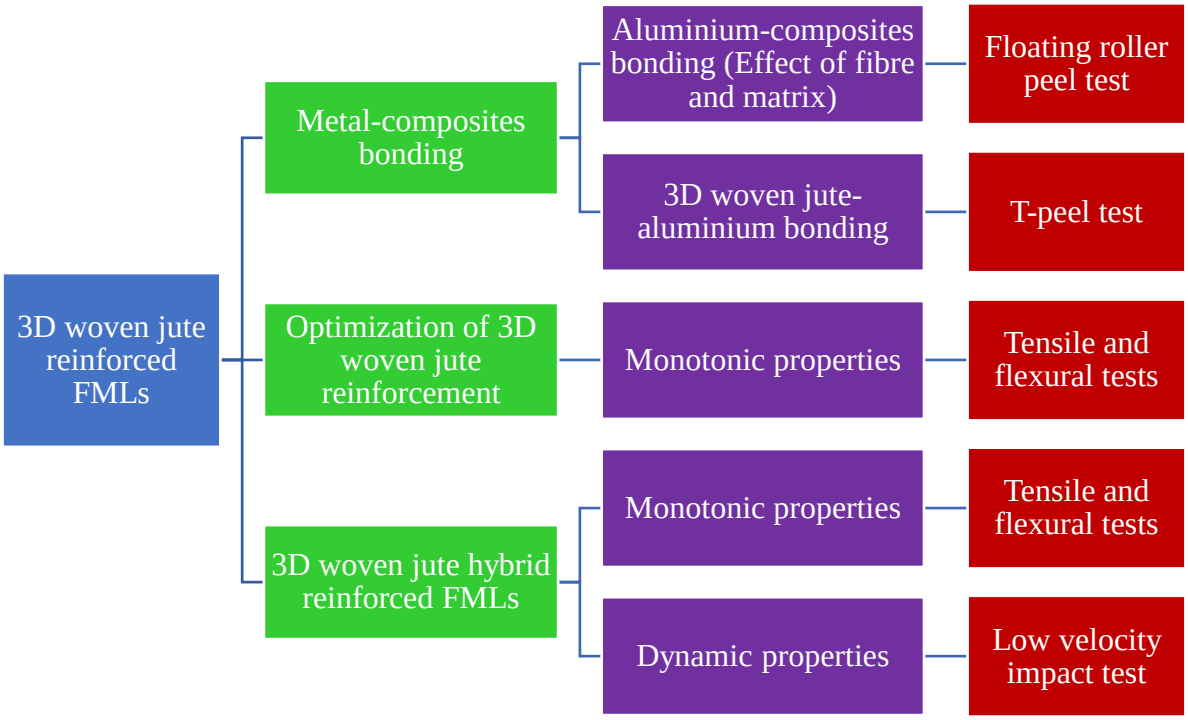

Figure 1.31 Specific objectives of research and flow chart of study

Chapter 2. Materials and Experimental Methods

Different kind of materials and manufacturing techniques were used to manufacture the fibre metal laminates in the current study. Both qualitative and quantitative assessments were carried out to characterize the fibre metal laminates. The jute was used as main fibre for the weaving of 3D woven reinforcement. Once the structure of weave was optimized, the 3D woven jute was sandwiched with 2D woven jute, aramid, carbon, and glass, respectively. The FMLs with hybrid reinforcement were developed using epoxy, PP and PVB matrix. In the first step vacuum infusion was used to make 3D woven jute FMLs. For the fabrication of hybrid composites and FMLs the compression hot press techniques was used. The quality of adhesive bonding between composite and aluminium was accessed using T-peel and floating roller peel tests. The monotonic properties were investigated using tensile and flexural tests, while impact performance was examined using drop weight low velocity impact test.

2.1 Materials

The jute yarn was used to make all type of 3D woven reinforcements. 3D woven jute reinforcement was jute in both parts of studies. Table 2.1 shows the physical properties of jute yarn.

Table 2.1 The properties of jute yarn used for 3D woven fabric

Yarn linear density [Tex]	**Breaking force (cN)**	**CV% strength**	**Uster hairiness (H)**	**CV % hairiness (sh)**
256.3	2015±39.29	22.83	6.94	2.83

As the jute is a natural fibre and degrades with the exposure to temperature, therefore, Thermo-Graphic Analysis TGA was done of jute yarn to check the degradation rate. As thermoplastic composite is made using the compression hot press, it is usually done at high temperature. The PP especially has a high melting temperature. From the graph, it is clear that within the operating temperature ranges used in the current study for the fabrication of composites and FMLs, the jute yarn properties do not affect much (*Figure 2.1*).

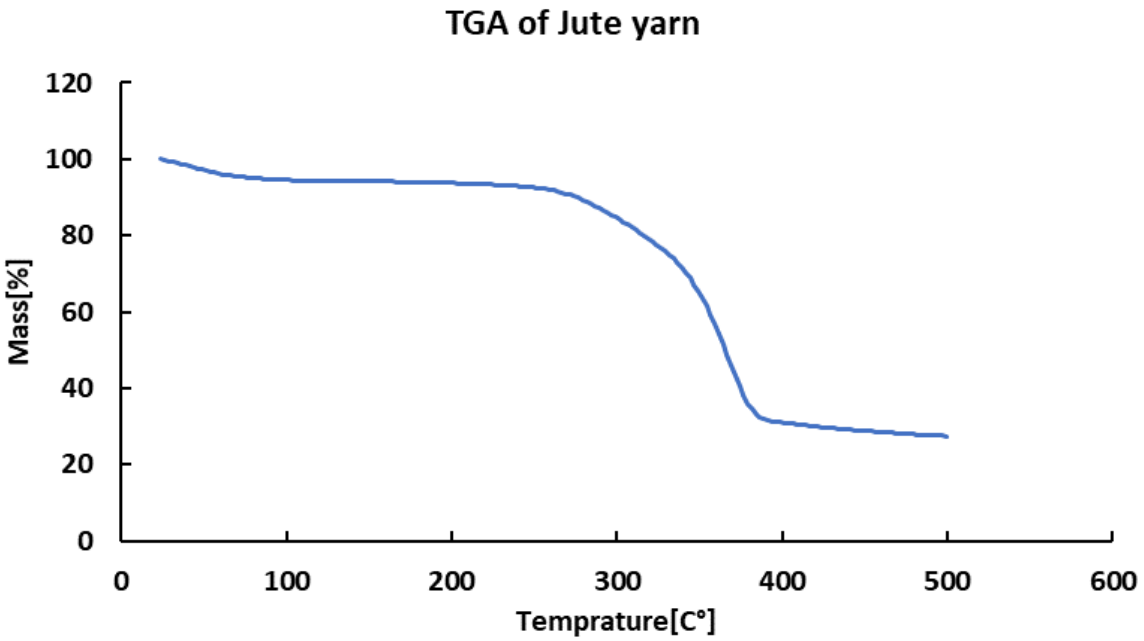

Figure 2.1 Thermo-Gravimetric Analysis TGA of jute yarn

While for the fabrication of 2D plain-woven fabric jute, aramid, carbon, and glass yarn were used. The linear density of all yarn used for the fabrication of reinforcement is shown in Table 2.2.

Table 2.2. The linear density of yarns used for the hybrid reinforcement manufacturing

Type of yarn	**Jute**	**Aramid**	**Carbon**	**Glass**	
Yarn linear density [Tex]	256.3	165	200	Warp	Weft
				96	141

The matrix used in the first part was low viscosity thermoset epoxy as all the samples in the first part were made using vacuum infusion technique which requires low-viscosity resin. The resin was supplied from NAN YA NPEF-170 (Taiwan), and hardener was Aradur HY 159. The average viscosity of resin after mixing was around 220-270 *mPa.s(50°C)*. Both parts were mixed with a ratio of 100:12.5, with an average curing time of 30 minutes as per supplier's instructions.

Both thermoset and thermoplastic matrix was used in the second part. The epoxy was used as a thermoset matrix as it is a more established matrix system used to make FML, While PP and PVB were used as a thermoplastic matrix. The reason for using two different kinds of the thermoplastic matrix was to find a better candidate for the replacement of epoxy. Epoxy and PP are used frequently for FMLs fabrication and reported in the literature, the PVB is surprisingly not used for FML fabrication, despite its excellent mechanical properties. The PVB can be cured relatively at low temperature as compared to PP. Further, due to low-temperature fabrication, the residual stresses and ductility problem can be minimized. The PVB exhibits excellent impact resistance and unique mechanical properties compared to PP. The physical and mechanical properties of all matrix systems are shown in Table 2.3.

Table 2.3. Physical and mechanical properties of matrix systems used to make hybrid composites and FMLs

Matrix	**Density [kg/m³]**	**Manufacturer**	**Tensile Modulus [GPa]**	**Tensile Strength [MPa]**	**Elongation [%]**	**Glass Transition Temperature (Tg) [°C]**	**Melting Temperature [°C]**
Epoxy	1.2	Araldite® LY 556 Aradur® 22962	2.7-3	62-72	3.0-4.0	148-158	
PP	0.9	Chawla Industries, Pakistan	1.2	30	115	-10°C	170
PVB	1.1	Tanyun, China	2.5	40-50	41	66-84	165-200

The Differential Scanning Calorimetry DSC curves of both PP and PVB shows the glass transition temperature Tg and melting temperature. The PP was used in the felted sheet form,

while PVB was used in fine powder form. The DSC of thermoplastic resins is very crucial as the subsequent temperature setting during compression moulding is kept as per DSC findings (Figure 2.2).

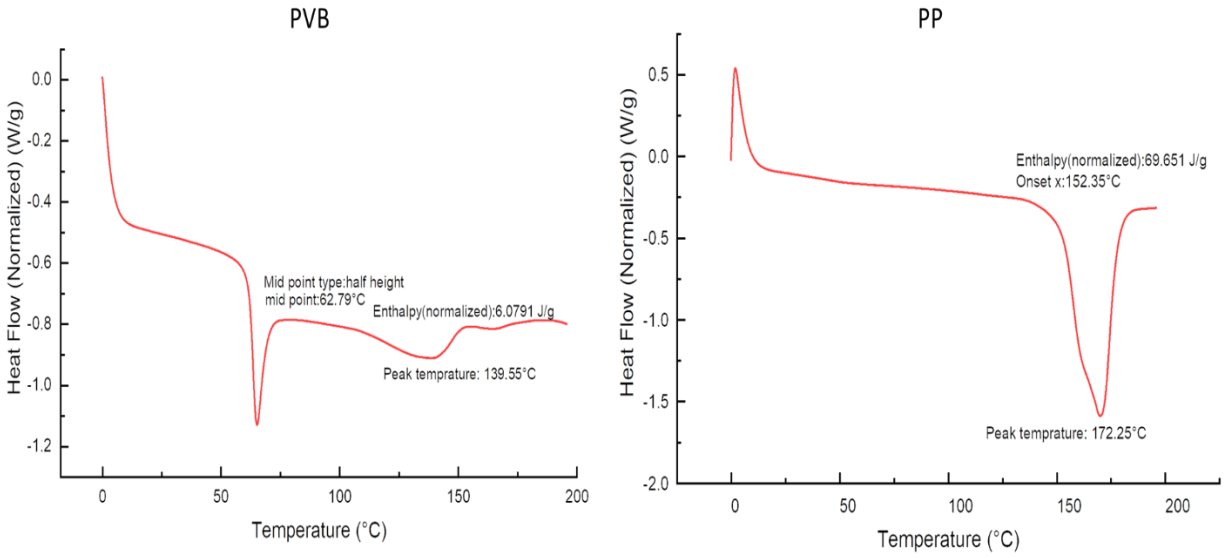

Figure 2.2. DSC curves of PVB and polypropylene

The 7075-T6 alclad aluminium sheet was used for all the FMLs with an average thickness of 0.6 mm supplied by Kaiser, USA (Table 2.4).

Table 2.4. Mechanical properties of Aluminium 7075-T6 alclad

Code	**Manufacturer**	**Density [kg/m³]**	**Tensile Modulus [GPa]**	**Yield Strength [MPa]**	**Tensile strength [MPa]**	**Elongation [%]**
7075-T6 Alclad	Kaiser ,USA	2.81	71.7	462	524	5-11

The chemical composition of 7075-T6 aluminium metal shows that the main constituent after aluminium in the alloy is Zn. This is high strength and low ductility alloy used for aerospace application and one of the oldest aluminium alloy used for aerospace applications (Table 2.5).

Table 2.5. Chemical composition of the 7075-T6 alloy

Composition	**Al**	**Si**	**Fe**	**Cu**	**Mn**	**Mg**	**Zn**	**Cr**	**Ti**	**Other, each**	**Other, total**
Percentage [%]	87.1-94.4	0.4	0.5	1.2-2.0	0.3	2.1-2.9	5.1-6.1	0.18-0.28	0.2	0.5	0.15

All the chemicals used for the anodizing were lab-grade supplied by the following suppliers. As the anodizing is a very sensitive process and can cause variation in the results, non-lab grade chemicals are being used (Table 2.6).

Table 2.6. Chemicals used for anodizing of aluminium surface

Chemical	**Ethanol [CH_3CH_2OH]**	**Acetone [C_3H_6O]**	**Sodium hydroxide [NaOH]**	**Sodium dichromate [$Na_2Cr_2O_7$]**	**Sulphuric acid [H_2SO_4]**
Supplier	Sigma aldrich	Daejung	Sigma Aldrich	Merck	Daejung

2.2 Fabrication Processes of Reinforcement and FMLs

The fabrication of both the composites and FMLs was carried according to protocols for thermosets and thermoplastics matrices. The singeing of jute yarn was done before weaving. The surface treatment of aluminium was done before the fabrication of FMLs. The vacuum infusion technique was used to make all the samples in part 1, while for part 2 the hot press compression moulding technique was used. In the end, all the samples were cut as per standard. The details of all the reinforcement manufacturing and composite fabrication process are given below in detail.

2.2.1 Reinforcement Preparation Process

The 2D and 3D woven structure were weaved on the dobby shuttle loom. Before starting any subsequent process, the jute yarn was singed to remove the protruding fibre. These fibres cause

the entanglement with the mechanical parts of the weaving machine during shed opening and closing (Figure 2.3).

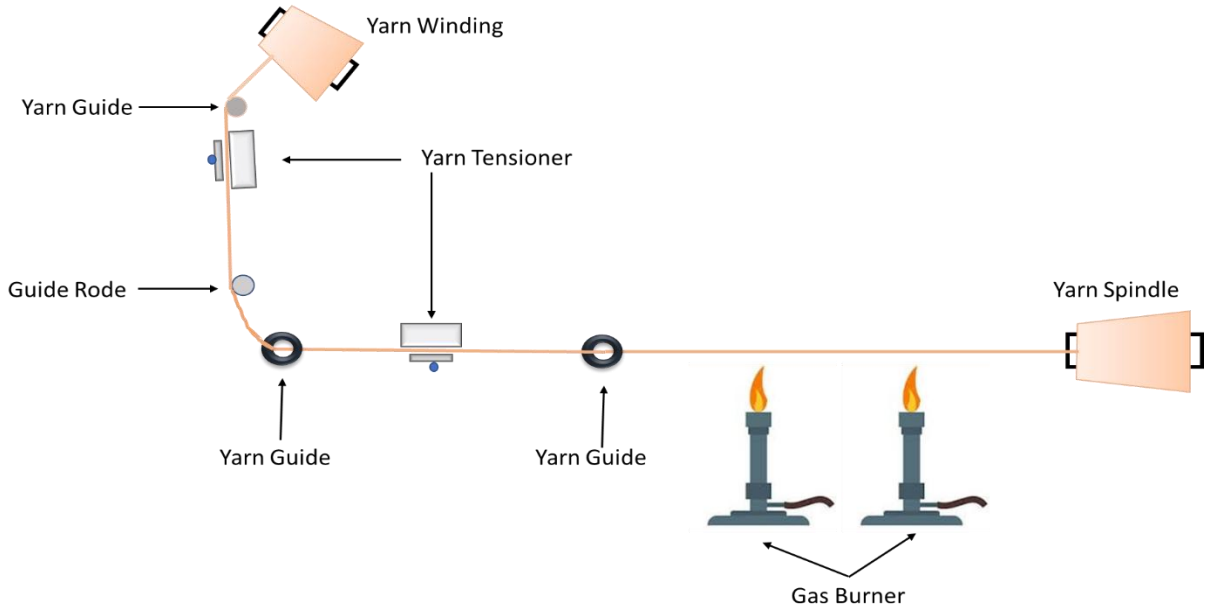

Figure 2.3. Schematic view of the yarn singeing process

After the singeing, the warping was done to prepare the beam for weaving. The warping was done on CCI automatic single end warping machine. The total 970 ends were achieved on the warping as per the requirement of final width of the fabric on the weaving machine. The warper beam was then taken to the weaving machine for subsequent weaving (Figure 2.4).

Figure 2.4. (a) Warping and (b) weaving process for 3D jute reinforcement manufacturing

The singeing had caused a clear difference of appearance along with the ease of weaving. The other option to carry out the weaving of unsinged yarn is by applying sized material. Still, the problem with the sizing of jute is that the removal of sized material is very difficult, which cause a problem with the fibre-matrix interface (Figure 2.5).

Figure 2.5. The difference in fabric appearance of the un-singed and singed yarn

As discussed earlier, the experimental study was carried out in two parts. The 1st part concerned the investigation of the jute-metal interface and optimization of 3D jute reinforcement. The manufacturing details are given in the below section. The 3D woven fabric reinforcement had four layers each and layers were interlocked using four different types of interlocking patterns. All 3D woven fabrics had square quality with 13 ends/cm and picks/cm, respectively. The areal density was between 770-780 g/m^2. The thickness of woven fabrics was taken at a dry, relaxed state. The notations and details of samples are also given below in Table 2.7.

Table 2.7. 3D woven jute reinforcement's structures, cross-sections, and samples notations

Type of Interlocking	Preform Cross-section	Fabric	Thickness [mm]	Fabric Notation
Hybrid TT Warp-LL Weft interlock	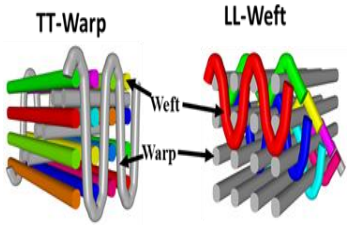		3.85	JWF1
Hybrid LL Warp -LL Weft interlock	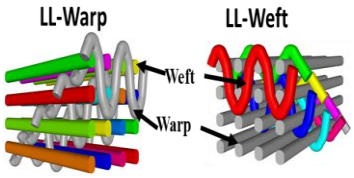		4.1	JWF2
Hybrid TT Warp- TT Weft interlock	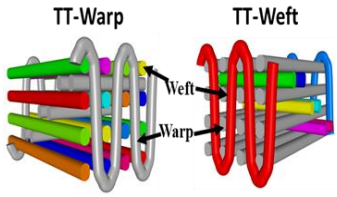		3.3	JWF3
TT-Weft interlock	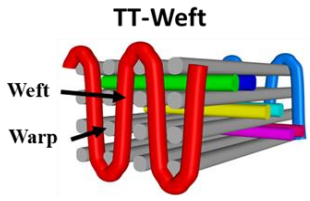		3.1	JWF4

For the 2nd part, the hybrid reinforcement was used in which the outer layer of composite was 2D plain woven structures made with jute, glass, carbon, and aramid fibre. At the same time, the inner core of hybrid composite was of 3D jute woven fabric. The structures of 3D and 2D woven fabrics are shown in Figure 2.6. The reason behind using plain woven structure was to use a stable structure which provides smooth adhesion with the metal layer.

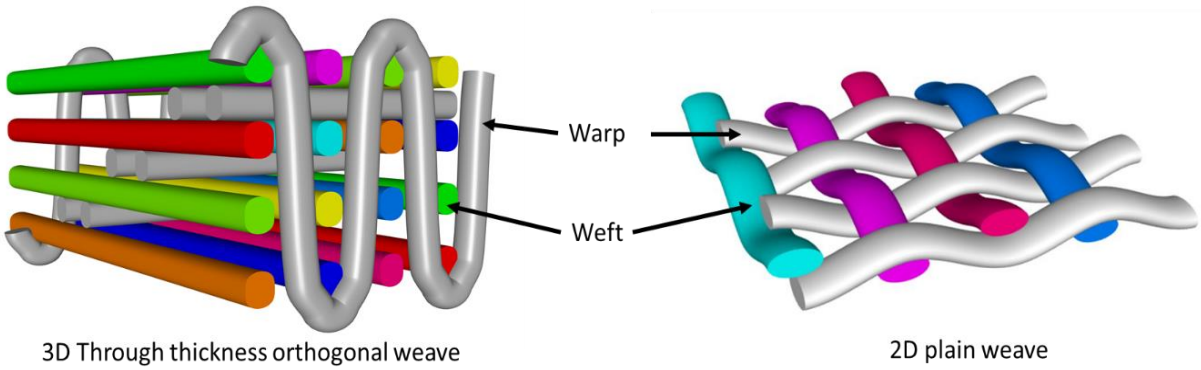

Figure 2.6. The weave structures of reinforcements used for hybrid composite and FML fabrication

The GSM of all kinds of 2D reinforcement was in the same range. The 2D plain weave design was used for all type of 2D reinforcement. The synthetic 2D reinforcement was commercially procured, while the 2D and 3D jute reinforcement was made on the weaving machine using the same kind of jute yarn Table 2.8.

Table 2.8. Reinforcement properties used to make hybrid FMLs

Reinforcement	**Areal Density [g/m²]**	**Fabric**	**Ends/cm**	**Picks/cm**	**Thickness [mm]**
3D Jute	760-780		13	13	2.5
2D Plain Woven aramid	220	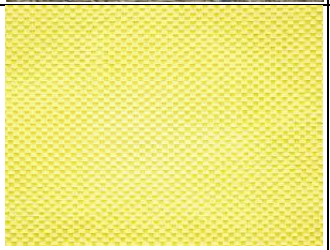	6.8	6.8	0.32

2D Plain Woven Carbon	200	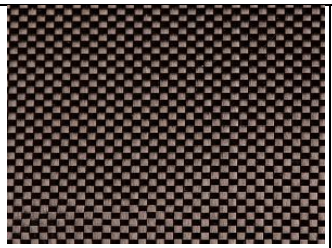	5.5	4.7	0.34
2D Plain Woven Glass	231	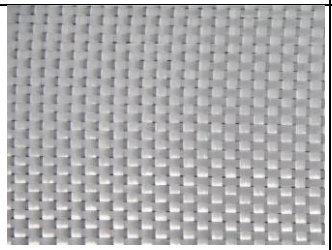	10.2	10.2	0.25
2D Plain Woven Jute	220	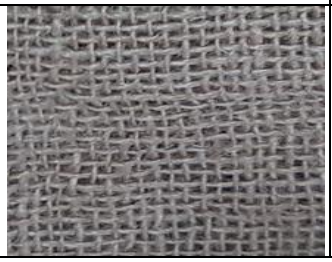	4	3.5	1.13

2.2.2 Surface Treatment of Aluminium

Aluminium surface preparation is an important and necessary part of FMLs fabrication. Before surface preparation, the sheets were cut in the smaller sizes so the subsequent chemical process could be carried out smoothly. The manual cutter was used to cut the sheets. After cutting, the surface was prepared in the following steps.

The aluminium surface has dirt, dust, impurities, and waxes on it; a good clean surface is required for further processes. Acetone was used to de-grease the surface. After degreasing, the plates were mechanically abraded with 800,1000 and 1200 grade sandpaper, respectively. It was made sure that the shiny protective layer is appropriately removed, as shown in below Figure 2.7.

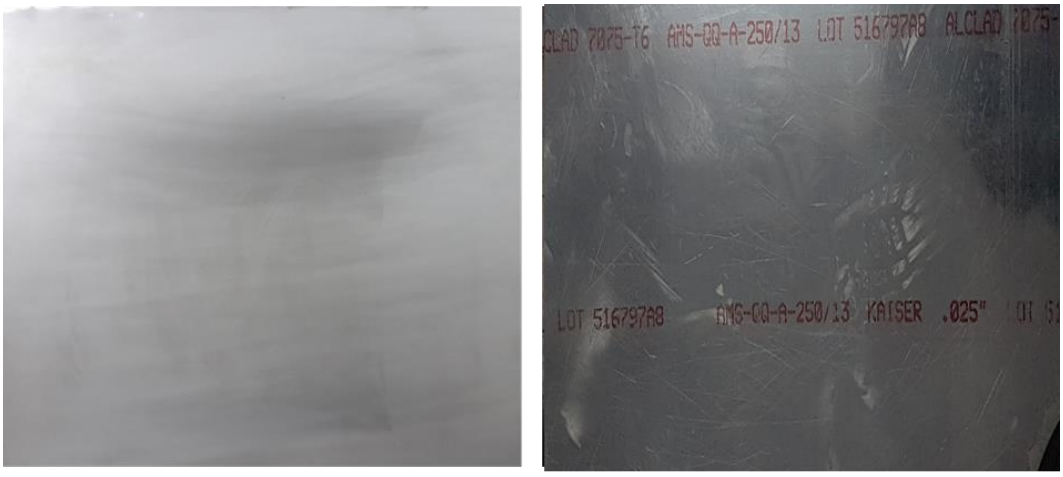

Figure 2.7. The surface of Al plate (a) after abrasion (b) before abrasion

After abrasion, the plates were cleaned with, detergent, acetone, and distilled water respectively to make sure that no residuals of the previous process left on the surface of the plate. After mechanical abrasion, the plate was ready for further chemical processing. The anodization of aluminium is done to create the porous oxide layer. The oxide layer provides sites for interlocking. The anodizing process is very sensitive; any mishandling or skipping of a step may lead to the inappropriate surface of the aluminium.

Alkaline cleaning was done for 10-15 minutes in 11% by weight solution of NaOH made in distilled water. After that, the plates were cleaned and immersed in hot distilled water for 5 minutes to clean the surface properly. Then the plate was checked for water break test to make sure that there was not impurity on it. After alkaline cleaning, the plate was deoxidized in a solution having the following composition:

- 10 % by weight Sodium dichromate
- 30 % by weight Sulphuric acid
- 60 % by weight distilled water

The deoxidation was done for 10-15 minutes at 80°C.

After deoxidation, plates were removed from the solution. After removing from solution, the plates were rinsed and immersed in distilled water for 5 minutes to remove residual chemicals properly. After that, the plates were moved to the anodizing bath. The electrolyte for anodizing contained 12% by weight Phosphoric acid prepared in distilled water. The operating voltage for anodizing was 12 ± 0.5V DC, and anodizing was done for 20-25 minutes. The complete anodizing process was carried in the specially designed fume hood as very hazardous fumes produce during the whole process (Figure 2.8).

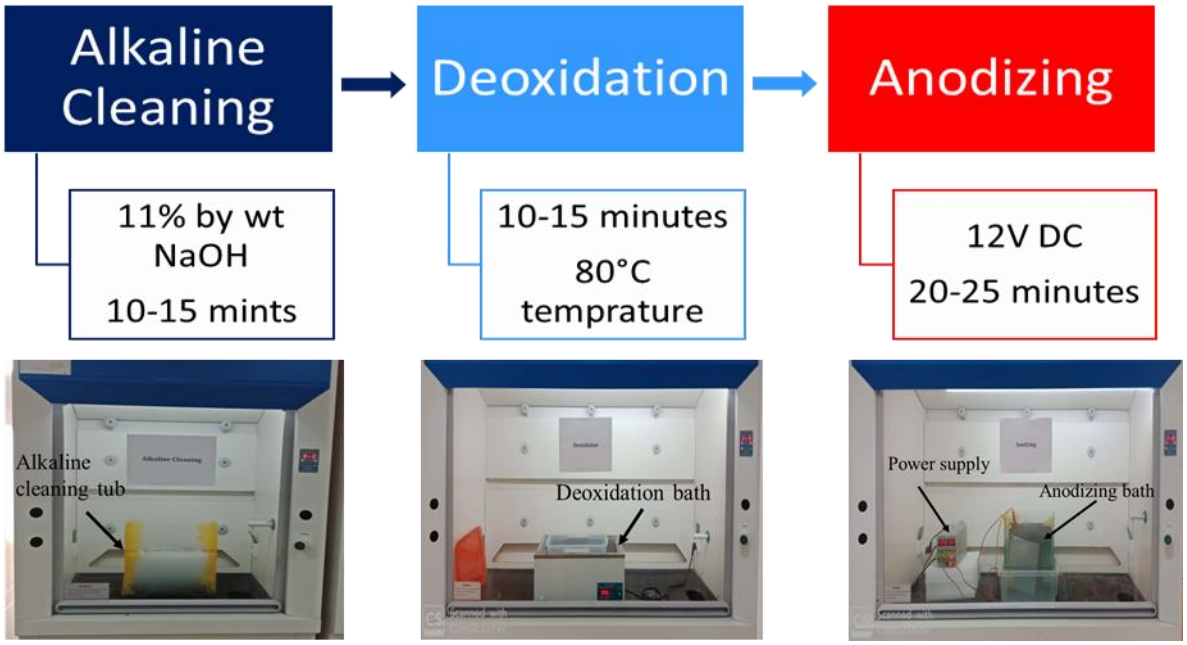

Figure 2.8. Operating parameters of the PAA process and complete process set-up of the PPA process

As soon as the DC supply was turned off, the plate was removed from the electrolyte. After removing from the electrolyte, the plate was cleaned with distilled water for 5 minutes. Then the surface was dried using hot air. After drying, the plates were placed in airtight bags to protect the anodized layer. Distilled water was used in all processes to get repeatable results. The water break test was performed after alkaline cleaning, deoxidation and anodizing to make sure no impurities were carried out from the previous process. The surface of the aluminium

plate should not be touched during the whole process to avoid the transfer of foreign contaminants on the surface. After anodizing, the plates were used immediately.

The anodized surface should be continuous smooth and regular. There should not be any scratches, irregularities, burnt mark or areas that are not anodized. There are often some irregularities at the point of electrical contact, which are acceptable. The surface after anodizing was inspected visually to confirm whether the surface is anodized or not. The anodized plate was placed at a low angle (0-10°) at white polarized light to confirm the anodizing. The surface showed a rainbow of colors. All plates after anodizing inspected visually to check the formation of the rainbow. The water contact angle test was also conducted to check the angle of a water droplet with the anodized surface. The procedure is discussed below in detail.

A water break test is conducted to check the surface energy of metals. Typically with impurities, the aluminium has lower surface energy. With a surface having high surface energy will form a continuous film of water. A surface which is not chemically treated or have impurities will show isolated drops. The distilled water is used to conduct a water break test. The surface is inspected for the 30s usually to observe if there is any water break. The water break test is conducted after every process, and if it fails at any stage, the process will be again started from the beginning [157]–[159]. The water break test was conducted for all the plates before the subsequent operation (Figure 2.9).

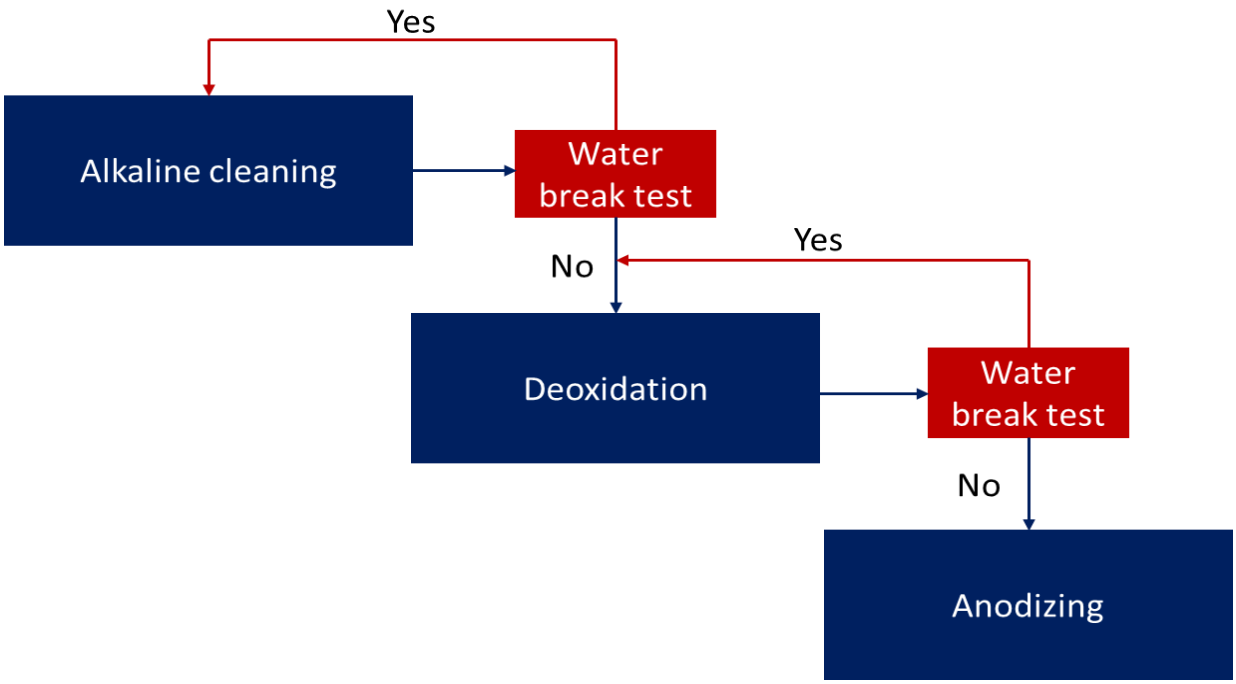

Figure 2.9. Water break tests sequence for PAA

2.2.3 3D Jute Reinforced Composites and FMLs Vacuum Infusion Fabrication Technique

The Jute Fibre Reinforced Composites JFRCs and Jute Reinforced Aluminium Laminates JuRALs developed in the 1st part of the study were made using the materials mentioned earlier in the following sequence. For the fabrication of JFRCs and JuRALs, all types of reinforcements were cut in the weft direction. The surface of aluminium was anodized, as mentioned earlier, to enhance the adhesion between metal and composite [33], [34].

All the FMLs were made using simple 2/1 configuration, with one composite plate sandwiched between two aluminium plates (Figure 2.10).

Figure 2.10. 2/1 lay-up configuration used for FMLs fabrication

After reinforcement cutting and surface preparation of aluminium, the vacuum infusion technique was used for JFRC and JuRAL fabrication. The vacuum infusion process is a simple one-step process and can be used instead of the autoclave to manufacture FMLs (Figure 2.11) [10].

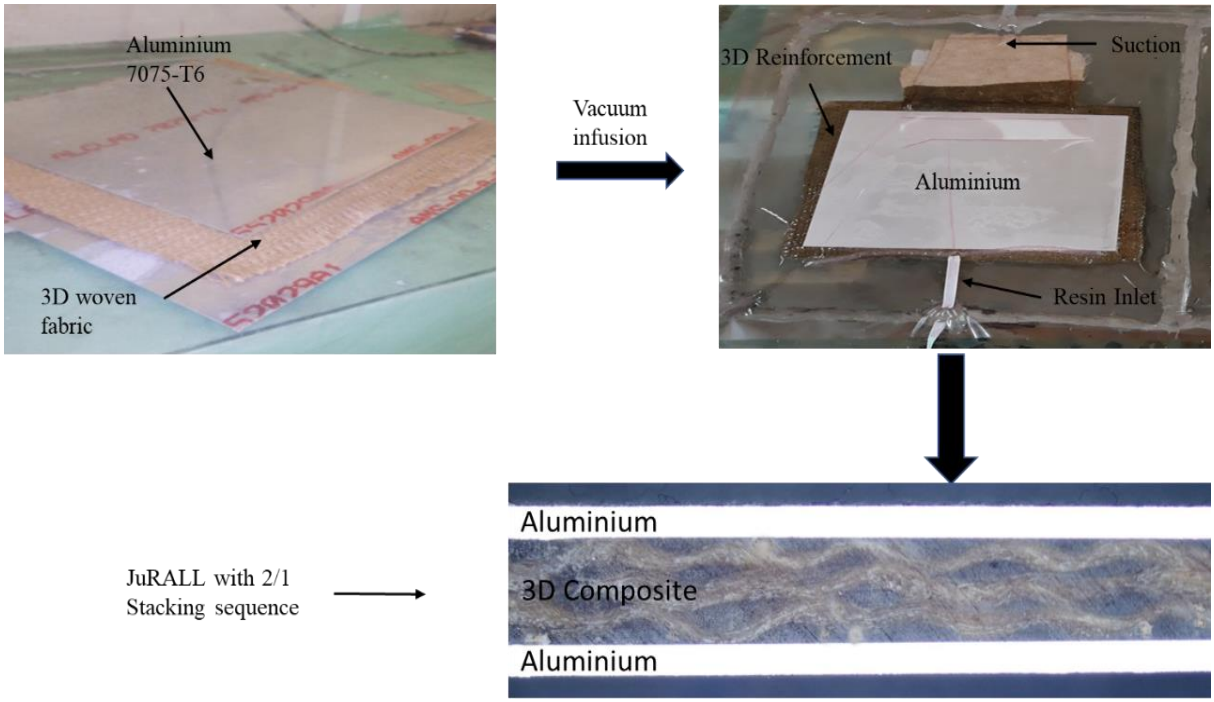

Figure 2.11. JuRAL vacuum infusion fabrication process

The details of JFRCs and JuRALs notations and corresponding thicknesses are shown in Table 2.9.

Table 2.9. JFRCs and JuRALs samples detail with notations

Sr#	Type of Interlocking	JFRC Thickness [mm]	JuRAL Thickness [mm]	JFRC Notation	JuRAL Notation	Fiber Volume Fraction [V_f]
1.	Hybrid TT Warp-LL Weft interlock	3.3	3.65	JFRC1	JuRAL1	0.27
2.	Hybrid LL Warp-LL Weft interlock	3.02	3.45	JFRC2	JuRAL2	0.27
3.	Hybrid TT Warp-TT Weft interlock	2.84	3.29	JFRC3	JuRAL3	0.295
4.	TT-Weft interlock	2.58	3.3	JFRC4	JuRAL4	0.305

The thickness of different type of JuRALs was different depending upon the thickness of the reinforcement used. The volume fraction of different type of samples was not concerned by the thickness of reinforcement. The thickness was different due to different type of interlocking while the GSM of all type of reinforcement was in the similar range, hence fibre volume fraction was also in similar range. The MVF of JuRAL1, JuRAL2, JuRAL3 and JuRAL4 was 0.33, 0.35, 0.36 and 0.36, respectively.

2.2.4 Hybrid Composites and FMLs Compression Hot Press Fabrication Process

For the second part of the experimental study, all the composite and FMLs were prepared using compression hot press. The purpose of using compression hot press instead of vacuum infusion was that the thermoplastic matrix was being used.

In the second part of experimental work, the lay-up configuration for FMLs was 2/1, the FRC part of FMLs was also made with 2/1 lay-up configuration in which the core of FRC was made with 3D orthogonal jute woven fabric which was sandwiched with 2D plain woven fabric. The structure of 3D reinforcement was selected from the second part (Figure 2.12).

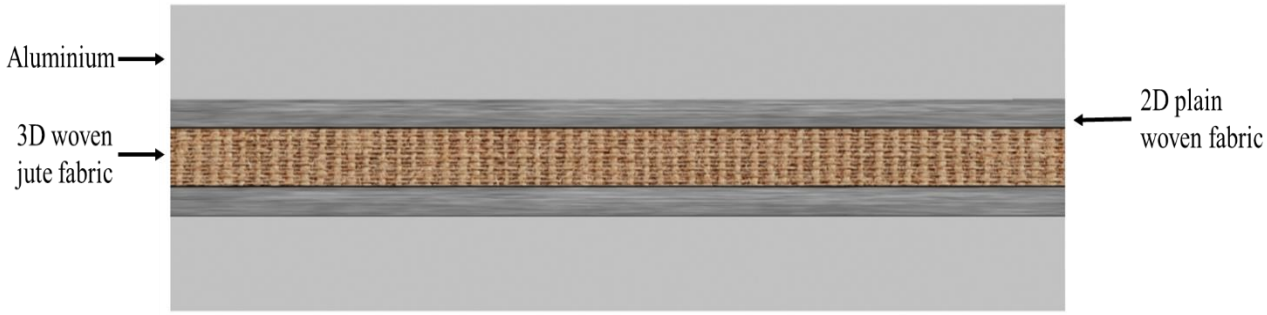

Figure 2.12. 2/1 FML configuration with hybrid reinforcement

Figure 2.13 shows the schematic configuration and stacking sequence of plies used to make the composites and FMLs.

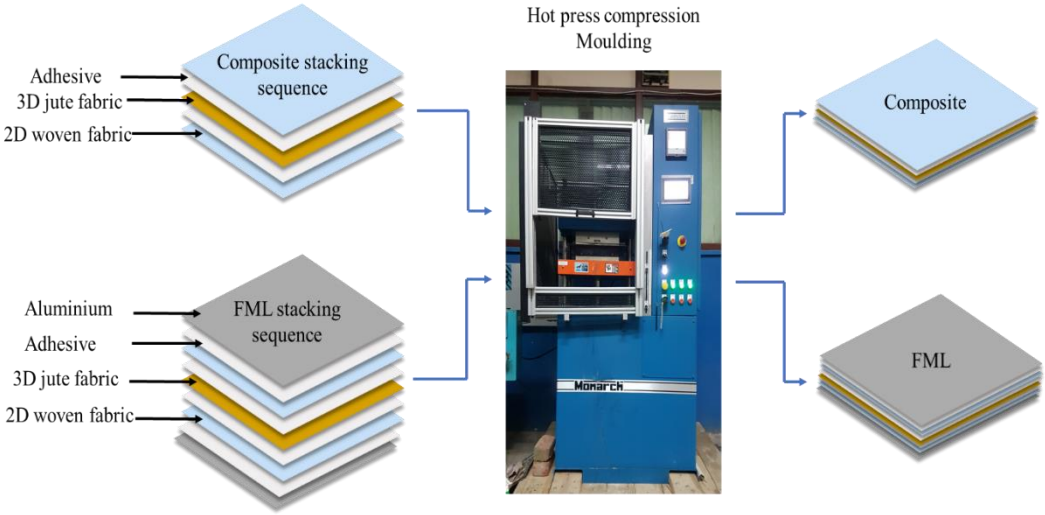

Figure 2.13. The schematic view of the configuration used to manufacture the composites and FMLs

The operating conditions were kept constant for all the samples during the manufacturing on compression hot press. Figure 2.14 shows the stacking sequence of the hybrid configuration of FML and sample placement in the machine.

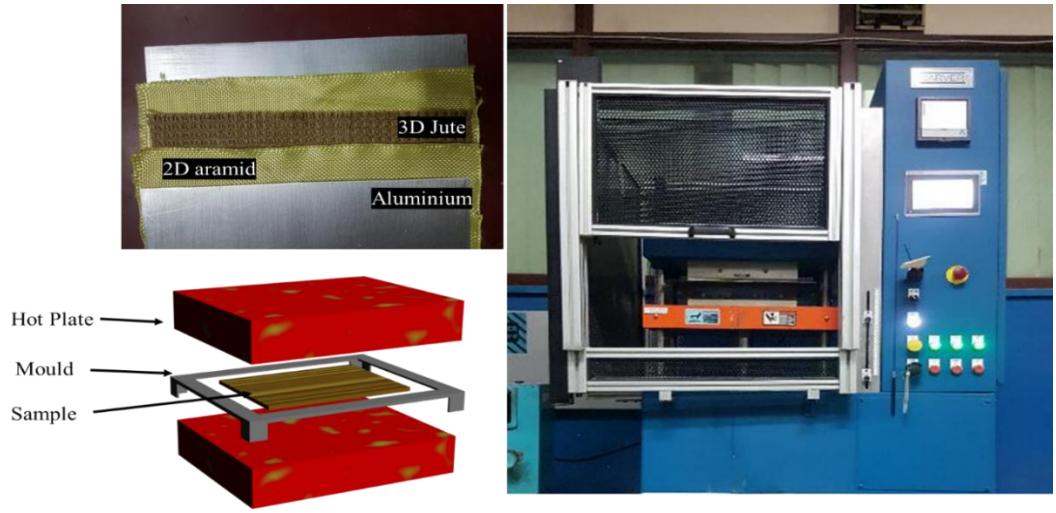

Figure 2.14. Fabrication of FMLs on compression hot press and stacking sequence of FMLs for fabrication

The compression hot press has a working capacity of 30 ton and upper-temperature limit of 300 °C. Each hot plate has a size of 77.4 cm². The difference between the temperature of the two plates was kept at 5°C to facilitate the conduction of heat. During the fabrication of PVB based FMLs and composites, the samples were removed from the machine once the temperature of the machine was below the Tg of PVB. For PP, as it has very low Tg, so the samples were removed from the machine just below 100°C (Figure 2.15).

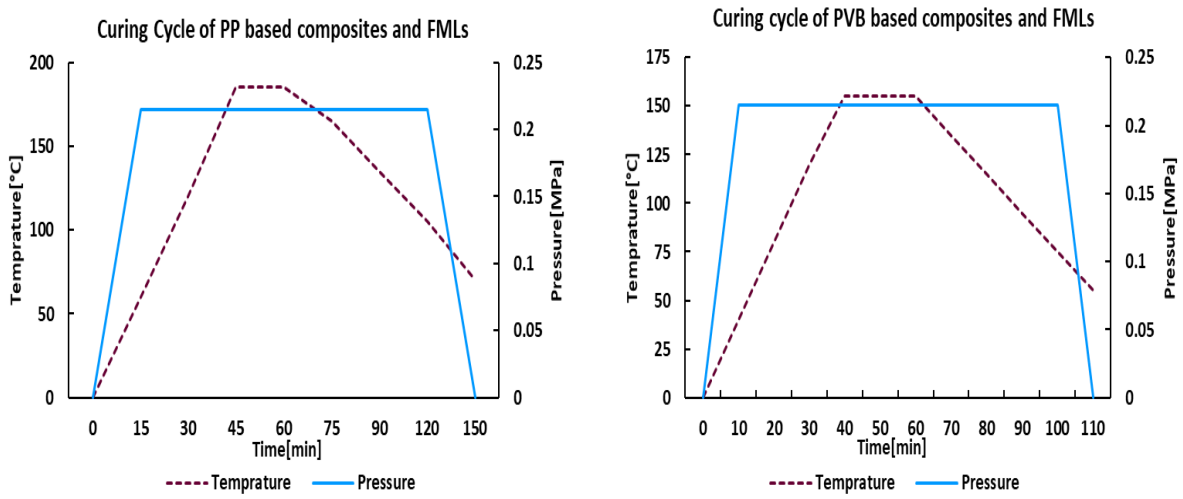

Figure 2.15. The curing cycle of PP and PVB based composite and FMLs during fabrication on compression hot press

Teflon sheets were used above and below the samples to avoid any sticking with the plates of hot press. A square mould made with stainless steel was used to achieve constant MVF for all type samples. It can also be seen in (Figure 2.14). The PVB samples were kept for a longer time in the hot press as it takes longer time to powder to melt and uniformly distribute throughout the sample. The thermoset epoxy-based samples were post-cured after removing from the compression hot press as per suppliers' instructions. For post-curing, the curing oven was used. The temperature was kept a bit higher than the melting temperature due to the thickness of the sample and the hybrid configuration of reinforcement. As the epoxy needs a long curing cycle as compared to thermoplastic resin systems. Due to this longer curing cycle, an additional cost is added during sample preparation (Figure 2.16).

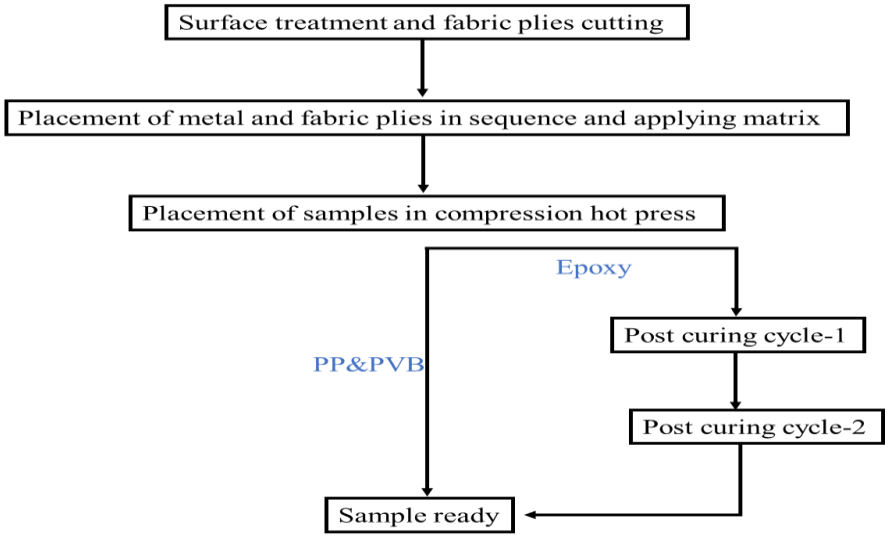

Figure 2.16. The sample preparation route of thermoset and thermoplastic matrix-based samples used in the current study

The reason for this longer curing at elevated temperature is complete curing of unfixed polymers. The usually PVB has shortest curing cycle followed by PP and epoxy in the following order, Epoxy > PP > PVB.

Table 2.10 shows the sample notations used to distinguish the different samples. Five different sets of samples were made with each having three variations depending upon the kind of matrix is used. The name of each sample has three words donating the variations used for each sample and easy recognition. The first letter shows the type of material used for 2D plain hybrid structure; the second letter shows that whether composite or FML. The third letter shows the kind of matrix being used. For example, in AFB, letter A indicates aramid, F indicates FML, and B representing PVB.

Table 2.10. No of samples and sample notations used for hybrid composites and FMLs fabrication.

Configuration	Schematic of plies	Notations			Thickness [mm]	Fiber Volume Fraction [V_f]
		Epoxy	PP	PVB		
3D Jute		JCE	JCP	JCB	1.82±0.02	0.36±0.01
Al/3D Jute/Al		JFE	JFP	JFB	2.6±0.05	
Plain 2D Jute/3D Jute/ Plain 2D Jute		JJCE	JJCP	JJCB	2.65±0.05	0.36±0.01
Al/Plain 2D Jute/3D Jute/ Plain 2D Jute/Al		JJFE	JJFP	JJFB	3.40±0.03	
Plain 2D aramid/3D Jute/ Plain 2D aramid		ACE	ACP	ACB	2.20±0.05	0.43±0.015
Al/Plain 2D aramid/3D Jute/ Plain 2D aramid/Al		AFE	AFP	AFB	3±0.01	
Plain 2D carbon/3D Jute/ Plain 2D carbon		CCE	CCP	CCB	2.20±0.05	0.42±0.016
Al/Plain 2D carbon/3D Jute/ Plain 2D carbon/Al		CFE	CFP	CFB	3±0.01	
Plain 2D glass/3D Jute/ Plain 2D glass		GCE	GCP	GFB	2.2±0.05	0.40±0.02
Al/Plain 2D glass/3D Jute/ Plain 2D glass/Al	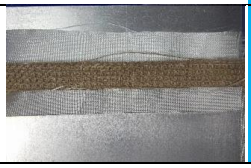	GFE	GFP	GFB	3±0.01	

2.2.5 Aluminium-Composite Bond Samples Preparation for Floating Roller Peel Test

The samples for the floating roller peel test were prepared using the compression hot press as described in section 2.2.4. The epoxy, PP and PVB were used as matrices. The floating roller peel test sample has two-component, flexible adherend and rigid adherend. The aluminium was used as flexible adherend, while composite was used as a rigid adherend. The detailed scheme of samples preparations is presented in Figure 2.17.

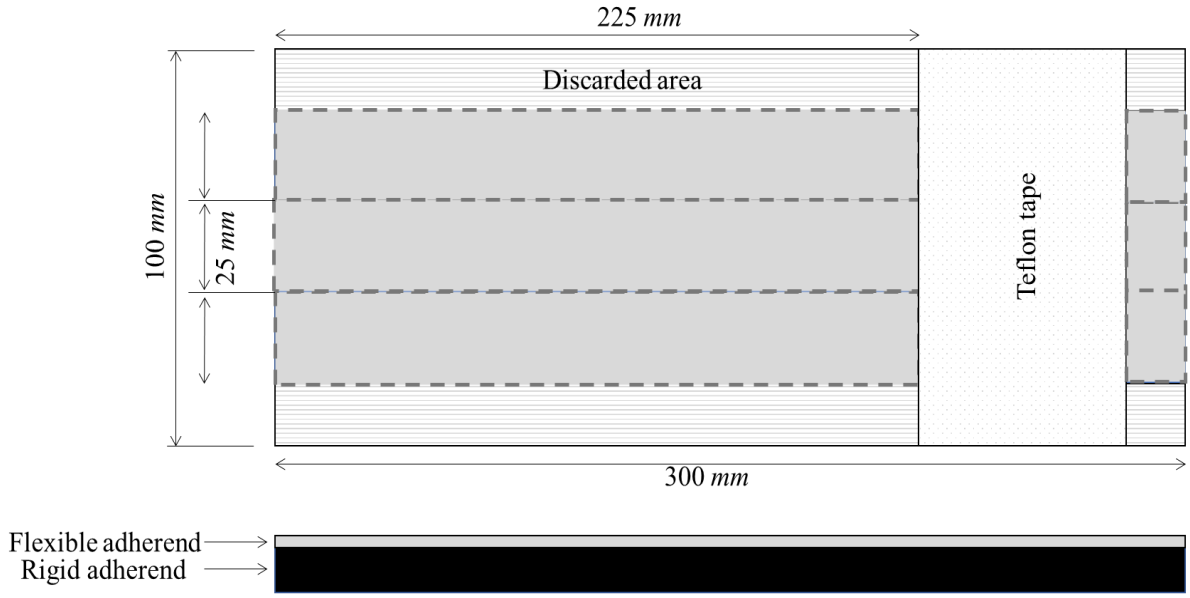

Figure 2.17. Scheme of test panel preparation for floating roller peel test [60]

The jute, aramid, carbon, and glass were used to make composites. All the samples details, notations, and types of adherend are given in Table 2.11.

Table 2.11. The detail of sample notations and materials details of the floating roller peel test

Matrix	Flexible adherend	Rigid adherend	Notations	Figure of sample
Epoxy		Jute composite	JE	
PP			JP	
PVB			JB	

Epoxy	Aluminium (0.6*mm*)	Aramid composite	AE	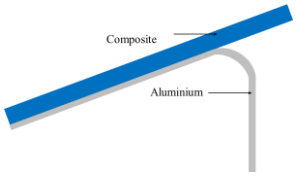
PP			AP	
PVB			AB	
Epoxy		Carbon composite	CE	
PP			CP	
PVB			CB	
Epoxy		Glass composite	GE	
PP			GP	
PVB			GB	

The average thickness of adhesive layer for epoxy, PP and PVB was 0.26±0.02*mm*, 0.35±0.015*mm* and 0.36±0.016*mm*, respectively. The thickness of composite part was around 3.2*mm* for all the samples.

2.3 Composites and FMLs Mechanical Characterization

As already discussed in the first part, the assessment of jute-aluminium bonding and static properties of 3D jute reinforced FMLs and its constituents were investigated. While the second part concerns the qualitative assessment of metal-composite bonding of aluminium with jute, aramid, carbon, and glass. While tensile, flexural and LVI properties of both hybrid composites and FMLs were also investigated. The samples for testing were prepared using a diamond profile cutter. Three repetitions were performed per configuration throughout the study. The details of all the samples and test methods is given below.

Before using aluminium alloy for any subsequent process after anodizing, the water contact angle test was performed to check the wettability and hydrophilicity of the surface. The water contact angle was measured using water contact angle goniometer.

The T-peel test was used to check the bonding strength between aluminium and 3D jute composite. The T-peel test was performed according to ASTM D1876 standard at a crosshead

speed of 4.23mm/sec. The Zwick / Roell UTM Z100 was used to conduct the T-peel test. Figure 2.18 shows the schematic view of the T-peel specimen and specimen mounted on the machine.

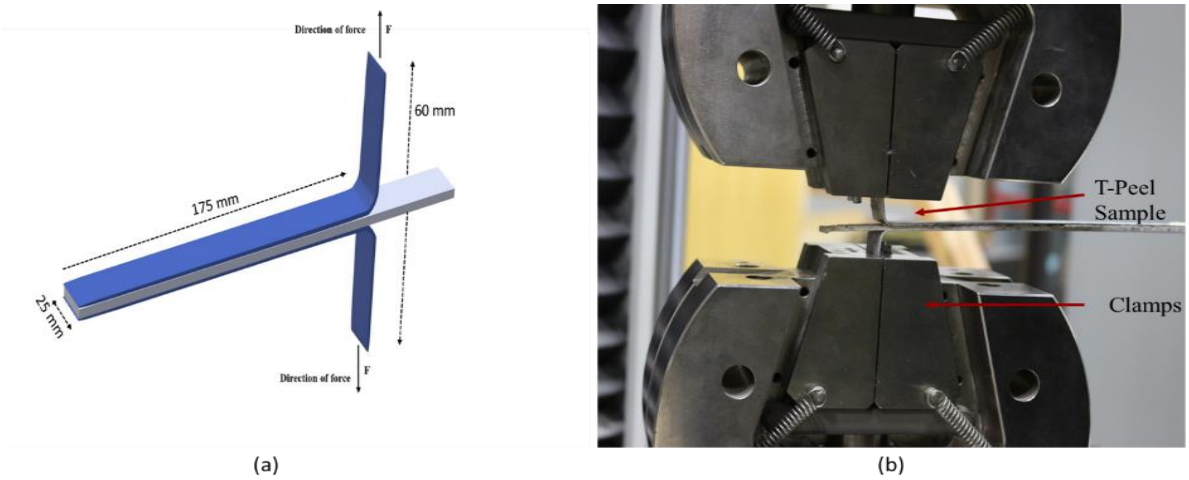

Figure 2.18. (a) Schematic view of specimen for T-Peel test (b) T-Peel sample mounted on the machine

The DIN EN 2243-2 was used to determine the peel performance of metal-composite adhesive bonds. The test was performed on Zwick / Roell UTM Z100. The testing speed was 152 mm/min (Figure 2.19).

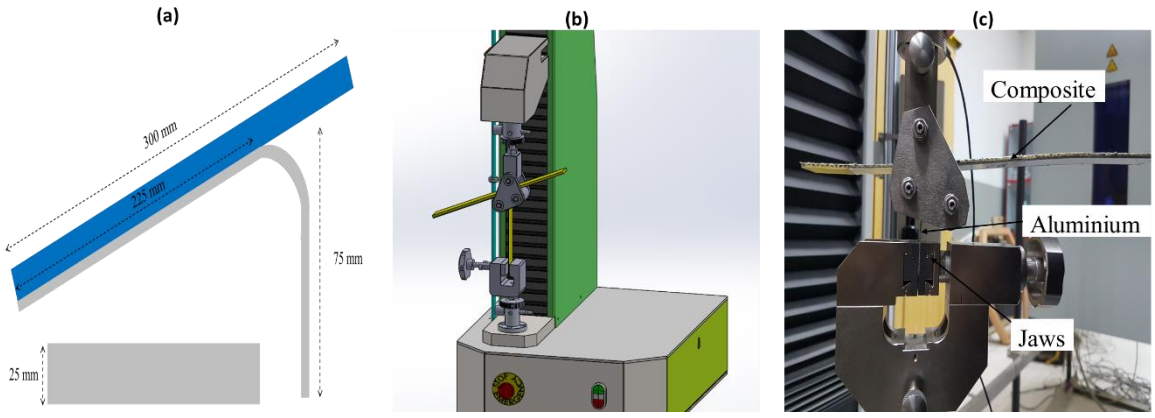

Figure 2.19 (a) sample dimensions (b) The schematic of the floating roller peel test (c) sample mounted on the machine for the floating roller peel test

The tensile test was carried out using the ASTM D3039 standard at a crosshead speed of 2 mm/min. While the flexural test was conducted according to ASTM D7264 standard at a

crosshead speed of 1 mm/min and span length of 32×thickness of sample. After the tests, the specimens were examined microscopically to check the mode of failure. The Zwick / Roell UTM Z100 was used to conduct tensile and flexural test.

The LVI test of all the samples was performed as per ASTM D7136. The sample size was 150×100 mm (L×W). The tests were performed on HIT230F, Zwick Roell having an impactor of hemispherical shape with a diameter of 16 mm (Figure 2.20).

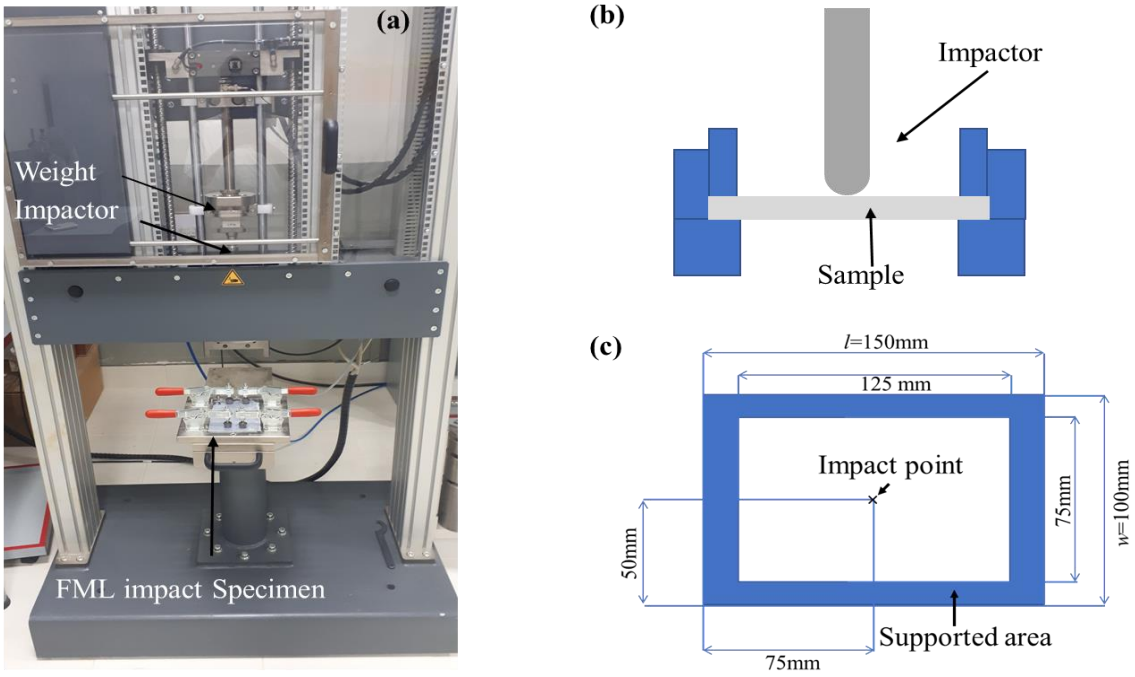

Figure 2.20. (a) Samples mounted on hydraulic impact testing machine (b) schematic of impact testing (c) LVI sample dimensions

The impactor had a hydraulic brake to avoid multiple strikes. After placing the sample on the platform was tightened with the neoprene rubber grips to avoid slippage / bouncing due to impactor. The composites and FMLs were tested on different energy levels; the reason behind different energy levels was that the composites would be perforated at a very low energy level compared to FMLs. As the LVI is a dynamic test, so both composites and FMLs will behave differently. By sandwiching the structures, the parameters influencing the properties will also

be different. For the composites, the 8 J impact energy was used while 35J was used for FMLs. Several pre-trials were done to select the energy level. Then energy level was selected based on the perforation of epoxy-based composites and FMLs. The parameters used for LVI of composites and FMLs are given in Table 2.12.

Table 2.12. Parameters of impact testing of composites and FMLs

Composites		**FMLs**	
Parameters	**Values**	**Parameters**	**Values**
Drop Height	676 mm	Drop Height	192 mm
Impact velocity	3.641 m/s	Impact velocity	1.941 m/s
Work Capacity	35 J	Work Capacity	8.02 J
Drop Weight	5.278 kg	Drop Weight	4.258 kg

After the tests, both composites and FMLs were inspected to check the type of damage. The delamination pattern, crack propagation, perforation, First Visible Crack FVC and Second Visible Crack SVC were inspected carefully to get an insight into the nature of the damage. The impacted and non-impacted sides were carefully examined for all type of samples to compare the behaviour of matrix and hybridization against the impact.

The impact energy was calculated as follow:

$$E_i = \frac{mv_i^2}{2} \qquad (2)$$

Where *Ei* is measured impact energy *J*, *m* is mass of impactor (*kg*) and v_i is impact velocity at initial position (*m/s*).

Following the ASTM D7136 [160] the force signal provided by the load cell were integrated to compute impactor velocity and deflection as follow to get deflection vs time curve:

$$v(t) = v_i + gt - \int_0^t \frac{F(\tau)}{m} d\tau \quad (3)$$

$$\delta(t) = \delta_i + v_i t + \frac{gt^2}{2} - \int_0^t (\int_0^t \frac{F(t)}{m}) d\tau \quad (4)$$

Where δ_i is initial deflection at t=0 (m/s), $\delta(t)$ is deflection at time t (m/s), g is acceleration due to gravity (9.8m/s^2), t is time during test (s), $F(t)$ is measured impact force at time t (N), The contact force and impact velocity being known, the absorbed energy as a function of time was determined as follow:

$$E_a = m\frac{v_i^2 - v(t)^2}{2} + mg\delta(t) \quad (5)$$

Where E_a is absorbed energy (J)

The residual deflection was also gauged after removing the sample from the machine with a digital depth gauge. The residual deflection shows the part of the deformation which does not return to its original position. The damaged area of all the samples was also measured to check the extent of damage (Figure 2.21).

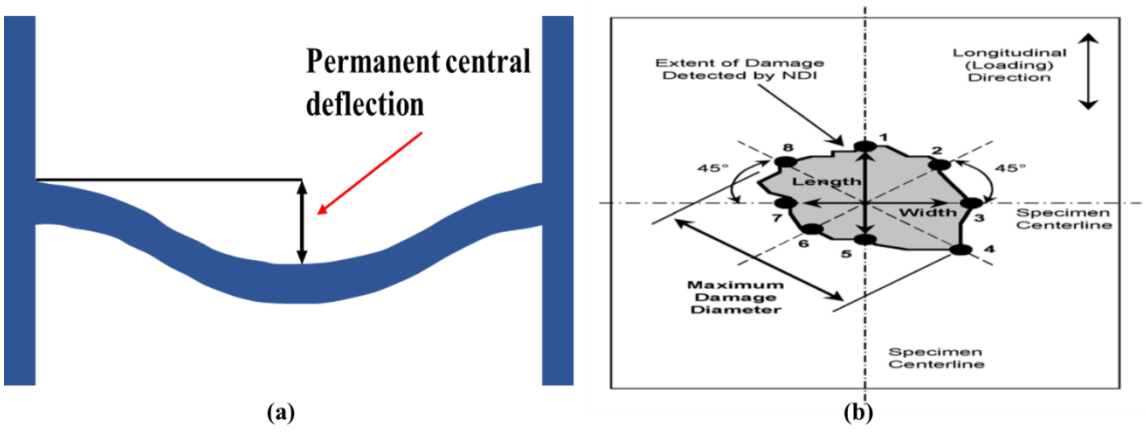

Figure 2.21. Measurement of (a) residual deflection (b) damaged area

Chapter 3. Adhesive Bonding Quality Assessment

This chapter presents the water contact angle results of pre-treated and post-treated aluminium surfaces along with T-peel and floating roller peel test results of the aluminium-composite bonds. The surface of aluminium was prepared using phosphoric acid anodizing before FMLs fabrication. The water contact angle of the anodized aluminium was lower than non-ionized aluminium showing higher surface free energy of anodized aluminium. The T-peel test results showed that the aluminium-3D jute composites bond properties solely depend upon the type of bonding materials rather structure type of reinforcement. The floating roller peel test was used to explore the effect of different fibres and matrices on the adhesive properties. The result shows that the overall PVB matrix has the highest properties. Even though the failure type was not cohesive, the ductility of the matrix played a vital role in the final properties.

3.1 Water Contact Angle

The water contact angle test of aluminium surfaces was carried out to check the quality of surface treatments. The water contact angle was measured for the anodized and un-anodized aluminium surface using water contact angle goniometer. The deionized water is used for the contact angle measurement. The mechanical preparation only increases the hydrophilicity partially with a water contact angle of 78.2°. The anodizing process increased the hydrophilicity substantially with almost equal to zero (6.55º), showing super hydrophilicity (Figure 3.1).

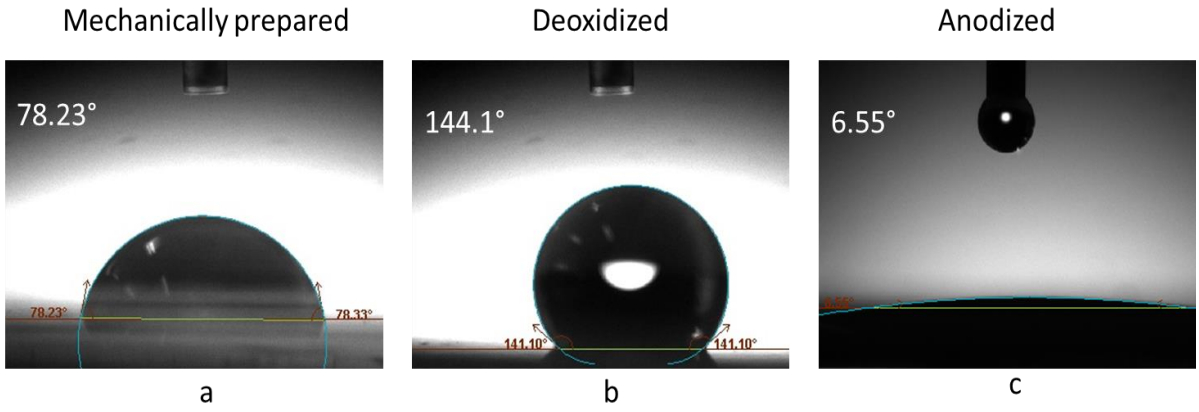

Figure 3.1. The water contact angle of the aluminium surface after (a) Mechanical preparation (b) De-oxidation and, (c) Anodizing

The small contact angle indicates that the liquid is wetting the surface properly, while the larger contact angle shows the wetting is difficult for certain reasons. The high contact angle indicates the presence of hydrophobic substances, *e.g.* the film, coating, contamination, *etc.* [157]–[159]. The low contact angle shows the hydrophilicity, while the high contact angle is concerned to hydrophobicity. The hydrophobic surface causes poor wetting and ultimately poor bonding. The hydrophilicity of the aluminium surface is increased by introducing micro-roughness [161]. For a hydrophobic surface with low surface free energy, the hydrogen bonding between water molecules is greater than the affinity between water molecules and substrate. For the

hydrophilic surface, the association between substrate and a water molecule overcome the hydrogen bonding within water molecules, causing wetting of surface [162].

3.2 3D Jute Composite-Aluminium Bond Adhesive Performance

The T-peel test results of JuRALs are very important to understand the delamination behaviour of metal-composite bonding in NFML. As most of the natural fibre reinforcement is made using spun yarn, so the delamination will be almost similar for all the JuRALs with slight variation depending upon the properties of the individual material.

Figure 3.2 shows the typical load extension curve of T-Peel test of JuRALs. The curve shows the nature and pattern of delamination of aluminium-3D woven jute composite bond.

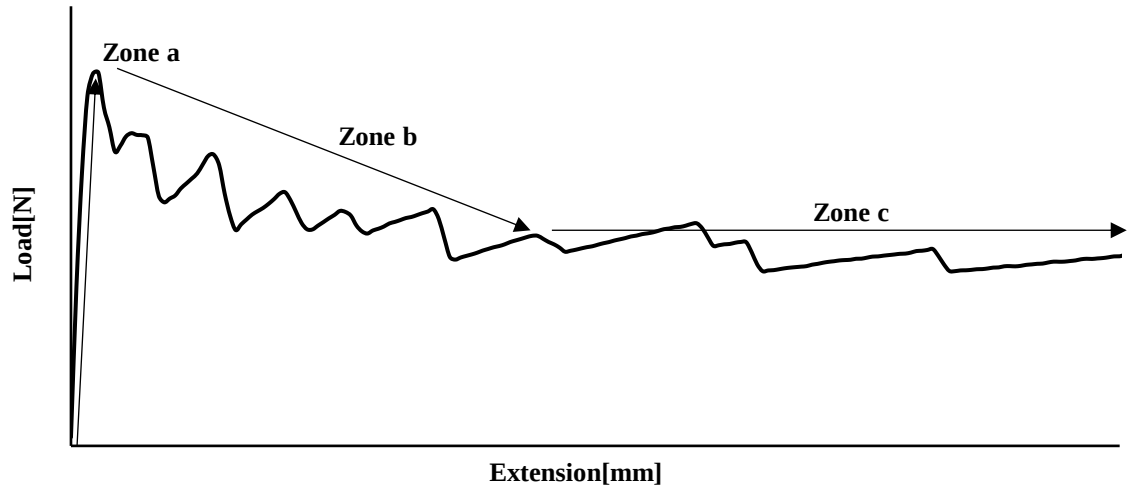

Figure 3.2. Typical load-extension curve of T-Peel test of JuRALs

The T-Peel test curve for JuRAL can be divided into three principal zones; (a) In the first zone, the crack initiation occurs. As the applied load increases rapidly until reaching its maximum value with very small delamination; (b) In second zone the softening starts due to decrease in fibre bridging, that is why the value of load start decreasing; (c) In third zone the curve follows the stable pattern until complete delamination. This kind of behaviour of the load-extension curve is also reported in previous works [34]. The reason for this kind of curve is that the crack

initiation required the highest amount of force, with this force the matrix cracking starts. The matrix crack in case of T-peel test is in the adhesive layer joining aluminium and composites. After the crack initiation, the force decreases because once a crack has been initiated, it will only be propagated with a constant force. The trend of the curve also indicates the brittle behaviour of the epoxy matrix; that is why there are sharp slopes in the curve.

Figure 3.3 shows the load-extension curves of JuRALs T-Peel test. The results of the T-peel test show that the delamination properties of all types of JuRALs were in a similar range and there was not much difference in the average values of the load. The delamination pattern shows that, there was no sudden drop in the curve showing the even adhesion. The failure during delamination was either cohesive or adhesive. The adhesive failure is a type of failure between adhesive and adherend, such kind of failure occur if bonding of the matrix is not very good with aluminium or composite and cohesive failure is in the matrix layer. The cohesive failure is an indicator of good adhesion of matrix with metal and composite [60], [64]. The intra-laminar failure was not seen as the reinforcement was 3D woven. The main reason of this absence of intra-laminar failure was high epoxy content in the 3D woven jute composite.

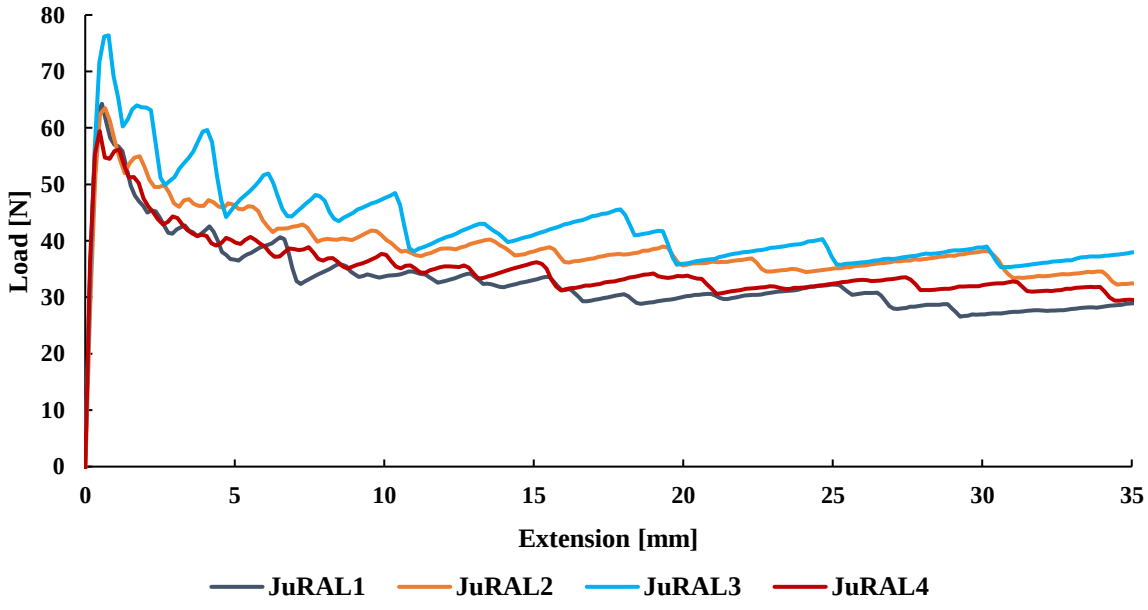

Figure 3.3. The average Load-extension curves of T-Peel test of JuRALs

The graph also indicates that the delamination pattern of all the JuRALs was almost the same, the justification for that similar behaviour was the nature of the raw material used to make JuRALs, *e.g.* epoxy, aluminium and jute. The delamination properties were concerned by the adhesion between jute, aluminium and epoxy. As the materials were same so the trend was also nearly similar. The graph also illustrates clearly that there was no link between delamination properties and different types of structures of reinforcement of JuRALs. Now as per previous argument the properties should be identical but there was a variation in values of the peak as well as the average load for different JuRALs. The reasons for this change are as follow: a– nature of raw material of reinforcement (protruding fibre and yarn unevenness); b– manufacturing technique (vacuum infusion); c– uneven fabric top surface due to 3D woven structure. The reinforcement was made with spun jute yarn, the placement of fibres in the spun yarn are not that aligned as in case of filament yarn. The loose fibres of jute spun yarn provide different resistance towards delamination force during crack initiation and propagation. The irregularity of jute spun yarn and different packing compactness on the top of fabric surface generates resin rich and resin poor areas. These resin rich and poor areas trigger different effects on the delamination pattern and properties. All these factors lead to a different type of load–extension curves for different JuRALs specimen. Figure 3.4 also displays the delaminated surfaces of both metal and composites. As the delamination properties are only concerned with the contacting part of the materials being used, so this behaviour of JuRALs is understandable. Since the samples were made using the Vacuum infusion, so there is possibility of slight variation of the adhesive layer from sample to sample. Unlike autoclave in which prepregs are used, the VI use infusion for resin injection.

The work done (Fracture energy) and the fracture toughness (G1) during T-peel tests were calculated using the following Equation:

$$G = \frac{A}{aw} \quad (6)$$

In Equation 6, A is area under the curve [*J*], *a* is the propagated crack length [mm], *w* the width of the tested sample [*mm*].

Table 3.1 presents the different properties of the T-peel test of JuRALs and corresponding fracture toughness. In the t-peel test mainly average force is most reliable parameter, as can be seen in the below table that the F*av* of all the JuRAL was in similar range [60].

Table 3.1. T-Peel force and fracture toughness properties of JuRALs

Parameters	**JuRAL1**	**JuRAL2**	**JuRAL3**	**JuRAL4**
F_{max} [N]	64.27±3	63.50±7.92	76.39±8.2	59.43±11
F_{av} [N]	28.51±5	33.69±0.5	35.31±3.6	30.37±5.5
Fracture Toughness (G) [KJ/m²]	1.14±0.2	1.34±0.02	1.41±0.13	1.21±0.22

Figure 3.4 shows the microscopic images of delaminated surfaces of aluminium and composite. It can be seen clearly that the epoxy and jute fibres are adhered to the aluminium. When analyzed the composite surface, it presents that at some points there were fibre pull-out and cohesive failure. Some spots were showing cracking in the adhesive layer, especially the resin rich areas. The reason of the resin rich and resin poor areas is already discussed. It is also evident from the delaminated surfaces of aluminium and composite that the delamination occurred on the composite side mostly rather towards aluminium. The porous oxide layer of anodized aluminium offered even interlocking as compared to jute composites. As the reinforcement of composite was made with low modulus yarn so the impact of fibre bridging was not as obvious as it should be in case of synthetic fibres. Therefore the complete, cohesive failure cannot be observed for reinforcements made with natural fibre.

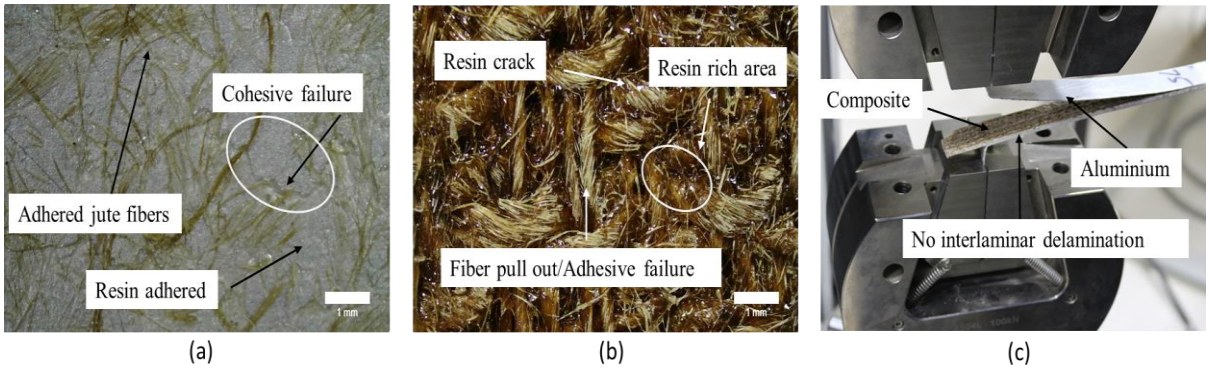

Figure 3.4. Microscopic images of the delaminated surface of (a) aluminium (b) composites (c) delamination phenomenon of JuRAL

3.3 Aluminium-Composite Bond Assessment with Floating Roller Peel Test

Figure 3.5 shows the typical force-extension curve of the floating roller peel test of the aluminium-composite bond. The curve has two zones: (a) crack initiation zone, (b) crack propagation zone. The crack initiation zone refers to the part of the curve where crack initiation starts. The highest force is required most of time in this part for the initiation of crack and matrix cracking. The second zone relates to crack propagation zone as in this zone the crack propagates with some fluctuation in the curve. The behaviour in this zone depends heavily on the type of failure, whether cohesive, adhesive, or intra-laminar fibre failure. Another factor which contributes to delamination properties in floating roller peel test is ductility of flexible adherend and adhesive layer. Since in current study only the type of adhesive material is changed for each set of samples so that its ductility will contribute significantly to final properties.

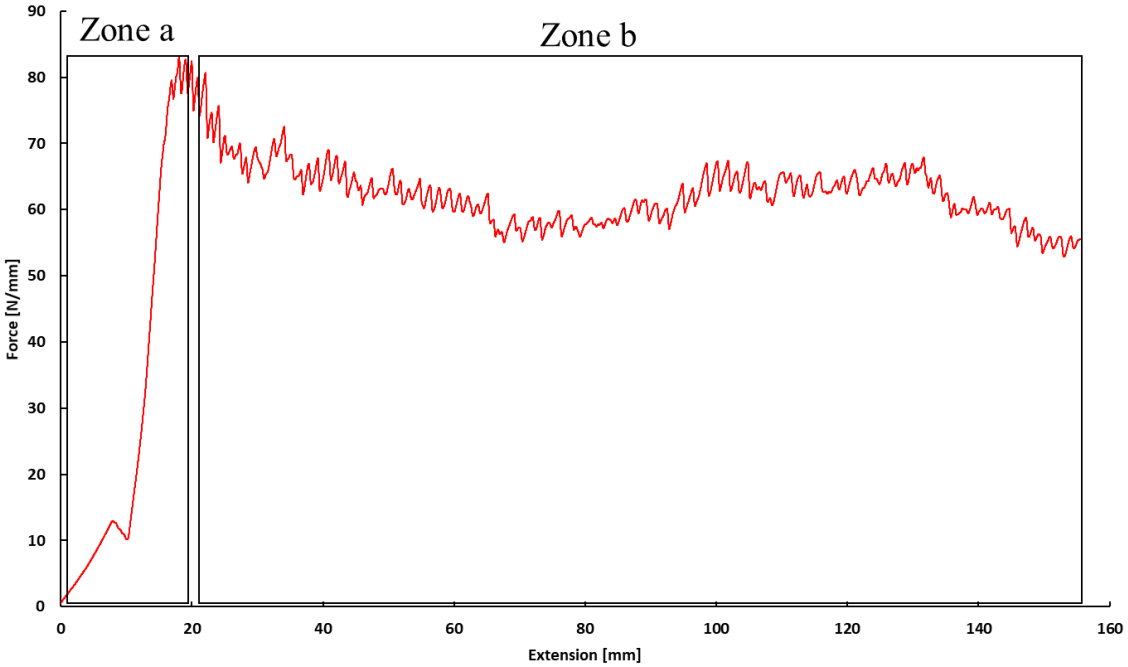

Figure 3.5. Typical force-extension curve of the floating roller peel test of the aluminium-composite bond

3.3.1 Aluminium-Jute Composite Bond Delamination Properties

Figure 3.6 shows the load-extension curves of aluminium-jute composite bond made with epoxy, PP and PVB matrix. The curves are clearly showing different delamination behaviour of each of aluminium-jute composite bond. The JE shows that there are sharp peaks in the curve. These multiple sharp peaks are due to the epoxy matrix, which is brittle. The curves of JP and JB show that there are different regions in the crack propagation zone; in some regions, the force increases while in some regions it decreases. This increase and decrease are due to non-uniform delamination. These non-uniform patches in the curve refer to different failure mechanism of each of bond. When the delamination behaviour of all three samples is compared, the JB has highest delamination force, followed by JP and JE.

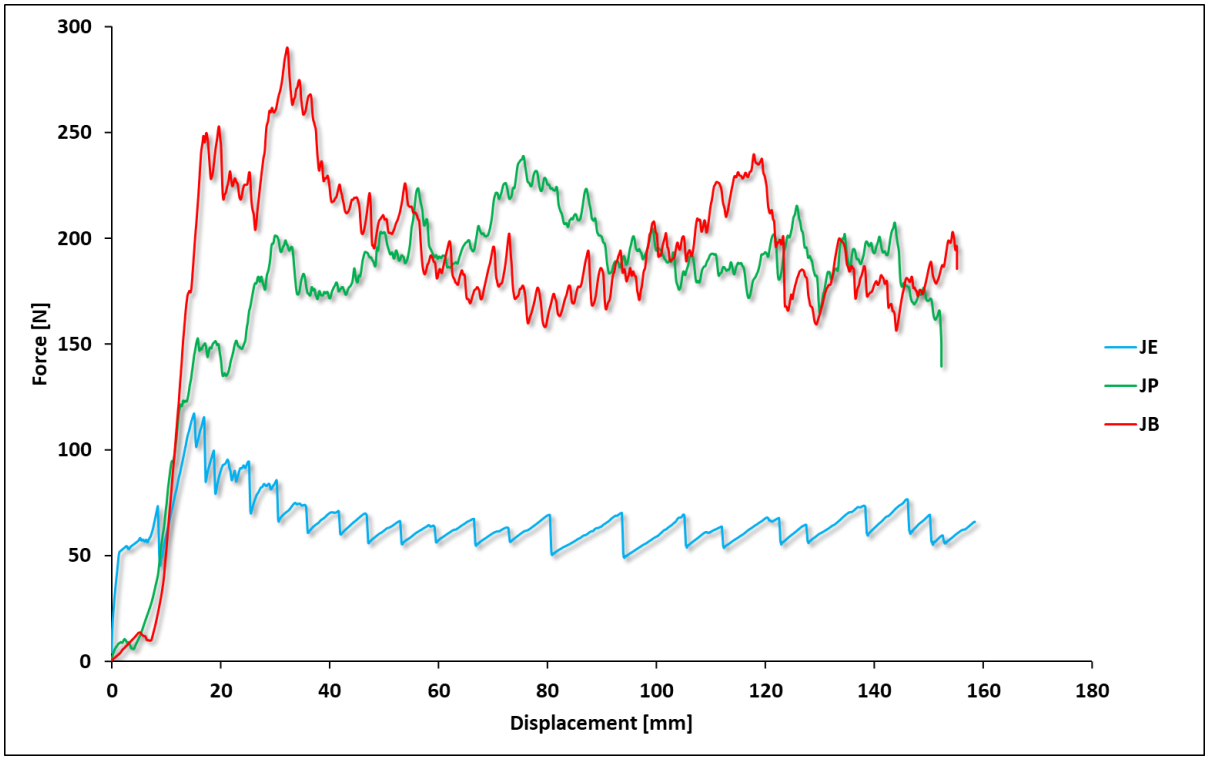

Figure 3.6. Typical force-extension curve of floating roller peel test of jute-aluminium bond with epoxy, PP and PVB

Figure 3.7 shows the delaminated surfaces of JE, JP and JB. From the figure, it can be seen that for JE, the aluminium surface was entirely wet with epoxy. For the JP and JB the aluminium has patches of adhered resin and delaminated surface, same is with the composite surface. The delaminated surfaces also show that there was some intra-laminar fibre failure for both PP and PVB matrix. The fibres can be seen clearly on the matrix, adhered with aluminium for JP and JB. The flexible adherend shape after removing from the machine also suggest about the delamination behaviour. In Figure 3.7 for JB, the aluminium is tilted backwards, showing the higher resistance offered by PVB based bond followed by JP and JE. This kind of delamination pattern also determines that the PVB bond showed higher ductility than counter PP and epoxy matrix. The failure between different interfaces, e.g. aluminium, composites, and adhesive layers, is another angle to understand this kind of behaviour. In jute-epoxy, it is evident that the interface of the adhesive layer with aluminium was too good that failure occurs towards the

composite interface. In jute-PP composite the mixed failure is seen, the failure occurs both towards aluminium and composite interface as the PP form mechanical interface, unlike epoxy. The jute-PVB composite is an interesting case as in spite of showing higher adhesive failure; it has high delamination force. It had excessive adhesive failure as well mainly towards the aluminium interface. This behaviour was due to high ductility and fibre-matrix interface that failure occurs towards the aluminium interface.

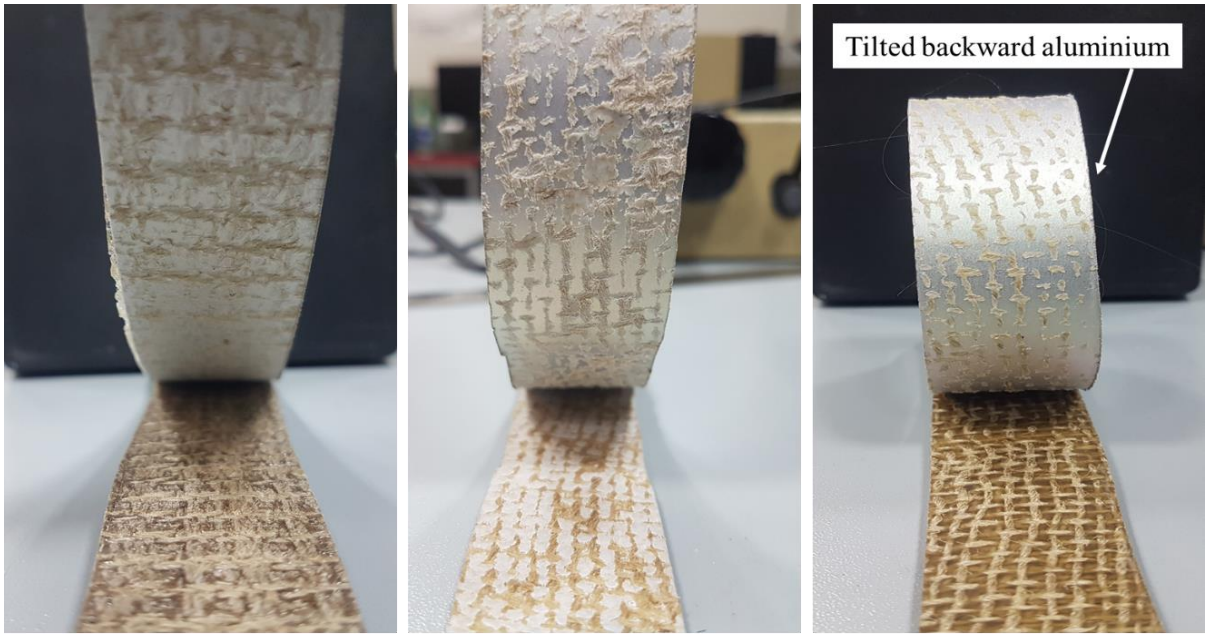

Figure 3.7. Comparison of de-bonded surfaces of the jute-aluminium bond of (a) JE (b) JP (c) and JB

Figure 3.8 shows the microscopic images of delaminated surfaces of JE, JP and JB. The JE is showing that matrix is uniformly distributed on aluminium with some jute fibre adhered. The composite part of JE is showing exposed jute fibres and matrix cracking. For both JP and JB, the delamination pattern for aluminium and composite is the same, with part of matrix adhered to aluminium and composite. When the composite part is observed, the jute fibres are clearly exposed in some places where the resin adhered to aluminium. Both JP and JB are also showing some intra-laminar fibre failure; this intra-laminar failure still considered better than adhesive

failure as the failure does not occur at the interface. The JE is also showing some adhered jute fibre on flexible adhered, but those fibres are usually loose fibres of jute yarn.

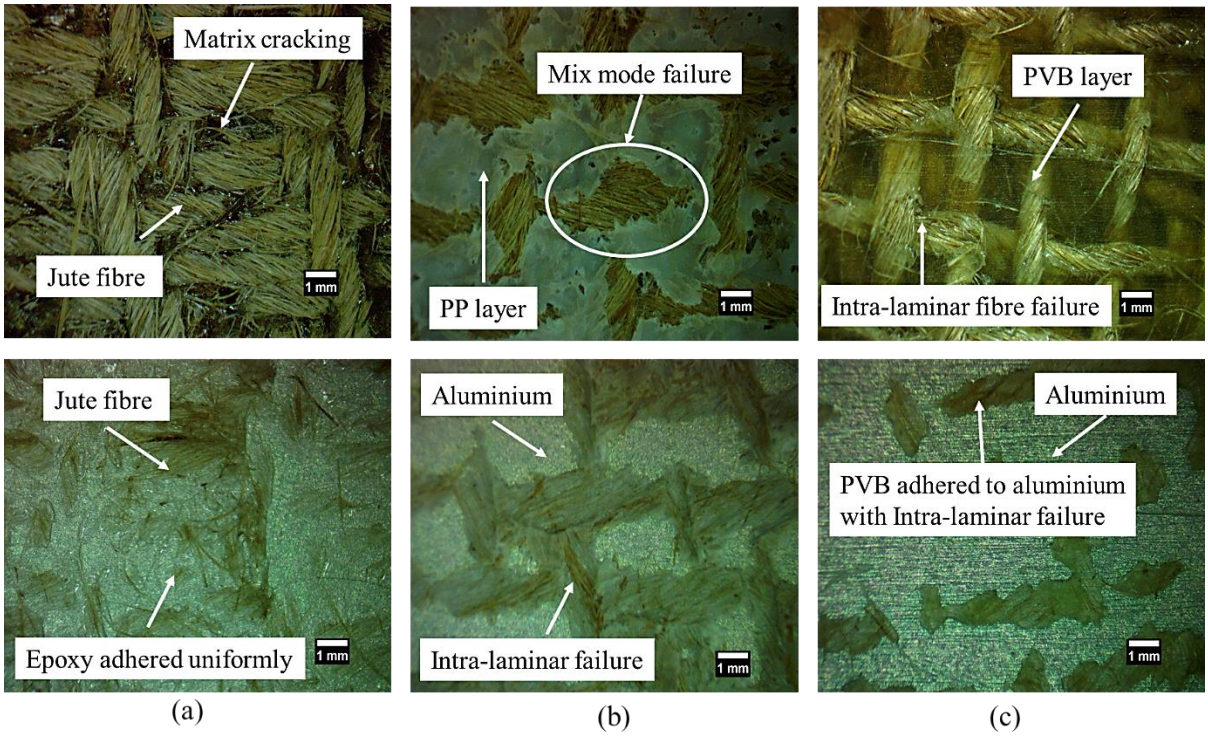

Figure 3.8. Microscopic view of delaminated surfaces of the jute-aluminium bond of (a) JE (b) JP and (c) JB

3.3.2 Aluminium-Aramid Composite Bond Delamination Properties

Figure 3.9 shows the typical force-extension curves of AE, AP, and AB. The curve shows that the AP has the highest delamination force, followed by AB and AE. When the behaviour of the AE is observed, despite the epoxy matrix, showing small spikes on the curve. The crack propagation zone is showing smooth delamination, and fibre did not adhere with matrix during delamination. The AB is also showing that after crack initiation, the crack propagated smoothly. The AP, however, had some unevenness in the curve both in crack initiation and crack propagation zone, which relates to uneven cracking of PP matrix.

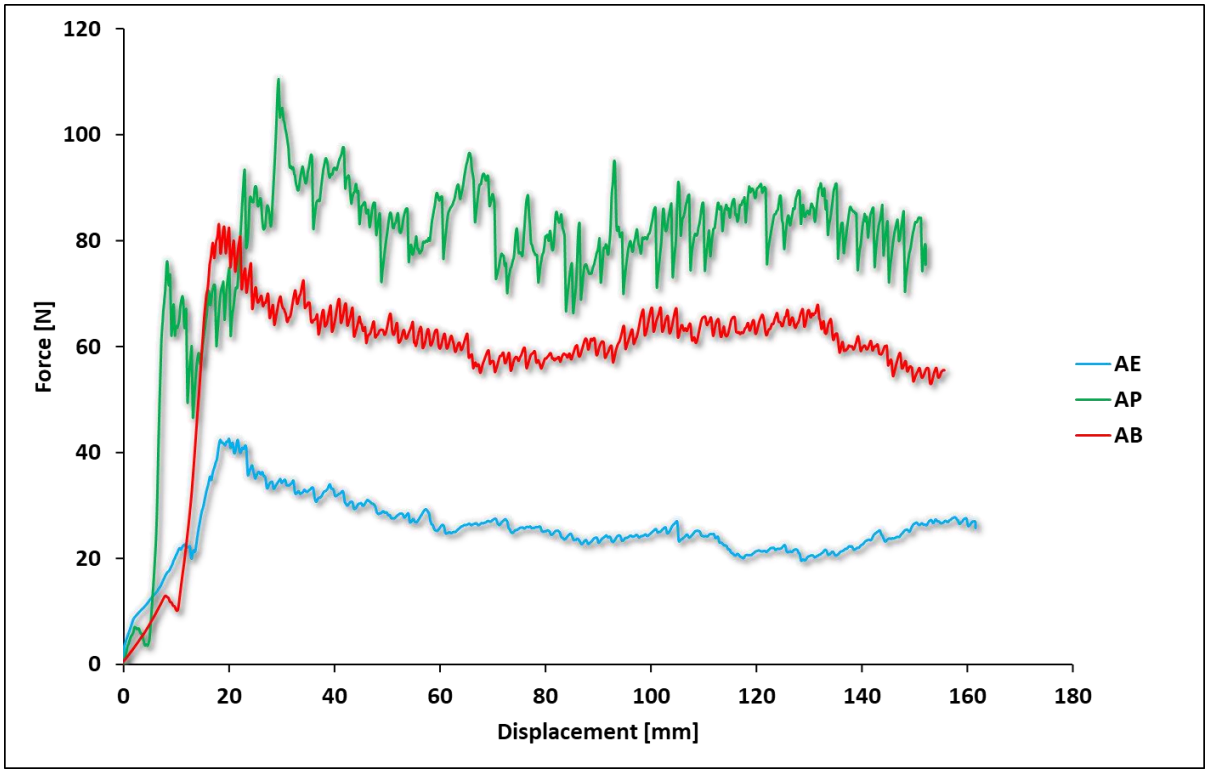

Figure 3.9. Typical force-extension curve of floating roller peel test of aramid-aluminium bond with epoxy, PP and PVB

The delaminated surfaces of AE, AP, and AB are showing that the matrix adhered with the aluminium clearly with no sign of aramid fibre pull-out (Figure 3.10). The composite is showing no sign of intra-laminar failure due to the nature of aramid fibres. The aramid fibres have excellent transversal strength. The flexible adherend (aluminium) of all three samples have different tilt, with highest in the AB followed by AP and AE. The adhesive layer adhered to aluminium is also showing the cross-weaving pattern of 2D plain woven aramid. This indicates that failure was a mainly adhesive failure, and the interface between aluminium-matrix was stronger than the composite interface. Even the failure pattern was the same, the different in the force was due to the ductility of the matrix and fibre-matrix interface.

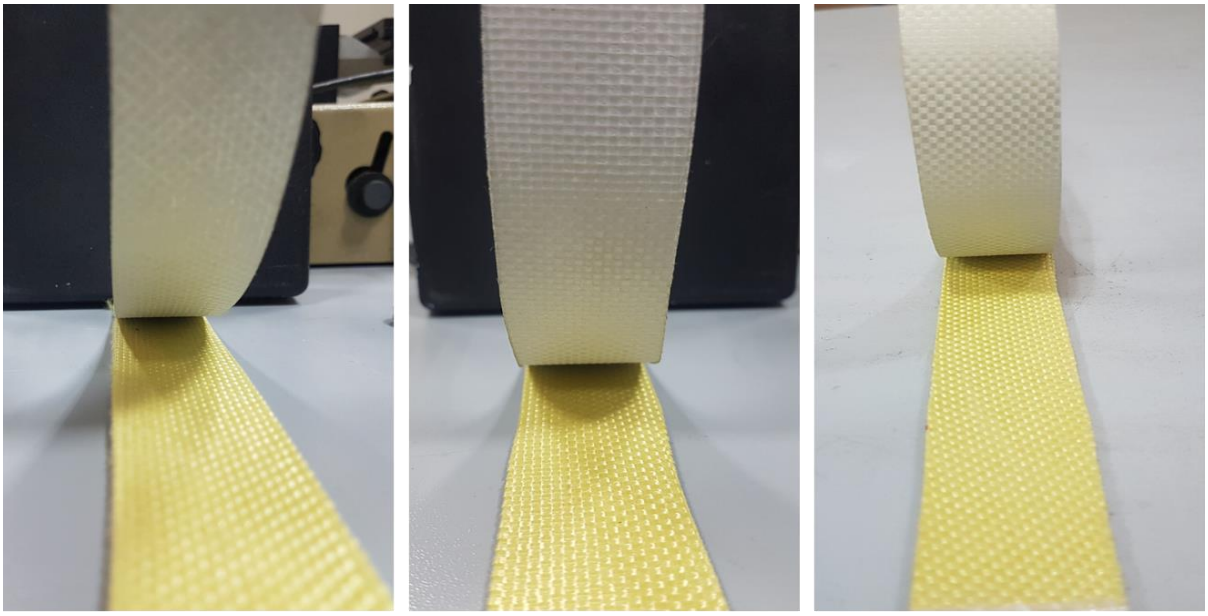

Figure 3.10. Comparison of de-bonded surfaces of the aramid-aluminium bond of (a) AE (b) AP (c) and AB

The microscopic images of AE, AP, and AB showing a similar kind of delamination surfaces and nature as presented in Figure 3.11. The composite part is showing that the fibres are intact to surface with no interlaminar or intra-laminar fibre failure. The aluminium surface is showing that the matrix adhered to the surface uniformly with no-sign of broken pattern. The possible failure was between composite and adhesive layer interface. The aluminium-matrix bonding dominated the bonding between matrix-composite. That is why this kind of failure mechanism was seen.

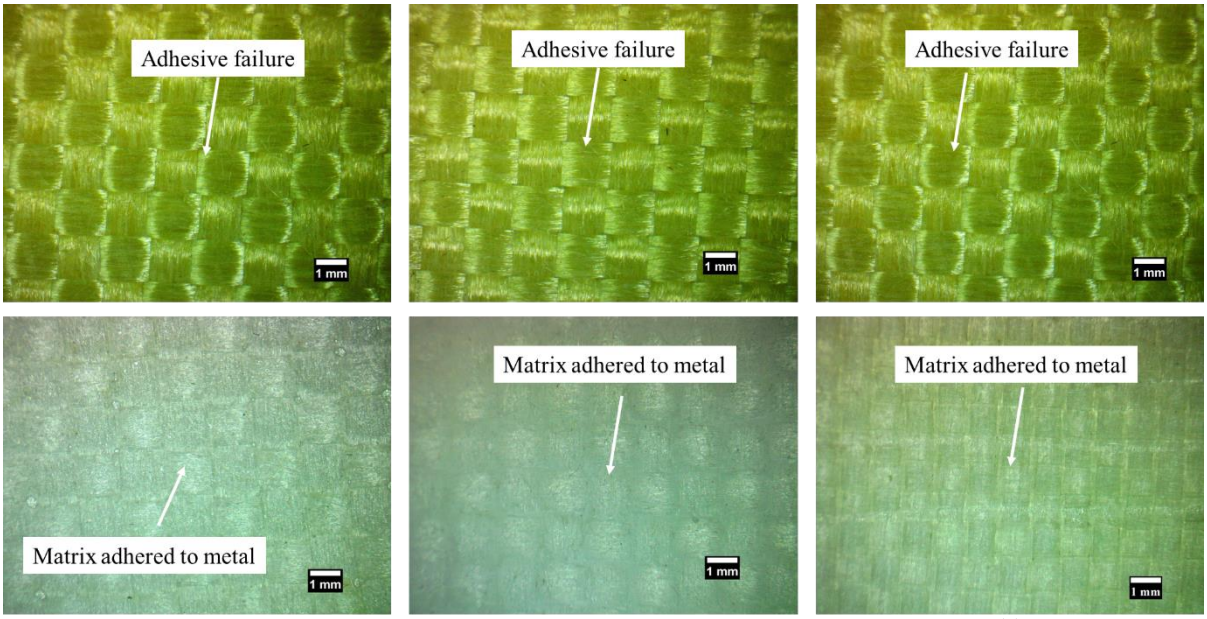

Figure 3.11. Microscopic view of delaminated surfaces of aramid-aluminium de-bonded surfaces of (a) AE (b) AP and (c) AB

3.3.3 Aluminium-Carbon Composite Bond Delamination Properties

Figure 3.12 shows the typical force-extension curves of CE, CP, and CB. The CE after initiation of crack follows the very smooth path. That mainly shows even crack propagation. The CP and CB are, however showing very different behaviour, the CP initially had very high crack imitation force followed by a decrease in force in the crack propagation zone. For the CB, the force keeps on increasing in the crack propagation zone with some variations.

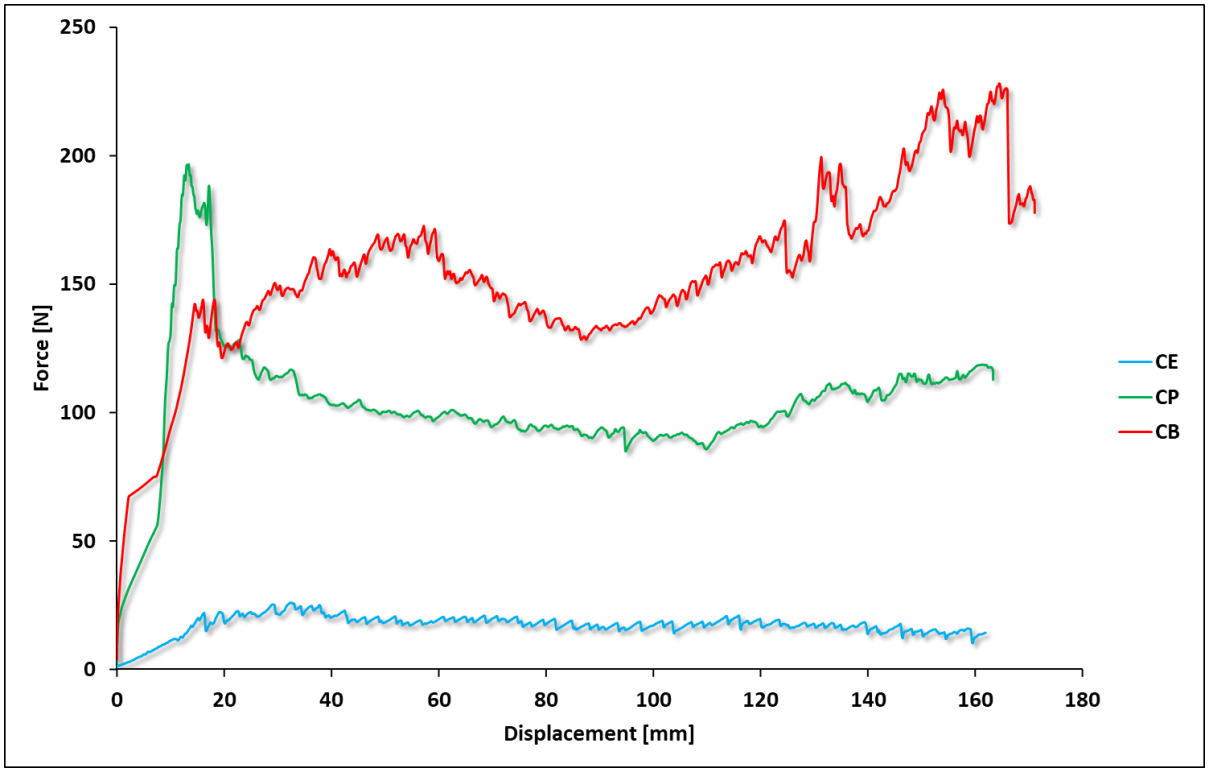

Figure 3.12. Typical force-extension curve of floating roller peel test of carbon-aluminium bond with epoxy, PP and PVB

The de-bonded surfaces of CE are showing that the matrix adhered to the aluminium and composite. There were some carbon fibres adhered with matrix showing the intralaminar failure, but the overall failure was a cohesive failure. The CP is showing adhesive failure with some intra-laminar failure. In intra-laminar failure patches, the adhesive layer was intact with aluminium and the carbon fibre can be seen on the matrix layer as well. For the CB, the adhesive failure occurred with intra-laminar failure. The adhesive failure was towards metal interface and with the progression, it converted to intra-laminar failure. The behaviour of CB curve shown in Figure 3.12 is also due to this kind of failure pattern. The intra-laminar and adhesive portions are mixed in CB (Figure 3.13). It can be established from the failure mechanism of these aluminium-carbon composite bonds, that in spite of dominant cohesive failure in CE the delamination force was higher in CP and CB. This was mainly due to highly

ductile thermoplastic matrix. Further, the intra-laminar failure is also considered better due to non-existence of interface failure.

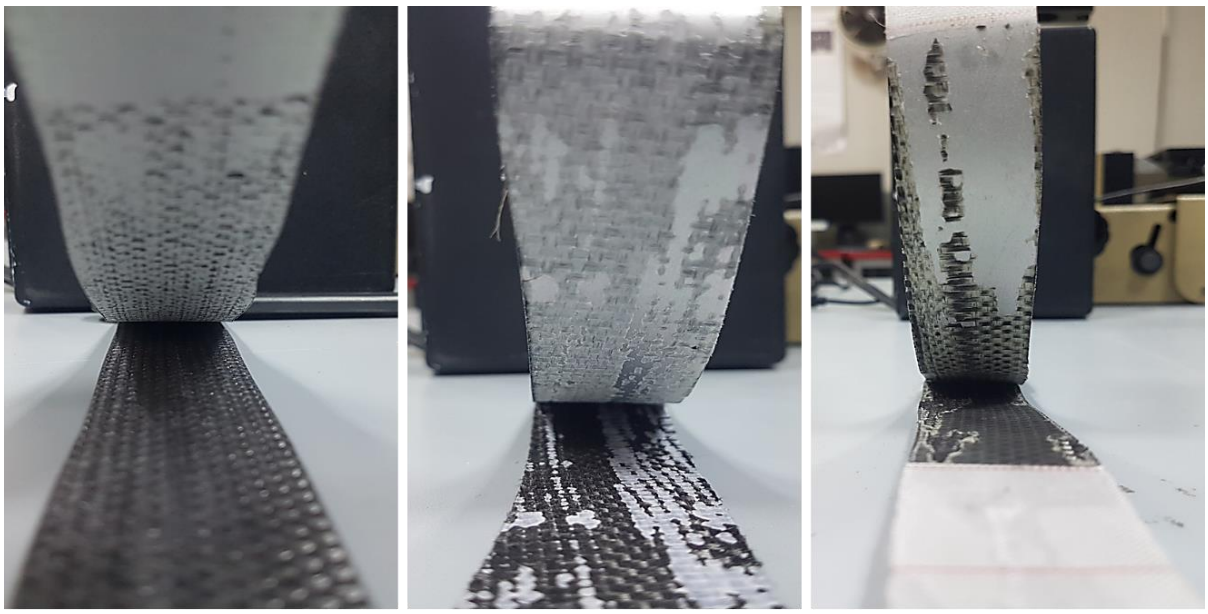

Figure 3.13. Comparison of de-bonded surfaces of the carbon-aluminium bond of (a) CE (b) CP (c) and CB

The microscopic images of delaminated surfaces clearly show the pattern of delamination of all three types of bond. The composite part of CE had visible matrix cracking and fragments of intra-laminar failure. The aluminium surface is showing that its surface is completely covered with epoxy and a small portion of the fibres also adhere to the matrix. On the other hand, the CP shows that there was a very low number of carbon fibres adheres to matrix which was adhered to the aluminium surface. The aluminium of CB had shown a very high amount of carbon fibres adhered to it; these higher intra-laminar failures was the reason of an increase in the delamination force in CB (Figure 3.14).

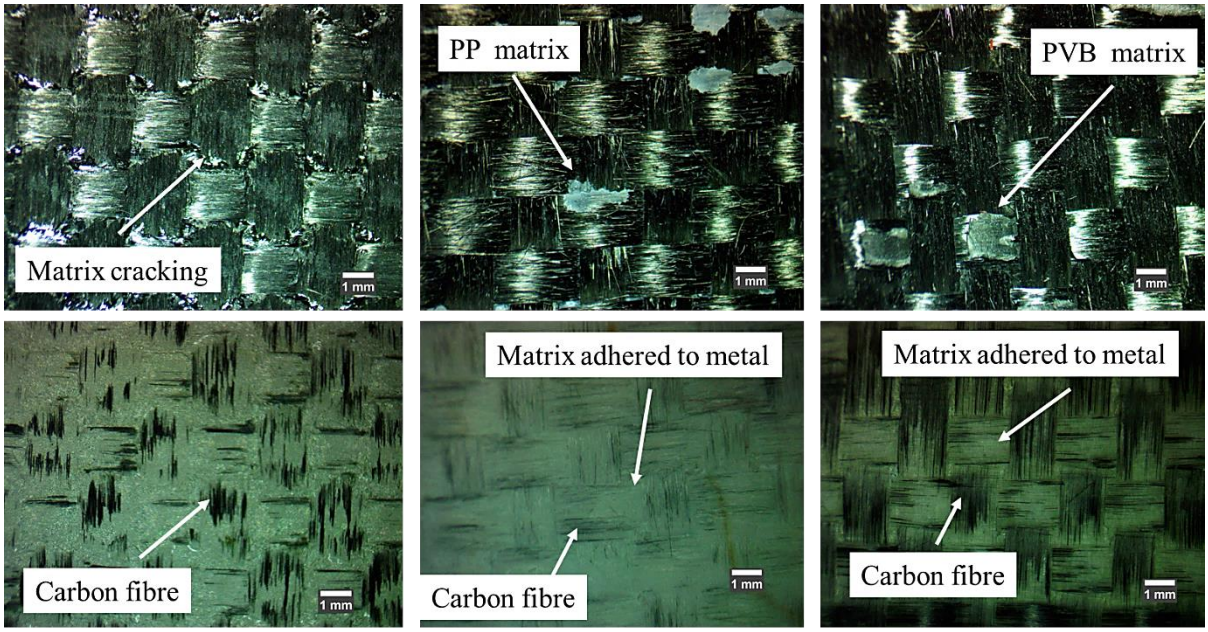

Figure 3.14. Microscopic view of delaminated surfaces of the carbon-aluminium bond of (a) CE (b) CP and (c) CB

3.3.4 Aluminium-Glass Composite Bond Delamination Properties

The typical force-extension curves of floating roller peel test of GE, GP and GB are shown in Figure 3.15. Unlike previous aluminium-composite bond with epoxy, the GE is showing the higher crack initiation and propagation force, the reason for this behaviour is excellent glass-epoxy interface. The GB had very steady crack propagation zone while GP had the crack propagation with some fluctuation.

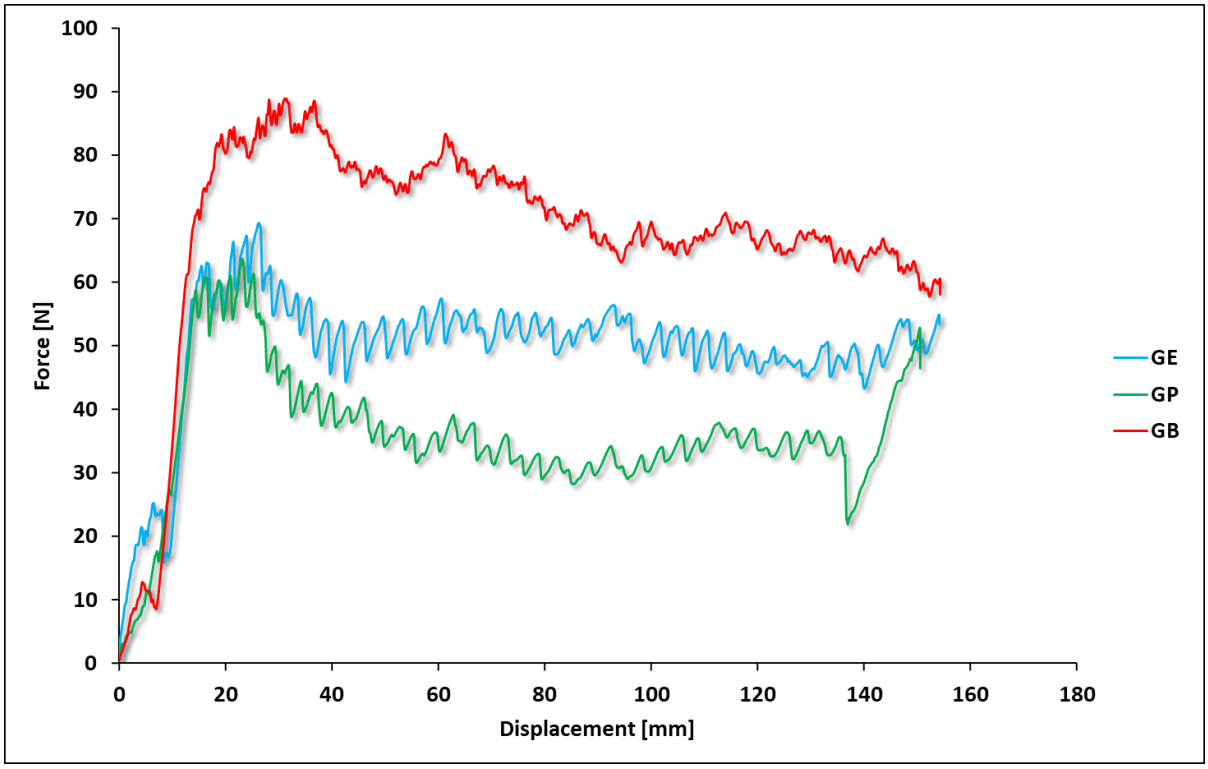

Figure 3.15. Typical force-extension curve of floating roller peel test of glass-aluminium bond made with epoxy, PP and PVB

The delaminated surface of GE is showing that the resin is adhered with aluminium along with some fibres. These fibres adhere as a result of the intra-laminar fibre failure. The overall failure mechanism was cohesive failure. The GP had fully covered aluminium surface with PP, while the composite surface is clearly exposed with no sign of resin and intra-laminar fibre failure. The dominant failure was adhesive failure and it happened at composite interface. The GB is also showing the aluminium surface fully covered with the PVB matrix. There was small intra-laminar fibre failure as well but the prominent failure mechanism was adhesive failure. The composite surface is showing light yellowish shade which is due to the PVB matrix (Figure 3.16).

Figure 3.16. Comparison of de-bonded surfaces of the aluminium-glass bond of (a) GE (b) GP (c) and GB

The microscopic images of delaminated surfaces show that for both GE and GB the composite part had some intra-laminar fibre failure. The aluminium surface of both GE and GB is showing that the matrix adhered to the metal completely. For the GP, although the matrix was adhered to the surface of aluminium, the composite part, however not showing any kind of fibre pull-out (Figure 3.17).

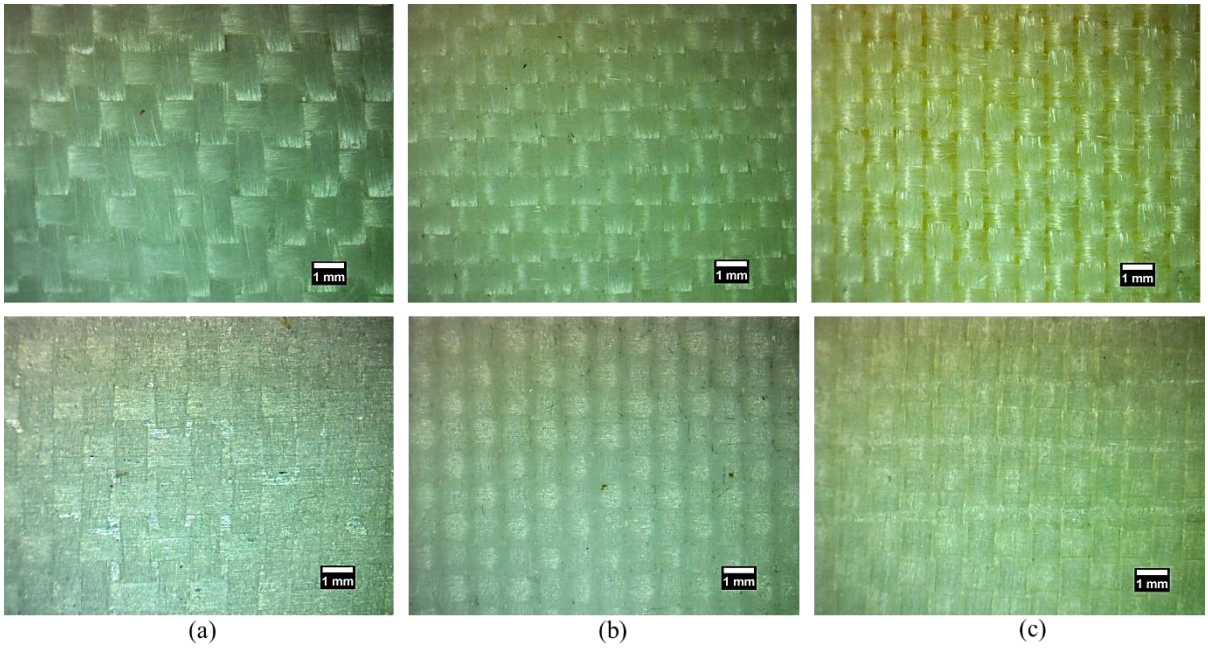

Figure 3.17. Microscopic view of delaminated surfaces of the aluminium-glass bond of (a) GE (b) GP and (c) GB

3.3.5 Aluminium-Composites Bond Properties Comparison

Figure 3.18 shows the comparison of F*av*, F*min* and F*max* of aluminium-jute composite bond made with epoxy, PP and PVB matrix for floating roller peel test. The JB had the highest F*max*, followed by the JP and JE. The reason of the highest properties of JB is its excellent adhesion with aluminium and plastic deformation of the thermoplastic matrix. The plastic deformation of the thermoplastic matrix caused difficult crack initiation and propagation. The JE, on the other hand, had a relatively low value of the maximum, average as well as minimum force. The reason is the high brittleness of the epoxy matrix, which cause it breakage at a lower force. For the JE there is not a vast difference in F*max* and F*av*, showing even delamination. For both JP and JB, the difference, however, is higher, which is showing an uneven delamination pattern.

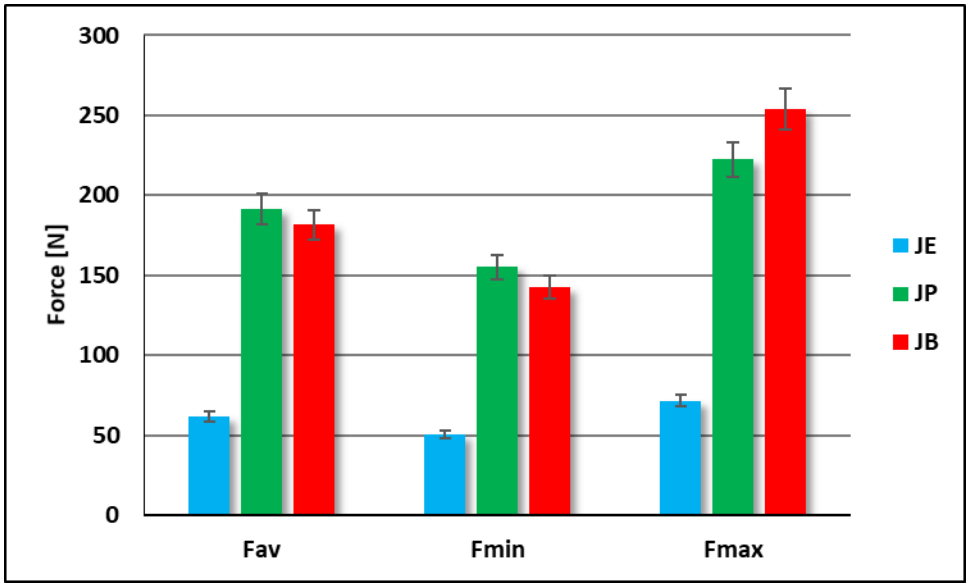

Figure 3.18. Comparison of average, minimum and maximum force of floating roller peel tests of jute-aluminium bond with epoxy, PP and PVB

The comparison of average, maximum and minimum force of AE, AP and AB is presented in Figure 3.19. The AP had highest F*max* followed by AB and AE. The F*av* and F*min* also follow the same pattern. The low value of the average, minimum and maximum force of AE is due to poor fibre-epoxy bonding that leads to poor delamination performance. For the AP and AB, although they have a high value of force, due to lack of intra-laminar fibre failure caused the relatively lower delamination force compared to other aluminium-composite bond.

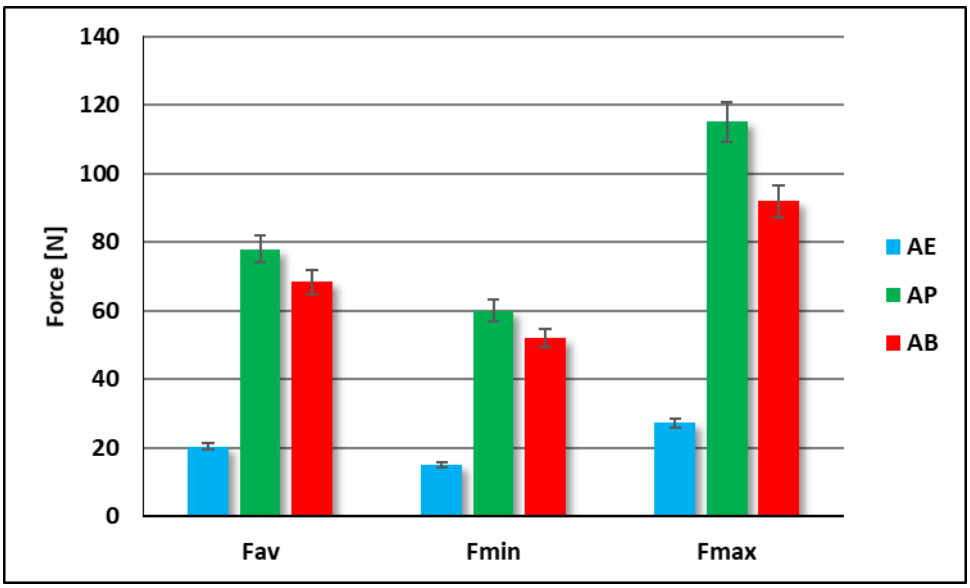

Figure 3.19. Comparison of average, minimum and maximum force of floating roller peel tests of aramid-aluminium bond with epoxy, PP and PVB

The comparison of average, minimum and maximum value of force for CE, CP and CB are shown in Figure 3.20. There is a huge difference in the properties of all three specimens. The CB has the highest values of force, followed by CP and CE. There are different factors which contribute to such kind of behaviour: (a) fibre-matrix interface; (b) metal-matrix interface and (c) nature of the matrix, as can be seen in Figure 3.13. The CE had very even delamination but due to poor matrix-fibre interface had lower properties. The CB, however, showed better fibre-matrix interface, but the pattern of delamination suggests that there was some adhesive failure also exist. The higher properties of the thermoplastic matrix as compared to thermoset matrix is due to the plastic nature of PP and PVB.

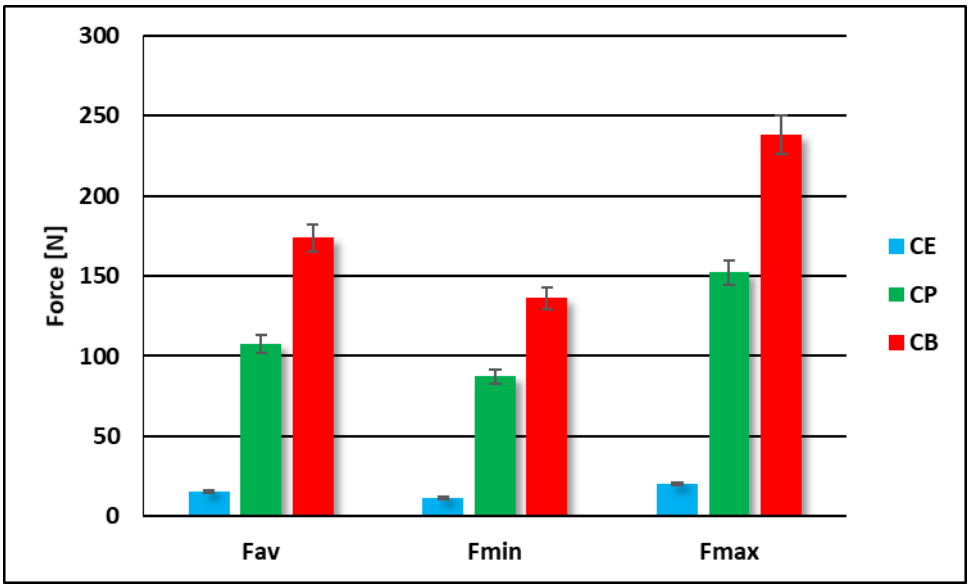

Figure 3.20. Comparison of average, minimum and maximum force of floating roller peel tests of carbon-aluminium bond with epoxy, PP and PVB

Aluminium-glass composite made with epoxy, PP and PVB had different behaviour compared to previous metal-composite bond. The relatively better properties of GE were due to improved fibre-matrix interface of glass-epoxy. Along with cohesive failure, the intra-laminar fibre

failure was also seen in GE. The GB had overall better properties due to better fibre-matrix interface and plastic deformation of the matrix (Figure 3.21).

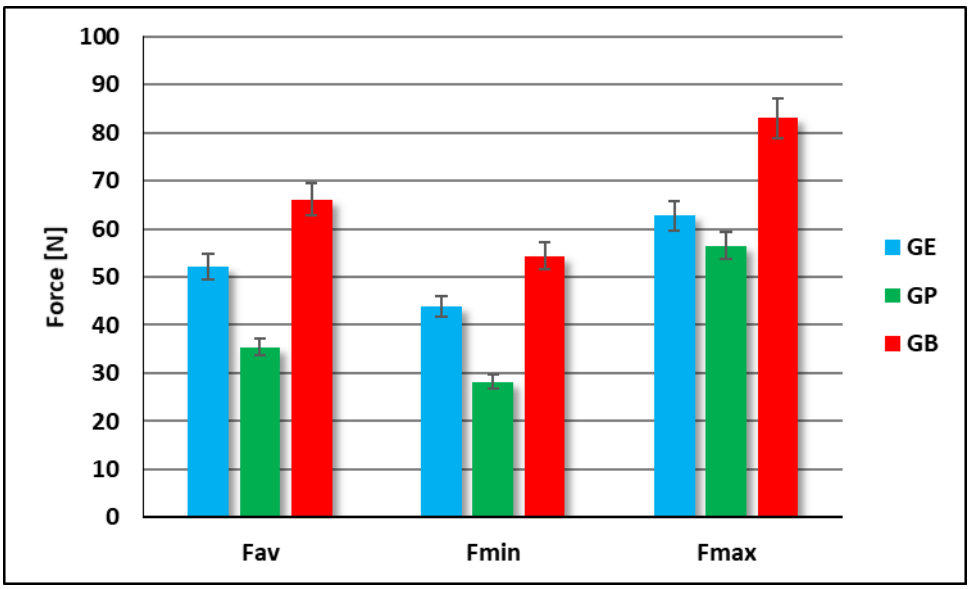

Figure 3.21. Comparison of average, minimum and maximum force of floating roller peel tests of glass-aluminium bond with epoxy, PP and PVB

3.3.6 Fracture Toughness Comparison of Aluminium-Composite bonds

The fracture toughness of all the samples was calculated as per standard mentioned earlier in section 2.3 and using equation 6. The fracture toughness comparison tells about the overall properties of materials and how the failure mechanism effect it. Figure 3.22 shows the comparison of fracture toughness of different metal-composites bonds made with different fibers and matrix. It is showing the overall the thermoplastic matrix has high fracture toughness as compared to epoxy. Within the different thermoplastic matrix high fracture toughness was achieved for jute and carbon due to its high intra-laminar failure. The high adhesive failure in case of aramid and glass caused overall low fracture toughness. The epoxy has high fracture toughness with jute and glass due to high fraction of intra-laminar failure and further these are low modulus yarn. If overall fracture toughness is compared with all fiber and matrix, the PVB showed that it was effective with all kind of reinforcements.

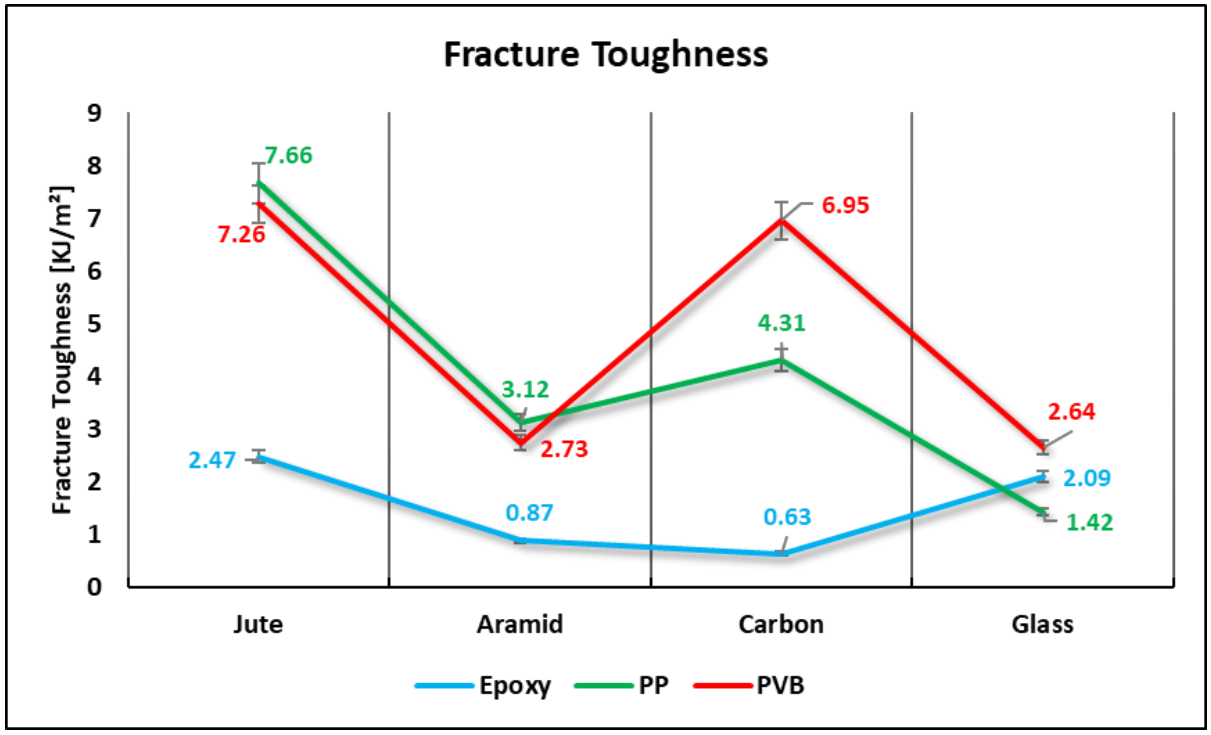

Figure 3.22 Comparison of fracture toughness of different composites-metal bond made with epoxy, PP and PVB

3.4 Conclusion

The surface of aluminium was prepared using PAA, the quality of anodized surface was checked using a water contact angle. The water contact angle gives the estimation of surface free energy. The metal surface with a lower water contact angle has a high surface energy and one with high contact angle has lower surface energy. The anodized aluminium surface had a lower water contact angle as compared to bare, mechanically prepared, and oxidized aluminium surfaces. The delamination properties of 3D woven jute composites and aluminium were accessed using T-peel test. The results showed that the delamination properties were governed by the nature of material rather the different type of structures. As long as the nature of bonding material is same the properties will also remain same. The properties of aluminium-composites bond made with different fibres and matrices was accessed using a floating roller peel test. The rigid adherend was made with composite and flexible adherend was of

aluminium. When the properties of aluminium-jute composites were compared made with epoxy, PP and PVB matrix. The highest delamination force was obtained from PVB matrix followed by PP and epoxy. The PVB and PP had an adhesive failure as a predominant failure mechanism. The PP and PVB matrix were adhered with aluminium throughout the delaminated surface, the jute fibres were also adhered with the matrix showing intra-laminar fibre failure. The aluminium surface of epoxy was fully covered with a matrix, showing predominately cohesive failure. For the aluminium-aramid bond the PP has the highest delamination force followed by PVB and PP. The delamination pattern suggests the surface of aluminium was fully covered with the matrix with no sign of intra-laminar fibre failure. The aluminium-carbon fibre bond showing poor delamination properties of epoxy and superior for PVB matrix, the properties of PP were in between. The delamination pattern suggests that the epoxy covered the surface of metal completely, while for PP and PVB there was mix adhesive failure. However, for both PP and PVB the intra-laminar fibre failure was also observed, the PVB however had more extensive intra-laminar fibre failure. The aluminium-glass bond had the highest properties for PVB followed by epoxy and PP. The epoxy glass interface caused better delamination response as compared to previous aluminium-composite bond. Both epoxy and PVB had some intra-laminar fibre failure, showing excellent bonding. The PP had a cohesive failure, but no intra-laminar fibre failure was observed. Results of thermoplastic based bonds also shows that in spite of absence of cohesive failure the delamination force was still higher than epoxy, it shows that the plasticity and ductility of matrix has more significant effect than type of failure. The fracture toughness comparison shows that the thermoplastic matrix have high fracture toughness and PVB was effective with all type of reinforcements.

Chapter 4. 3D Jute Reinforced Composites and FMLs Monotonic Properties

This chapter concerns the monotonic properties of optimizing 3D woven structure for FML fabrication and then subsequent hybridization of optimized 3D woven jute fabric with 2D woven fabric. The tensile and flexural tests were conducted for both optimization and hybridization of 3D woven structures. The result shows that the OTT woven structures are better for FML fabrication than other types of structures. While the hybrid reinforced FMLs were made with 2D /3D reinforcement and epoxy, PP, and PVB matrix, respectively. The hybrid FMLs had more consistent properties than constituent composites. The epoxy-based composites and FMLs showed overall higher tensile and flexural properties, but the PVB based composites and FMLs also showed very promising performance as a possible replacement of epoxy. The flexural properties of hybrid-PP-based FMLs were very poor due to premature failure.

4.1 Optimization of 3D Woven Reinforcement for FML Fabrication

4.1.1 Tensile Test of 3D Reinforced Composites and FMLs

JuRAL is made of aluminium and Jute fibre reinforced composite, so present very distinct tensile properties compared to its constituents. Figure 4.1 shows the typical stress-strain curve for JuRALs. The curve presents that at the start, both stress and strain increase proportionally until the start of the matrix crack around 2.2% strain, then the strain keeps on increasing with little to no rise in tensile stress. Then at the end of the curve there are two slopes, at lower and higher stress level. The explanation of high tensile fracture strain is that the JuRAL is comprised of aluminium and composite, as a tensile fracture strain of aluminium is higher than composite layer so damage begin from composite layer and then transmit to aluminium layer [163]. In JuRALs sandwiching JFRCs with aluminium has given both extensibility and load-bearing capability which is not achievable alone with composites.

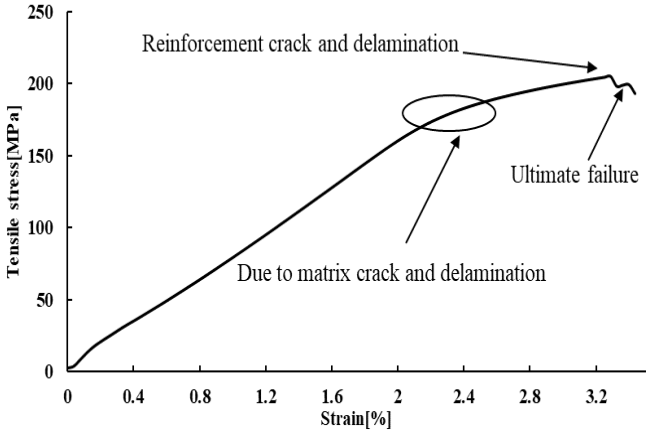

Figure 4.1. Typical tensile stress-strain curve of JuRAL

Out of two slopes at the end of the curve as mentioned earlier, one slope at ultimate load and other which is relatively at lower force is at ultimate failure. After reaching at maximum load the curve shows a steep decrease triggered by the interface debonding due to matrix cracking. Consequently, the applied load rose at a comparatively smaller slope compared with the former until ultimate failure [164]. There is a net increase in tensile strength of JuRAL as compared to

JFRC due to two reasons; first adding aluminium above and below the jute composite and the second reason was anodizing of aluminium which improved bonding significantly [165]. In JFRC, only fibres and epoxy determines the mechanical properties, while in JuRAL metal also played a crucial role in properties along with fibre and epoxy [38].

Figure 4.2 shows the comparison of stress-strain curves of static tensile test of JFRCs, JuRALs and aluminium.

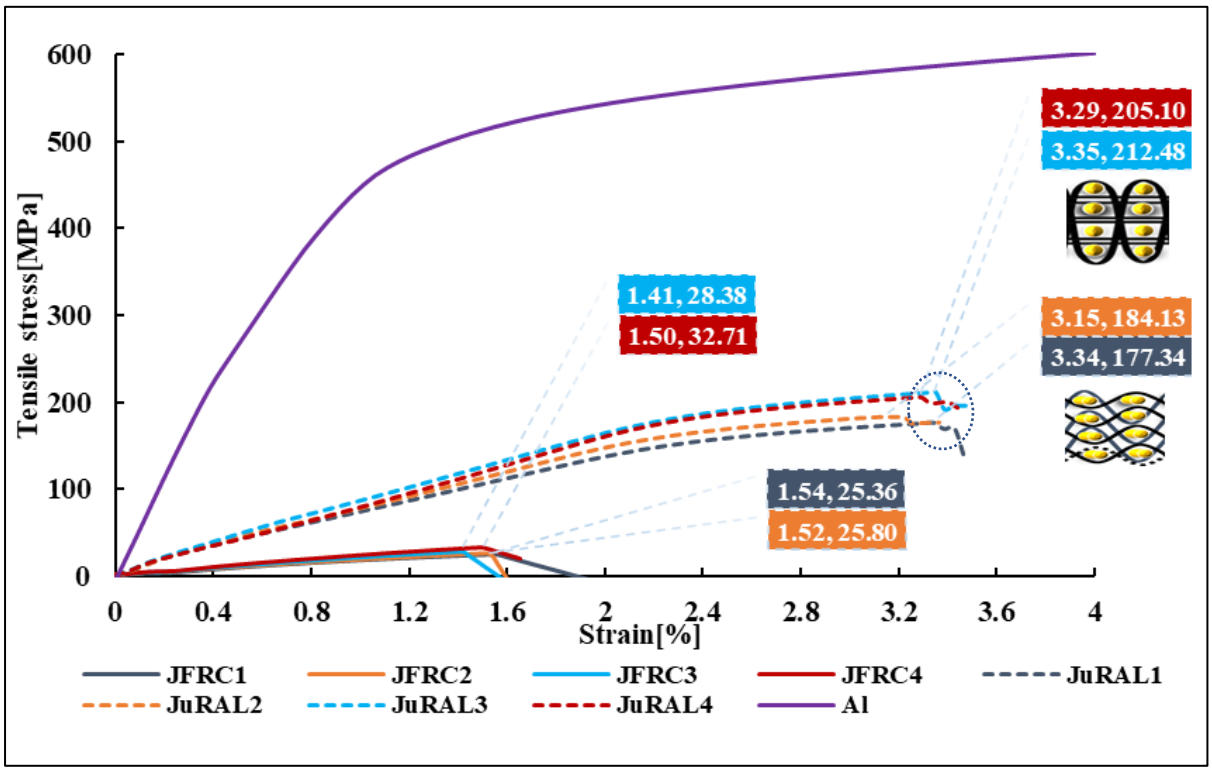

Figure 4.2. The average tensile stress-strain curves of JFRCs, JuRALs and aluminium

The JFRCs and JuRALs reinforced with TT-interlocked fabrics, both have high tensile strength. This increase in composites had been due to low crimp of TT interlocked structures than LL interlocked structures. while in JuRALs there was another factor which had influenced to the tensile properties was MVF. The higher the MVF more dominant will be the effect of the metal. That is why higher tensile strength was achieved for JuRAL3 and JuRAL4 than JuRAL1 and JuRAL2, due to the coupled effect of MVF and interlocking pattern of the jute

reinforcement. The tensile fracture strain is almost double for JuRALs as compared to JFRCs, the reason for this high fracture strain is already described. JFRC break with a sharp, steep curve, unlike JuRAL due to brittle nature of thermoset resin and absence of aluminium. In JuRALs before failure the sample experience different mechanism, the failure trigger with resin cracking which leads to delamination between aluminium and composite. Once the delamination begins, the crack spread more quickly. Table 4.1 shows the tensile properties of JuRALs and its constituents composites.

Table 4.1. Tensile properties of JFRCs and JuRALs

Properties	**JFRC1**	**JFRC2**	**JFRC3**	**JFRC4**	**JuRAL1**	**JuRAL2**	**JuRAL3**	**JuRAL4**
Tensile Strength [*MPa*]	25.36± 0.0.38	25.80± 0.43	28.38± 0.59	32.71± 0.43	177.34± 2.39	184.13± 3.40	212.48± 2.82	205.10± 3.48
Tensile Strain [%]	1.54± 0.045	1.52± 0.047	1.41± 0.052	1.50± 0.05	3.34± 0.1	3.15± 0.11	3.35± 0.12	3.29± 0.09

The dominant failure mechanism observed in JuRAL was delamination, matrix crack, metal crack and fibre failure, as shown in Figure 4.3.

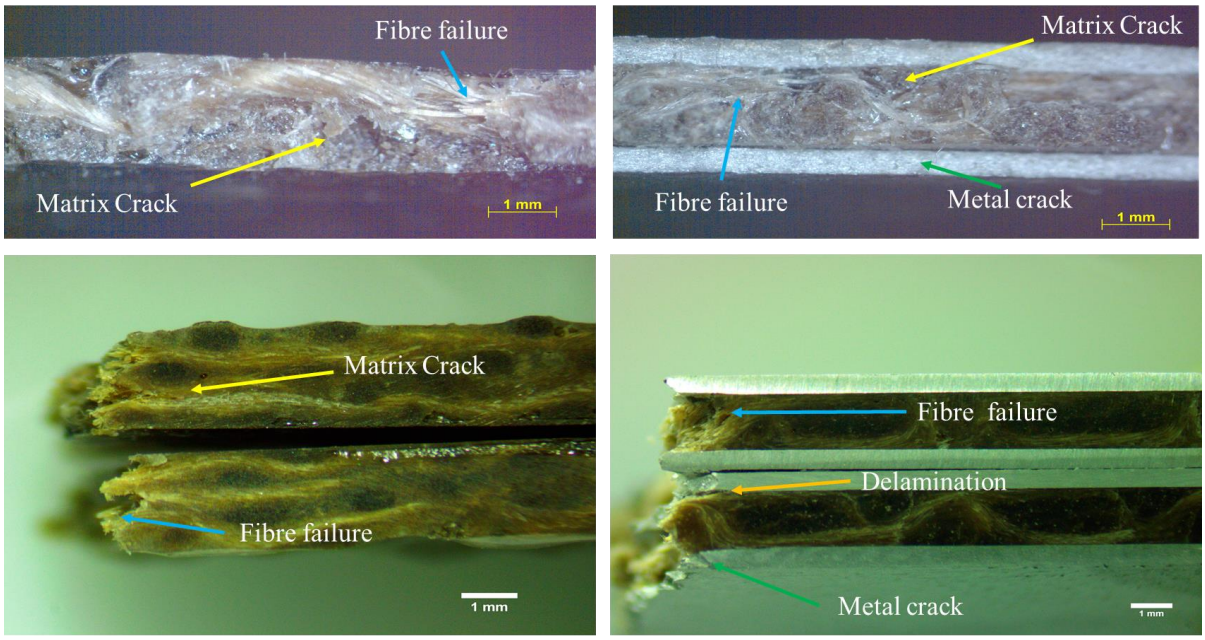

Figure 4.3. Microscopic images of (a) JFRC and (b) JuRAL showing side and fracture face after the tensile test

It confirms that there was a small debonding among the aluminium and composite layer. This debonding before complete failure caused two slopes at the failure point in the curve as can be seen in Figure 4.1. There was one more element which contributed for such kind of failure was the low modulus and low stiffness of jute fibre, the fibre bridging effect is not very obvious with jute reinforcement in JuRALs as that is more apparent with synthetic reinforcement, so the sharp crack was observed running across the thickness direction without spreading. As the major role against loading was from aluminium, and the pattern of failure also justifies such behaviour [166].

4.1.2 3D Jute Reinforced Composites and FMLs Flexural Properties

The flexural properties of JFRCs and JuRALs were got using the already explained procedure. Figure 4.4 shows the typical stress-strain curve of the flexural test of JuRAL.

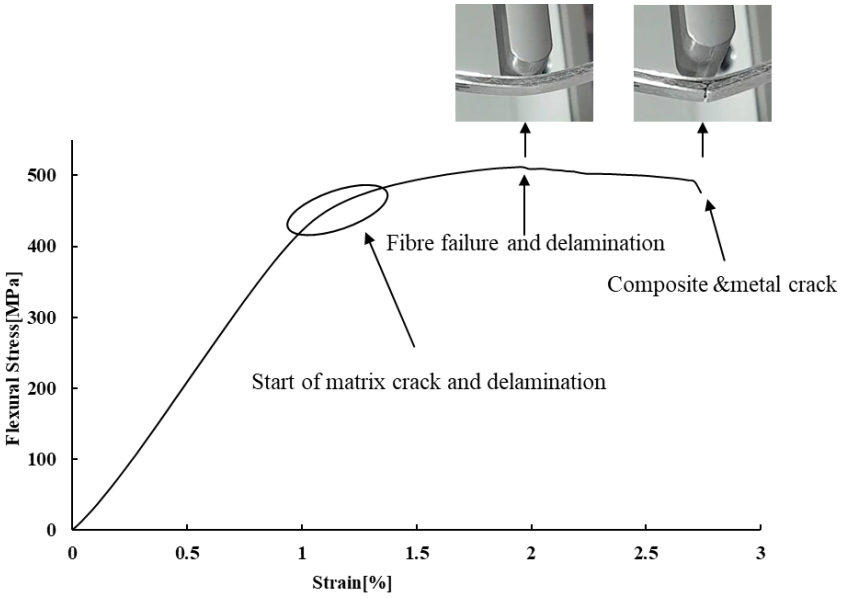

Figure 4.4. Typical flexural stress-strain curve of JuRAL

Generally, during a flexural loading of JuRAL, the stress keeps on increasing with bending, then a specific point comes when aluminium alloy delaminates and break. The delamination starts as a result of matrix cracking. Once the matrix cracks, the delamination spread to a larger area. This delamination of the aluminium layer in the case of the bending test is due to an increase in shear forces [96]. In the FMLs, unlike FRC, there are other factors involve which determine the properties, e.g., delamination, metal cracking. The curves show that for JuRAL, there is a region of strain hardening where smaller strain is produced with higher force than in the second region more strain is produced with little force up to failure, the reason of the strain hardening is that both aluminium and JFRC resist the bending. At maximum stress, the shear forces reach to the maximum extent. The maximum stress point can also be seen in the graph. There is a slight drop in the curve after reaching maximum stress; this drop is due to matrix cracking or sometimes fibre breakage at the micro-level. After the initial drop in stress, the aluminium-composite start delamination. At the ultimate failure, the delamination spread to a larger area, the composite and non-loading side aluminium breaks. During the flexural test, both aluminium sheets act in a different way; the outer aluminium sheet cracks while the

loading side aluminium sheet tends to delaminate, the delamination occur between aluminium-composite. Flexural properties of JuRAL are not only governed by properties of constituent materials, but the adhesion between aluminium and composite also plays a major role in deciding the final properties. The trend of rise in bending properties is the same for all types of JuRALs. The overall flexural properties of JuRALs were higher than respective JFRCs as shown in Table 4.2.

Table 4.2. Flexural Properties of JFRCs and JuRALs

Sample ID	**JFRC1**	**JFRC2**	**JFRC3**	**JFRC4**	**JuRAL1**	**JuRAL2**	**JuRAL3**	**JuRAL4**
Flexural Strength [MPa]	38.91± 1.16	43.80± 1.36	26.59± 0.56	17.38± 0.37	511.98± 6.91	495.81± 9.17	553.54± 7.36	554.02± 9.42
Flexural Strain [%]	2.58± 0.08	2.17± 0.06	2.26± 0.07	2.12± 0.04	1.94± 0.07	1.70± 0.06	1.97± 0.07	2.05± 0.06

Figure 4.5 shows the average flexural stress-strain curves for the flexural test of JFRCs and JuRALs. The flexural strength of JFRC1 and JFRC2 was higher than JFRC3 and JFRC4. The JFRC1 and JFRC2 are LL interlocked while JFRC3 and JFRC4 are TT-interlocked, for LL-interlocked structures the yarns are placed in layers so more resistance to bending as compared to TT-interlocked structures, that is why the flexural strength of JFRC1 and JFRC2 was more than JFRC3 and JFRC4. On the contrary, the flexural strength of JuRAL3 and JuRAL4 was higher than JuRAL1 and JuRAL2, that was mainly due to higher MVF as discussed previously. Both interlocking pattern of reinforcement and MVF have contributed to determine the final properties. There is a sudden dip in the JuRAL2 curve after reaching ultimate stress even though its MVF is higher than JuRAL1, this dip was due to the concentration of shear forces and debonding to a larger area as can be seen in Figure 4.5.

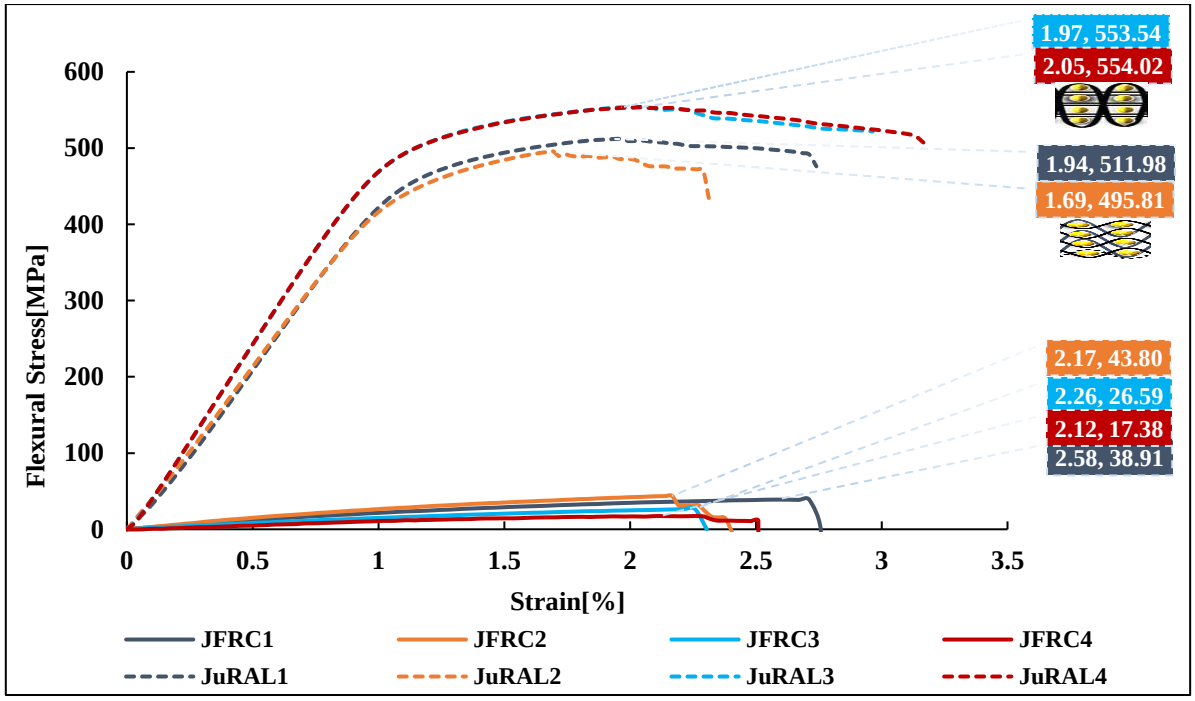

Figure 4.5. The average flexural stress-strain curves of JFRCs and JuRALs

The most common failure mechanisms observed in JuRALs were metal cracking, fibre pull out, matrix cracking and delamination as observed in the case of the tensile test while in JFRCs the dominant failure mechanism were matrix cracking and fibre pullout. However the mechanism of failure in flexural loading was different as compared to tensile loading. In flexural test, the metal cracking was observed in the non-loading aluminium sheet, which was due to stress concentration. Matrix cracking indicated the brittle failure, and this pattern of cracking was due to the nature of reinforcement material as already explained. From Figure 4.6 it can also be seen that the failure region of JuRALs is limited to the area where the bending force is applied, the delamination was not spread to larger areas. This is due to: (a) excellent metal-composite bonding (b) 3D woven reinforcement which reduce the crack propagation [11].

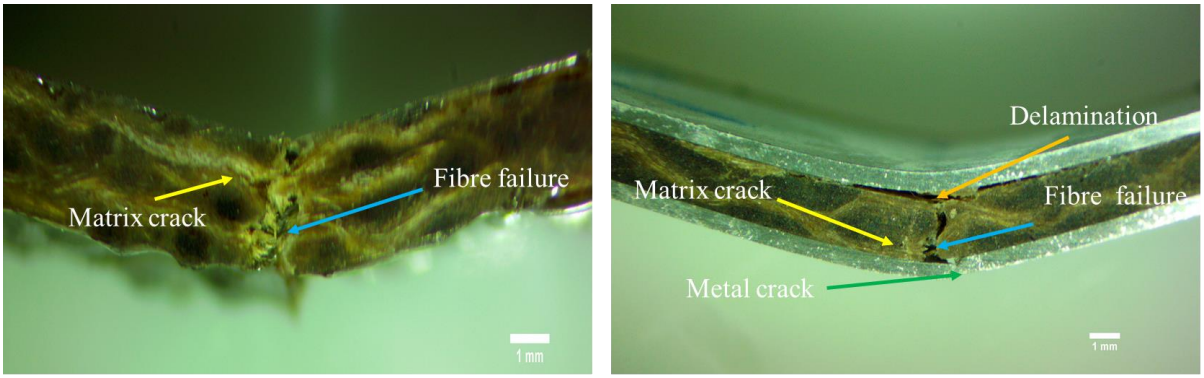

Figure 4.6. Microscopic images of tested specimens of (a) JFRCs (b) JuRALs after the flexural test

4.2 3D Jute Reinforced Hybrid Composites and FMLs Characterization

4.2.1 3D Jute Reinforced Hybrid Composites and FMLs Tensile Properties

The tensile properties of different hybrid reinforced composites and FMLs was determined to check the effect of hybridization and matrix. As the 3D jute reinforcement was sandwiched between 2D woven skin and along with different matrix, so all these parameters will alter the final tensile properties.

A. 3D Jute Composites and FMLs

Figure 4.7 shows the stress-strain curve of 3D jute reinforced FMLs and its constituent composites. The JCP curve depicts the behaviour of PP matrix, low modulus, and low strength. The slight hook at the end of the curve in JCP was appeared due to mismatch of PP and jute interface, as the reinforcement get exposed after the crack of the PP matrix, and the PP did not impregnate the fibre completely. Between JCE and JCB, the JCE initially showed high stiffness and then broke with a relatively lower value of tensile stress. The fracture of JCE earlier than JCB was due to the brittleness of epoxy resin. On the other hand, the JCB had shown more strain with high rigidity. When compared the JCB and JCP, the tensile strength was quite higher for JCB. The factors which contributed towards this kind of stress-strain

behaviour of 3D jute reinforced composites were the nature of the matrix and fibre-matrix interface. For JCB overall better properties were achieved due to improved fibre-matrix bonding and high stiffness of PVB. Figure 4.7 shows the stress-strain curves of 3D jute reinforced FMLs. The trend of the results is almost similar to composite with failure strain pattern follows the pattern of matrix properties. Another factor which plays a vital role in the final properties' determination of FMLs was the metal-composite interface. All three FMLs shows similar behaviour until the elastic region. In the non-elastic region, all three FMLs deforms differently. The JFE had a brittle breakage and relatively low strain to failure. The JFB after reaching ultimate tensile strength show further strain, as at ultimate tensile strength there was slight delamination due to resin crack and then ultimate failure at a relatively lower strength. The JFP showed a substantial amount of strain before ultimate failure. That is due to delamination between aluminium-composite and after that aluminium keeps on elongation. The elongation in JFP was due to aluminium as the composite and aluminium delaminated at F*max.*

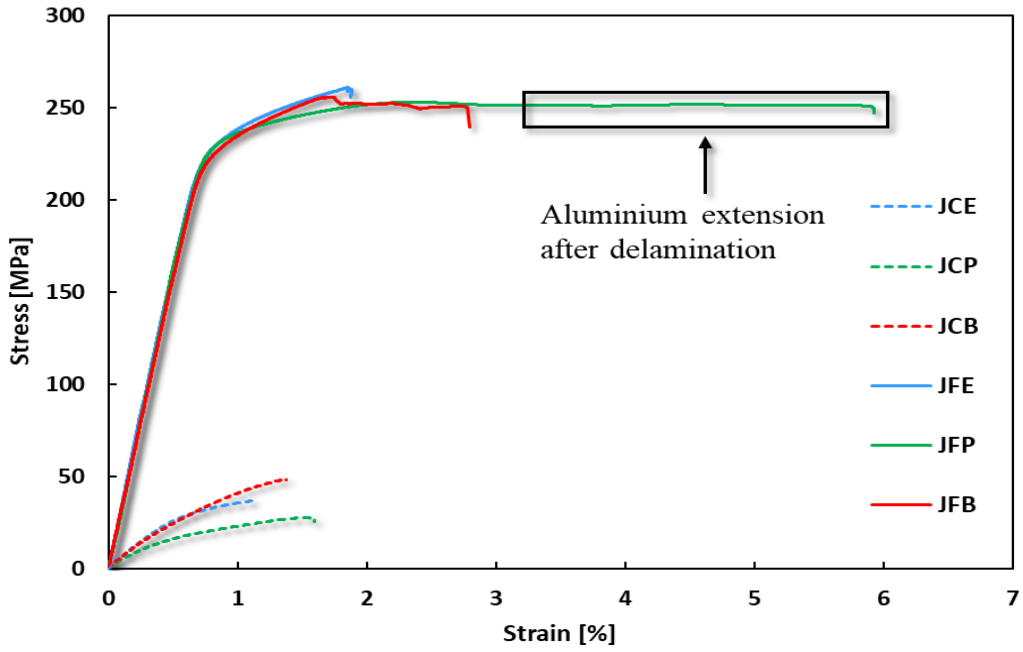

Figure 4.7. The tensile stress-strain curve of 3D jute reinforced composites and FMLs

Figure 4.8 shows the tensile strength, strain, and modulus of 3D reinforced FMLs and its constituents composites. The tensile strength of JCB was highest among the 3D jute reinforced composites than JCE, followed by JCP. The highest failure strain was observed in the JCP, followed by JCB and JCE. The elastic modulus was highest for JCE, followed by JCB and JCP. The reason for this kind of behaviour is already well explained. Among three composites JCB showed overall high strength and stiffness, with relatively higher strain and strength. When the properties of FMLs are compared, the JFE showed higher strength, followed by JFB and JFP. The JFP showed the highest strain, followed by JFB and JFP. When the elastic modulus is discussed, the JFE showed the highest modulus, followed by JFB and JFP. The properties of both composites and FMLs follow the quite linear pattern. When the overall performance of all the three composites and FMLs were compared the PVB based composites and FMLs showed balance properties.

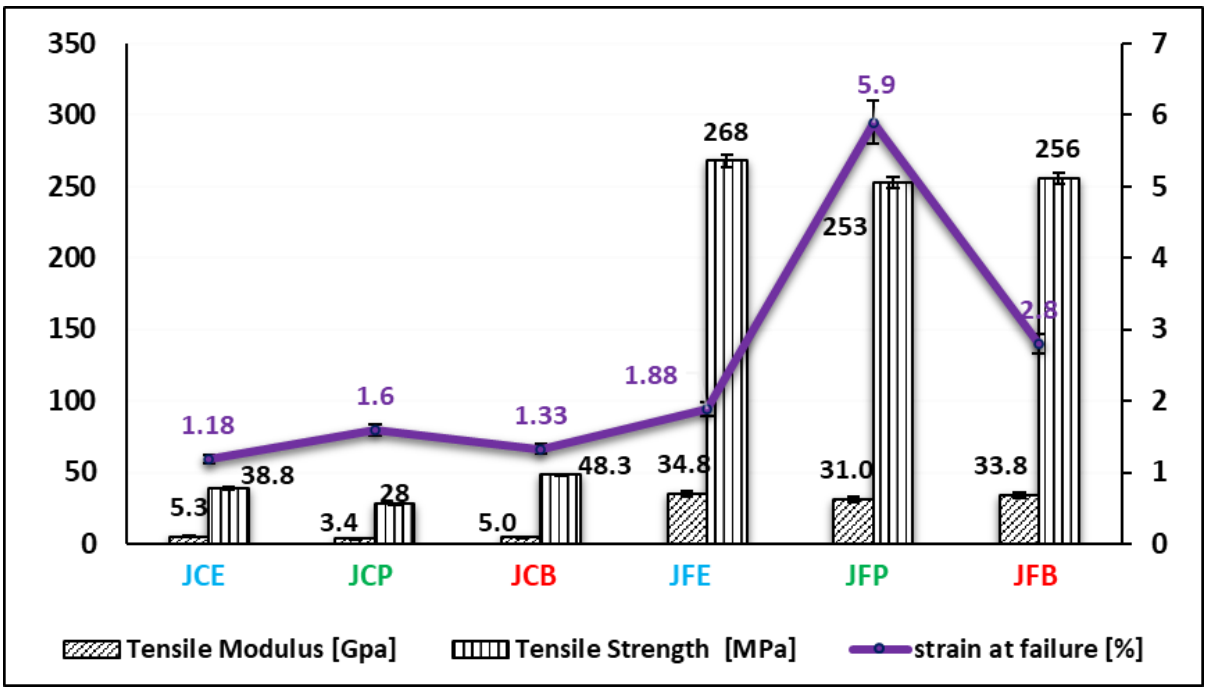

Figure 4.8. Tensile properties of 3D jute composites and FMLs

Figure 4.9 shows the microscopic images of fractured samples of composites and FMLs. The composites and FMLs have a different pattern of failure. When the composite failure pattern was compared, the JCP showed a lot of fibre pullout, that was due to resin crack followed by reinforcement failure. While JCE and JCB shows brittle failure, the JCE showed slight tapper breakage that caused a slight bend in the curve as can be seen in Figure 4.9. When analyzed the fracture pattern of FMLs, The JFE shows quite a brittle failure with slight delamination and resin crack. The JFP showed very obvious fibre pullout; this pullout was due to cracking of PP, once the resin cracked the jute fibres get exposed and then break. The JFB showed intermediate failure between JFE and JFP, with slight fibre pullout and brittle breakage.

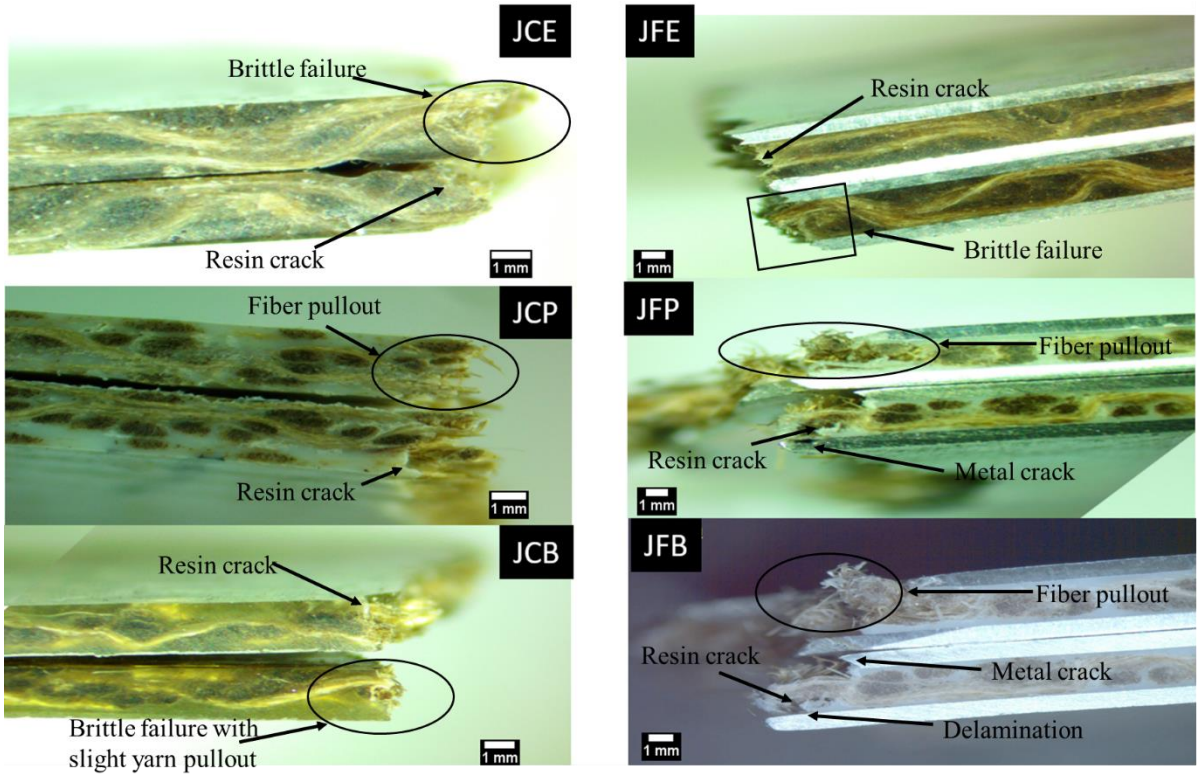

Figure 4.9. The cross-section of fractured samples after the tensile test of 3D jute composites and FMLs

The fractured face of all the samples is showing how the metal, matrix and reinforcement behaved against tensile load. The epoxy and PVB based samples are showing that the matrix

had fully impregnated the reinforcement and failure was brittle. For the PP based samples the failure was with fibre pullout and resin crack quite before fibre break (Figure 4.10).

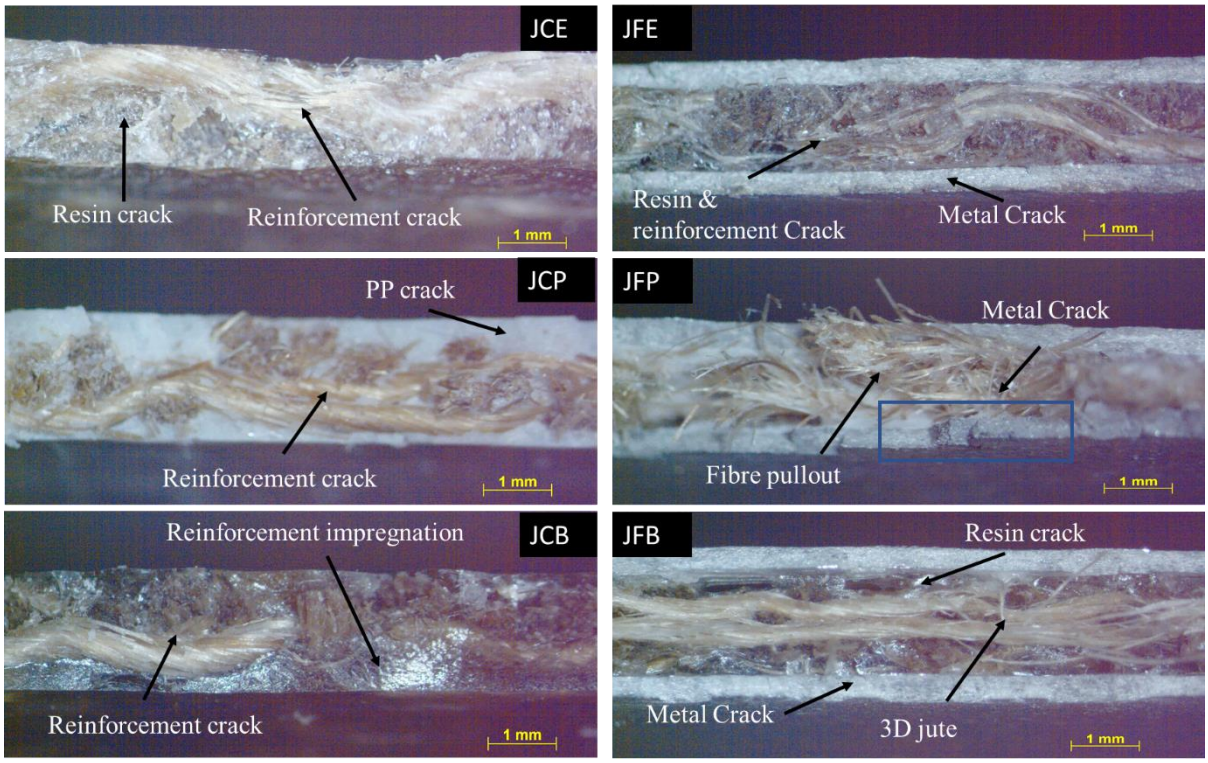

Figure 4.10. The cross-section of fractured face of samples after the tensile test of 3D jute composites and FMLs

B. 2D Jute / 3D Jute Composite and FMLs

Figure 4.11 shows the stress-strain curves of 2D jute + 3D jute reinforced composites and FMLs. The JJCE showed quite a brittle response with high modulus, low strain, and brittle fracture. The JJCP showed the ductile response with high strain, low modulus, and low strength. The reason for bend at the end curve of JJCP had already explained in the previous section. The JJCB showed high strain and high strength with quite steady properties. When the properties of FMLs were compared, the JJFE had a brittle breakage, JJFP like JFP showed the high strain. The reason for the high strain of pp based FMLs is that the after delamination between aluminium and composites the aluminium keeps on extending and then break. The JJFB somewhat showed superior mechanical performance. The curves of all three FMLs were

same in elastic region and in non-elastic region the trend gets changed due to the start of failure. Overall, when the results of 2D jute + 3D jute composites are discussed the PVB based composites and FMLs showed better performance in term of failure strain and strength. The PVB matrix had a better fibre-matrix interface. The metal-composite bonding was also better in PVB based FMLs, which resulted in better tensile performance.

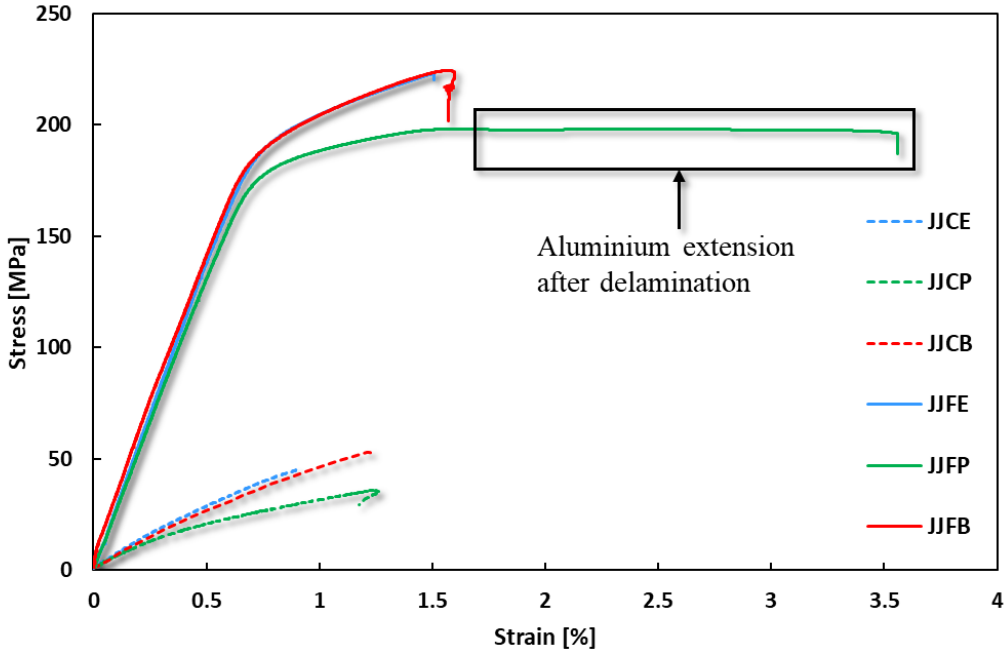

Figure 4.11. The tensile stress-strain curve of 2D jute + 3D jute composites FMLs

Figure 4.12 shows the comparison of the tensile properties of composites and FMLs. When the properties of composites were compared, the JJCB has the highest tensile strength, followed by JJCE and JJCP. The JJCE had a lowest failure strain followed by JJCB and JJCP. The elastic modulus of epoxy-based composites and FMLs was highest. Out of thermoplastic resins, the PVB based composites and FMLs had higher elastic modulus.

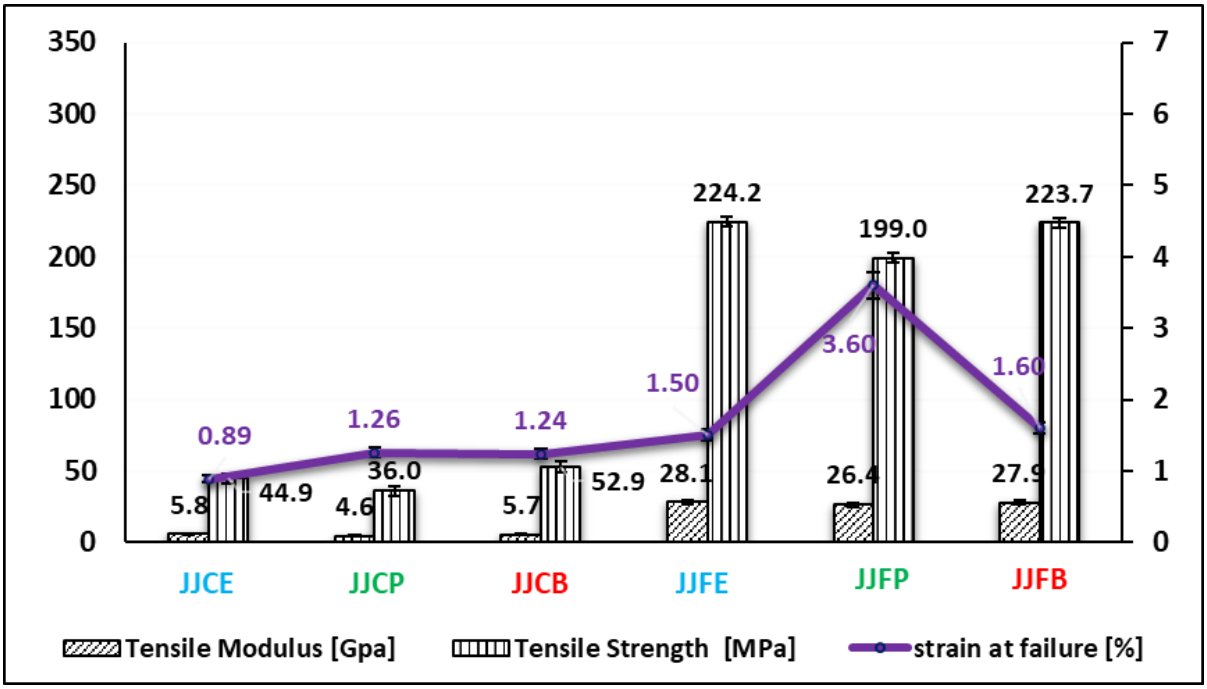

Figure 4.12. Tensile properties of 2D jute + 3D jute composites and FMLs

Figure 4.13 shows the microscopic images of fractured samples after the tensile test. The JJCE showed the brittle failure with resin cracking. The fractured sample of JJCP showing that there was an extensive fibre pullout, the reason of fibre pullout was poor impregnation of jute fibres by resin. Once the resin cracks, the fibre was exposed to a tensile force. The JJCB had shown high brittle failure; there was no sign of fibre pullout, showing excellent impregnation of fibres. The dominant failure phenomenon in the FMLs is fibre pullout, delamination, resin crack and matrix crack. In the hybrid 2D jute + 3D jute FMLs the delamination between 2D and 3D jute plies was not observed. The JJFE had a brittle failure with slight delamination and resin crack. In the FMLs, the failure starts with resin crack followed by delamination and then complete failure. The JJFP had delamination, resin crack and extensive fibre pullout as a dominant failure mechanism. The JJFB had delamination around crack position between aluminium-composite, resin crack and metal crack as a dominant failure mechanism. Overall, when the thermoplastic matrices are discussed, the PVB had a very stable failure mechanism.

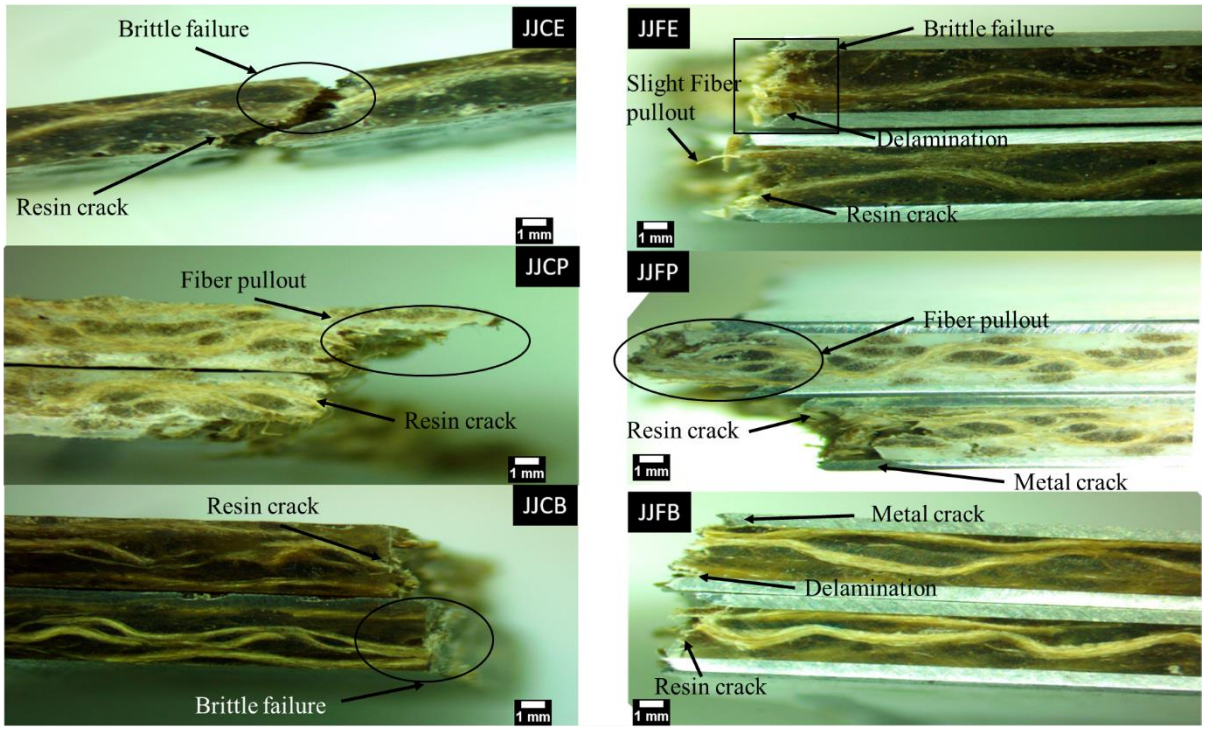

Figure 4.13. The cross-section of fractured samples after the tensile test of 2D jute + 3D jute composite and FMLs

Like 3D jute reinforced composites and FMLs, the 2D / 3D jute reinforced samples are also showing similar behaviour. The fractured faces of epoxy and PVB samples are showing impregnation of reinforcement with matrix, the failure was dominantly brittle with fibre and matrix crack. The failure in the PP based samples was slight ductile as matrix crack followed by fibre pullout. The impregnation of reinforcement was also not as good as seen in case of epoxy and PVB (Figure 4.14).

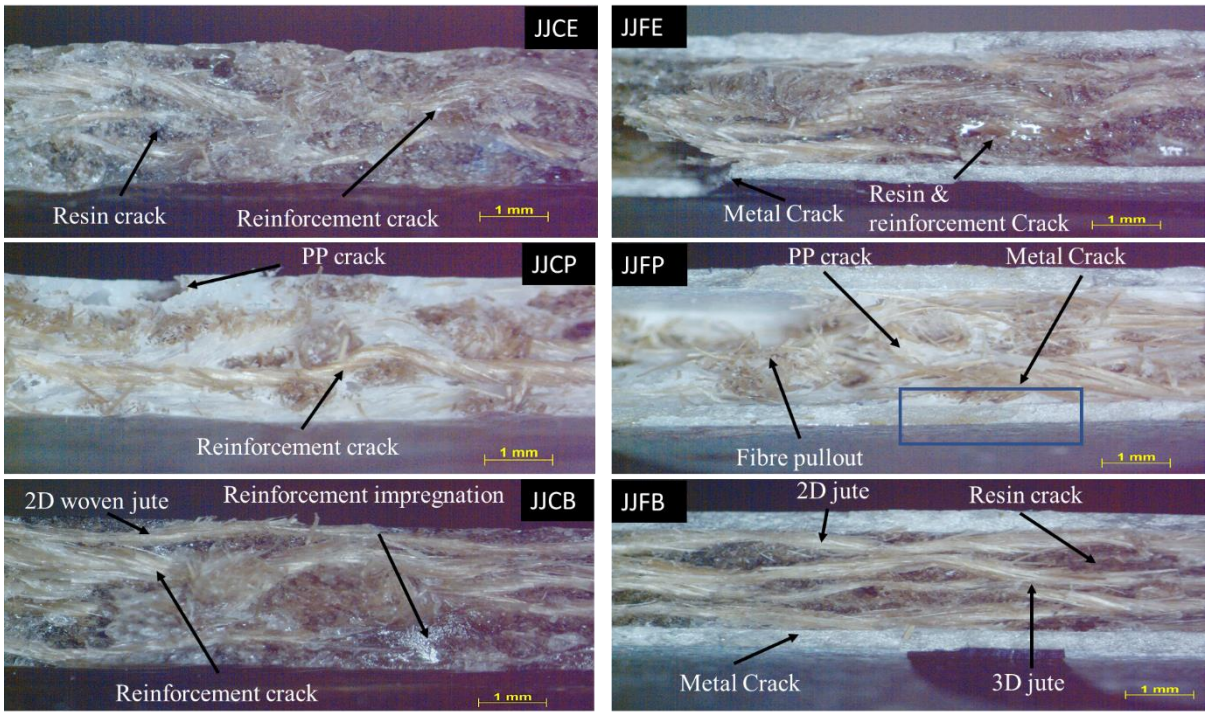

Figure 4.14. The cross-section of fractured face of samples after the tensile test of 2D jute + 3D jute composite and FMLs

C. 2D Aramid / 3D Jute Composite and FMLs

Figure 4.15 shows the tensile stress-strain curves of 2D aramid + 3D jute composites and its associated FMLs. When the behaviour of the composite was observed, the epoxy-based composite had the highest modulus, strength, and brittle fracture. The ACB had properties in between ACE and ACP. The modulus was higher than ACP but lower than ACE. The ACB showed somewhat lower tensile strength. The ACP showed higher tensile strain as compared to ACE and ACB. The higher strain of the ACP was due to PP, which imparted ductility in the composite. The FMLs were also showing very distinct characteristics when compared with 100% jute reinforced FMLs. The FMLs had three zones in the stress-strain curve. The linear region (elastic), non-linear region (inelastic), and failure zone. The AFP had a relatively very large non-linear region that is due to the nature of both matrix and reinforcement. Both AFE and AFP had unique failure zone with a sudden drop in the curve after reaching maximum stress. As at maximum stress, there is a slight delamination between jute composite core and

2D aramid fabric layer and then the jute reinforcement core crack. This different failure strain of all the components causes a different type of failure zone. The failure of AFB occurs at relatively at lower strain and lower stress due to fracture of the reinforcement layer rather delamination.

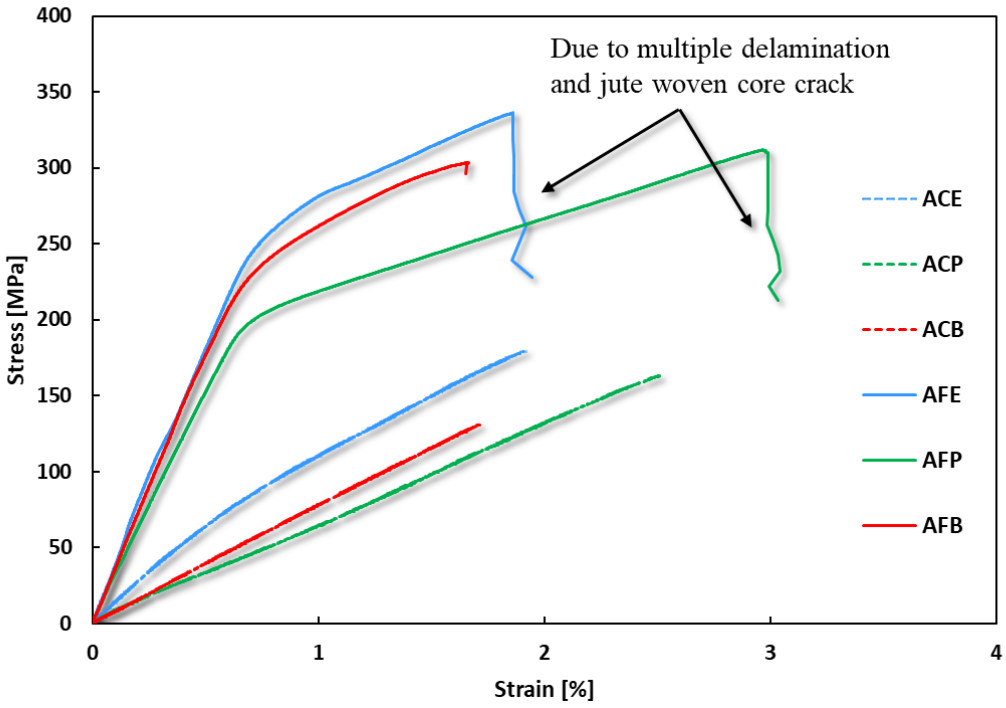

Figure 4.15. The tensile stress-strain curves of 2D aramid + 3D jute reinforced composites and FMLs

Figure 4.16 shows the properties of 2D aramid + 3D jute reinforced composites and FMLs. The tensile strength of ACE was highest, followed by ACP and ACB. The tensile modulus of ACE was highest, followed by ACB and ACP. The tensile failure strain of the ACP was highest, followed by ACE and ACB. The lower tensile failure strain of ACB was unusual as it must be higher than ACE. The reason for the lower failure strain of ACB was that the delamination between jute and aramid did not happen; instead, there was a fracture; this sudden fracture caused the lower strain. When the properties of FMLs are accessed, the AFE had the highest tensile strength followed by AFP and AFB. The tensile failure strain of AFP was higher

than both AFE and AFB. The AFE had a higher failure strain than AFB; even the AFE was made with epoxy which had high brittleness and low strain. The high failure strain in case of AFE is achieved due to the start of delamination between 2D aramid and 3D jute composite core before ultimate failure. The failure strain is quite high for 2D aramid+3D jute reinforced composites and FMLs as compared to rest of composites and FMLs that is due to a high strain rate of aramid fibres.

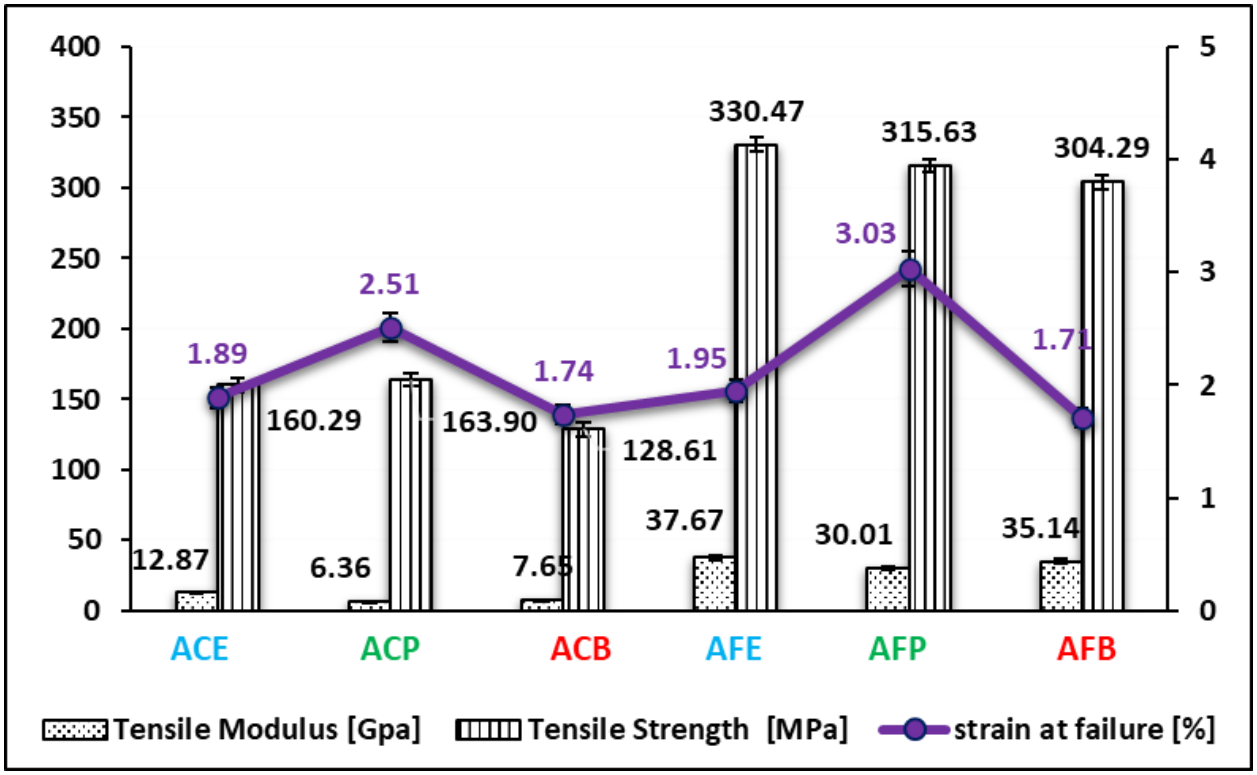

Figure 4.16. Tensile properties of 2D aramid + 3D jute composites and FMLs

Figure 4.17 shows the cross-section of fractured samples of composites and FMLs. When the cross-section of composites is compared, all the composites are showing aramid fibre pullout. The ACP is also showing jute fibre pullout along with aramid fibre pullout. That is due to poor bonding of PP and reinforcement. The ACB was showing aramid fibre pullout, but when the jute composite core is compared, it showed brittle failure as the matrix had impregnated the jute fibbers thoroughly. The ACE is also showing aramid fibre pullout along with brittle composite core failure. The FMLs fracture is very interesting as both AFE and AFP showing

incomplete failure. The aluminium layer was not cracked. There was delamination between the aramid and jute layer, while the jute layer was cracked after certain strain. The reason for not cracking of aluminium layer is a delamination between 2D aramid layer and 3D jute core. The AFB was showing complete failure crack, unlike AFE and AFP. The delamination between aramid and jute woven core was not to be seen. The jute woven core shows a brittle failure, while the aramid fibre layer has fibre pullout. Another reason of the incomplete failure of AFE and AFP was that the adhesion between aluminium and aramid was higher than the adhesion between jute woven core and aramid, that is why the jute and aramid delaminated, and jute woven core cracked. In the AFB the adhesion was even between all the components caused complete failure.

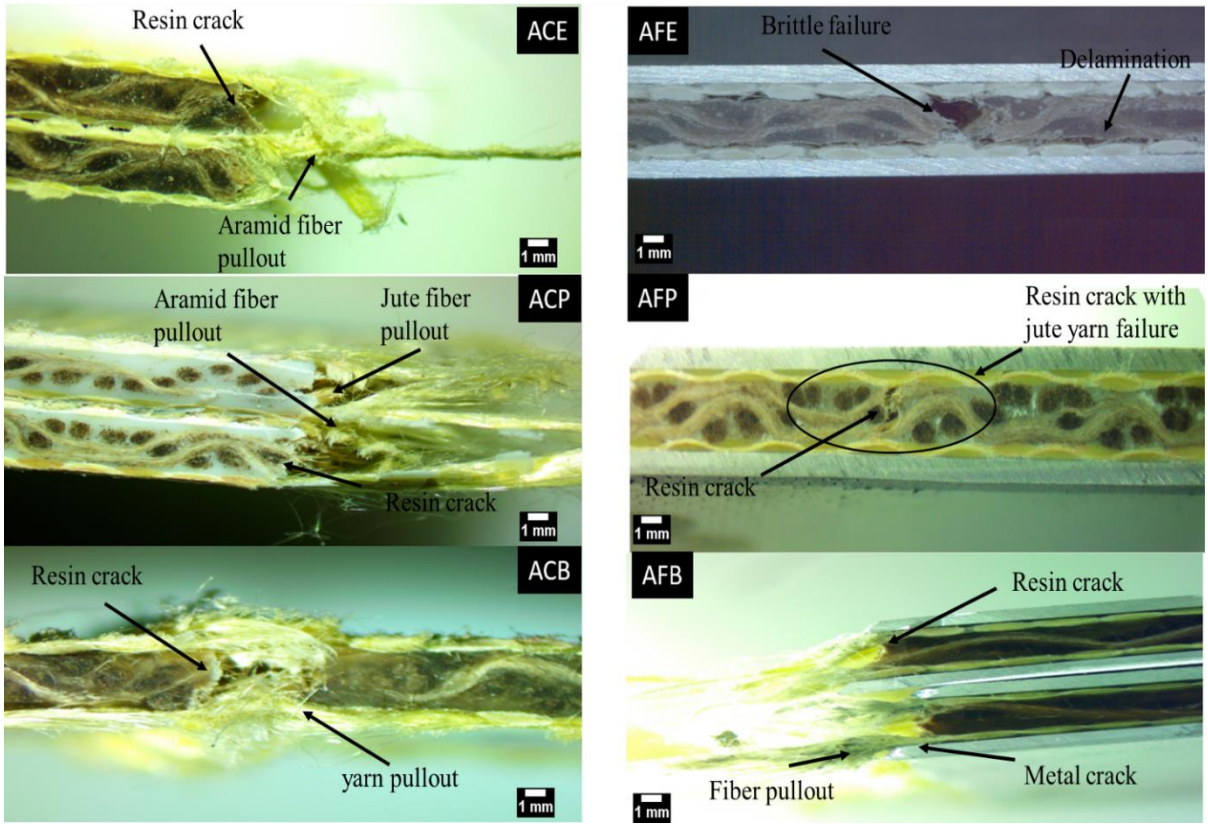

Figure 4.17. The cross-section of fractured samples after the tensile test of 2D aramid+3D jute composite and FMLs

Figure 4.18 shows the microscopic images of fractured faces of 2D aramid / 3D jute reinforced composites. The fractured faces of FMLs are not added as the AFE and AFP were not fully fractured. The ACE is showing that the 3D reinforcement had brittle failure, while aramid fibre suffered fibre pullout before breaking. The ACP also showing similar failure additionally jute fibre pullout due to PP matrix. The AFB however had partial failure as the jute reinforcement suffered brittle failure followed by incomplete aramid fibre breakage.

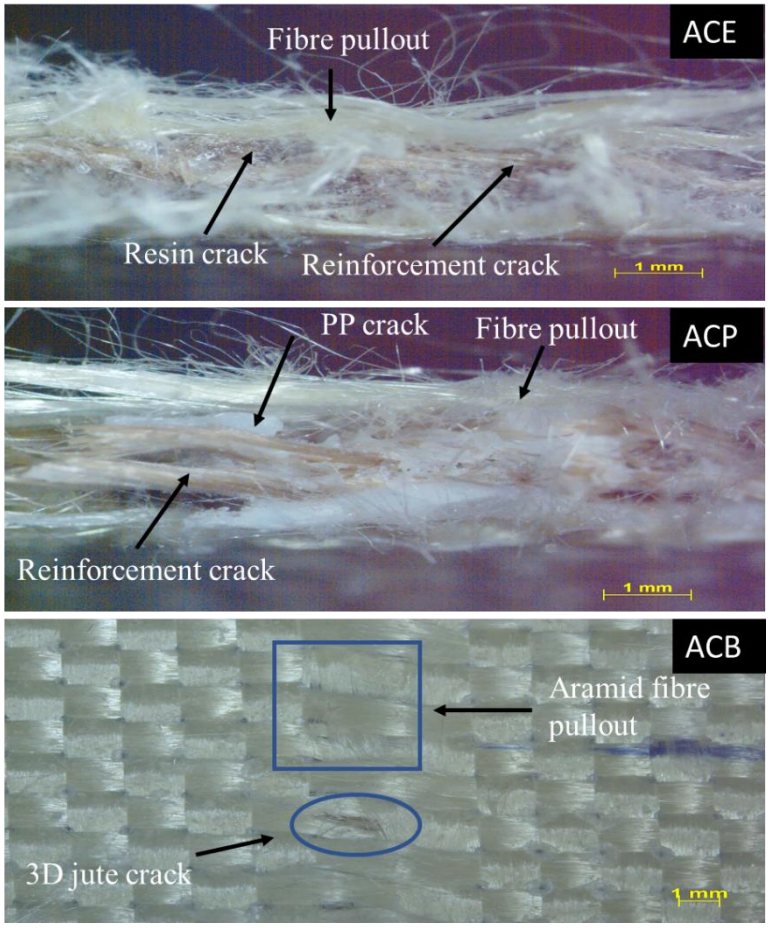

Figure 4.18. The cross-section of fractured face of samples after the tensile test of 2D aramid + 3D jute composite

D. 2D Carbon / 3D Jute Composite and FMLs

Figure 4.19 shows the tensile stress-strain curves of 2D carbon + 3D jute reinforced composites and FMLs. The CCE is showing very brittle failure with low strain to failure and high modulus. The CCB showed properties in between CCE and CCP, with intermediate brittleness and

failure strain higher than CCE but lower than CCP. The CCP showed a ductile fracture, and the stress-strain curve had two portions, the smaller linear portion and then higher non-linear portion. The addition of carbon fibres imparted overall low failure strain to all the composites. When the stress-strain curves of FMLs were compared like 2D aramid-reinforced FMLs, the FML which have brittle failure will exhibit low failure strain while the FMLs in which delamination between reinforcement occur experience high failure strain. The CFE showed lower failure strain as compared to CFB due to already describer reason. The CFP had higher failure strain and the failure region also depicting multiple curves due to delamination before subsequent failure.

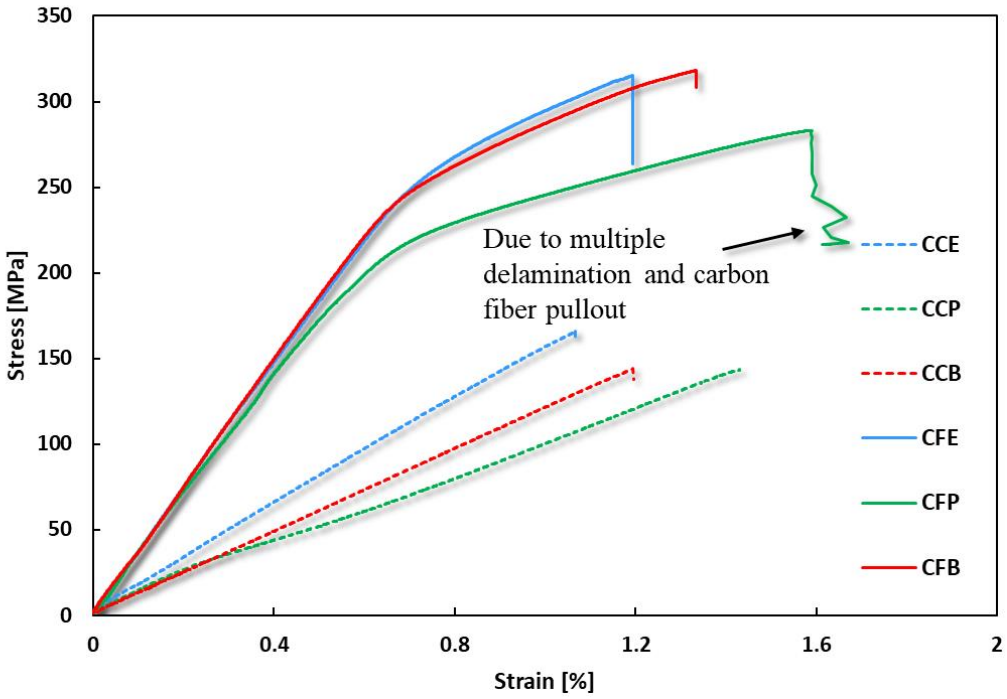

Figure 4.19. The tensile stress-strain curve of 2D carbon + 3D jute reinforced composites and FMLs

Figure 4.20 shows the tensile properties of 2D carbon + 3D jute reinforced composites and FMLs. The CCE was showing higher tensile strength while CCP and CCB were showing almost similar tensile strength. When the tensile failure strain was compared, the CCP had the

highest failure strain followed by CCB and CCE. The tensile modulus was higher for CCE, followed by CCB and CCP. When the tensile properties of FMLs were compared, the CFB had the highest tensile strength, followed by CFE and CFP. The tensile modulus was highest for CFE, followed by CFB and CFP. The failure strain of CFP was highest, followed by CFB and CFE. There was a slight variation in the failure strain of composites and FMLs; in fact, the failure strain of FMLs was slightly higher than composites. The reason for the higher failure strain of FMLs was the addition of aluminium which added more extensibility. The FML which experience a brittle failure usually show lower strain with lower tensile strength compared to other FMLs.

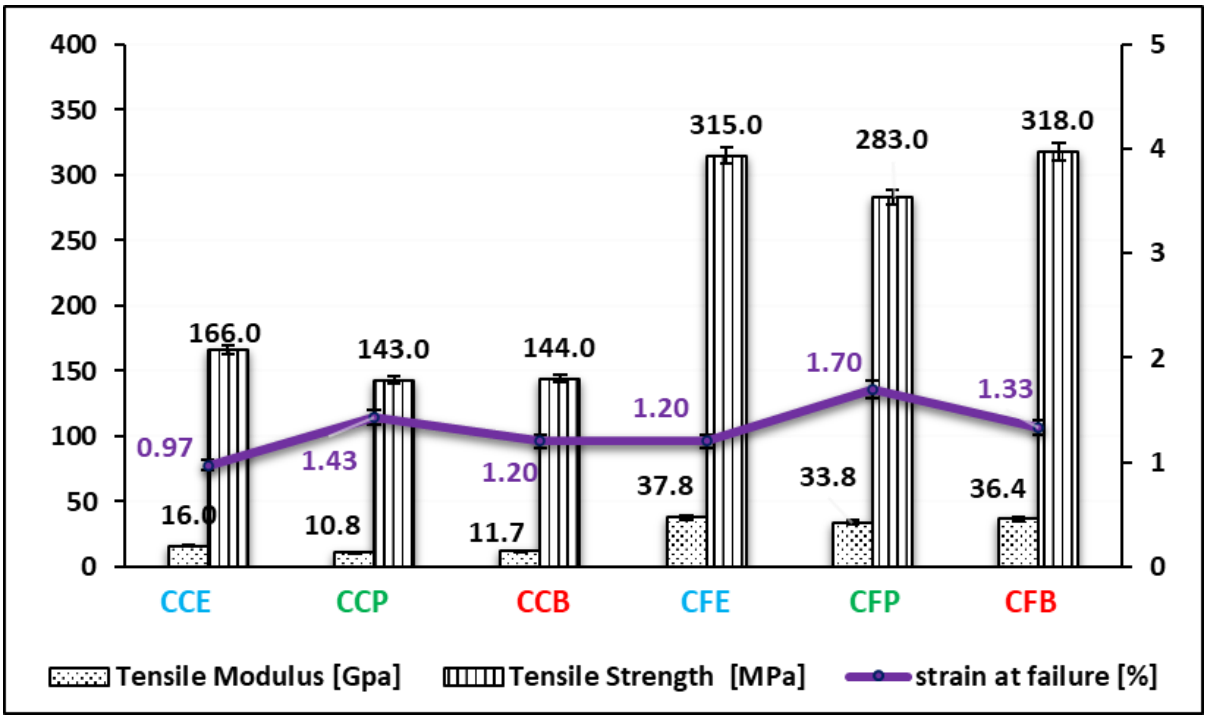

Figure 4.20 Tensile properties of 2D carbon + 3D jute composites and FMLs

Figure 4.21 shows the cross-section of fractured samples of 2D carbon + 3D jute reinforced composites and FMLs after the tensile test. The CCE was showing brittle failure with resin crack and slight carbon yarn pullout. The overall pattern of failure of CCE was brittle. The CCP was showing fibre pullout of both jute and carbon. The reason for this kind of behaviour

of CCP was PP matrix which mechanically fastens the reinforcement and once the matrix was cracked the reinforcement get exposed. The impregnation of reinforcement was also not very good with the PP matrix. The CCB showing portion of carbon yarn pullout and brittle failure of jute woven core. The overall impregnation of reinforcement by PVB matrix was quite good. The FMLs were showing similar kind of failure pattern as of composites. The CFE was showing brittle failure with the very sharp vertical crack line. There was slight carbon yarn pullout. Only slight delamination was seen between composites core and aluminium. The CFP was showing large fibre pullout with delamination within composites core and with aluminium as well. The CFB showed overall brittle failure with slight carbon yarn pullout; there was also slight delamination between aluminium and composites.

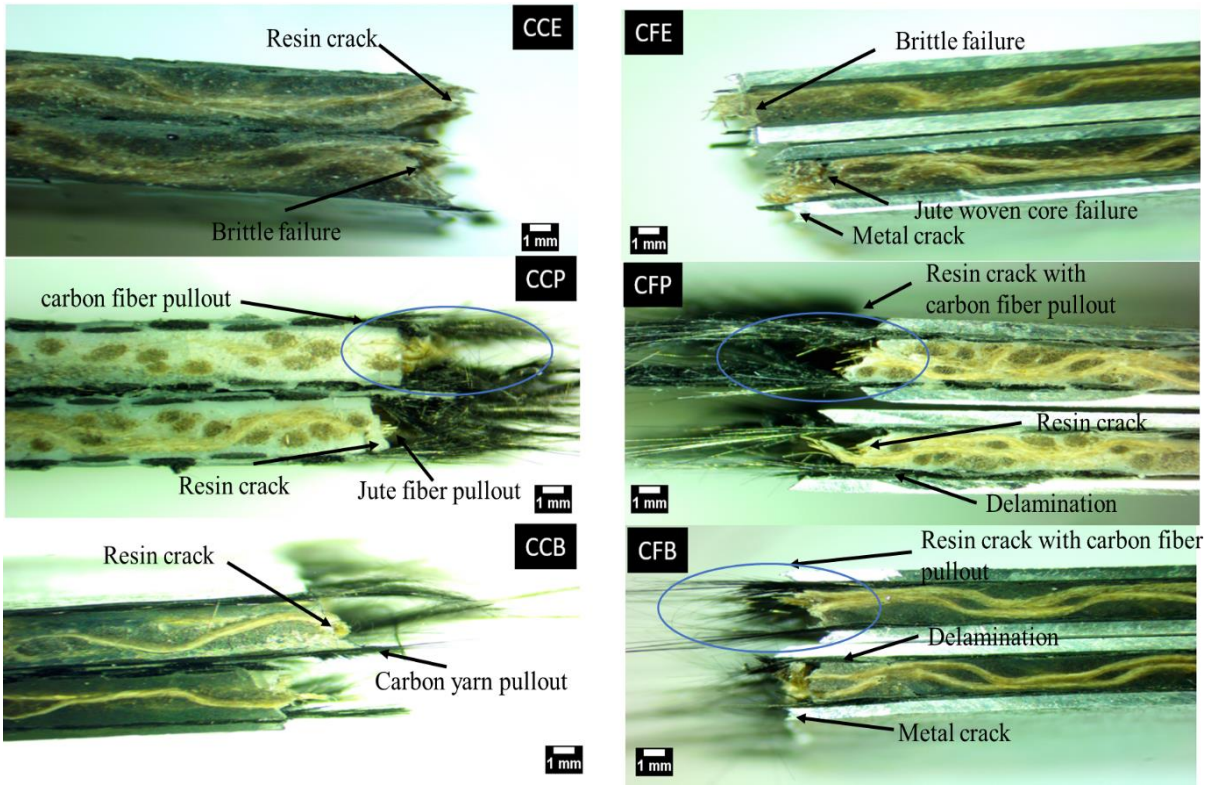

Figure 4.21. The cross-section of fractured samples after the tensile test of 2D carbon + 3D jute composite and FMLs

Figure 4.22 shows the microscopic images of fractured faces of tested samples of 2D carbon / 3D woven jute reinforced composites and FMLs. The BCE is showing that the reinforcement

is impregnated fully, and failure is brittle. The BFE is also showing brittle failure, but there was a slight carbon fibre pullout. Both BCP and BFP is showing fibre pullout of carbon and jute before cracking. The BCB and BFB had brittle failure, the fibres were impregnated completely, however there was a slight carbon fibre pullout for BFB.

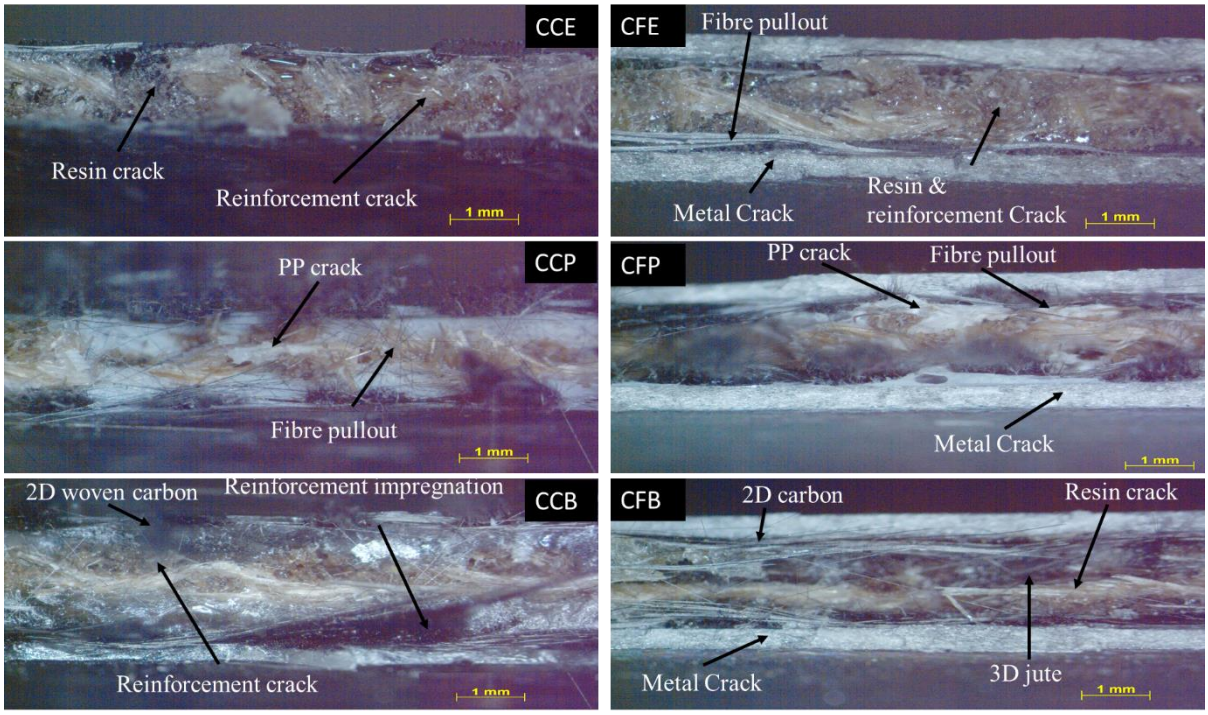

Figure 4.22. The cross-section of fractured face of samples after the tensile test of 2D carbon + 3D jute composite and FMLs

E. 2D Glass / 3D Jute Composite and FMLs

Figure 4.23 shows the tensile stress-strain curve of 2D glass + 3D jute reinforced composites and FMLs. The stress-strain curves of composites showing very incremental behaviour form GCE to GCB. The curve of GCE showing low strain with brittle failure and high modulus. The properties of GCB were in between GCE and GCP. The strain was slightly higher than GCE, and the failure was in between brittle and ductile. The GCP had a ductile failure with large non-linear portion. The stress-strain curves of FMLs had three parts, linear, non-linear, and fracture part. The linear part had a very sharp increase in the stress with a small increase in the strain.

Then non-linear part showing high strain with low stress. The non-linear portion represents the start of matrix crack and delamination. The fracture zone was indicating the complete failure of FMLs. The fractured part of all three FMLs was different, with the GFE had multiple curves indicating the excessive delamination between composite core and aluminium. The GFB was showing brittle failure with slight delamination. The GFP was showing excessive delamination between composites and aluminium. Once there was delamination between composites and aluminium, the aluminium keeps on elongating until failure. The factors which contribute to such behaviour of FMLs are the nature of constituent materials and composite-metal bond.

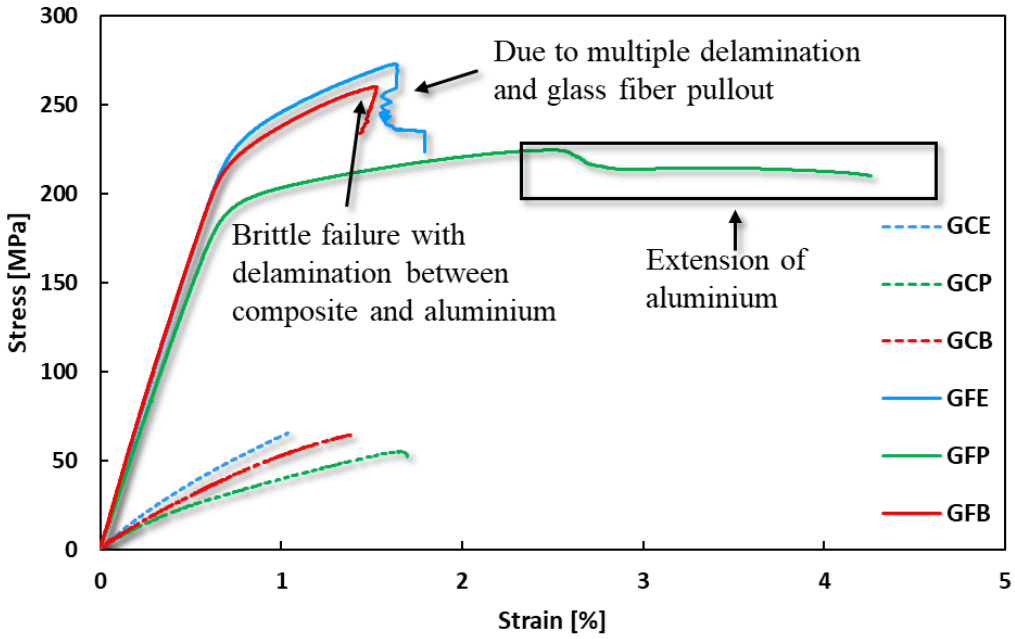

Figure 4.23. The tensile stress-strain properties of 2D glass-3D jute reinforced composites and FMLs

Figure 4.24 shows the tensile properties of 2D glass + 3D jute composites and FMLs. The GCE showed overall high tensile strength and modulus, followed by GCB and GCP. The failure strain was higher for GCP, followed by GCB and GCE. For the FMLs the tensile strength was higher for GFE followed by GCB and GCP. The tensile modulus of GFB was highest, followed by GFE and GFP. Unlike previous FMLs, the tensile modulus of GFE was

lower than GFB, showing the effectiveness of PVB with glass hybrid FML. Another factor which possibly can contribute for the better properties of GFB could be aluminium composite adhesion. The tensile failure strain of GFP was highest, followed by GFE and GFB. The reason for the high failure strain of GFE was due to delamination between glass-aluminium and glass fibre pullout as already seen in the previous sections.

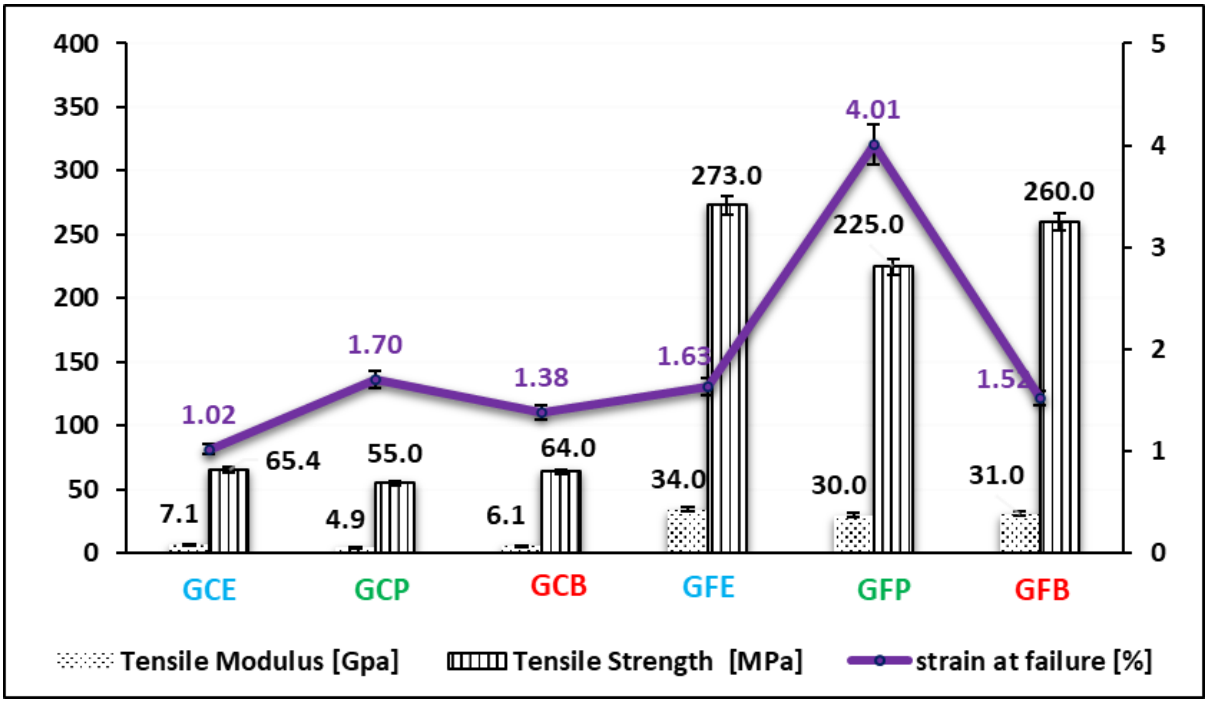

Figure 4.24. Tensile properties of 2D glass + 3D jute composites and FMLs

Figure 4.25 shows the cross-section of the fractured sample of 2D glass + 3D jute composite and FMLs after the tensile test. The GCE sample showed that there was extensive delamination between 2D glass and jute woven core, yet the jute experienced a brittle failure. The GCP, like the previous synthetic + jute, reinforced composites experienced both glass and jute fibre pullout. The GCB had a brittle failure with slight glass fibre pullout. For the FMLs the GFE had delamination between composites and aluminium along with glass fibre pullout. The jute woven core experienced a brittle failure. The GFP had an extensive glass and jute fibre pullout with delamination within the composite and between composite-aluminium. The GFB had a

brittle failure with some delamination between composite-aluminium. The GFB was showing overall stable cracking.

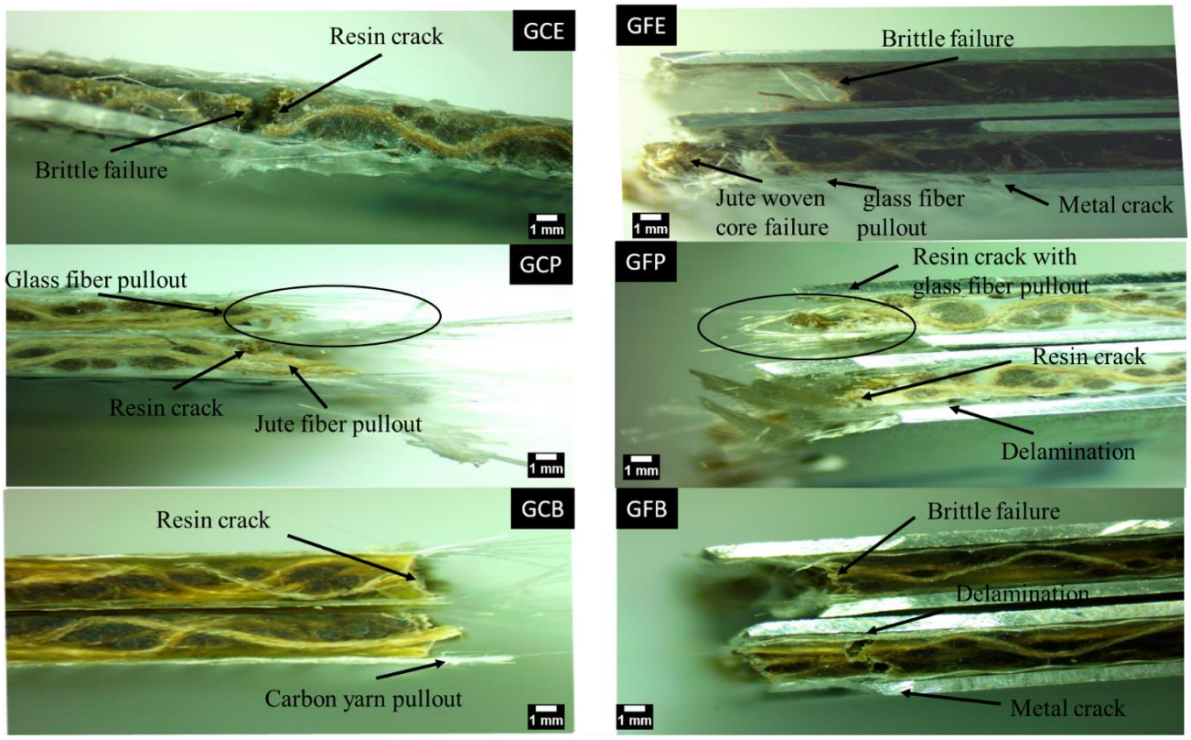

Figure 4.25. The cross-section of fractured samples after the tensile test of 2D glass + 3D jute composites and FMLs

Figure 4.26 shows that JCE had incomplete failure. The 3D jute had brittle failure, while there was delamination between 3D jute and 2D glass followed by glass fibre breakage. The GFE had metal crack after delamination. The 3D jute had brittle crack and glass fibres are showing fibre pullout. The pattern of failure of JCP and JFP was similar to previous PP based samples, the main reason of this kind of failure was PP matrix which do not impregnate the reinforcement. The GCB and GFB however are showing very brittle failure, the reinforcement was impregnated completely with matrix.

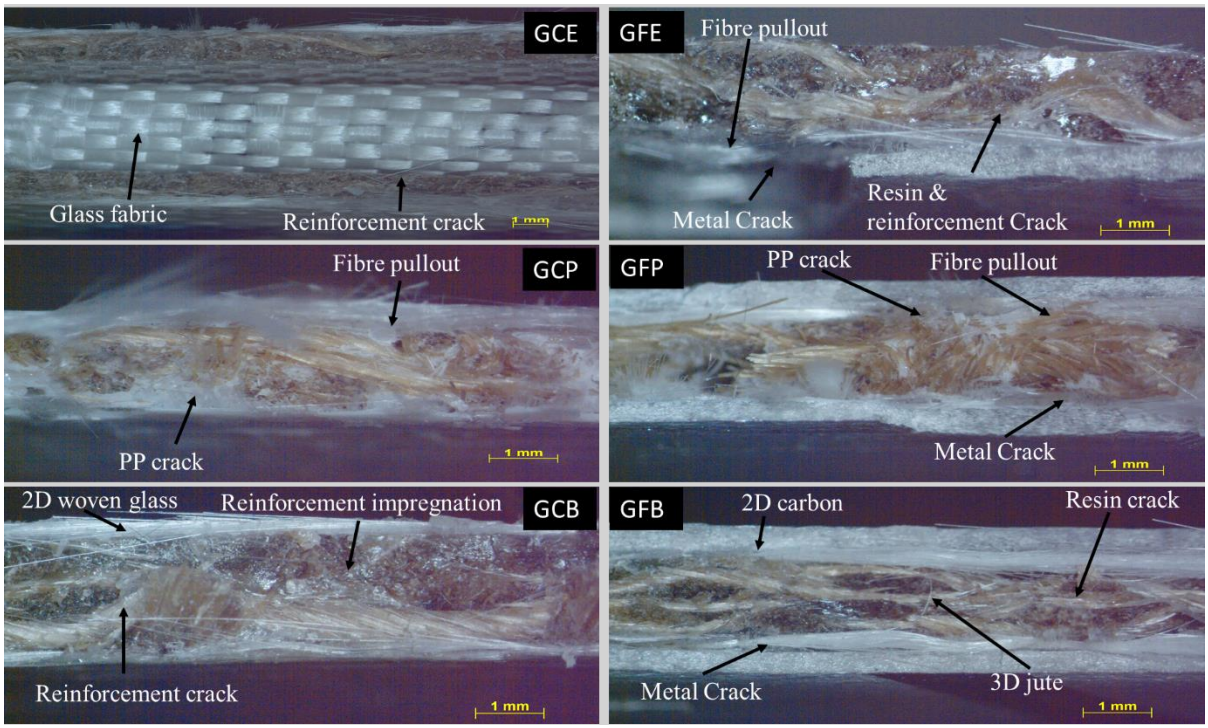

Figure 4.26. The cross-section of fractured face of samples after the tensile test of 2D glass + 3D jute composites and FMLs

4.2.2 3D Jute Reinforced Hybrid Composites and FMLs Flexural Properties

A. 3D Jute Composites and FMLs

Figure 4.27 shows the flexural stress-strain curve of 3D jute composites and FMLs. As can be seen from the curves of composites that the JCE initially had high modulus as compared to JCB and JCP, but eventually cracked due to the brittleness of epoxy matrix. The JCB, on the other hand, showed higher flexural strength and relatively higher strain to failure as compared to JCE. The JCP had shown overall low flexural strength and high failure strain, indicating ductile behaviour of composite. The reason for better flexural strength of JCB was that the PVB had impregnated the reinforcement entirely, which formed better network. The stress-strain curves of FMLs are almost similar with a very identical linear and non-linear part, and there was a slight difference in the non-linear part. Once the sample delaminated than more deformation occurs with almost identical stress. The difference in flexural strength was also

not very large, indicating the dominating effect of aluminium and indicating better composite-metal bonding.

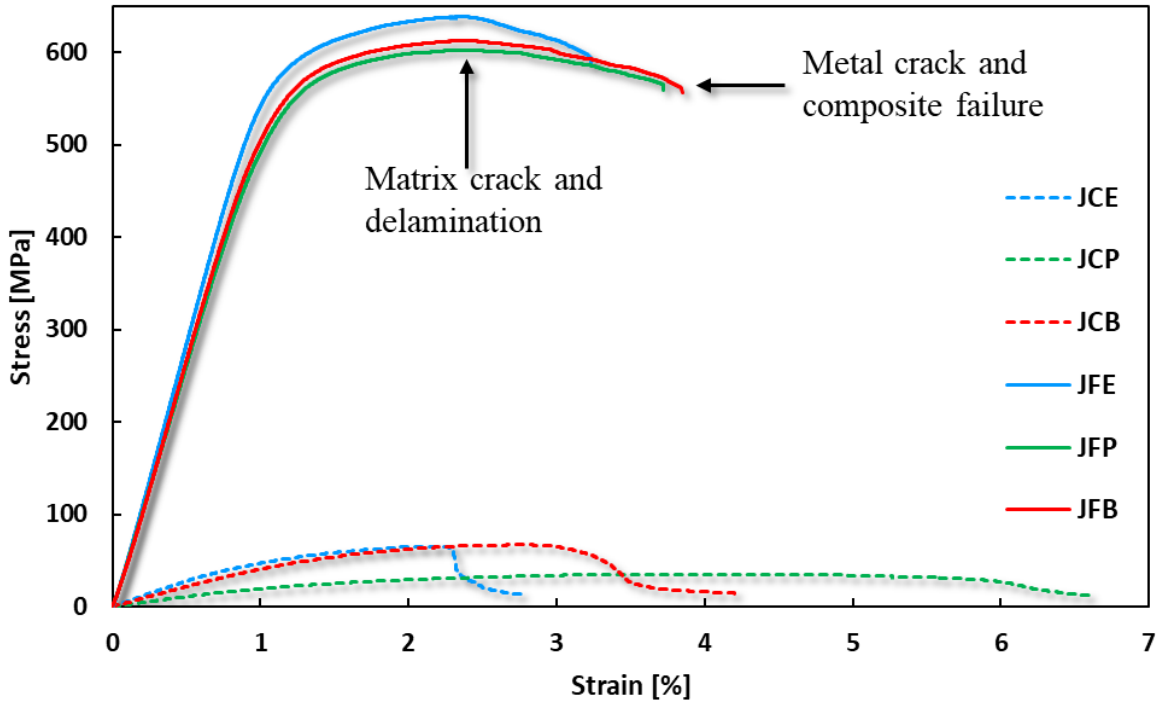

Figure 4.27. The flexural stress-strain curve of 3D jute composites and FMLs

Figure 4.28 shows the flexural properties of 3D jute reinforced composites and FMLs. The flexural strength of JCE was slightly lower than JCB but higher than JCP. The flexural strength of the JCP was almost half of both JCE and JCB. The flexural strain of the JCP was highest, followed by JCB and JCE. The flexural modulus of JCE was highest and then for JCB and JCP, respectively. The flexural properties of composites were mainly governed by reinforcing material, especially matrix type. When the flexural properties of FMLs were analyzed, these properties had a very linear trend, JFE had higher tensile strength and modulus followed by JFB and JFP. The flexural strain was at the almost same level for all the FMLs. The metal-composite bond also drove the flexural properties of FMLs along with constituents' properties. That is from JFE to JFP the properties tend to decrease. The highest strength and modulus were achieved with epoxy, followed by PVB and PP.

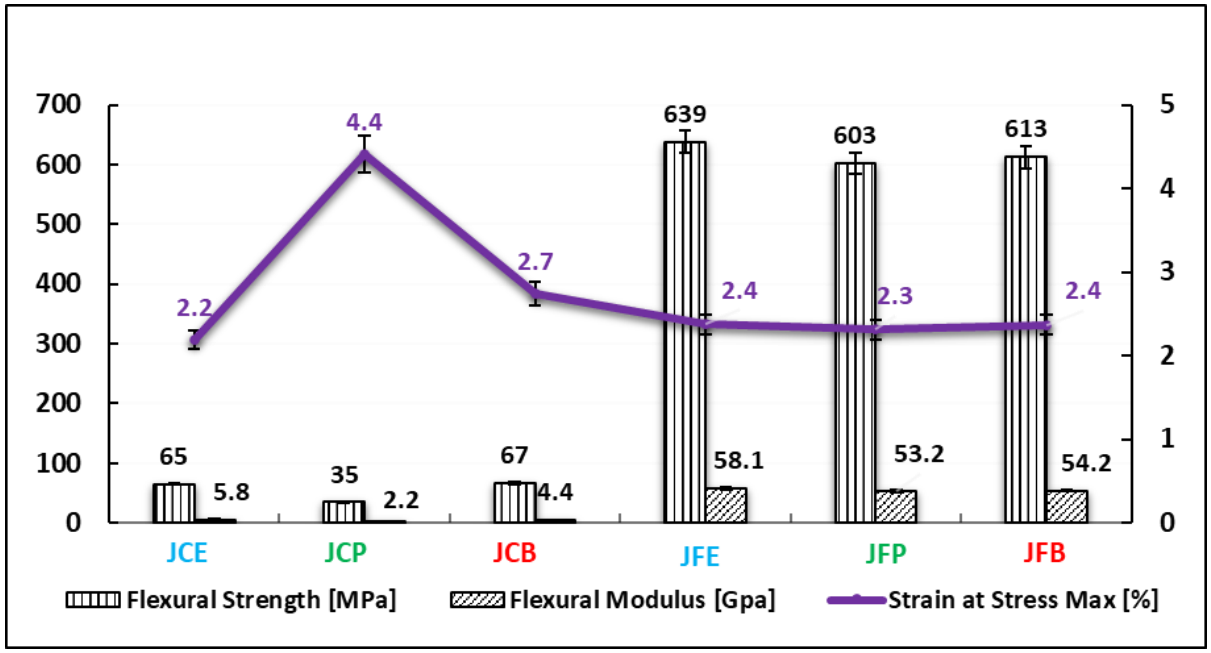

Figure 4.28. Flexural properties of 3D jute composites and FMLs

Figure 4.29 shows the cross-section of fractured samples of 3D jute composites and FMLs after the flexural test. When the sample of composites were analyzed, the dominant failure mechanism was resin crack followed by reinforcement break. In the FMLs, the failure starts with resin crack, which tends to cause delamination, as the shear forces keep on increasing at a certain point, the lower aluminium sheet crack along with reinforcement. The failure pattern of PVB and epoxy-based FMLs was almost similar, but for PP the bending was relatively easier, that is why showing resin cracking followed by reinforcement and metal crack.

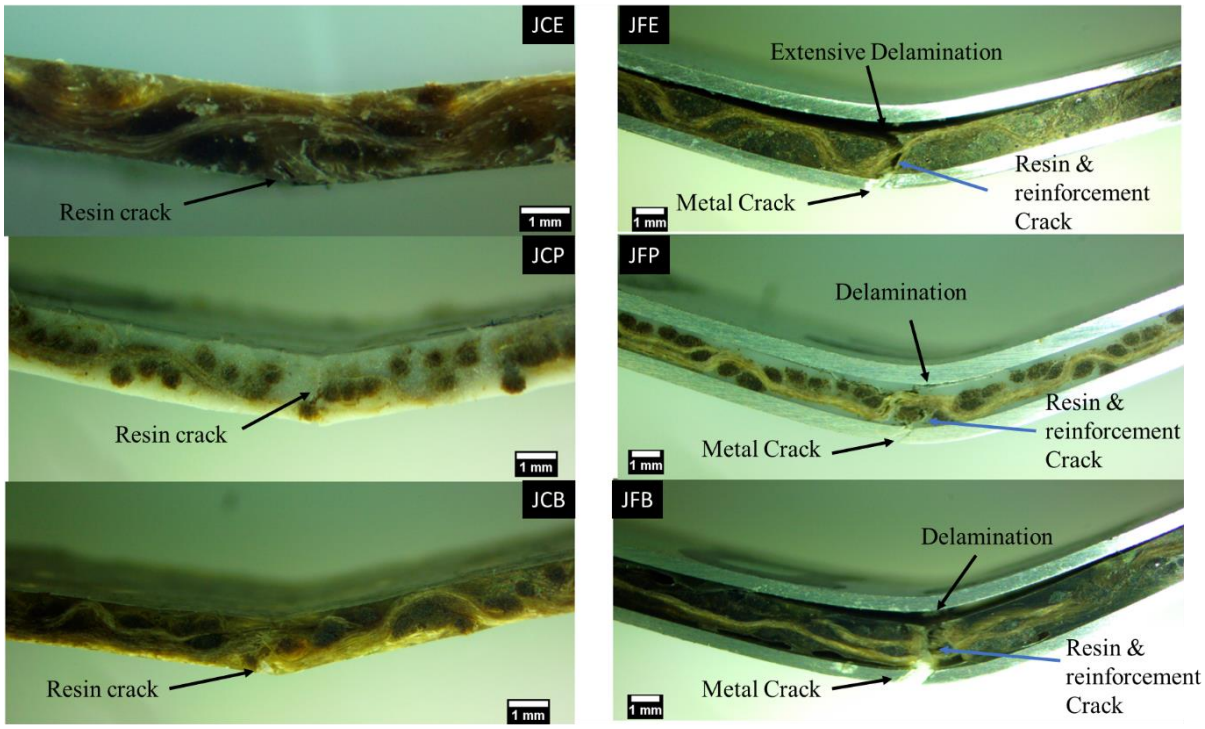

Figure 4.29. The cross-section of fractured samples after flexural test of 3D jute composite and FMLs

B. 2D Jute / 3D Jute Composite and FMLs

Figure 4.30 shows the flexural stress-strain curves of 2D jute + 3D jute composites and FMLs. The JJCE showed a brittle failure with initially high modulus as compared to JJCB and JJCP. JJCB, on the other hand, showed initially low modulus but had relatively high strength as compared to JJCE. The JJCP showed ductile failure with low strength and low modulus. The strain is also different for all three composites mainly governed by the nature of the matrix being used. When the curves of FMLs were compared, the behaviour of all three FMLs was similar to 3D jute FMLs. As once the resin cracks the delamination starts, and FMLs soften causing extensive bending. The failure strain was also similar mainly due to the effect of aluminium, unlike composites in which the matrix had a major part to play.

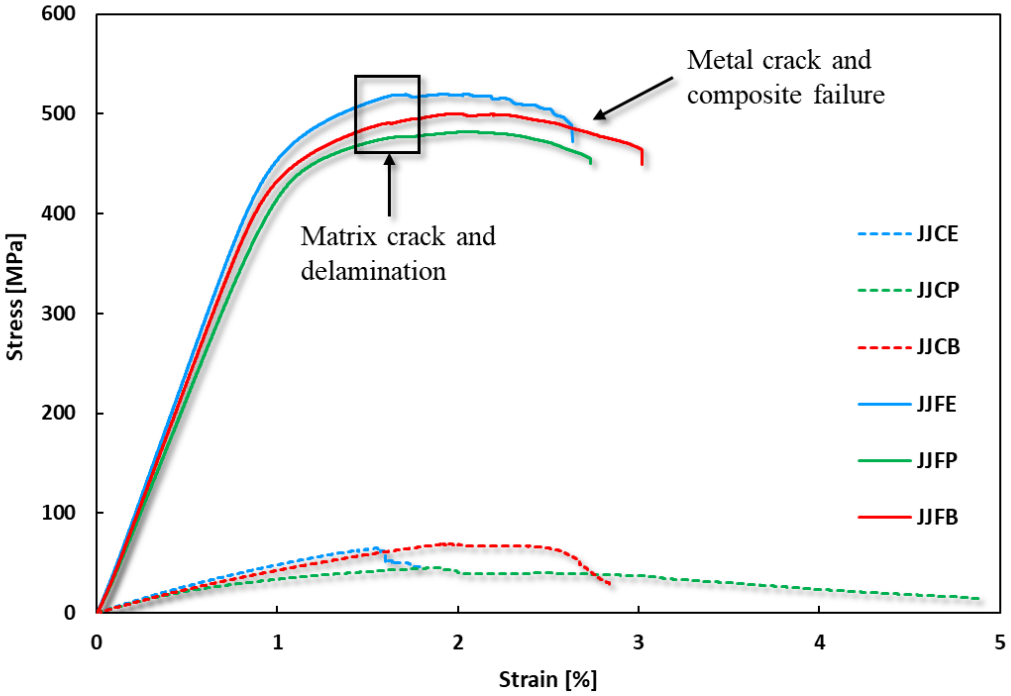

Figure 4.30. The flexural stress-strain properties of 2D jute-3D jute reinforced composites and FMLs

Figure 4.31 shows the flexural properties of 2D jute + 3D jute composites and FMLs. When the properties of composites are compared, the JJCB had the highest flexural strength, followed by JJCE and JJCP. The flexural modulus of JJCE and JJCB was almost equal, while JJCP had lowest modulus. The strain was also higher for JJCB, followed by JJCP and JJCE. The reason for the better properties of JJCB was better impregnation of reinforcement, which form even network. Further, the PVB based composite offered better resilience with jute reinforcement as compared to epoxy and PP. As epoxy is brittle and PP is more ductile. When the properties of FMLs are compared, the JJFE had higher flexural strength and modulus followed by JJFB and JJFP. The flexural strain of JJFP was the highest then JJFB and JJFE, respectively. As discussed before that the properties of FMLs are also contributed by a metal-composite bond other than the matrix and reinforcement.

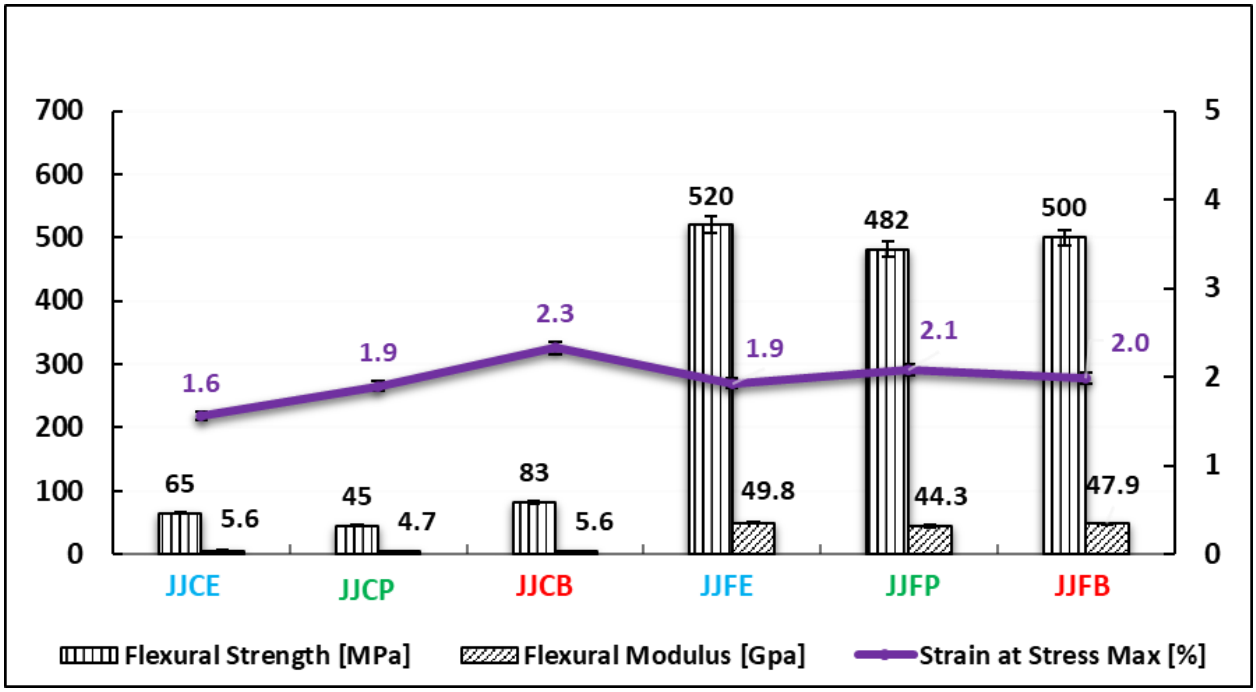

Figure 4.31. Flexural properties of 2D jute + 3D jute composites and FMLs

Figure 4.32 shows the cross-section of fractured samples after the flexural test. As can be seen from the sample of composites that JJCE and JJCB were completely fractured while JJCP partially fractured with resin and reinforcement crack. The JJCE and JJCB breakage pattern indicate that the failure was more brittle while JJCP had a ductile failure. The dominant failure mechanism as discussed earlier for FMLs was delamination, metal crack, resin, and reinforcement failure. The more brittle is matrix more will be delamination between metal-composite, once the resin cracks the delamination propagates further between metal-composite.

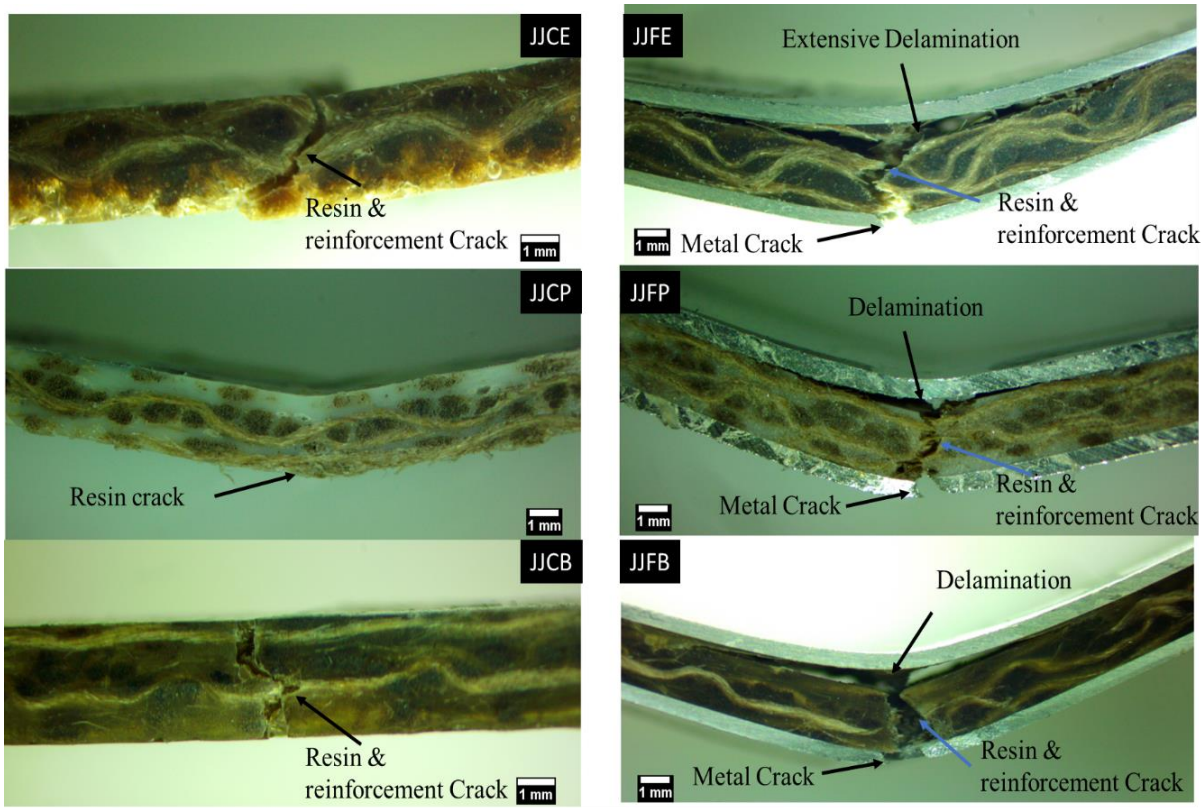

Figure 4.32. The cross-section of fractured samples after flexural test of 2D jute + 3D jute composite and FMLs

C. 2D Aramid / 3D Jute Composite and FMLs

Figure 4.33 shows the flexural stress-strain curve of 2D aramid + 3D jute reinforced composites and FMLs. The curves of all three composites are different from each other. The ACE had high modulus with a sharp increase in stress relative to strain. The ACP had ductile behaviour, while ACB had intermediate behaviour. The multiple peaks in ACE were indicating resin crack as the reinforcement was not cracked. As in all three composites the aramid fibres were not cracked, so the different behaviour of composites was governed by the properties of the matrix. The FMLs curve had three parts: linear (elastic), non-linear (inelastic) and the failure zone. The AFE and AFB had similar kind of stress-strain curves. The failure zone of AFE and AFB showed multiple delamination between aramid-jute and aramid-aluminium while AFP was showing premature failure due to delamination between composites and metal.

The reason of delamination between aramid and jute woven core was that the bonding between aluminium and aramid was stronger than the jute-aramid.

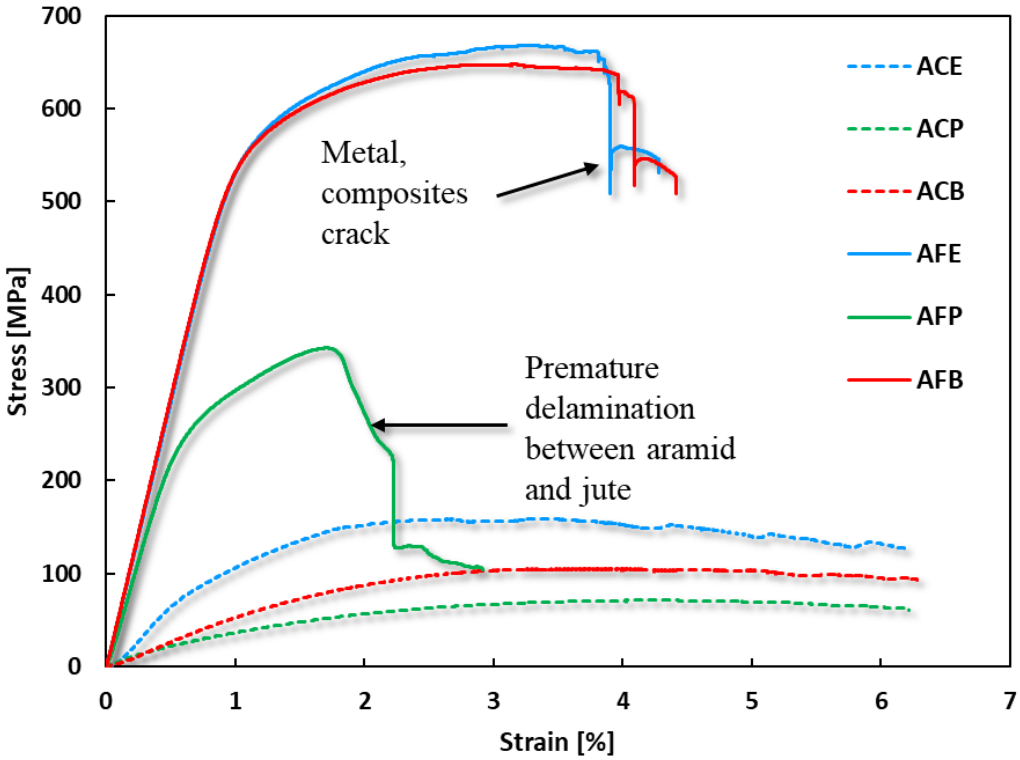

Figure 4.33. The flexural stress-strain properties of 2D aramid + 3D jute reinforced composites and FMLs

Figure 4.34 shows the flexural properties of 2D aramid + 3D jute reinforced composites and FMLs. There was a significant difference in the properties of three composites, that was due to the matrix as none of the composite experience fractures. Aramid woven outer layer rendered cracking. The failure strain of composites was also higher due to the effect of 2D aramid and matrix. The FMLs, on the other hand, showed higher flexural strength for AFE followed by AFB and AFP. The flexural modulus was higher for AFB, followed by AFE and AFP. The failure strain was higher for AFE and then for AFB and AFP, respectively. The reason for the lower properties of AFP is already explained as the extensive delamination cause premature failure of FML.

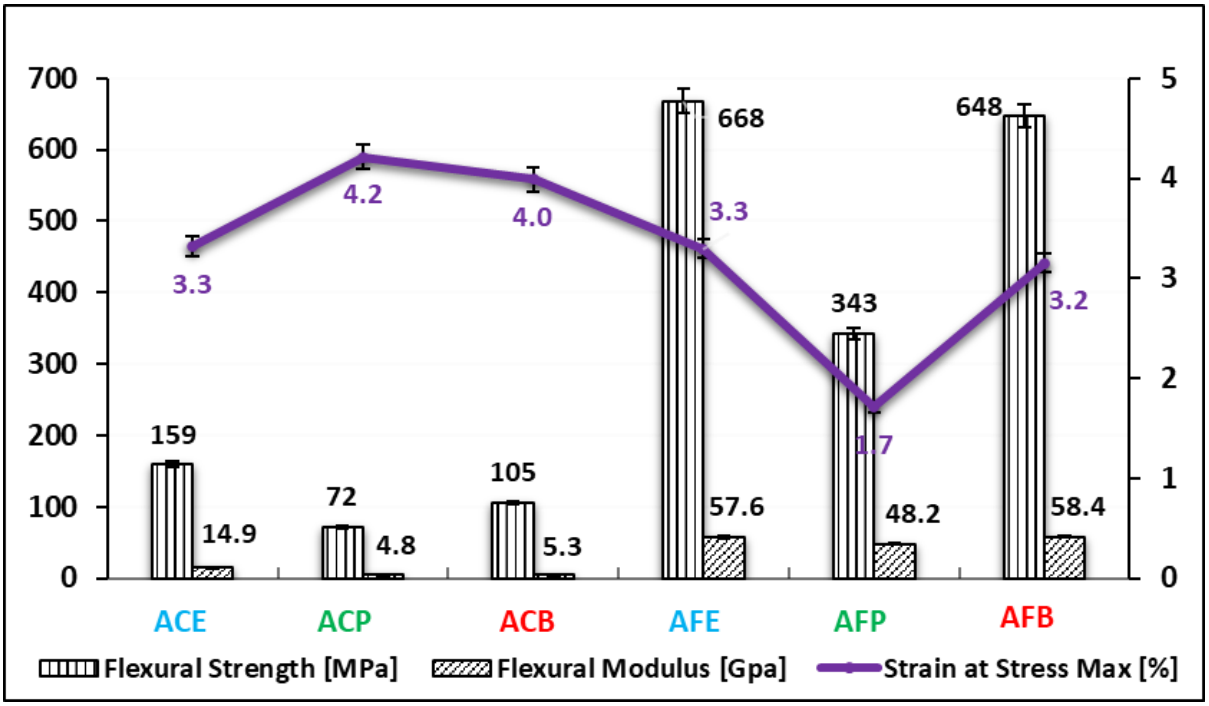

Figure 4.34. Flexural properties of 2D aramid + 3D jute composites and FMLs

Figure 4.35 shows the cross-section of fractured samples after flexural test of 2D aramid + 3D jute reinforced composite and FMLs. The composite samples showed extensive bending, and there was no sign of fibre failure. There was a slight resin crack in the composites, but fibre failure was rendered due to aramid fibre. The failure pattern of AFE and AFB was almost similar, in AFE there was extensive delamination seen between aramid and jute woven core while in AFB the delamination was slightly lower. The dominant failure mechanism in AFE and AFB was metal crack, delamination, resin, and reinforcement crack. In AFP there was delamination observed between aramid and jute woven core. The bonding between aramid and jute was not very well, resulted in delamination. The reason for weak bonding between aramid and jute woven core is PP matrix as it caused inferior bond.

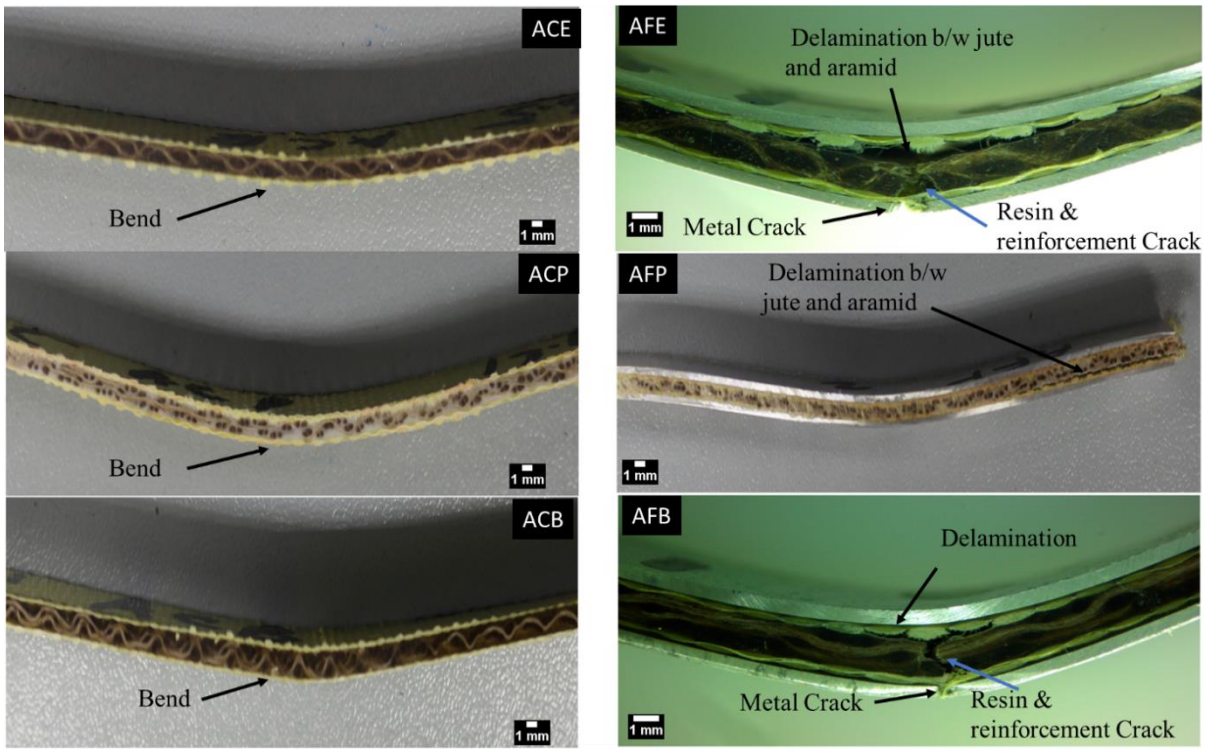

Figure 4.35. The cross-section of fractured samples after flexural test of 2D aramid + 3D jute composite and FMLs

D. 2D Carbon / 3D Jute Composite and FMLs

Figure 4.36 shows the stress-strain curves of 2D carbon + 3D jute reinforced composites and FMLs. The composite curve shows the high brittleness of CCE and brittle failure. The CCP had very ductile failure as it experienced tremendous strain relative to other composites. The CCB had intermediate properties as the curve is in between CCE and CCB. As far as the composites are concerned, the properties are mainly governed by the reinforcement and matrix. For the FMLs, the curve can be divided into three principal zones: linear, non-linear and failure zone. In the linear zone, the curve rises very sharply with very little strain, in the non-linear zone, the curve tends to experience considerable strain with low stress, as in the non-linear zone the resin crack and delamination start. In the failure zone, there was reinforcement failure, and multiple delaminations were experienced, causing multiple peaks. The behaviour of CFE and CFB curves was almost similar. For CFP, in the linear zone the curve tends to follow the

CFE and CFB but in the non-linear zone due to premature delamination between 2D carbon and 3D jute woven core the failure occurs prematurely.

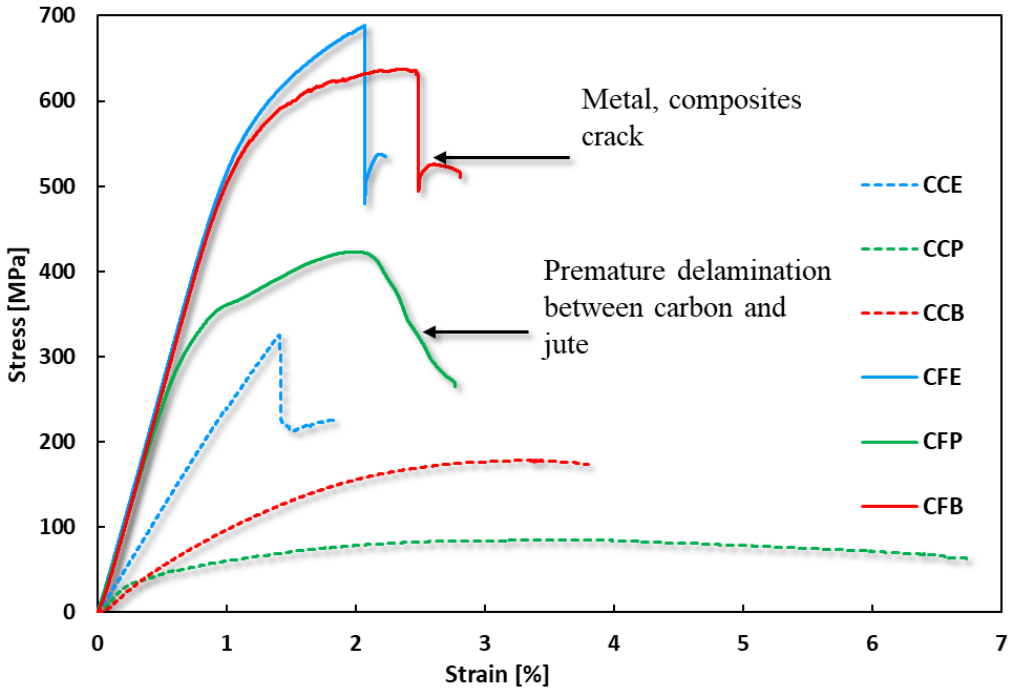

Figure 4.36. The flexural stress-strain properties of 2D carbon + 3D jute reinforced composites and FMLs

Figure 4.37 shows the flexural properties of 2D carbon + 3D jute reinforced composites and FMLs. When the properties of composites are discussed, the CCE had the highest flexural strength, followed by CCB and CCP. The flexural modulus also follows the same pattern. For flexural strain, the CCP had the highest strain, followed by CCB and CCE. For the FMLs the CFE had the highest flexural strength followed by the CFB and CFP. The flexural modulus of CFE and CFB was almost equal, while the CFP had the lowest modulus. The failure strain of CFB was higher than for CFE and CFP respectively. The reason for the lower failure strain of the CFP was a premature failure due to delamination between reinforcement. The low flexural strength of the CFP was also due to the previously discussed reasons.

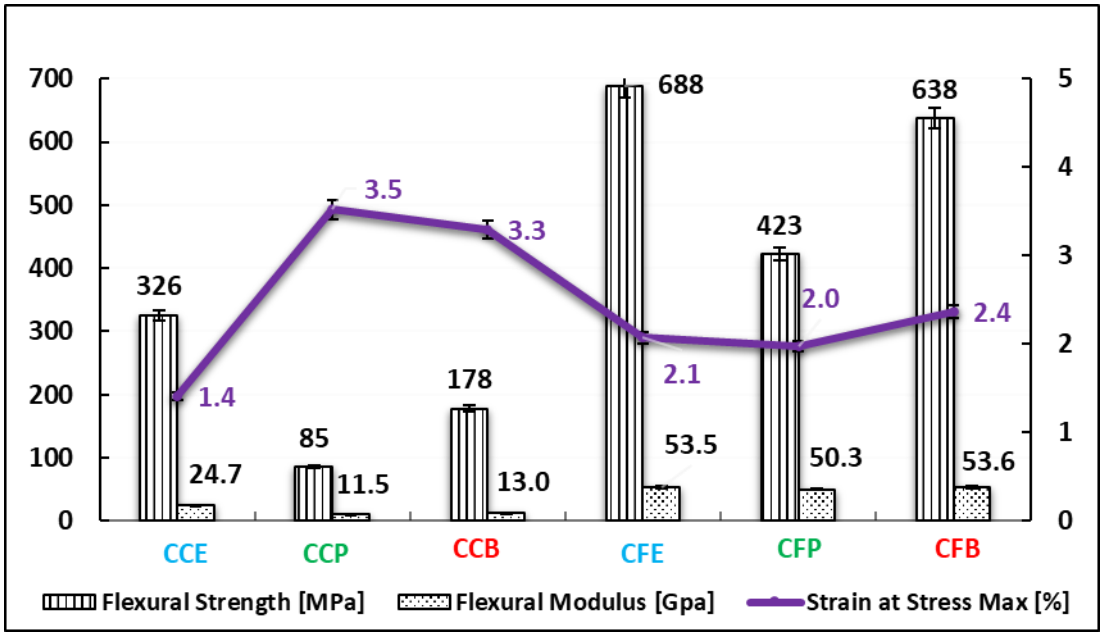

Figure 4.37. Flexural properties of 2D carbon + 3D jute composites and FMLs

Figure 4.38 shows the cross-section of fractured samples of 2D carbon + 3D jute reinforced composites and FMLs after the flexural test. The CCE had a brittle failure due to epoxy and carbon fibre. The CCB also experienced brittle failure along with delamination between carbon and jute. The CCP did not experience any crack due to the ductile nature of PP, and there was delamination seen between carbon and jute woven core. For the FMLs, CFE and CFB experienced a similar kind of failure. The dominant failure mechanism includes delamination, metal crack, resin, and reinforcement failure. The CFP failed prematurely due to delamination between carbon and jute woven core, that's why lower properties were experienced for the CFP.

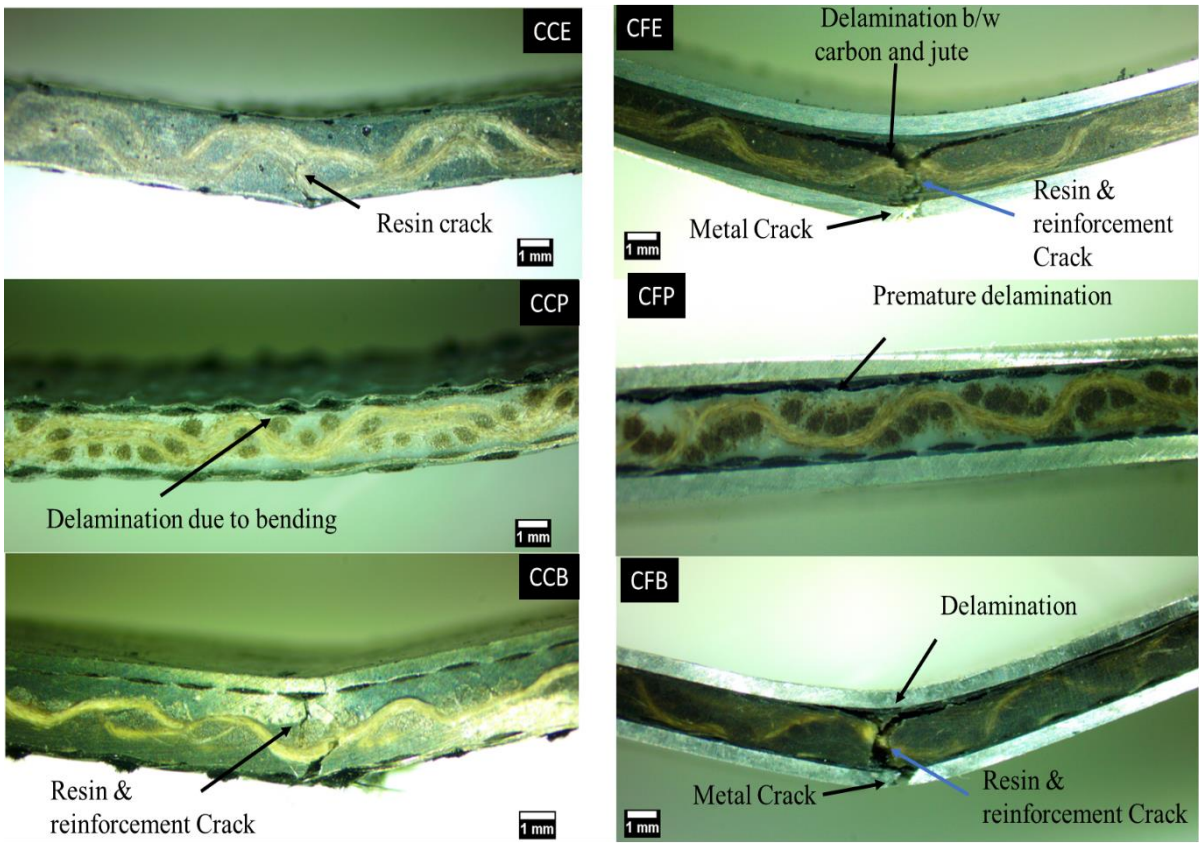

Figure 4.38. The cross-section of fractured samples after flexural test of 2D carbon + 3D jute composite and FMLs

E. 2D Glass / 3D Jute Composite and FMLs

Figure 4.39 shows the flexural stress-strain curves of 2D glass + 3D jute reinforced composites and FMLs. The GCE showed high modulus and high flexural strength. The GCB had relatively lower flexural strength as compared to GCE. The GCP showed more ductile behaviour with relatively lower strength and modulus. The GCE had a high strain followed by GCP and GCB. The reason for the high failure strain of GCE was that glass-epoxy composite form more durable structure which offers more resistance to deformation. Further, the aluminium, glass and epoxy had a stronger interface which causes better properties. When the curves of FMLs are analysed, the linear portion of all three FMLs was similar. In the non-linear part, the GFP experienced a sudden drop in the curve due to premature delamination between glass and jute

woven core. The GFE had highest strength. The failure strain of GFB was higher due to the already explained reason.

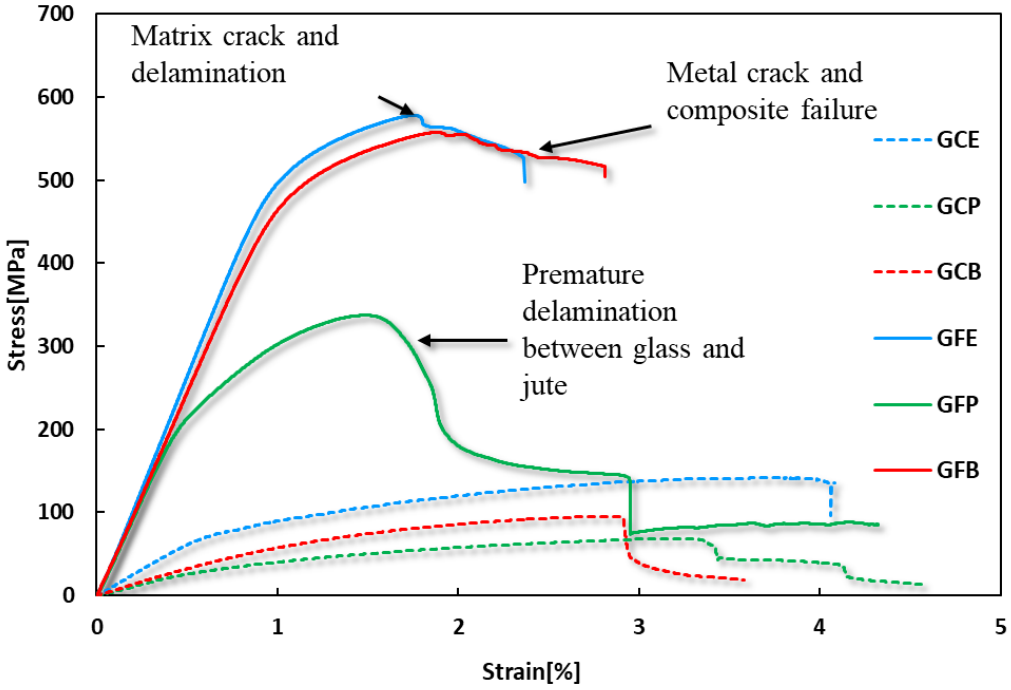

Figure 4.39. The flexural stress-strain properties of 2D glass + 3D jute reinforced composites and FMLs

Figure 4.40 shows the flexural properties of 2D glass + 3D jute reinforced composites and FMLs. The GCE had the highest strength and modulus, followed by GCB and GCP. The failure strain of GCE was the highest and then for GCP and GCB, respectively. The reason for the higher strain of GCE is already explained. For the FMLs properties, the GFE had the highest strength. Between GFB and GFP, the GFB had higher strength. The strain of GFB was highest, followed by GFE and GFP. The reason for the lower failure strain of GFP was that it disseminated prematurely, the glass and jute woven core delaminated due to poor bonding.

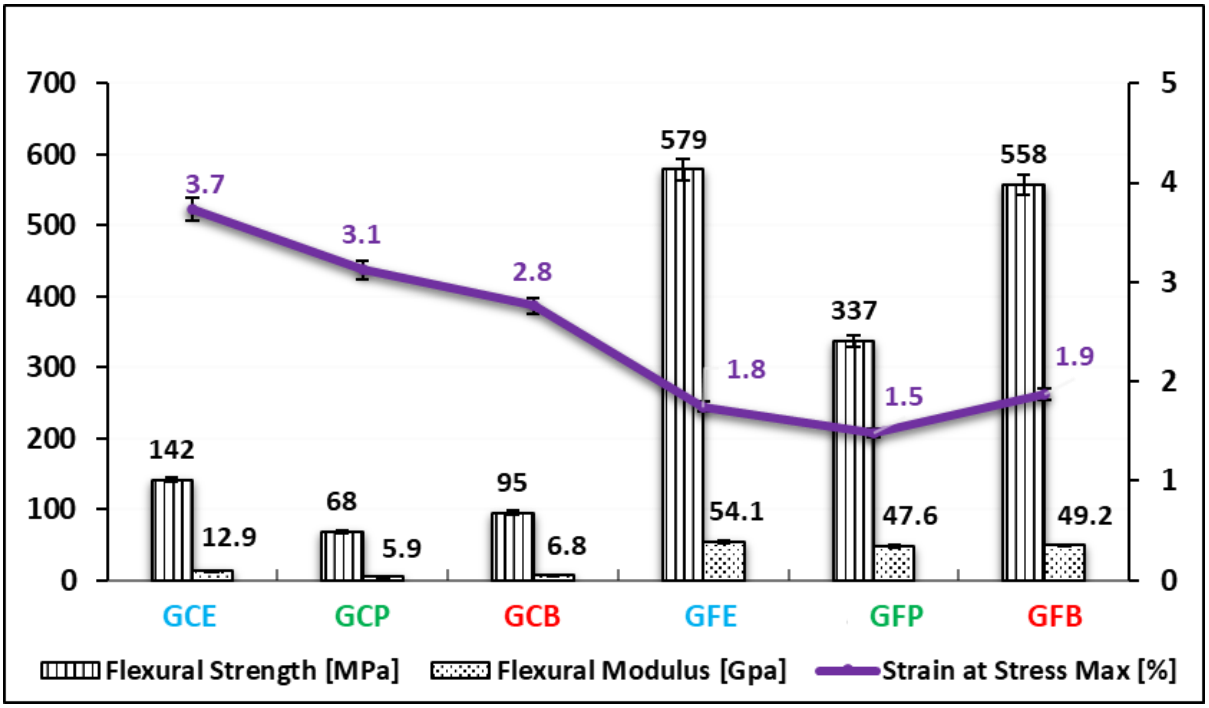

Figure 4.40. Flexural properties of 2D glass + 3D jute composites and FMLs

Figure 4.41 shows the cross-section of fractured samples after flexural test of 2D glass + 3D jute reinforced composite and FMLs. All the composite samples experienced resin and reinforcement crack. The GCE experienced brittle failure of jute woven core. The GCB also experienced a similar kind of failure. In GFE and GFB the dominant failure mechanism was delamination, resin, metal, and reinforcement crack. The metal crack was experienced due to large shear forces. The GFP, like previous synthetic + jute FMLs, experienced delamination between glass and jute woven core. This premature delamination caused its failure before GFE and GFB.

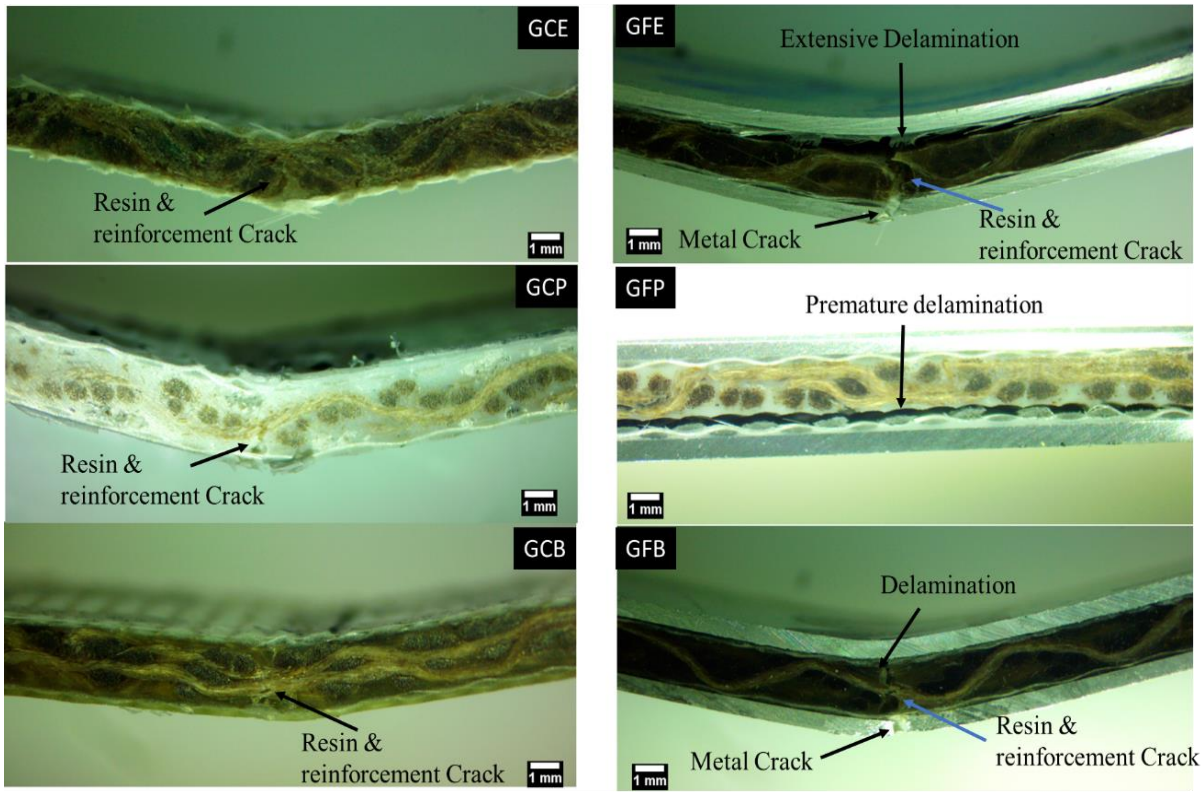

Figure 4.41. The cross-section of fractured samples after flexural test of 2D glass + 3D jute composite and FMLs

4.3 Conclusion

The properties of composites were different from FMLs. Normally after addition of aluminium above and below the composite improved its tensile and flexural properties to many folds. The properties of 3D woven reinforcement depend heavily on the type of interlocking being used to make them. The 3D woven reinforced composite which has TT interlocking offer much improved tensile properties due to low crimp. While the LL interlocked structures offer better bending properties due to placement of yarn in layer and in the thickness direction. When the FMLs are made, another factor which contributes significantly is MVF, the FML with higher MVF will have better properties. The highest MVF is achieved for TT interlocked reinforcement so the properties of FMLs made with that will also be higher. The TT interlocked

structure is more compact and have a thickness less than LL interlocked structures. The hybrid structures offer the added advantage of synthetic and natural fibres. The properties of these structures will be governed by the type of material used for hybridization. Along with the material type, the matrix also plays an important role in the final properties. The 100% jute reinforced composites and FMLs, both suffer brittle breakage when made with epoxy. The 100% jute reinforced composites and FMLs made with PP matrix offer inferior properties due to poor metal-matrix interface. Once the composite and aluminium delaminate the aluminium keeps on elongating. The PP hybrid composites and FMLs show ductile behaviour and higher elongation. The tensile stress-strain curve shows that hybrid PP FMLs had excessive delamination due to poor metal-matrix, metal-composite, and fibre-matrix interface. The flexural stress-strain curve also shows that the PP based FMLs had suffered premature failure due to delamination between 2D woven and 3D woven fibre layer. The tensile properties of PVB composites and FMLs depended on the type of reinforcement, the 100% jute reinforced composites performed relatively better due to better interface of fibre matrix. The FMLs made with 100% jute and PVB performed better than PP and its properties were also comparable to epoxy based FMLs. The flexural properties of PVB based composites reinforced with 100% jute were better than other composites, while for the FMLs lower than epoxy and higher than PP based FMLs. The epoxy-based hybrid composites and FMLs showed overall better tensile and flexural properties. The tensile properties of epoxy-based composites were the highest, followed by PVB and PP, while for the FMLs both epoxy and PVB showed similar modulus and the difference in the tensile strength was not very large. When the properties of hybrid composites and FMLs are compared, the PVB based FMLs perform better than composites as compared to other FMLs, the reason of this improvement is that the PVB offer better metal-matrix interface which result in improved mechanical performance. It can be concluded the

PVB matrix can be used as a replacement for the FML fabrication due to its overall better metal-matrix and fibre-matrix interface.

Chapter 5. Hybrid Composites and FMLs Low Velocity Impact Properties

This chapter concerns the low-velocity impact properties of FMLs and corresponding composites made with hybrid reinforcement and different matrices. The purpose of hybridizing 3D jute with 2D synthetic reinforcement was to access the improvement in the properties w.r.t metal-matrix, metal-composite, and composite-matrix interface. The crack propagation, damage, and failure mechanism were also accessed. The effect of thermoplastic and thermoset matrices was also determined to examine how the energy dissipation and crack propagation characteristics changes for different matrices. The PVB based composites and FMLs showed overall higher impact performance as compared to both epoxy and PP matrix. The plasticity of matrix and energy dissipation characteristics of PVB based composites and FMLs was the reason behind improved impact performance. Out of different types of hybrid reinforcement, the aramid /3D jute combination showed better impact performance due to nature of aramid fibre.

5.1 LVI Properties of 3D Jute Composites and FMLs

Figure 5.1 shows the different curves of JFRC after LVI. As can be seen from the curves that for each type of composite the curve has 4 slopes indicating the different stages of fracture. This type of slopes in the curves purely indicates the response of 3D structures. The first slope indicates the initial matrix cracking and exposing to the fibre top layer. Then the second slope indicates the further matrix cracking with damage in the fibre layer. As the crack keeps progressing in the vertical direction so there will be more resistance towards the cracking as the fibres are placed in the layers, so more resistance is offered. That is why it can be seen that every slope is at higher force. The third slope is showing highest resistance towards impact and it is a bit wider as compared to the other slopes. This is coupled effect of fibre layer and matrix. As deformation continues, it has become difficult for structure to deform depending on the matrix and fibre interface. With more matrix cracking the fibre layers get exposed and further it becomes difficult to crack to propagate without deforming fibre layer, so that is why the third slop is a bit wider and at higher force. Then the last slop shows the complete failure of the structure. The type of damage will depend upon the nature of the matrix system. The JCB offered more resistance to impact and more stiffness compared to rest of two composites. The JCB also has least central deflection during impact. The JCP has comparably maximum central deflection showing higher damage, even more than JCE. The reason for this behaviour is that the PP do not have a very good interface with jute fibres, due to this poor interface the reinforcement and PP are getting exposed to impact.

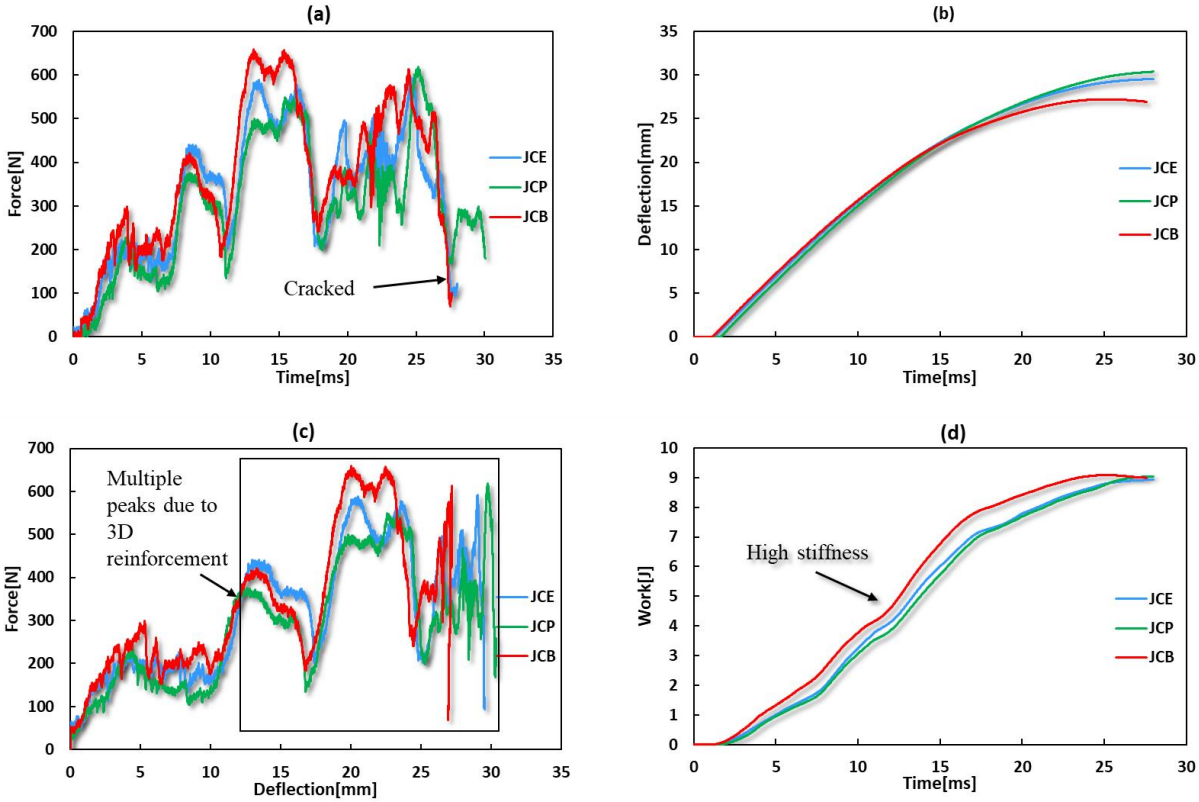

Figure 5.1. Typical curves of 3D jute composites (a) force-deflection (b) force-time (c) work-time (d) deflection-time

The *Figure 5.2* shows the tested samples of 3D composites after LVI test. The tested samples closely correlate with the force-deflection curve of the sample. Both JCE and JCP have a similar pattern of crack, mainly showing the impact performance is fibre dominated. The crack is propagated in the warp and weft direction, normal to each other. In the JCB the crack did not follow any specific path rather propagated randomly. The impact properties in the JCB are matrix dominated. Due to this matrix dominated behaviour the maximum deflection is also less than both JCE and JCP. Further, as the cracks propagate randomly, so it has to bear more resistance from reinforcement, so that is another reason of better impact performance of JCB. The matrix fully impregnates the fibres in JCB that is the reason of the dominance of matrix during LVI test.

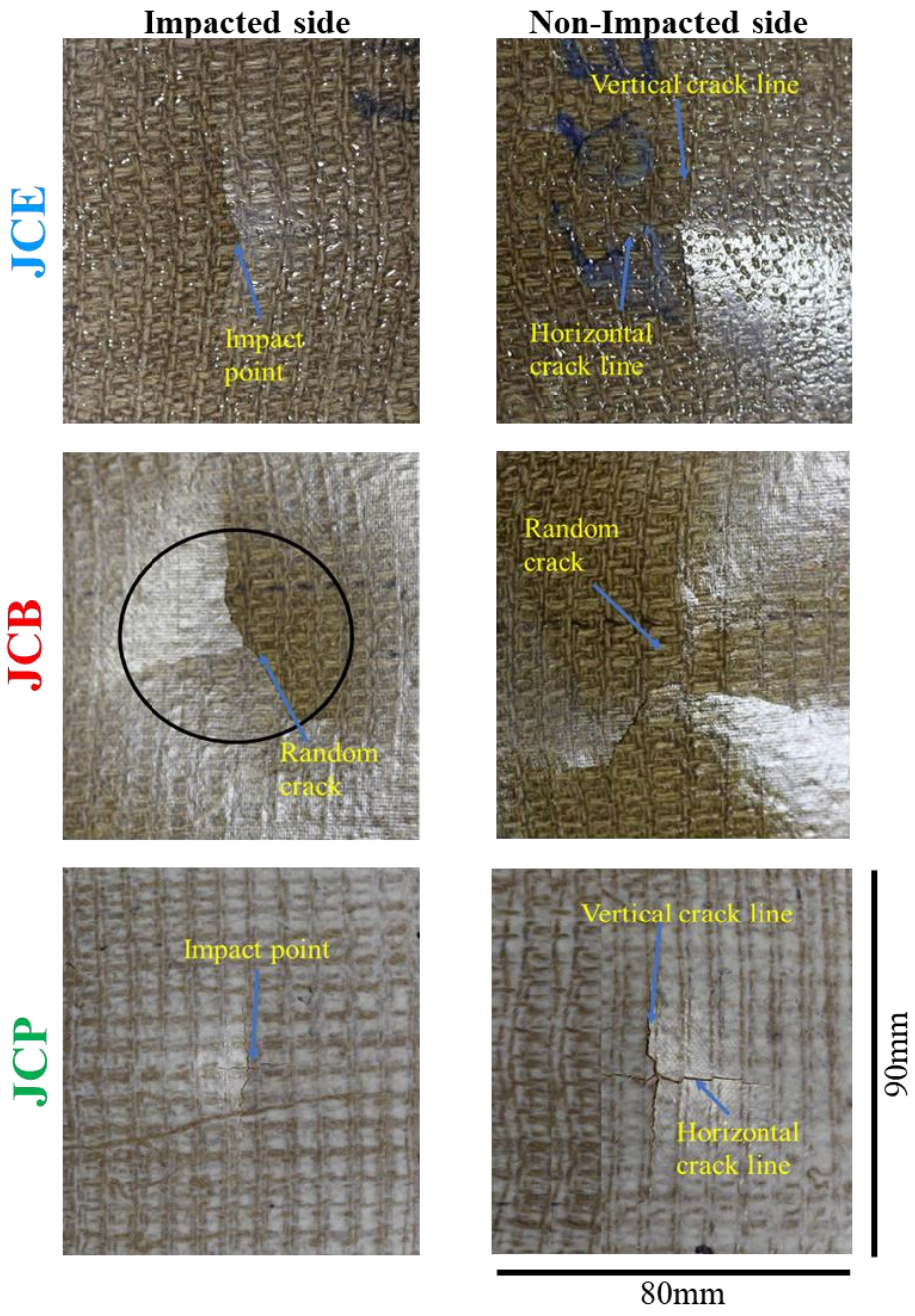

Figure 5.2. The images of cracked composites samples after LVI showing different crack types

Figure 5.3(a) shows the force-time curve of 3D jute reinforced FMLs. The JFB had the highest impact force. The JFP and JFE show almost similar behaviour. The first major drop in the force was observed around 2*ms* for all samples. This drop in force indicates the delamination between metal and composite due to the plastic deformation of aluminium. Both the JFE and JFB

initially offered similar resistance towards LVI and showed the same kind of bending stiffness. Then after the first drop in the curve, the JFB offered better resistance towards impact. The parameters which affect the LVI impact properties are the nature of the matrix, fibre-matrix interface, and metal-matrix interface. When the effect of the matrix is discussed, the PVB offered more stiffness than PP and epoxy, so more impact tolerant. The PVB offered more resistance towards perforation as well. The epoxy due to brittle nature is least impact tolerant so more and easier perforation when compared to PVB. The PP is also stiffer, but in the case of jute reinforcement, the impregnation of reinforcement and bonding is not very good so offered poor impact resistance even compared to epoxy. The first failure point in the FMLs relates to damage initiation force, at that point mainly the drop in the peak is observed due to sufficient deep indenter penetration, matrix cracking or significant delamination. The delamination is usually a result of matrix cracking [110]. The sharp drop in the force-time curve in case JFE and JFP was due to excessive delamination followed by reinforcement failure. Another interesting aspect is contact time, which is less for PVB based FMLs shows excellent resistance towards the impact due rebound of the impactor. Figure 5.3(b) shows the deflection-time curve and as can be seen that for both JFE and JFP the deflection goes on increasing with time as the impactor keeps on penetrating the sample, while in case of JFB the after attaining the maximum deflection the curve tends to bend down due to already described reason. Figure 5.3 (c) shows the force-deflection curve; the curve clearly indicates that both JFE and JFP suffered complete perforation while JFB suffered only FVC on NIS. It can also be seen from the curve that after reaching the maximum deflection, the PVB reinforced FML released more elastic energy back to the impactor. As discussed earlier in the case of JFB, only part of the energy was used while the rest was used to rebound the impactor. In the case of JFE and JFP, excessive energy was used in fibre damage and perforation. The PVB impregnated the reinforcement fully, making a stiffer network against the impact. Figure 5.3 (d) shows the work

done-time graph. It is very clear from the graph the PVB based FML released a portion of impact energy as elastic energy. Both JFP and JFE suffered perforation. The JFP suffered perforation even at a low energy level showing its poor performance. The curve also shows the less stiffness of JFP and the highest stiffness of JFB.

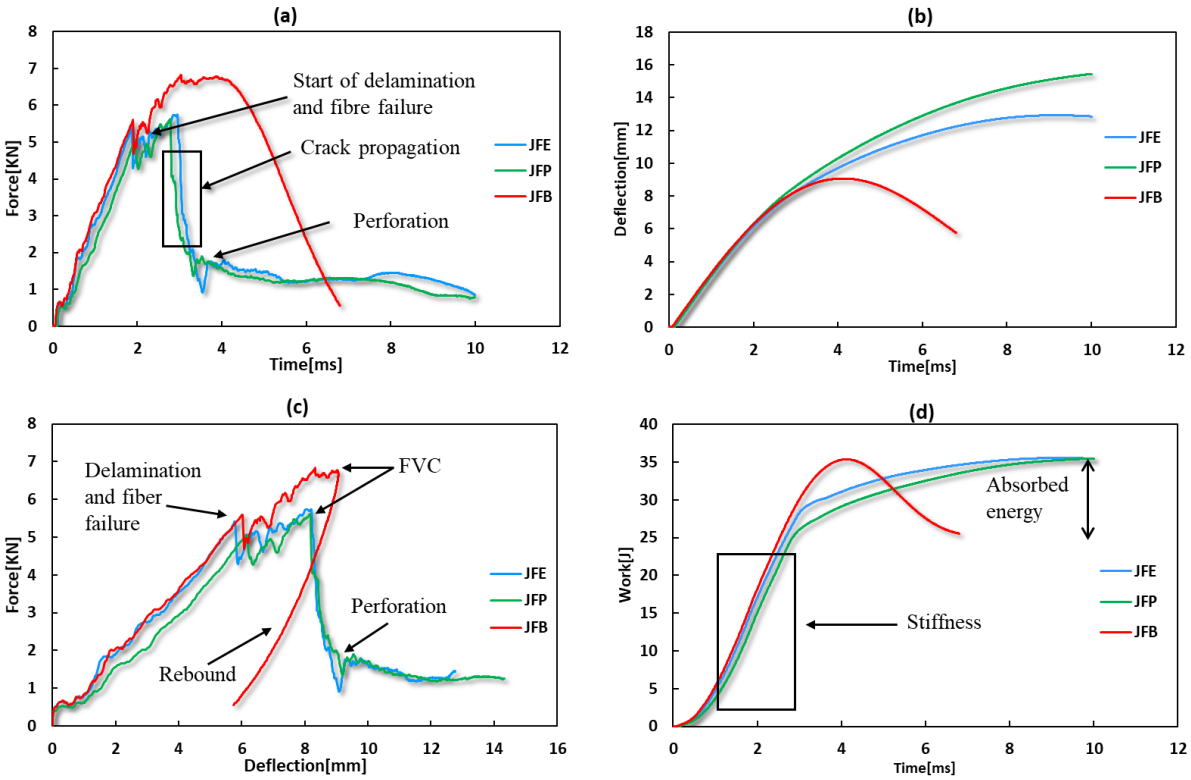

Figure 5.3. Typical curves of 3D jute FMLs (a) force-deflection (b) force-time (c) work-time (d) deflection-time

The Figure 5.4. shows the LVI tested samples of 3D jute reinforced FMLs and cross-section of damage area. Both JFE and JFP had been perforated completely. Before going to perforate they had an FVC and SVC crack. This behaviour can also be seen in the force-deflection curve Figure 5.4 (c). The FMLs experience FVC on the NIS rather than IS, the reason for this metal break on NIS is that the fibre cracking in the composite starts due to compressive stresses which are generated due to micro-fibre buckling. This micro-cracking makes ways to meso and macro fibre cracks in the composites. These micro-cracking points create the pressure points on the surface of the NI aluminium plate, which cause the cracking of metal [111], [127]. While the

JFB has FVC with plastic deformation of aluminium. That shows the JFB has better ability to store elastic energy and then rebound that elastic energy as compared to JFE and JFP as can be seen from the cross-section that the JFB mainly experienced plastic deformation. Both aluminium and PVB deformed plastically. The JFE and JFP have a similar type of perforation, but the nature of perforation is different from each other due to different matrix systems.

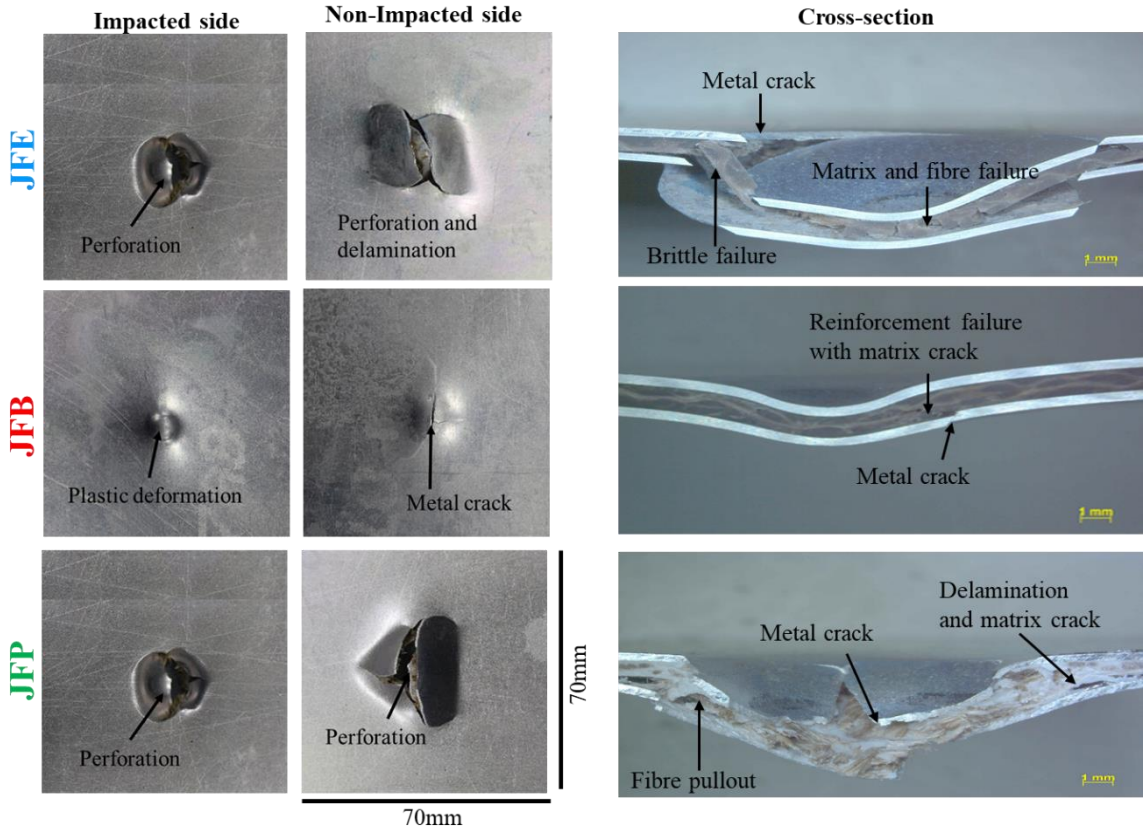

Figure 5.4. The cracked samples of 3D jute reinforced FMLs and the cross-section of the damaged area

5.2 2D Jute / 3D Woven Jute Composite and FMLs LVI properties

The Figure 5.5. shows the LVI test response of 3D jute reinforced composites sandwiched between 2D plain jute woven fabric made using three different kind of resin systems. Globally the trends are almost similar when it is related to effect of matrix systems, due to already explained reasons. The JJCB show much more stiffness and resistance to impact. Figure 5.5(a) shows that there are not multiple peaks like JJCE and JJCP in the curve of JJCB. That is due

to dominance of PVB in determining the properties of JJCB. The JJCB curve shows that the impactor stops after hitting the palate and then shows some rebound due to elastic stored energy. JJCP and JJCE both shows almost similar kind of behaviour towards LVI. Even the 3D reinforcement was sandwiched between 2D plain woven fabric the global behaviour did not change. As discussed in the previous section, the jute-epoxy and jute-PP composites show a fibre dominant deformation due to the nature of bonding of both the matrix systems, so there are multiple peaks like simple 3D jute composites made with same metrices once the matrix crack then the reinforcement determine the properties. The initial part of force-deflection curve of JJCE and JJCP is different from the JCE and JCP due to sandwiching of 3D fabric with 2D fabric, the deformation starts at higher force even with higher stiffness. As the 2D reinforcement also have the same material, so overall there is small change in the properties. Figure 5.5(b) shows that the JJCB has least central deflection as compared to JJCE and JJCP.

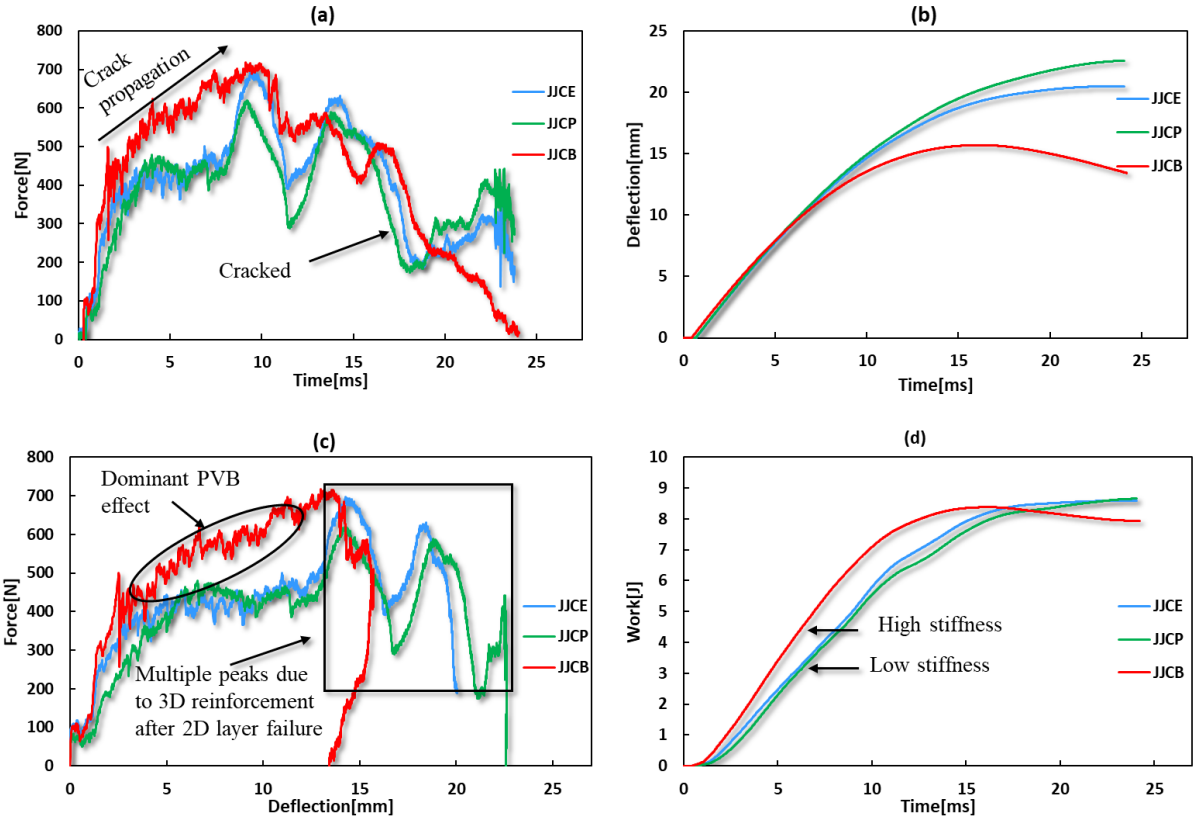

Figure 5.5. Typical curves of 2D jute + 3D jute composites (a) force-deflection (b) force-time (c) work-time (d) deflection-time

The images of tested samples of 2D jute + 3D jute reinforced composites are showing similar damage characteristics as the simple 3D jute reinforced composites showed. The JJCE and JJCP has similar kind of cracking / fracture behaviour dominated by fibres, with vertical and horizontal crack lines normal to each other. The JJCB has random crack with almost similar size on the IS and NIS. While in the JJCE and JJCP the crack is propagated more on the NIS side (Figure 5.6).

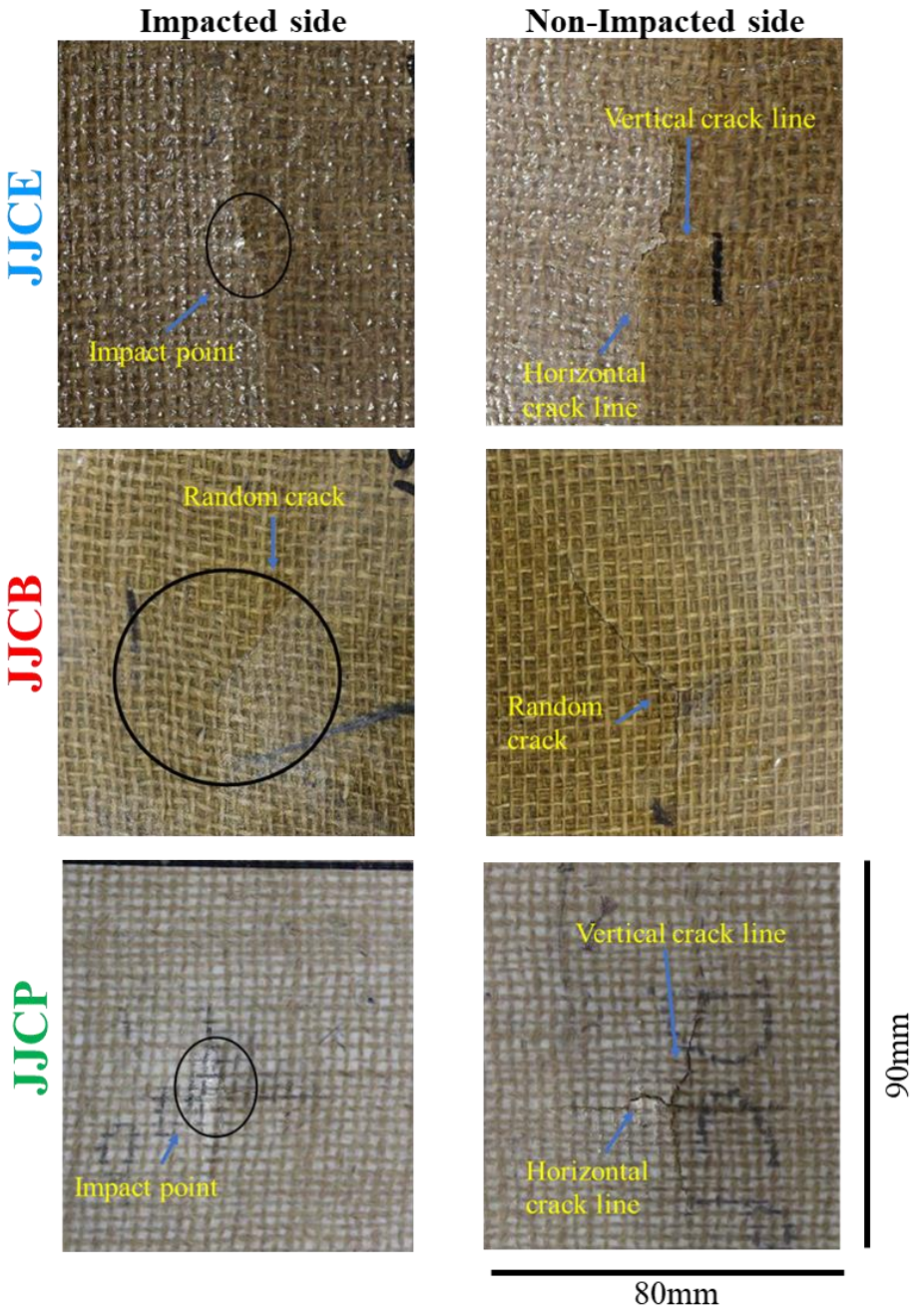

Figure 5.6 The fractured samples of 2D jute + 3D jute composites after LVI

Figure 5.7(a) shows the force-time curves of 2D jute + 3D jute reinforced FMLs. The curves show that the behaviour of 2D jute + 3D reinforced FMLs is also similar to the FMLs made with only 3D woven jute reinforcement. The curve drops sharply after the second peak in the force for the JJFE and JJFP, this sharp drop in case of JJFE was due to the brittleness of epoxy resin. While for JJFP, that was due to poor fibre-matrix interface as once the crack initiates, it

propagates easily. The JJFE suffered partial perforation and JJFP suffered complete perforation. As in case of JJFE the crack spread to larger area which render its complete perforation (Figure 5.8). The JJFB offered overall better resistance to impact with a high impact force compared to JJFE and JJFP. The plastic nature of both aluminium and PVB added up in a way that it offered better resistance towards impact due to better metal–composite adhesion and fibre-matrix interface. The contact time of impactor with JJFB is also shorter than the other two FMLs, as the impactor rebound due to unused elastic energy. Figure 5.7(b) shows the deflection-time curve, the curve shows that all three FMLs have different behaviour. The JJFP was showing a gradual increase in the deflection, indicating impactor penetration. The JJFE also showing an initial increase in the deflection, but then curve bend slight downward. This bending was due to deflection of impactor by delaminated aluminium layer, as aluminium delaminated to larger due crack spreading, which caused deflection rather complete penetration (Figure 5.8). The JJFB however, showed a similar kind of behaviour as experienced in case of JFB. The force-deflection curves also show that the JJFB experienced only FVC while JJFE and JJFP experienced perforation after first and second cracking. Figure 5.7(c) JJFB is showing the two slops at almost similar force in the force-deflection curve. The first slope is showing matrix cracking and subsequent fibre damage. The second slope relates to FVC. At this point, first visible failure occurs on the NIS of FML. The impactor experiences a rebound after reaching the maximum central deflection; due to release of elastic energy by FMLs in case of JJFB. The JJFE showed higher stiffness initially, but then decrease gradually due to the start of delamination as a result of matrix cracking. After the FVC the curves of both JJFE and JJFP are showing a sharp drop in the force, but as the crack spreads the JJFE suffered delamination to a larger area between metal-composite which caused a deflection of impactor by aluminium that is why there is a slight inward rebound seen. Figure 5.7(d) shows work-time curves, the curves clearly shows high stiffness of JJFB followed by JJFE and JJFP. The bend in the curve

also indicating that the JJFB had transferred back stored elastic energy to the impactor, unlike JFE the JJFE showing a slight bend in the curve that is due already explained reason.

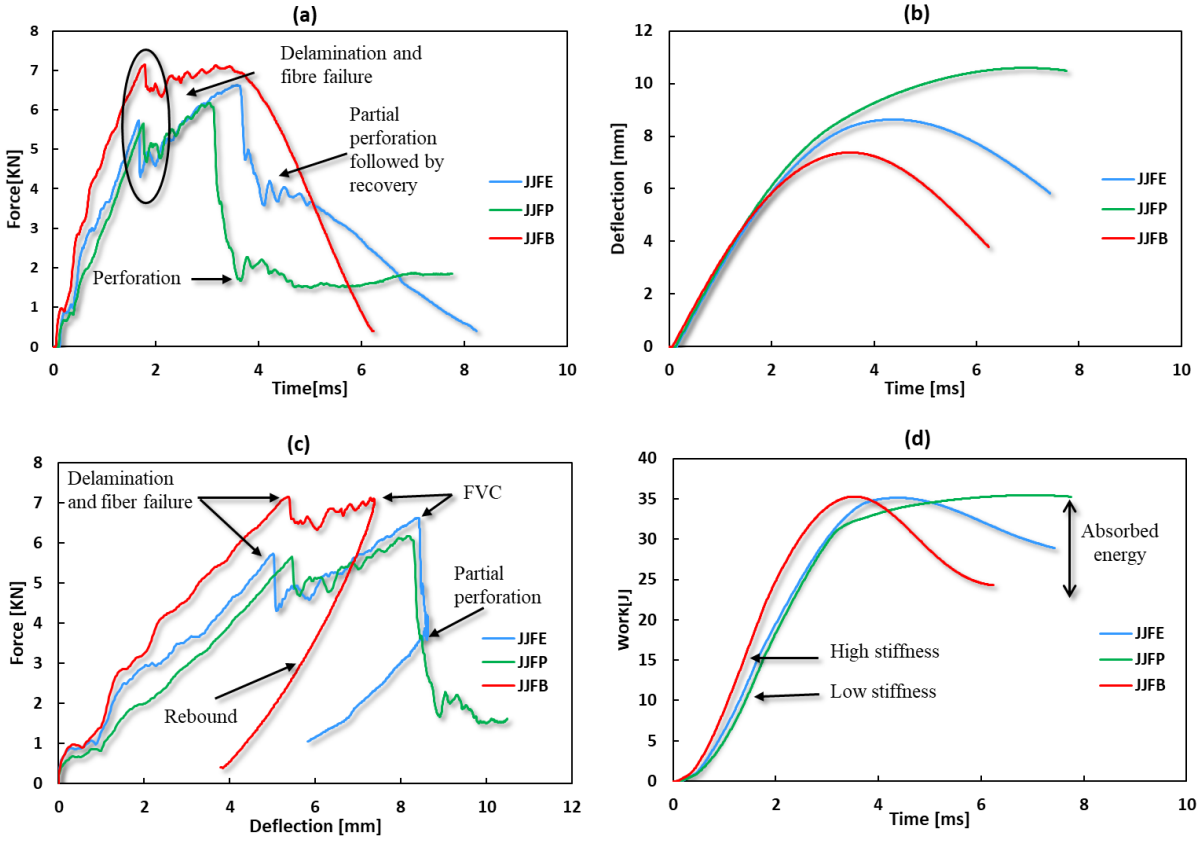

Figure 5.7. Typical curves of 2D jute + 3D jute FMLs (a) force-deflection (b) force-time (c) work-time (d) deflection-time

The tested samples of 2D jute + 3D woven jute reinforced FMLs and cross-section of damage area are shown in Figure 5.8. From the damage assessment of impacted samples, it can be established that both JJFE and JJFP has similar kind of fracture behaviour, both having FVC and SVC crack followed by the perforation. But the JJFE do not experience complete perforation due to delamination between composite and metal to a larger area. The aluminium is also deflected more in JJFE as compared to JJFP; Figure 5.7(c) also verifies this behaviour. The JJFB showed no apparent SVC only FVC. Unlike JJFE and JJFP the aluminium remained intact with the reinforcement showing excellent adhesion as well. As there was no perforation in JJFB so normally after reaching the maximum deflection, it will have elastic recovery.

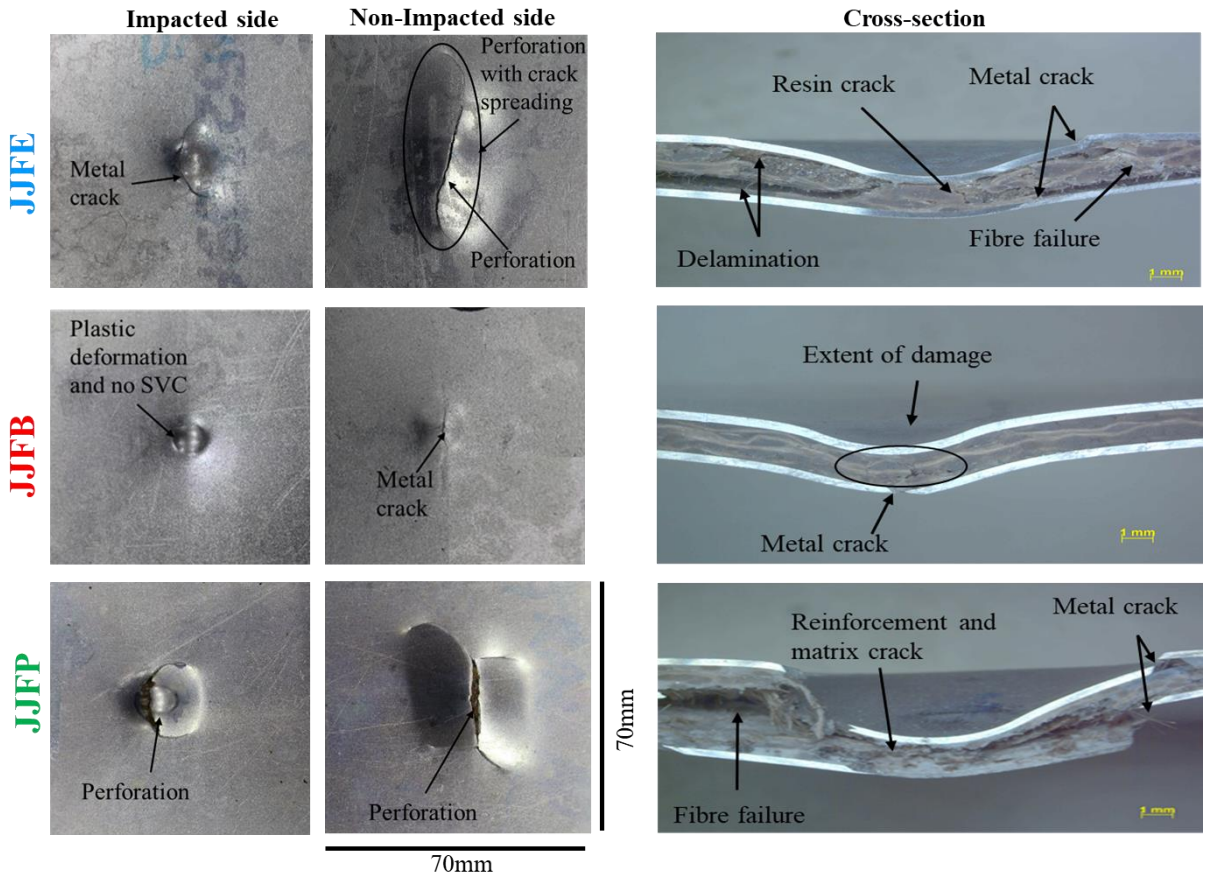

Figure 5.8. The cracked sample of 2D jute + 3D jute FMLs after LVI tests and cross-section of damaged area

5.3 2D Aramid / 3D Woven Jute Hybrid Composite and FMLs LVI Properties

The Figure 5.9 shows the graph of impact behaviour of 2D aramid + 3D jute composites after LVI test. It can be seen that ACE has suffered complete perforation. The ACP has also experienced some fibre damage on NIS side and there was also rebound due to elastic energy stored during impact. The ACB did not face much deformation during LVI. It offered sufficiently high resistance towards impact and the rebound also started earlier than the ACP. In spite of different kind of behaviour towards LVI, the overall resistance offered by all composites is showing contributions from aramid layer. The aramid fibres have exceptional resistance towards the impact due to its structural configuration. The ACE shows high initial

stiffness as compared to both ACP and ACB before experiencing matrix cracking until the first drop in the force. This trend is also visible in work-time graph (Figure 5.9(d)). The ACB has shown more rebound with less central deflection. The ACP has also shown similar kind behaviour towards LVI as compared to ACB except suffering a crack on the NIS. When the effect of hybridization is compared with 2D / 3D jute reinforced composites, it has improved a lot, especially for PP based composite. The JCP and JJCP showed poor performance against LVI due to the inferior fibre-matrix adhesion, but with the addition of aramid fibres, the properties have enhanced to many folds. Both the ACP and ACB suffered an almost similar amount of deformation.

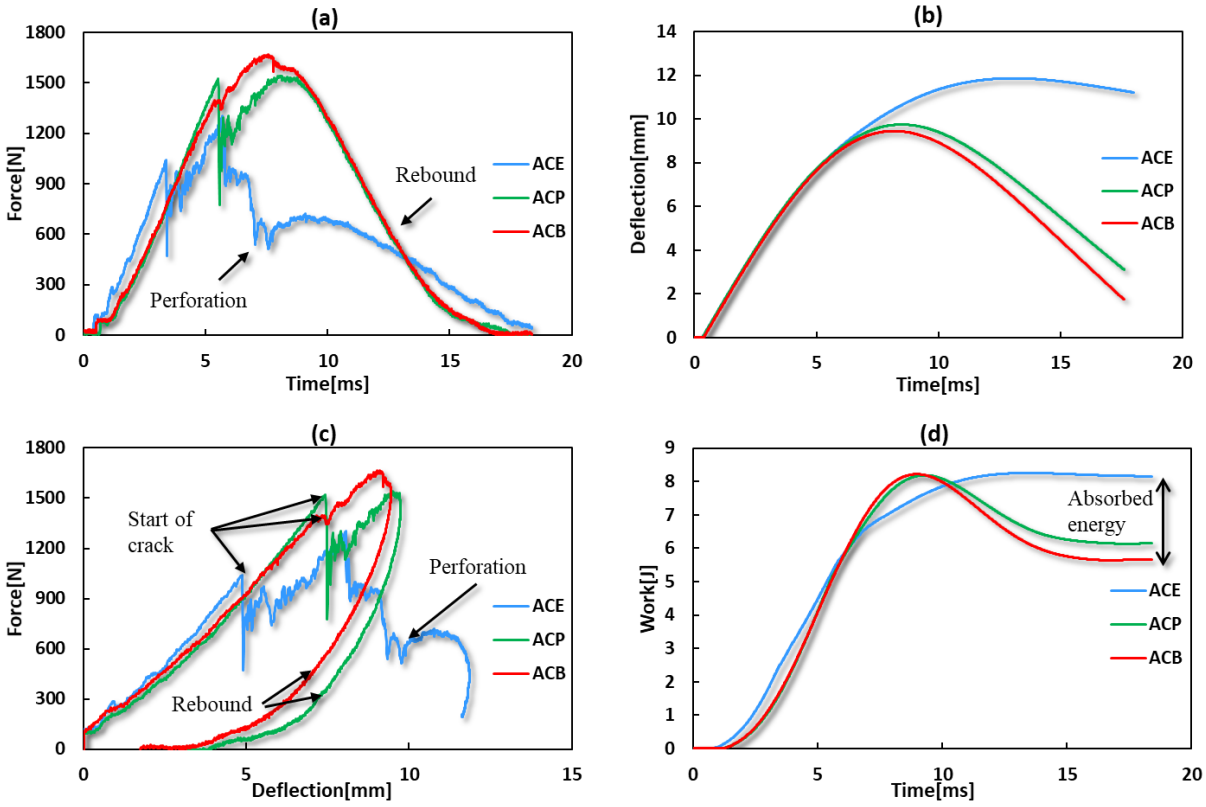

Figure 5.9. Typical curves of 2D aramid + 3D jute composites (a) force-deflection (b) force-time (c) work-time (d) deflection-time

From the images of impacted samples (Figure 5.10) it can be seen that only ACE has been perforated completely. That perforation can be seen on both IS and NIS of ACE. Both ACP

and ACB have suffered a minor crack on NIS side and invisible damage on IS. The ACE sample is also showing that some areas around the point of impact where some delamination can be seen between 2D aramid layer and 3D jute composite layer. This delamination is on both sides of the sample. This delamination on IS was distributed horizontally and vertically, normal to each other. This type of delamination was due to adhesion mismatch of 2D aramid and 3D jute when made with epoxy. This delamination between aramid and jute is also visible on NIS side and more concentrated around the perforation point. The ACP and ACB did not experience any such visible delamination between aramid and 3D jute composite layers. The reason of this different behaviour is nature of the matrix system.

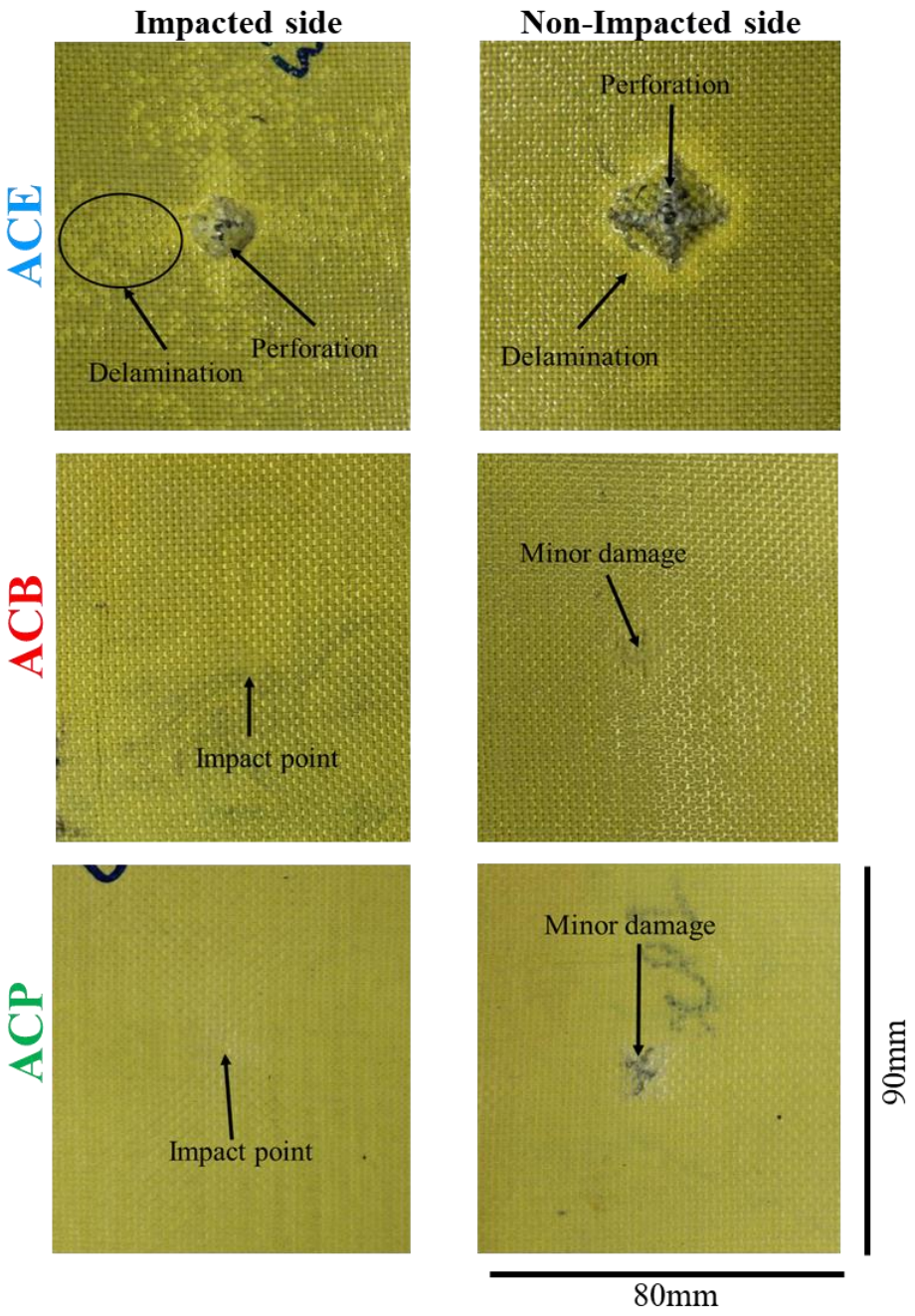

Figure 5.10. Cracked samples of 2D aramid + 3D Jute composites after LVI test

In Figure 5.11(a) it can be seen that the AFB is more impact tolerant than the AFP and AFE. All three FMLs had initially similar kind of behaviour, the AFP and AFB experienced first drop in the force at an almost similar point around 2*ms.* The AFE suffered a drop in force slightly earlier than AFP and AFB. Unlike 100% jute reinforced PP based FMLs, AFP showed improved characteristics due to the obvious effect of the addition of aramid fabric, as jute could

not get exposed to impactor directly. Further PP and aramid had also offered improved fibre-matrix interface. An interesting effect of hybridization of jute with aramid can be seen that unlike other FMLs, the sharp drop in the curve was not observed; rather, there was a gradual drop. The AFB, as usual, showed excellent impact properties, the AFP had also showed improved performance. The AFE had similar behaviour due to the effect of the epoxy matrix. Figure 5.11(b) shows the deflection-time curves, as can be seen, that for both AFP and AFB the curve faces a drop after an increase in deflection, showing the resistance of structure towards impactor, while for AFE the impactor kept piercing showing low resistance of the structure towards impact. Figure 5.11(c) shows the force-deflection curves. The curves show that the AFB experienced some permanent deformation and FVC on NIS, then rebound of the impactor. For AFP the behaviour is almost similar with a slight difference, at 9 *mm*, it experienced an SVC and AFB didn't experience SVC rather impactor rebound due to stored elastic energy. The AFP shows rebound after second crack. Both AFB and AFP show almost similar amount of recovery after the rebound. The AFE showed the poor performance against impact, and it can be seen that it had experienced FVC and SVC followed by complete perforation. The brittleness of epoxy renders composite to propagate energy. From Figure 5.11(d) it is clear that AFB has the highest stiffness, followed by AFP and AFE. The absorbed energy also follows the same pattern.

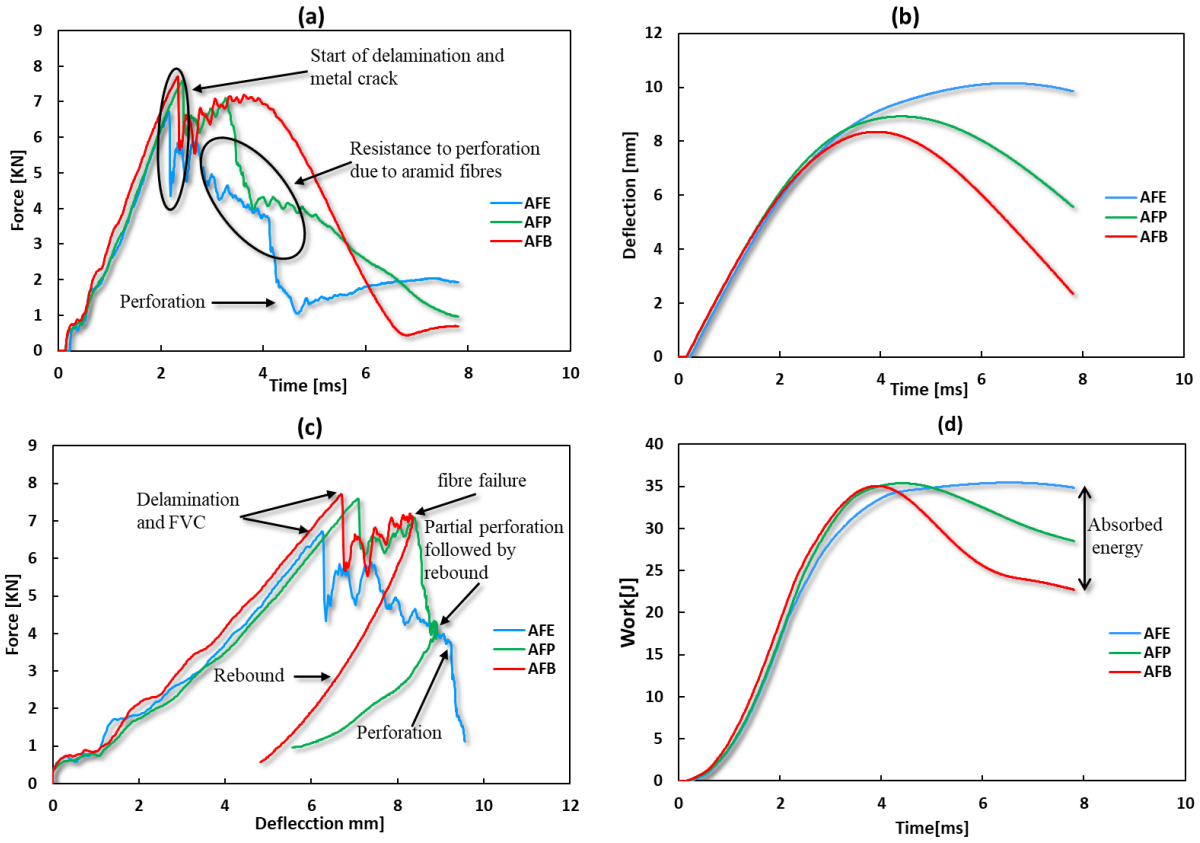

Figure 5.11. Typical curves of 2D aramid + 3D jute FMLs (a) force-deflection (b) force-time (c) work-time (d) deflection-time

Figure 5.12 shows the images of damaged samples of 2D aramid + 3D jute woven reinforced FMLs and cross section of damage area. These samples are very clearly correlating with the force-delamination curve (Figure 5.11(c)). The AFE had been perforated with delamination between composite and metal. The perforated area is also not very wide, only around the impacted point. AFP has suffered FVC and SVC crack with delamination and slight perforation. This minor perforation followed by rebound due to stored elastic energy. The AFB samples are showing only FVC crack.

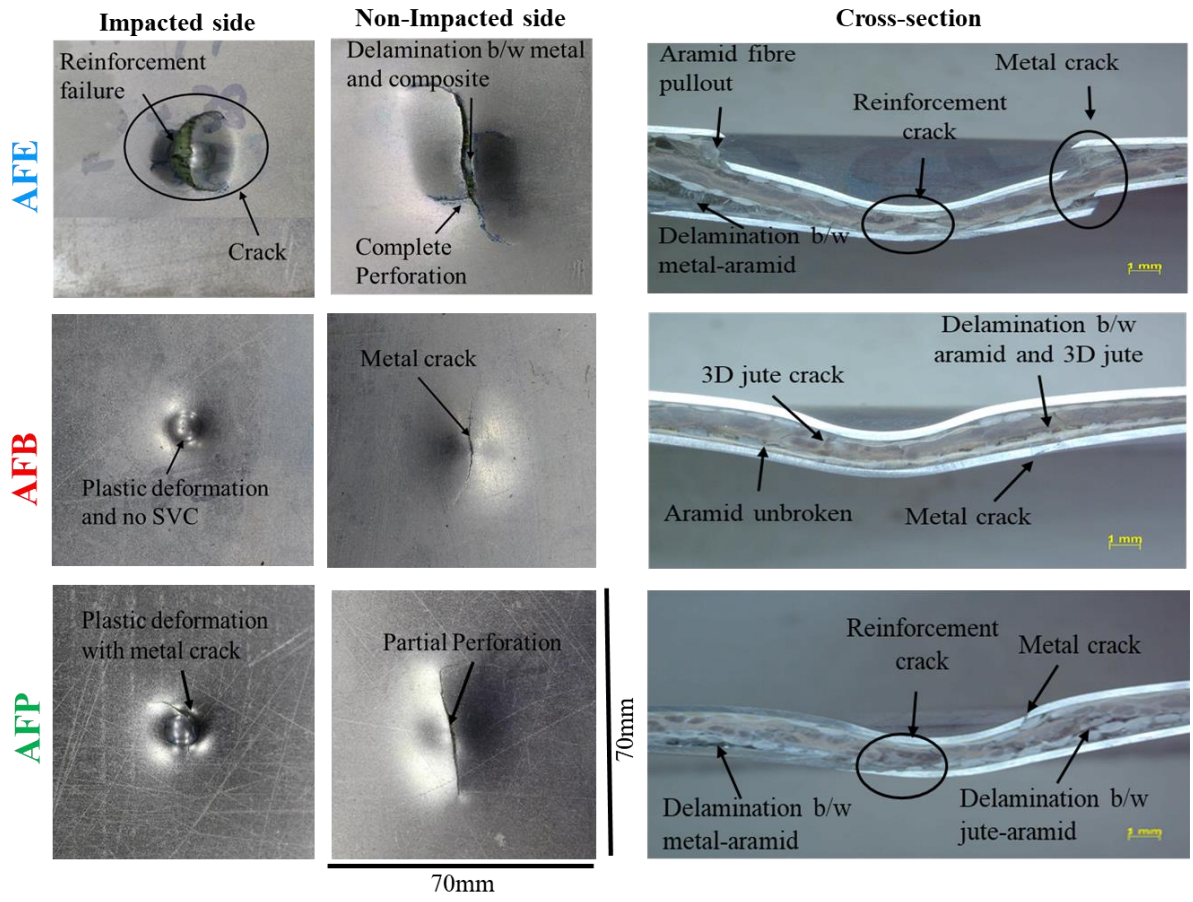

Figure 5.12. The cracked samples of 2D aramid + 3D jute hybrid FMLs after LVI tests and cross-section of damaged area

5.4 2D Carbon / 3D Woven Jute Composite and FMLs LVI Properties

The Figure 5.13 is showing the impact properties of 2D carbon + 3D jute composites. All the samples suffered some deformation, which varied from sample to sample depending upon the type of matrix. The CCB has shown initial stiffness which dropped significantly after the 1st crack at around 3mm. Same was with CCE but it suffered crack at relatively lower force. Even suffering the 1st crack at same point the nature of crack is different for both CCE and CCB, CCE is completely perforated relatively quickly while for the CCB the crack propagated rather perforation. The CCB lost a significant amount of force due to suffering larger crack which was propagated to even larger area. While the CCP has also been cracked, but that crack was at the relatively smaller area. The force-deflection curve of all three types of composite is

showing that the samples were cracked suddenly, unlike composites hybrid with aramid. Due to nature of 2D carbon, as the carbon has a very poor impact resistance. The small difference in the impact properties is due to the contribution of the matrix system. The CCE was perforated very quickly and contact time was also very small as compared to other two samples (Figure 5.13 (a)). The graph also shows that the impactor stopped after reaching the maximum deflection for the CCP and CCB, but the crack propagated differently due to nature of the matrices. The work-time graph shows that both CCB and CCP experienced little to no rebound after cracking and almost all impact energy was absorbed by the samples (Figure 5.13 (d)). The CCB initially had high stiffness which lost during the course of an impact event due to crack initiation. The curve becomes very straight at around 6ms for CCE for work-time and deflection-time graph, that is due to sudden perforation with no more resistance left by the composite against impactor. The CCB had suffered more deformation compared to CCP that is due to matrix and carbon fibres. As the crack initiates at the point of impact and once it has initiated, then it propagates to larger areas. As Both the epoxy and the PVB impregnate the fibres completely, but the epoxy-based composites perforates and PVB based experience crack propagation. The reason is that the epoxy is a brittle material with less stiffness so it gets perforated while PVB has high stiffness so it will propagate the crack rather perforation. In CCP the different behaviour of crack was due to polypropylene, as it was seen previously for bared jute fibre composites the performance of PP based composites was very poor. While hybridizing jute with synthetic fibres has improved it properties a lot. The PP-carbon combination has significantly improved the impact resistance of CCP. As it renders peroration and propagation both. Minimized the effect of both poor impact properties of carbon and least interference of PP with jute.

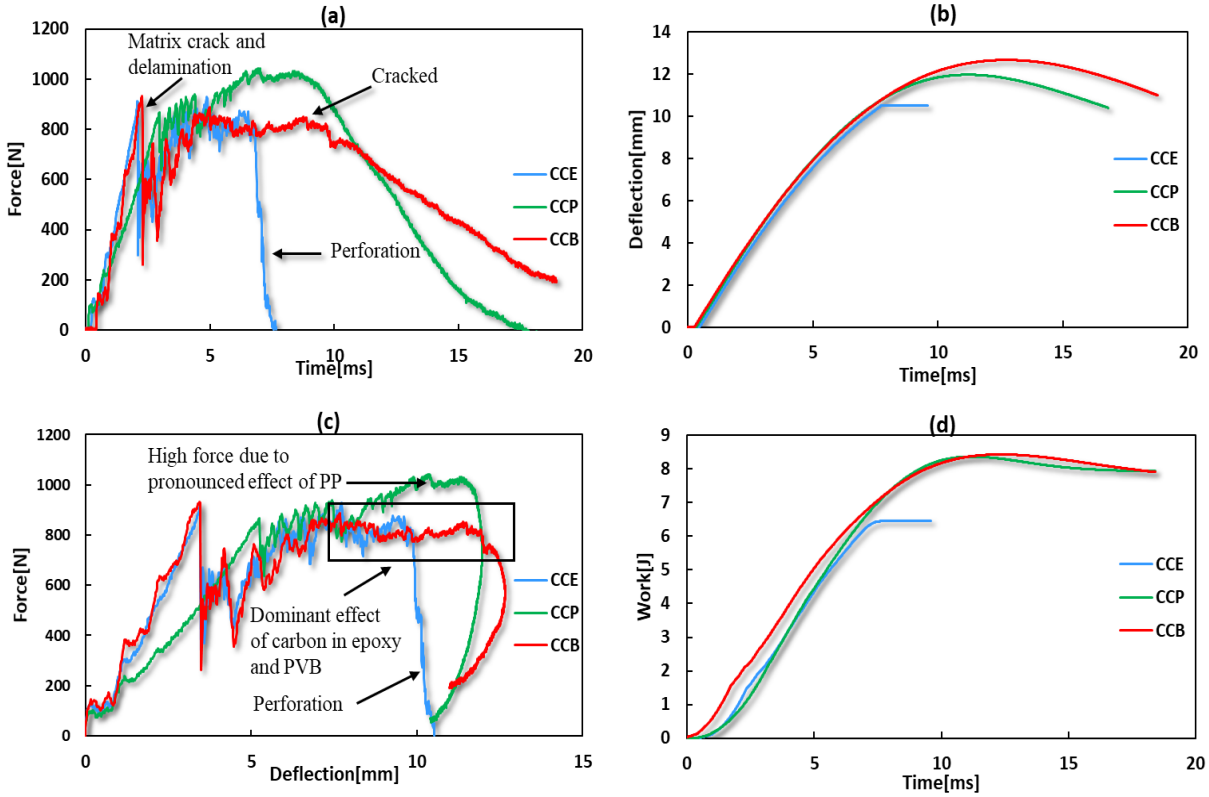

Figure 5.13. Typical curves of 2D carbon + 3D jute composites (a) force-deflection (b) force-time (c) work-time (d) deflection-time

The damaged samples of 2D carbon + 3D jute composites are showing that the CCE was perforated completely, while both the CCP and CCB damaged partially with later suffering wider crack (Figure 5.14). For the CCE the IS and NIS were completely perforated. The IS side of CCE is showing that the crack is just around the point of impact, while on the NIS it is spread in square direction that is due to bidirectional woven reinforcement. The CCP is showing the small damage on the IS side due to some delamination and interface disturbance between PP-carbon bonding. The NIS of CCP showing crack propagation with 2D carbon layer clearly cracked. As already discussed in detail about the nature of the crack in CCB the sample showing the visible propagated crack on the NIS of the sample, while IS side also has crack but not as large as on NIS.

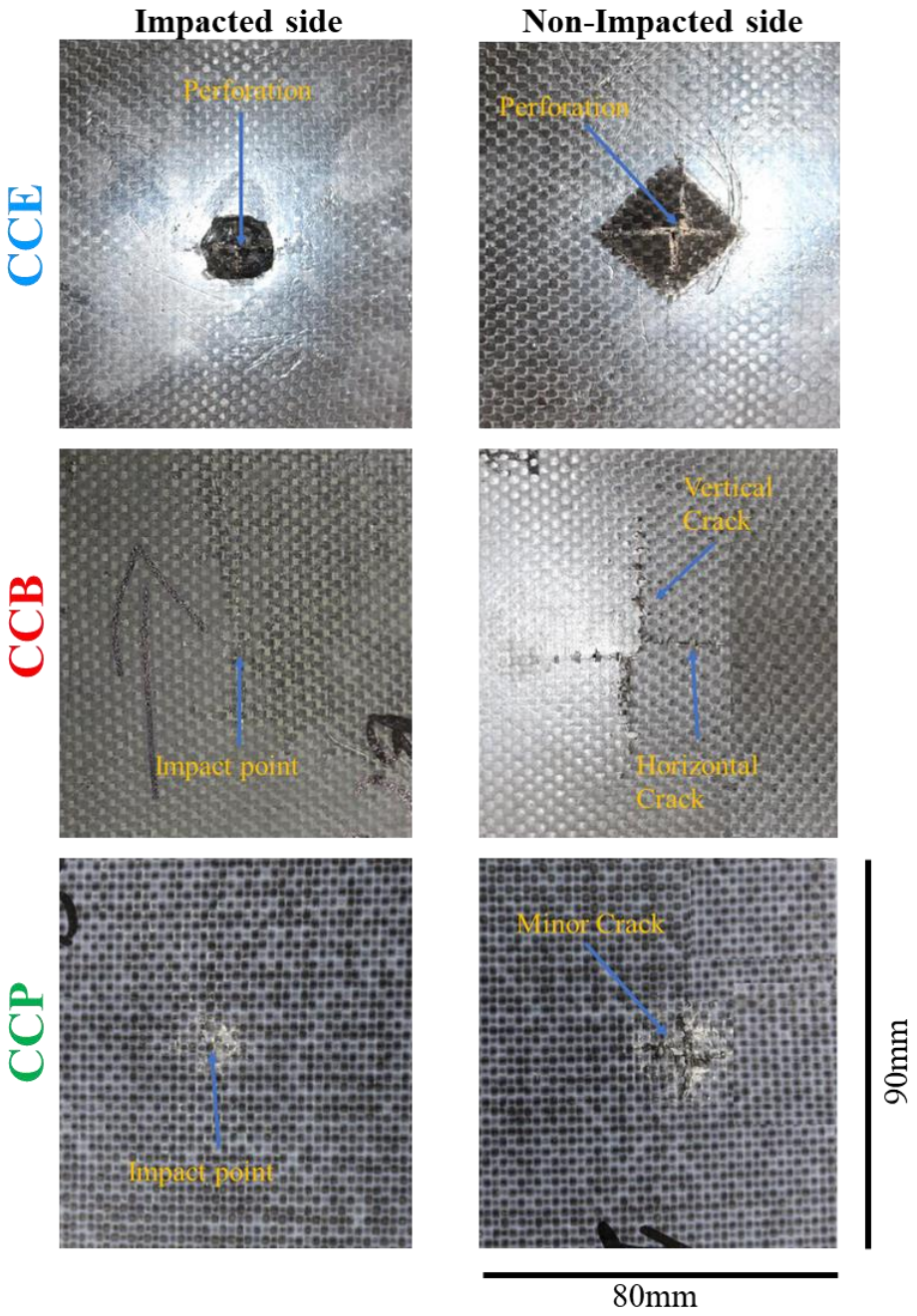

Figure 5.14. The cracked 2D carbon + 3D jute composites after LVI test

Figure 5.15(a) shows the force-time curve of 2D carbon + 3D jute woven reinforced FMLs. As can be seen from the curves that the effect of carbon fibres was very obvious, all three FMLs experienced a sharp drop in the force at around 3*ms*, this drop was due to brittle carbon fibres which get exposed and there was the failure. The CFE experienced a sharp drop due to carbon epoxy composite, which offered high brittleness and matrix crack at smaller impact force.

Figure 5.15(b) shows that both CFP and CFB suffered a similar kind of deflection, while the CFP experiencing slightly high deflection and then quick recovery. Figure 5.15(c) shows the force-deflection curves, The CFB and CFP both showing FVC and SVC. The CFP has more deflection compared to CFB. The rebound is also higher for CFP as seen in the case of AFP. Both CFB and CFE showed initial higher impact force, but for CFE the FVC is at smaller deflection around 4*mm* compared to CFB and CFP. The work–time graph also shows the higher initial stiffness of CFB and CFE (Figure 5.15(d)). The CFB sustained its stiffness and also offered more resistance to deformation. Both CFB and CFP have shown the rebound after reaching the maximum deflection. The CFB additionally presented better resistance for penetration and energy dissipation.

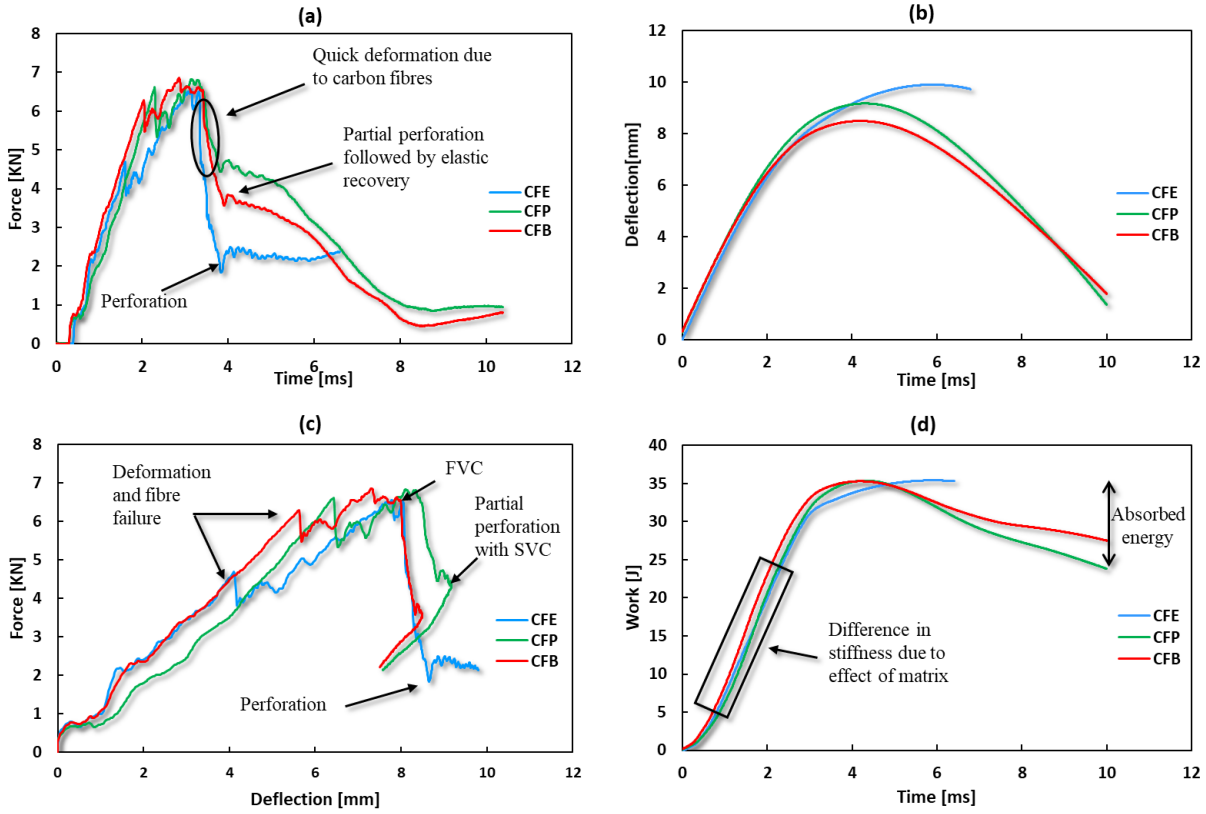

Figure 5.15. Typical curves of 2D carbon + 3D jute FMLs (a) force-deflection (b) force-time (c) work-time (d) deflection-time

Figure 5.16 shows the damaged samples of 2D carbon + 3D jute FMLs after LVI and cross section of damage area. As can be seen that the CFE has suffered complete perforation with

significant crack both on the IS and NIS. The crack is also limited to the point of impact not spread to a larger area. The CFP and CFB is showing a similar kind of crack, both suffered FVC and SVC with slight perforation. As can be seen from the force-deflection curves of both CFP and CFB that the sequence of damage as follows, (a) matrix crack and delamination, (b) FVC, (c) SVC, (d) partial perforation. The cross-sectional view, however, suggests that the CFP experienced delamination between lower aluminium and composite. In the case of CFB, the matrix deformed plastically and experienced a crack.

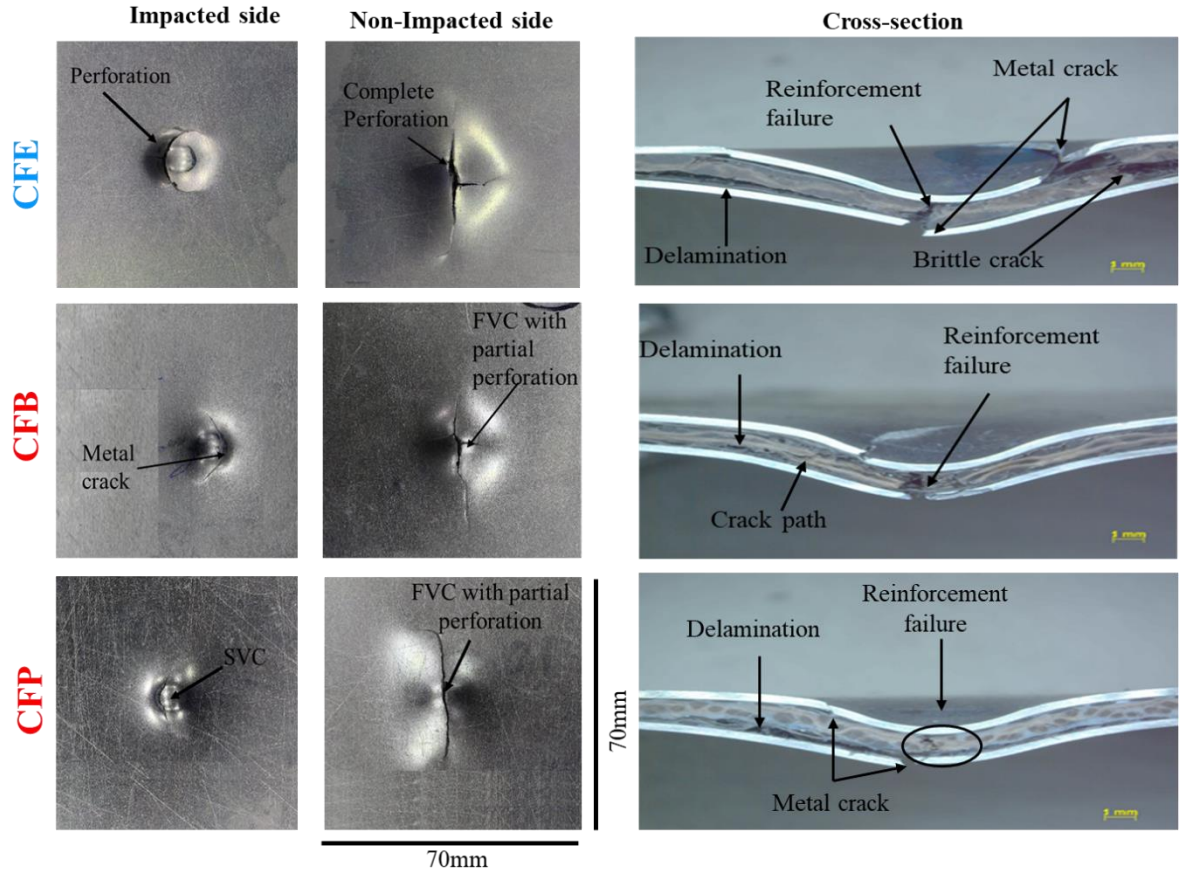

Figure 5.16. The cracked samples of 2D carbon + 3D jute woven hybrid FMLs after LVI test and cross-section of damaged area

5.5 2D Glass / 3D Woven Jute Composite and FMLs LVI Properties

2D glass + 3D jute composites impact properties are shown in Figure 5.17. All the composites have different behaviour against the LVI. The GCB shows initially high stiffness and resisting the incident impact. The crack initiation and crack propagation are at different force in GCB,

at around the 4mm there is a sudden drop in the peak this shows the delamination and matrix crack. Then at around 8mm there is another drop in the force, which is due to crack propagation. For GCE and GCP these two points start together at similar force. The GCE was perforated while both GCP and GCB suffered crack rather perforation. GCP shows rather steady damage characteristics, there was slight delamination and matrix cracking at 5mm. That damage point in case of PP based composite is not propagated to larger area. The GCE shows quite brittle behaviour and the sample perforate with small signs of matrix crack. The matrix cracking and perforation cannot be differentiated after seeing the force - deflection curve of GCE. The GCE perforate much earlier, even at a lower energy level. While GCB required much higher energy for damage propagation. The maximum deflection is lowest for GCB while highest for CCE. The reason of such kind of behaviour is already discussed in detail in previous sections. The impactor stops after dissipating all the impact energy to GCP and GCB, for GCB it stopped rather at small deflection. The work-time graph shows that the GCB has a higher stiffness while GCE and GCP has almost similar stiffness (Figure 5.17 (d)).

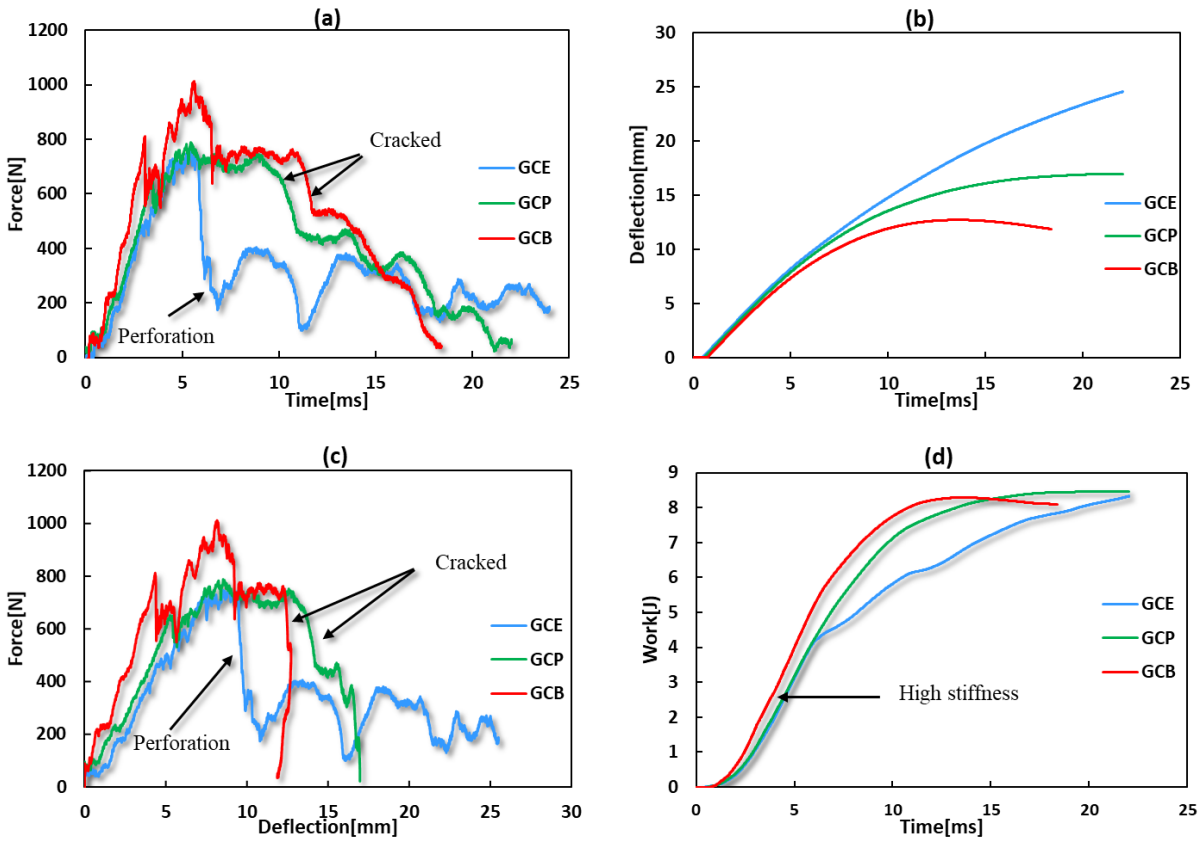

Figure 5.17. Typical curves of 2D glass + 3D jute composites (a) force-deflection (b) force-time (c) work-time (d) deflection-time

The impacted samples show the complete perforation of GCE with slight delamination on IS and NIS of the samples (Figure 5.18). The delamination is similar to the 2D aramid + 3D jute epoxy composites, but intensity is a bit less. As the delamination on IS was less in case of GCE than ACE. The reason for this behaviour is that the glass-epoxy interface is better than aramid-epoxy interface. The CCP is showing damage in the NIS with the crack propagated in the horizontal and vertical line, normal to each other in a square shape that was due to woven reinforcement. The GCB is also showing the damage propagation to a larger area with the crack line propagate horizontally and vertically normal to each other. The pure jute-based composites and synthetic hybrid composites made with PVB have different behaviour of damage propagation or different nature of crack in samples against LVI. Normally the pure jute-based composites have shown the random crack line not following any specific path unlike the

synthetic / jute composites. In the pure jute-based composite the dominance in the impact properties is by the PVB, while in synthetic / jute composites it is by both constituents.

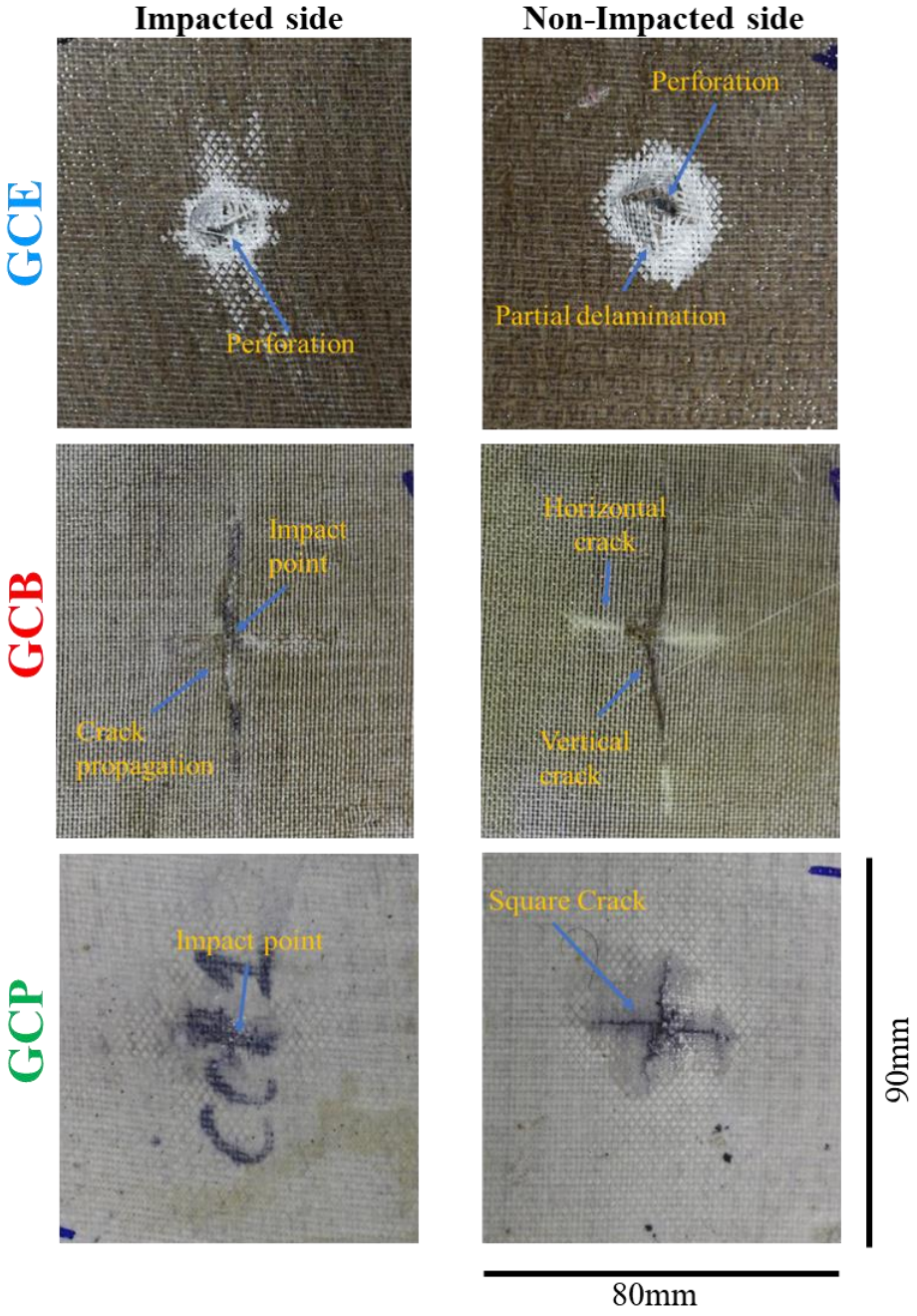

Figure 5.18. The cracked specimen of 2D glass + 3D jute composites after LVI test

The different graphs of impact test of 2D glass + 3D jute woven hybrid FMLs are shown in the Figure 5.19. Figure 5.19(a) showing that the force-time curve of GFB has similar behaviour like previous PVB based FMLs, however, GFE showed improved impact performance. As

between the first and second crack it had slightly bigger gap than the previous FMLs. The GFP experienced a sudden drop in the curve after the first peak that was due to delamination and reinforcement failure. The deflection-time curve was showing that both GFE and GFP had identical deflection, while GFB experienced the least deflection (Figure 5.19(b)). Figure 5.19(c) shows force-deflection curves, the GFB showing a drop in force around 5*mm*; this drop was due to matrix crack. After the FVC there is rebound observed in the curve. Both GFE and GFP suffer the perforation after receiving FVC and SVC. Unlike AFP and CFP the GFP is showing poorly as compared to the GFE, the reason for this behaviour is that the glass epoxy-based composites make a very stiff bond with aluminium, so it offers more resistance to impact. The GFB is also showing less contact time with the impactor due to rebound. The work-time curves of both GFP and GFE are showing cracks propagation (Figure 5.19(d)).

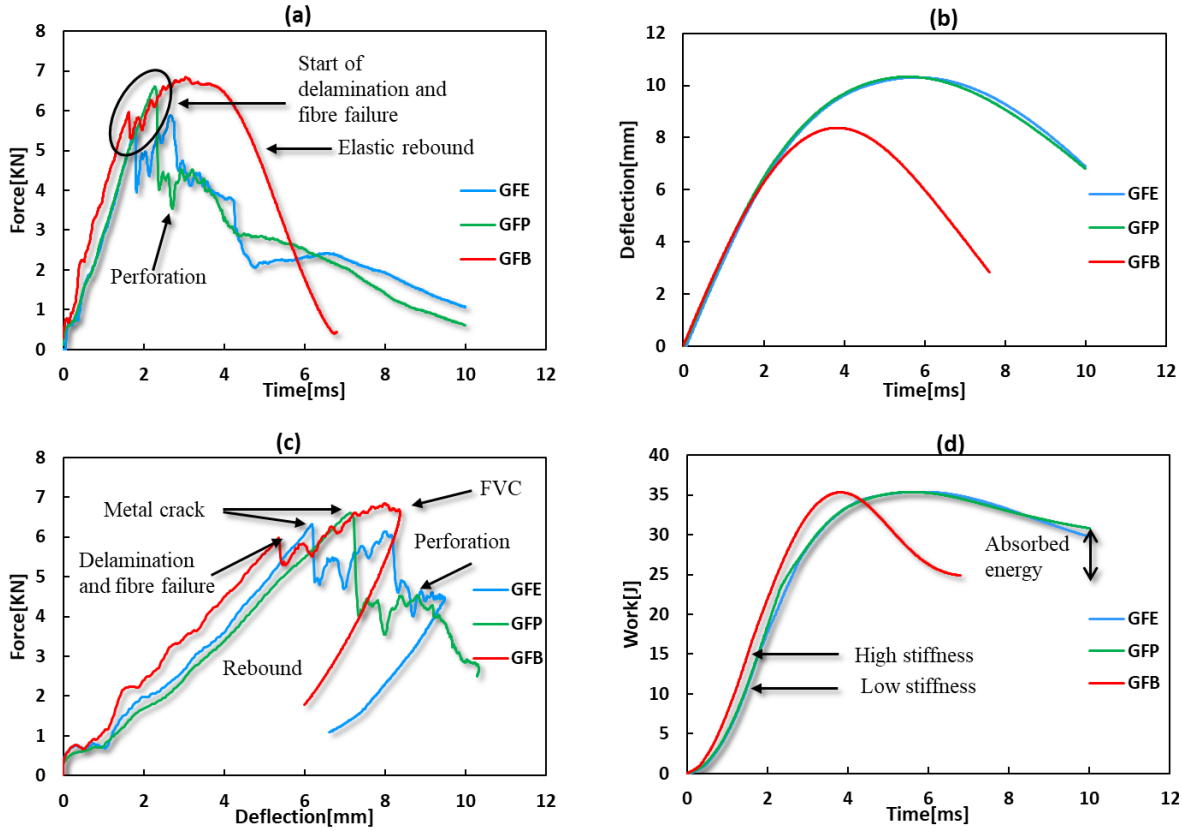

Figure 5.19. Typical curves of 2D glass + 3D jute FMLs (a) force-deflection (b) force-time (c) work-time (d) deflection-time

The damaged samples of the GFE and GFP are showing the perforation with the delamination while the GFB is displaying some plastic deformation with FVC **(**Figure 5.20**)**. The GFP and GFE demonstrated larger crack; this more massive crack is also showing the large delaminated area around the crack. Due to this delaminated aluminium on NIS, there was rebound seen in the force-deflection curve after perforation. The shape of the crack on the IS was similar to the previous FMLs. Like previous PP based synthetic / jute hybrid FMLs, the reason for the crack in GFP is also delamination between metal and composite. The GFB is displaying some matrix crack around impact point and overall a plastic deformation.

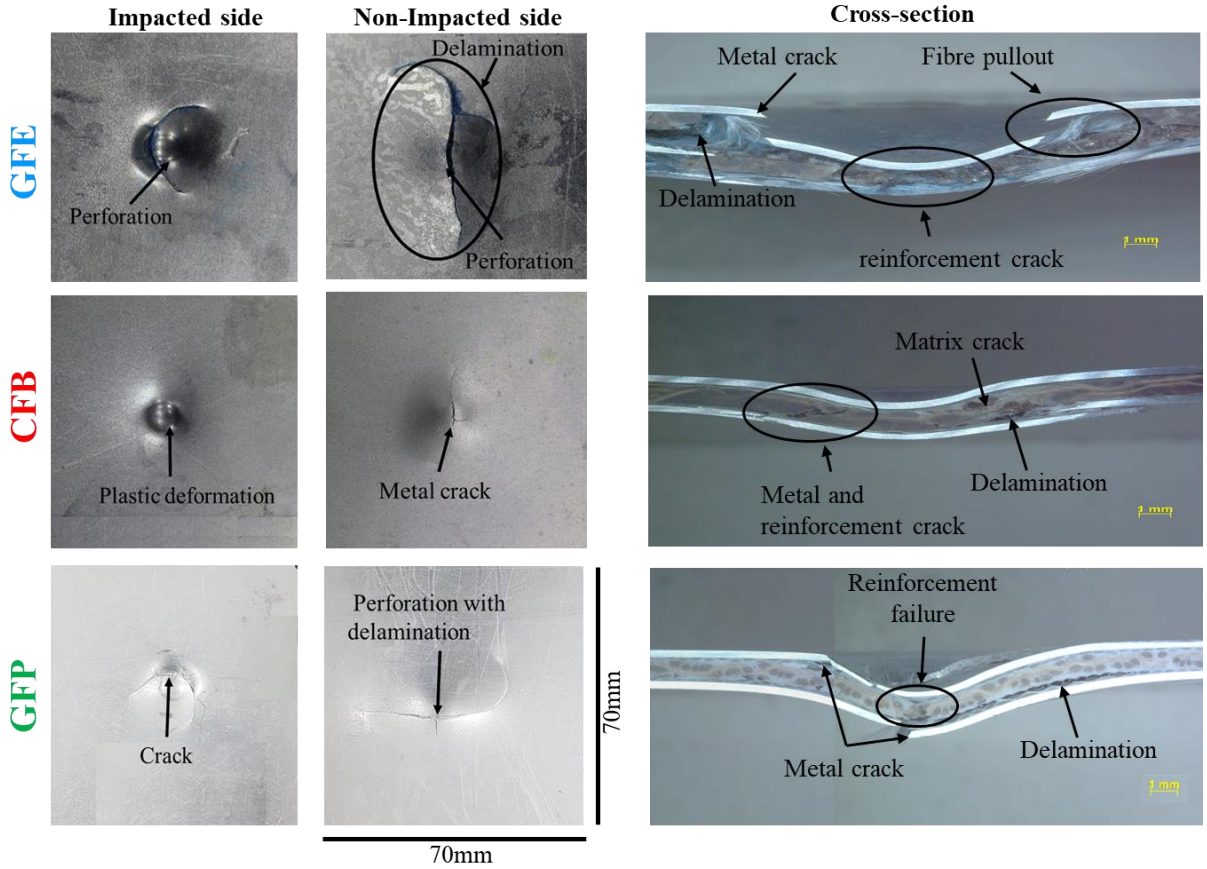

Figure 5.20. The cracked samples of 2D glass + 3D jute hybrid FMLs composites after LVI tests and cross-section of damaged area

5.6 Hybrid Composites and FMLs Performance Analysis

5.6.1 Maximum Deflection and Residual Deflection Comparison

The maximum deflection is good indicator to check the resistance of different kind of composites and FMLs subjected to low velocity impact. It shows the nature of deformation of structures made with different kind of matrix system. The Table 5.1 presents the maximum deflection and residual deflection of different composites and corresponding FMLs. It can be seen that both PVB based composites and FMLs had shown almost similar kind of behaviour. For the PP based composites and FMLs, the one reinforced with jute shows maximum deflection. The JCP, JJCP, JFP and JJFP are showing highest deflection. The reason of this maximum deflection of jute reinforced PP based composites and FMLs is that the PP has poor interface both with jute and aluminium. For the composites in which 3D jute fabric is sandwiched with synthetic fabric and PP matrix shows the better performance as compared to composites and FMLs in which reinforcement is 100% jute. As can be seen that ACP, CCP, GCP, AFP, CFP and GFP the deflection is lesser than epoxy-based structures but more than PVB based structures. When compared the central deflection of 100 jute reinforced and synthetic / jute hybrid structures the later performed better against LVI. The reason of better LVI performance of synthetic / jute combination is that the PP and synthetic fabric form good network and the 2D synthetic fabric expose to impactor before the 3D jute fabric so the LVI performance was improved. The performance of epoxy-based composites and FMLs similar in all cases with almost similar trends as all the structures were either cracked or perforated. This is due to brittle behaviour of epoxy. In the 2D carbon / 3D jute reinforced composites the trend line is different from other synthetic / jute hybrid composites. As the CCE was perforated very early so it is not showing the resistance towards impact, while CCB is showing slightly higher deflection as compared to CCP, this was due to crack propagation to higher area due to brittle behaviour of carbon yarn and energy propagation nature of PVB. The reason of larger crack

length as compared to CCP has already explained in the previous section in detail. The trends of deflection are very much similar in FMLs when compared to composites with slight variations. As in case of FMLs there are other factor which also effect the properties, e.g., The delamination between the composites and metal, plastic deformation of metal etc. In case of PVB based FMLs the delamination is rather minimum and so is the deflection.

The residual / permanent deflection shows the part of deformation which do not return to its original position. The permanent deflection was calculated for all type of samples. The Table 5.1 shows the values of permanent deflection of the composites and FMLs. The permanent deformation was not measured for the samples which were perforated or cracked. The measurement of residual deflection for composites is not an accurate parameter, as the composite material do not deform plastically. The better way to judge the composites after LVI is to measure the area of damage. As from the values of composites can be seen that the composites show very low permanent deformation as compared to maximum central deflection calculated during tests. The reason of this low value is that the composite does not show plastic deformation rather they experience a fracture. While the FMLs has plastic deformation, so for the composites only the part of deformation is recovered.

When the maximum and residual deflection values of FMLs are compared. The JFE, JJFP, AFE and CFE and JFP were perforated so there was no residual deformation recorded. The trend of residual deflection is almost similar to the trend of maximum deflection. Both PP and PVB based FMLs shows more restoration of permanent deformation as compared to epoxy based FMLs. The epoxy is brittle and have low plasticity, so the energy dissipation is very poor for it. When the PP and PVB based FMLs are compared with each other the PVB based FMLs whether 100% jute or synthetic / jute had shown higher residual deflection. For the PP based FMLs the synthetic/jute FMLs shown better residual recovery as compared to 100% jute reinforced FMLs. The reason of this behaviour is already explained in the previous section.

Table 5.1. Comparison of maximum central deflection and residual central deflection of composites and FMLs

Serial number	**FMLs**	**Maximum deflection[mm]**	**Residual deflection[mm]**	**Composites**	**Maximum deflection[mm]**	**Residual deflection[mm]**
1.	**JFE**	12.93	Perforation	**JCE**	29.67	Cracked
2.	**JFP**	15.71	Perforation	**JCP**	30.49	Cracked
3.	**JFB**	9.07	5.0	**JCB**	26.92	Cracked
4.	**JJFE**	8.63	4.7	**JJCE**	20.49	Cracked
5.	**JJFP**	10.59	Perforation	**JJCP**	22.63	Cracked
6.	**JJFB**	7.38	3.7	**JJCB**	15.71	1.9
7.	**AFE**	10.15	Perforation	**ACE**	11.86	Perforation
8.	**AFP**	8.92	4.6	**ACP**	9.74	1.95
9.	**AFB**	8.35	3.85	**ACB**	9.44	0.75
10.	**CFE**	9.90	Perforation	**CCE**	10.53	Perforation
11.	**CFP**	9.17	4.75	**CCP**	11.96	2.25
12.	**CFB**	8.49	4.6	**CCB**	12.66	1.65
13.	**GFE**	9.47	6.05	**GCE**	27.72	Perforation
14.	**GFP**	10.33	5.8	**GCP**	16.97	2.9
15.	**GFB**	8.37	4.45	**GCB**	12.72	1.65

From the values of permanent central deflection of composites, it can be seen that they show highest recovery in deformation. The results show that the permanent central deflection does not show the extent of deformation of composites materials. As the composites has high

fracture toughness and less plasticity so they show the low values of permanent central deflection. The damage area is true indicator of extent of damage.

5.7 F*max* of Composites and FMLs

The Fmax values of composite and FMLs is showing similar kind of trends but the FMLs are showing more consistent behaviour than the simple composites (Figure 5.21). The reason of more consistent behaviour of FMLs is aluminium, which first deform plastically before actually transferring load to composite part. The energy is initially consumed to impart plastic deformation before starting any delamination, matrix cracking and other type of damages. In almost all composites and FMLs the Fmax of PVB based structures is higher. The reason is already discussed in detail. The PVB based 2D carbon + 3D jute reinforced composites and FMLs are showing a bit odd behaviour. The CCB have lower Fmax values as compared to CCP, this trend is different from rest of composites as in all other PVB based composites have high Fmax values. The lower value of Fmax for CCB was due to crack initiation and propagation, which starts and propagate relatively to a larger area. The carbon is brittle and have low impact performance. While the PVB impregnate the composite completely. So after the failure of carbon fibres the matrix resist the impactor. While in case of CFB the Fmax of both CFB and CFP is almost same level. In the case of CCP it adds plastic deformation, which is the reason of higher value of Fmax. While compared to CCB the CFB show relatively better performance, the reason of this performance is that the bonding between composite and aluminium layer render the delamination to larger area. The aluminium deform plastically due to impact at the point of impact. The CCB it propagates the crack in the composite with minimum central deflation. So due to combination of these two a barrier is formed which reduce the crack penetration and more resistance to impactor.

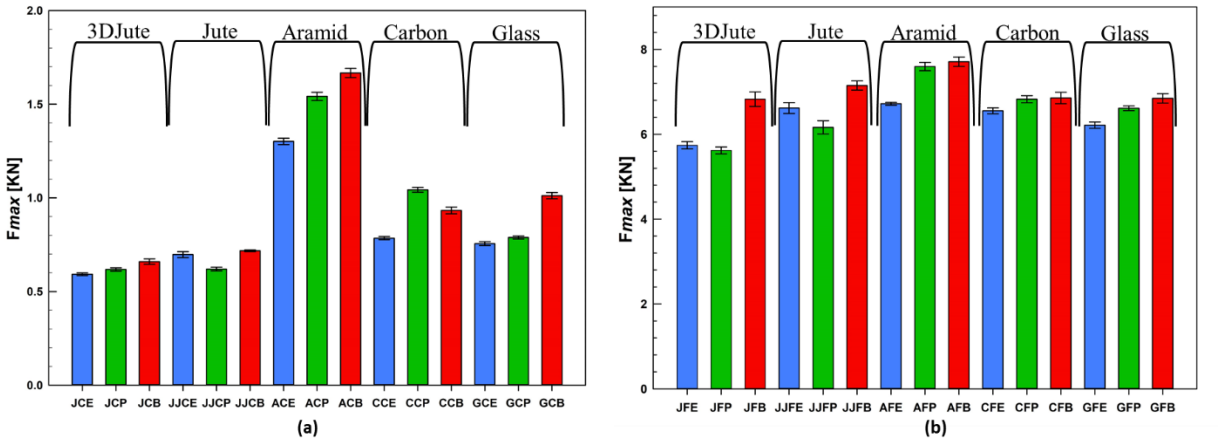

Figure 5.21. Comparison of Fmax of (a) composites and (b) FMLs made with different matrix

5.7.1 Composites and FMLs Absorbed Energy Comparison

The absorbed energy indicates the behaviour of a particular structure towards impact event. The absorb energy is usually difference of impact energy and rebound energy. The higher rebound energy indicates the excellent resistance of an object towards incident impact. There can be different scenarios for the LVI, a; A specimen can absorb a part of impact of energy and rebound a part of it (residual energy is lower than impact energy), b; the specimen can absorb all of impact energy with no perforation and impactor stops after transmitting all of its impact energy, c; the energy is absorbed by the specimen with the perforation (absorb energy can be equal or lower than impact energy).

When the absorbed energy of composites and FMLS are compared, it shows that the PVB based composites and FMLs absorbed lowest energy as compared to other samples, with showing rebound due to elastic undissipated energy. The JCP and JJP show the higher absorb energy than the counterpart, this shows the higher deformation of these composites. As the composites made with jute and PP has lower bonding with each other so they have lower resistance towards impact, in spite of the reason that the PP is more plastic and high energy absorption characteristics. The composites and counter FMLs showing similar kind of absorbed

energies. The epoxy-based composites show the highest amount of absorbed energy. Most of epoxy-based composites suffer perforation or relatively higher crack as compared to other specimens, this show that most of impact energy was used for deformation of specimens (Figure 5.22).

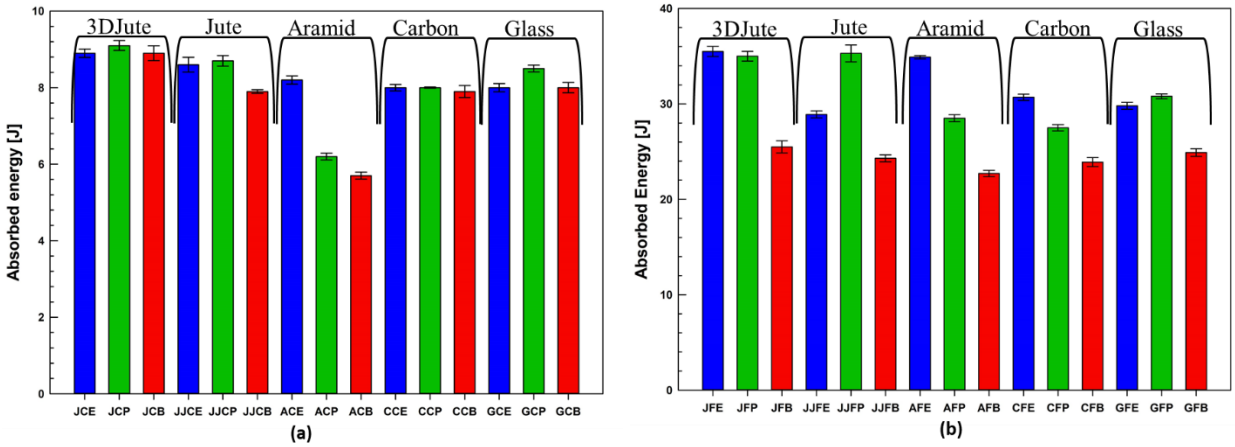

Figure 5.22. Comparison of absorbed energies of (a) composites and (b) FMLs

5.7.2 Damage Analysis

The degree of damage is ratio of absorbed energy to impact energy as:

$$Degree\ of\ Damage = \frac{Absorbed\ Energy}{Impact\ Energy} \qquad (7)$$

The degree of damage shows the amount of damage a specimen suffers after the LVI. If the value of degree of damage is less than one it shows the lower damage. From the Figure 5.23 it can be seen that the PVB based composites and FMLs suffered least damage. The results and damaged specimens shown in previous sections also justify the results. Almost all the composites samples except ACP and ACB suffered partial or complete crack. For the epoxy based FMLs almost all the FMLs suffered complete or partial perforation, the samples which suffered partial perforation was due to initiation of delamination on the NIS of samples between composites and aluminium. For the synthetic + 3D jute reinforced FMLs the PVB based FMLs

have lowest degree of damage followed by PP and epoxy, while for 100% jute based FMLs the PVB again has lowest degree of damage followed by epoxy and PP. The reason of this behaviour has already been discussed in detail in previous sections.

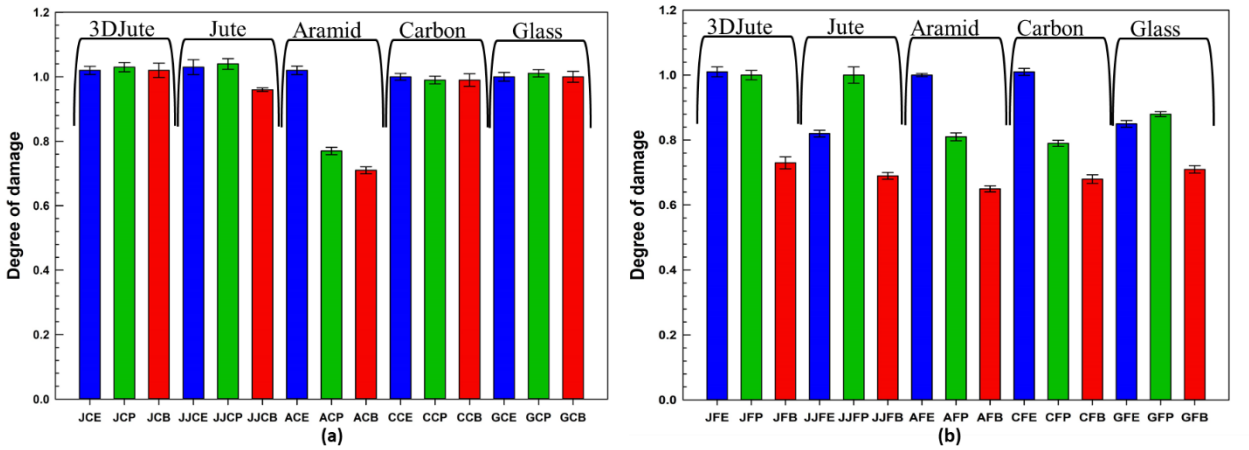

Figure 5.23. Comparison of degree of damage of (a) composites and (b) FMLs

The damaged area suggests the damage characteristics and extent of damage after LVI. The Figure 5.24 shows that the damage area of composites is usually larger than FMLs. The epoxy-based composites had larger damaged area for 100% jute reinforcements. The failure mode changed from cracking to perforation when using hybrid reinforcement for composite. That is why for hybrid reinforcement the damaged area is smaller. For CCB and GCB the damaged area is higher than the rest of counterparts, that is due cracking of composites. The cracking of composite shows excellent impregnation of reinforcement by matrix and dominant effect of matrix. The aramid / 3D jute reinforced composite showing the smallest damaged area, that is mainly due to effect of aramid skin, which render penetration of the impactor and diffuse the effect of impact. For the FMLs both reinforcement and type of matrix effected the properties, but another factor which added was aluminium-composite bonding. Due to effect of aluminium-composite bonding the trend of the damaged area is different for composites and FMLs. Almost all the PVB based FMLs showed a smaller damaged area, that has been due to

plastic deformation of aluminium, excellent metal-composite bonding and energy dissipation characteristics of PVB. The epoxy based FMLs had the largest damaged area compared to other FMLs due to the brittleness of epoxy and lower energy dissipation characteristics. PP had different behaviour for 100% jute reinforcement and hybrid reinforcement. For 100% jute reinforcement the damaged area is higher due to poor composite-matrix interface, whereas for hybrid reinforcement the damaged area relatively smaller as the jute did not expose directly to impact.

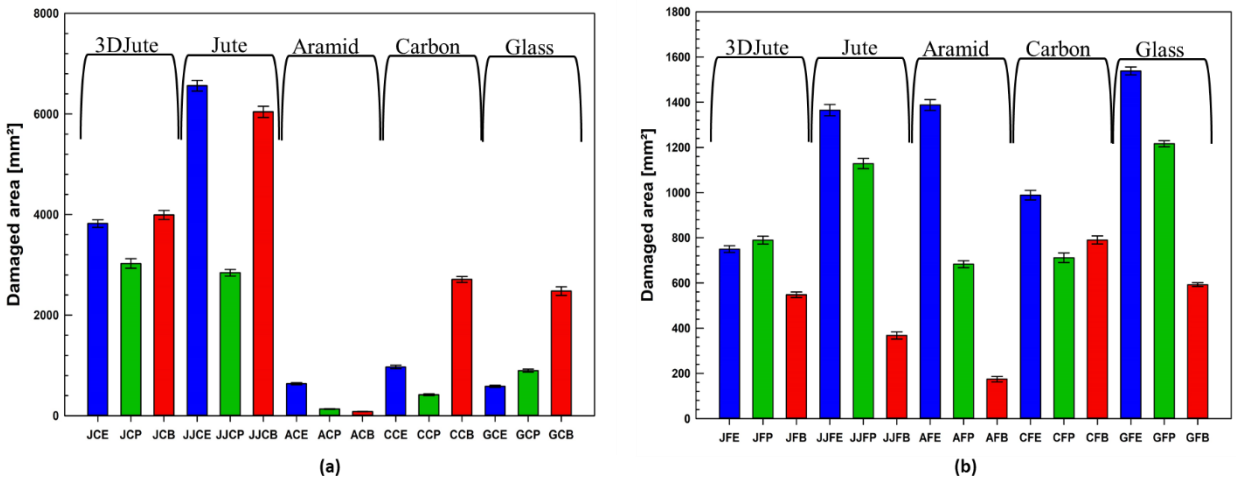

Figure 5.24. Comparison of damaged area of hybrid (a) composites and (b) FMLs

The degree of damage vs maximum deflection and degree of damage vs absorbed energy comparison of different composites is shown in Figure 5.25. The aramid / jute hybrid reinforced composites are showing least damage. while simple 3D jute reinforced composites are showing highest damage. The PVB based composites are showing slightly lowest energy absorption thus smaller damaged. This was also discussed earlier that PVB based composites were cracked rather than perforated. The 100% jute reinforced composites suffered highest damage with all type of matrices. While for hybrid reinforcement performed relatively better in term of deformation.

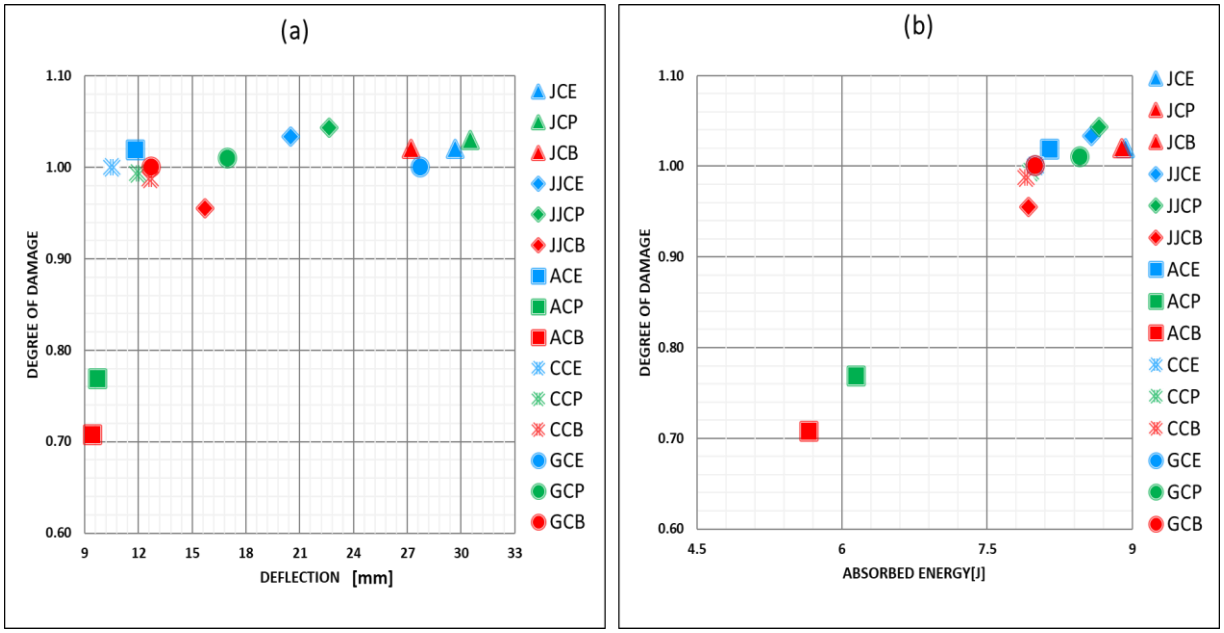

Figure 5.25. (a) degree of damage vs deflection and (b) degree of damage vs absorbed energy comparison of composites

From Figure 5.26 it can be clearly seen that the PVB matrix has clear effect on the properties of FMLs. All the FMLs made with PVB had least damage and deflection. The absorbed energy was also lower than rest of FMLs showing least damage. The hybrid reinforced FMLs made with PP matrix shown better properties than 100% jute reinforced counterparts. The hybrid glass / jute FML made with epoxy shown relatively better impact performance than other epoxy-based hybrid FMLs due to effect of better glass-epoxy interface.

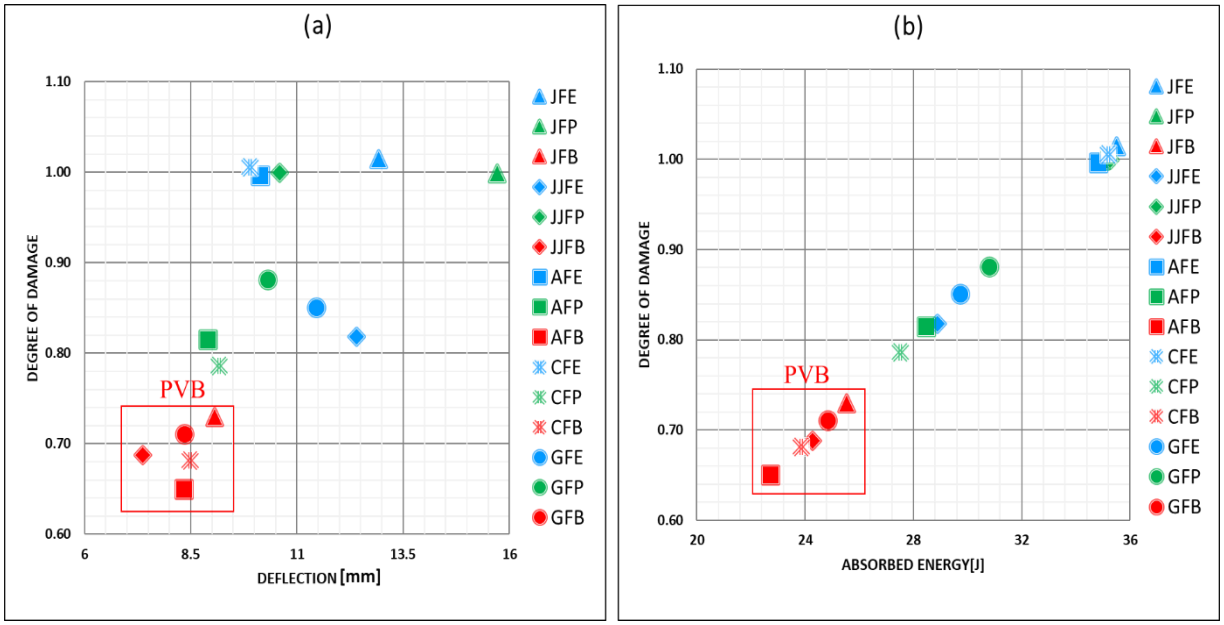

Figure 5.26. (a) degree of damage vs deflection and (b) degree of damage vs absorbed energy comparison of FMLs

5.8 Conclusion

This chapter explains the LVI properties of 3D woven jute reinforced composites and FMLs made with different matrices. The 3D reinforcement was further hybridized with 2D woven skin made with different types of fibres. The 100% jute reinforced composites and FMLs behaved in an almost similar manner. The samples made with PP matrix had low impact performance followed by epoxy and PVB. The poor impact performance of jute-PP reinforced composites and FMLs was due to poor fibre matrix interface. The epoxy is brittle in nature, so it has poor energy dissipation characteristics. When epoxy is used with jute it further dominates the properties. However, the PVB made relatively stiffer network and impregnated the fibres completely, so overall better impact performance with 100% jute reinforcement. When the impact properties of hybrid reinforced samples are compared, the properties were different for different reinforcements. The aramid / jute reinforcement showed overall high resistance, both for composites and FMLs. For the carbon / jute, the brittle carbon fibres determine the properties, as the crack propagation was relatively faster. For the glass/jute, the properties

depended on the matrix system. The dominant failure mechanism in the composites was cracking for 100% jute reinforcement. For the hybrid reinforcement and epoxy, the perforation was the dominant failure mechanism. For the FMLs, 100% jute reinforced with both epoxy and PP experienced perforation. The hybrid reinforced FMLs with epoxy experienced perforation with relatively more extensive cracking, however, hybrid-PP FMLs did not suffer perforation as seen for 100% jute reinforcement. The PVB based FMLs overall showed better resistance to impact and did not suffer complete failure due to high stiffness.

Chapter 6. Conclusion and Perspectives

In this work, two different sets of FMLs and their constituent's composites were studied made with 3D jute woven and hybrid 3D jute woven (2D plain woven + 3D jute woven) reinforcements for different static and dynamic mechanical loadings. The qualitative assessment of the quality of bonding between composites and aluminium were also done. The surface of aluminium was anodized using phosphoric acid anodizing to create micro-roughness to improve composite-metal bonding. In the first stage, mechanical properties of 3D orthogonal jute reinforced composites and FMLs were examined, i.e. Hybrid TT Warp-LL Weft interlock, Hybrid LL Warp-LL Weft interlock, Hybrid TT Warp-TT Weft interlock and TT-Weft interlock. The composites and FMLs were developed using vacuum infusion technique using these 3D reinforcements. The tensile and flexural properties were investigated to select the best 3D woven reinforcement. The TT weft interlocked structure showed overall better tensile and flexural properties for FMLs. In the 2nd part using TT interlocked structured as a core the jute-jute and synthetic-jute hybrid reinforced composites and FMLs were developed using three different kinds of matrices, *i.e*. epoxy, PP and PVB. The hybridization of 3D jute woven fabric was done with 2D plain woven jute, aramid, carbon, and glass fabric. The tensile, flexural and drop weight low-velocity impact properties were investigated to check the effect of hybridization and matrix. All the samples in the 2nd part were made using compression hot press moulding technique. The overall balanced properties of PVB based composites and FMLs for static and dynamic results were obtained.

- The water contact angle gives surface free energy while from the T-peel and floating roller peel test results the effect of material and matrix on the adhesive properties was accessed. The following conclusions were drawn from these results.

1) The anodized aluminium surface had a lower water contact angle as compared to bare, mechanically prepared, and oxidized aluminium surfaces. That shows higher surface free energy of anodized aluminium.

2) The T-peel test results show that the nature of constituents materials mainly drove the delamination properties, and interlocking pattern of 3D woven structure did not affect the adhesion between aluminium and composites as the contacting surfaces mainly determined the adhesion properties.
3) When the properties of aluminium-jute composites were compared made with epoxy, PP and PVB matrix, the highest delamination force was obtained from PVB matrix followed by PP and epoxy. The PVB and PP had an adhesive failure as a predominant failure mechanism. The PP and PVB matrix adhered with aluminium throughout the delaminated surface, the jute fibres also adhered with the matrix showing intra-laminar fibre failure. The aluminium surface of epoxy was entirely covered with a matrix, showing predominately cohesive failure.
4) For the aluminium-aramid bond, the PP has the highest delamination force, followed by PVB and PP. The delamination pattern suggests the surface of aluminium was fully covered with the matrix with no sign of intra-laminar fibre failure.
5) The aluminium-carbon fibre bond showing poor delamination properties of epoxy and superior for PVB matrix, the properties of PP were in between. The delamination pattern suggests that the epoxy covered the surface of metal completely, while for PP and PVB, there was mix adhesive and cohesive failure. However, for both PP and PVB, the intra-laminar fibre failure was also observed, the PVB, however, had more extensive intra-laminar fibre failure.
6) The aluminium-glass bond had the highest properties for PVB, followed by epoxy and PP. The epoxy glass interface caused better delamination response as compared to the previous aluminium-composite bond. Both epoxy and PVB had some intra-laminar fibre failure, showing excellent bonding. The PP had a cohesive failure, but no intra-laminar fibre failure was observed.

7) The fracture toughness of epoxy was lower as compared to thermoplastic counterparts due to its high brittleness. The PVB showed overall high fracture toughness for all kind of reinforcements.

▶ The composite and FMLs developed in the first stage using four types of 3D jute woven reinforcement to optimize the woven structure for FML fabrication. For the composites and FMLs, tensile and flexural properties were measured. Then in the second part using the optimized woven structures, the hybrid composites and FMLs were developed using epoxy, glass, and PP matrix. The tensile and flexural properties of those composites were accessed. The following conclusions were drawn from these tests.

1) The tensile properties of 3D woven composites in which orthogonal TT-interlock woven reinforcement was used resulted in highest strength and modulus due to least crimp of the structure. For the flexural properties of orthogonal LL-interlocked structures were highest due to more crimp and more yarn placed in layers resisting the bending load.
2) For FMLs, better tensile and flexural properties were obtained for TT-interlocked structured due to the coupled effect of MVF and 3D woven structure.
3) For the same areal density, the higher MVF was achieved for TT-interlocked structure due to tight construction. As for FMLs, along with the type of weave, the MVF also played a very crucial part in determining the final properties of FMLs.
4) The failure pattern suggested that for composite, the dominant failure mechanism was matrix and resin crack. In contrast, in the FMLs, the dominant failure mechanism was metal, matrix and resin crack along with delamination.

5) The vacuum infusion technique was successfully used for the development of FMLs, as it was first time employed to developed 3D jute woven reinforced fibre metal laminates.
6) For 100% jute reinforcement, the highest tensile and flexural properties were achieved for PVB based composites followed by epoxy and PP. As for the PVB impregnate jute reinforcement completely.
7) For the synthetic + 3D jute reinforced composites the highest tensile and flexural properties were achieved for epoxy followed by PVB and PP. As the epoxy and synthetic fibre outer layer formed a better network. While the failure was mainly dependent on the nature of synthetic material.
8) The PP based synthetic + jute reinforced FMLs suffered premature delamination between 2D synthetic woven outer layer and 3D woven core due to the stronger bonding between aluminium and synthetic layer as compared to between synthetic-jute woven core during the flexural test.
9) In all composites the failure mechanism for all type of composites was different, the epoxy-based composite had a brittle failure, the PP based composite had a ductile failure and PVB based composite also had a brittle failure.
10) When the compared w.r.t to bonding and impregnation point of view, the epoxy and PVB impregnated reinforced thoroughly, while for PP had poor impregnation. As for as bonding was concerned, the failure pattern suggested that both epoxy and PVB had excellent metal-composite bonding while PP had poor metal composite bonding.

▶ Drop weight low-velocity impact properties were investigated both for hybrid composites and FMLs made with three different kind of matrix, and the following conclusions were drawn.

1) For the impact properties, the composites and FMLs made with the epoxy showed overall poor impact performance due to the brittle nature of resin and lack of energy dissipation characteristics.
2) The impact properties of PP based FMLs depends heavily on the type of reinforcement and hybridization, the FMLs in which 100% jute fibre were used as reinforcement showed inferior impact performance due to poor bonding between PP and jute. While the PP based FMLs in which a hybrid of 2D plain synthetic + 3D jute was used showed relatively better impact performance as jute woven core was not directly exposed to an impact event.
3) The PVB based composites and FMLs overall showed better impact performance, due to better energy absorption characteristics and plastic deformation of both composite and aluminium as the PVB impregnated reinforcement completely and formed better network.
4) The failure pattern suggests that aramid / jute reinforced FMLs had an aluminium dominant failure. For rest of FMLs, only glass / jute reinforced FMLs made with epoxy and PP had an aluminium dominant failure, while 3D jute, 2D /3D jute, and carbon / jute reinforced FMLs had fibre dominant failure. As in the fibre dominant failure, the F_i is always lower than F_{max}.
5) The cross-section of damaged samples indicates that the epoxy-based FMLs experienced matrix crack, fibre breakage and delamination between metal-composites. The PP-based FMLs suffered damage due to poor jute-pp bonding, delamination between metal–composite and resin break. The PVB based FMLs showed excellent characteristics against LVI; it suffered damage due to resin crack, slight metal–composite delamination and fibre breakage. The overall reason for the excellent

resistance of PVB based FMLs was its superior metal-composite bonding and plastic deformation of the composite layer.

6) The energy absorption characteristics of composites and FMLs suggested that PVB based samples suffered the least deformation with higher fracture toughness.

The following recommendations can be valuable for the future development and applications of these novel FMLs.

1) The fracture and crack propagation mechanism can be investigated in detail since in sandwich structures made with hybrid reinforcement can involve multiple factors. The x-ray tomography can give a detailed insight of all these mechanisms.
2) The numerical validation of experimental results can be done using different finite element modelling tools.
3) Fatigue properties of FMLs is always point of interest due to the coupled effect of metal and composite. The fatigue testing can provide effect of hybridization, durability of metal-composites bonding and matrix on the final properties.
4) Thermal residual stresses effect the properties of FMLs. Since the TFML are being used so the effect of different parameters of compression hot press on the final properties of FMLs can be an interesting area to explore.
5) The hygrothermal properties can also be investigated as it can expand its area of applications to Navel uses.
6) In the next step the FMLs can be used for different non-loading parts for automotive applications especially cargo carrier, floors *etc.*

Bibliography

Bibliography

[1] C. A. J. R. Vermeeren, "An historic overview of the development of fibre metal laminates," Appl. Compos. Mater., vol. 10, no. 4–5, pp. 189–205, 2003.

[2] A. Asundi and A. Y. N. Choi, "Fiber metal laminates: An advanced material for future aircraft," J. Mater. Process. Technol., vol. 63, no. 1–3, pp. 384–394, 1997.

[3] T. Sinmazçelik, E. Avcu, M. Ö. Bora, and O. Çoban, "A review: Fibre metal laminates, background, bonding types and applied test methods," Mater. Des., vol. 32, no. 7, pp. 3671–3685, 2011.

[4] P. V. Straznicky, J. F. Laliberté, C. Poon, and A. Fahr, "Applications of fiber-metal laminates," Polym. Compos., vol. 21, no. 4, pp. 558–567, Aug. 2000.

[5] R. Alderliesten, "On the Development of Hybrid Material Concepts for Aircraft Structures," 2009.

[6] C. Meola, S. Boccardi, and G. maria Carlomagno, "Composite Materials in the Aeronautical Industry," in Infrared Thermography in the Evaluation of Aerospace Composite Materials, Elsevier, 2017, pp. 1–24.

[7] L. A. Louca and A. S. Fallah, "The use of composites in blast-resistant walls," in Blast Protection of Civil Infrastructures and Vehicles Using Composites, Elsevier Ltd., 2010, pp. 298–341.

[8] N. L. Feng, S. D. Malingam, and K. A. Zakria, "Influence of Kenaf Fibre Orientation Effect on the Mechanical Properties of Hybrid Structure of Fibre Metal Laminate Influence of Kenaf Fibre Orientation Effect on the Mechanical," Pertanika J. Sci. Technol., vol. 25, no. May, pp. 1–8, 2017.

[9] T. Heggemann and W. Homberg, "Deep drawing of fiber metal laminates for automotive lightweight structures," Compos. Struct., vol. 216, pp. 53–57, May 2019.

[10] J. Bienias, P. Jakubczak, and B. Surowska, "Properties and characterization of fiber metal laminates," in Hybrid polymer composite materials, V. K. . Thakur, M. K. . Thakur, and A. Pappu, Eds. Woodhead Publishing, 2017, pp. 253–271.

[11] L. M. G. Vieira, J. C. dos Santos, T. H. Panzera, J. C. C. Rubio, and F. Scarpa, "Novel fibre metal laminate sandwich composite structure with sisal woven core," Ind. Crops

Prod., vol. 99, pp. 189–195, 2017.

[12] J. Macheret and R. J. Bucci, "A crack growth resistance curve approach to fiber/metal laminate fracture toughness evaluation," Eng. Fract. Mech., vol. 45, no. 6, pp. 729–739, 1993.

[13] M. E. Kazemi, L. Shanmugam, L. Yang, and J. Yang, "A review on the hybrid titanium composite laminates (HTCLs) with focuses on surface treatments, fabrications, and mechanical properties," Composites Part A: Applied Science and Manufacturing, vol. 128. Elsevier Ltd, p. 105679, 01-Jan-2020.

[14] L. B. Vogelesang and A. Vlot, "Development of fibre metal laminates for advanced aerospace structures," J. Mater. Process. Technol., vol. 103, no. 1, pp. 1–5, Jun. 2000.

[15] P. Krishnasamy, G. Rajamurugan, and M. Thirumurugan, "Performance of fiber metal laminate composites embedded with AL and CU wire mesh," J. Ind. Text., p. 152808372093557, Jun. 2020.

[16] F. A. Arpatappeh, M. A. Azghan, and R. Eslami-Farsani, "The effect of stacking sequence of basalt and Kevlar fibers on the Charpy impact behavior of hybrid composites and fiber metal laminates," Proc. Inst. Mech. Eng. Part C J. Mech. Eng. Sci., vol. 234, no. 16, pp. 3270–3279, Aug. 2020.

[17] N. Zareei, A. Geranmayeh, and R. Eslami-Farsani, "Interlaminar shear strength and tensile properties of environmentally-friendly fiber metal laminates reinforced by hybrid basalt and jute fibers," Polym. Test., vol. 75, pp. 205–212, May 2019.

[18] M. A. Abd El-Baky, A. E. Alshorbagy, A. M. Alsaeedy, and M. Megahed, "Fabrication of Cost Effective Fiber Metal Laminates Based on Jute and Glass Fabrics for Enhanced Mechanical Properties," J. Nat. Fibers, 2020.

[19] H. Aghamohammadi, S. N. Hosseini Abbandanak, R. Eslami-Farsani, and S. M. H. Siadati, "Effects of various aluminum surface treatments on the basalt fiber metal laminates interlaminar adhesion," Int. J. Adhes. Adhes., vol. 84, pp. 184–193, Aug. 2018.

[20] A. Salve, R. Kulkarni, and A. Mache, "A review : Fiber metal laminates (FML ' s) - manufacturing , test methods and numerical modeling," Int. J. Eng. Technol. Sci., vol. 6, no. 1, pp. 71–84, 2016.

[21] *A. Elmahdy and P. Verleysen, "Tensile behavior of woven basalt fiber reinforced composites at high strain rates," Polym. Test., vol. 76, pp. 207–221, Jul. 2019.*

[22] *K. L. Pickering, M. G. A. Efendy, and T. M. Le, "Composites : Part A A review of recent developments in natural fibre composites and their mechanical performance," Compos. part A, vol. 83, pp. 98–112, 2016.*

[23] *J. Bienias, P. Jakubczak, and B. Surowska, "Hybrid Polymer Composite Materials," in Hybrid polymer composite materials, V. K. . Thakur, M. K. . Thakur, and A. Pappu, Eds. Woodhead Publishing, 2017, pp. 253–271.*

[24] *M. Sadighi, R. C. Alderliesten, and R. Benedictus, "Impact resistance of fiber-metal laminates: A review," Int. J. Impact Eng., vol. 49, no. 11, pp. 77–90, 2012.*

[25] *Aalco, "Aluminium - Specifications, Properties, Classifications and Classes, Supplier Data by Aalco," 2005.*

[26] *E. Poodts, D. Ghelli, T. Brugo, R. Panciroli, and G. Minak, "Experimental characterization of a fiber metal laminate for underwater applications," Compos. Struct., vol. 129, p. 3646, 2015.*

[27] *L. Pan, A. Ali, Y. Wang, Z. Zheng, and Y. Lv, "Characterization of effects of heat treated anodized film on the properties of hygrothermally aged AA5083-based fiber-metal laminates," Compos. Struct., vol. 167, pp. 112–122, 2017.*

[28] *G. Reyes and H. Kang, "Mechanical behavior of lightweight thermoplastic fiber-metal laminates," J. Mater. Process. Technol., vol. 186, no. 1–3, pp. 284–290, 2007.*

[29] *S. U. Khan, R. C. Alderliesten, and R. Benedictus, "Post-stretching induced stress redistribution in Fibre Metal Laminates for increased fatigue crack growth resistance," Compos. Sci. Technol., vol. 69, no. 3–4, pp. 396–405, 2009.*

[30] *Y. Huang, Q. Ouyang, D. Zhang, J. Zhu, R. Li, and H. Yu, "Carbon materials reinforced aluminum composites: A review," Acta Metall. Sin. (English Lett., vol. 27, no. 5, pp. 775–786, 2014.*

[31] *Y. Xia, Y. Wang, Y. Zhou, and S. Jeelani, "Effect of strain rate on tensile behavior of carbon fiber reinforced aluminum laminates," Mater. Lett., vol. 61, no. 1, pp. 213–215, Jan. 2007.*

[32] *Y. B. Hu et al., "Preparation and properties of Fibre-Metal Laminates based on carbon fibre reinforced PMR polyimide," Compos. Part B Eng., vol. 69, pp. 587–591, Feb. 2015.*

[33] *S. Y. Park, W. J. Choi, H. S. Choi, H. Kwon, and S. H. Kim, "Recent trends in surface treatment technologies for airframe adhesive bonding processing : A review (1995 – 2008)," J. Adhes., vol. 86, no. 2, pp. 192–221, 2010.*

[34] *H. Qaiser, S. Umar, A. Nasir, M. Shah, and S. Nauman, "Optimization of interlaminar shear strength behavior of anodized and unanodized ARALL composites fabricated through VARTM process," Int J Mater Form, vol. 8, no. 3, pp. 481–493, 2015.*

[35] *G. W. Critchlow and D. M. Brewis, "Review of surface pretreatments for aluminium alloys," Int. J. Adhes. Adhes., vol. 16, no. 4, pp. 255–275, 1996.*

[36] *V. MLCE, "Aramid reinforced Aluminum laminates: ARALL adhesion problems and environmental effects.," Delft university of technology, 1987.*

[37] *S. Y. Park, W. J. Choi, and H. S. Choi, "A comparative study on the properties of GLARE laminates cured by autoclave and autoclave consolidation followed by oven postcuring," Int. J. Adv. Manuf. Technol., vol. 49, pp. 605–613, 2010.*

[38] *E. C. Botelho, R. A. Silva, L. C. Pardini, and M. C. Rezende, "A review on the development and properties of continuous fiber / epoxy / aluminum hybrid composites for aircraft structures," Mater. Res., vol. 9, no. 3, pp. 247–256, 2006.*

[39] *S. Y. Park, W. J. Choi, H. S. Choi, and H. Kwon, "Effects of surface pre-treatment and void content on GLARE laminate process characteristics," J. Mater. Process. Technol., vol. 210, no. 8, pp. 1008–1016, 2010.*

[40] *J. Xue, W. Wang, Y. Takao, and T. Matsubara, "Composites : Part A Reduction of thermal residual stress in carbon fiber aluminum laminates using a thermal expansion clamp," Compos. Part A, vol. 42, no. 8, pp. 986–992, 2011.*

[41] *J. Bienias, "Fiber metal laminates-Some aspects of manufacturing process, structure and selected properties," Polish Soc. Compos. Mater., vol. 11, no. 1, pp. 39–43, 2011.*

[42] *B. J. Jensen, R. J. Cano, S. J. Hales, and J. A. A, "Fiber metal laminates made by VARTM process," in ICCM-17 17th International Conference on Composite Materials. 2009; Edinburgh; United Kingdom, 2009.*

[43] *R. J. Cano, B. W.Grimsley, E. S. Weiser, and B. J.Jensen, "Resin infusion of layered metal/composite hybrid and resulting metal/composite hybrid laminate," US 7,595,112 B1, 2009.*

[44] *A. C. Loos, G. Tuncol, K. Long, R. J. Cano, B. J. Jensen, and E. S. Weiser, "Flow Visualization and modelling of the resin infusion process during manufacture of fiber metal laminates by VARTM," in ICCM-17 17th international conference on composite materials. 2009: Edinburgh,United Kingdom, 2009.*

[45] *A. C. Loos, G. Tuncol, K. Long, and R. J. Cano, "Dvelopemnt and verification of the resin infusion process during manufacturing of fiber metal laminates by VARTM," in The 10th International Conference on Flow Processes in Composite Materials (FPCM10) Monte Verità, Ascona, 2010.*

[46] *R. J. Cano, A. C. Loos, B. J. Jensen, S. M. Britton, G. Tuncol, and K. Long, "Epoxy / Glass and Polyimide (LaRC PETI-8) / Carbon Fiber Metal Laminates Made By The VARTM Proces s," in SAMPE 2010 Conference & exhibition; new materials and processes for a new economy, 2010, p. 97.*

[47] *E. K. Baumert, W. . Johnson, R. J. Cano, B. J. Jensen, and E. S. Weiser, "Fatigue & Fracture of Engineering Materials & Structures Fatigue damage development in new fibre metal laminates made by the VARTM process," Fatique Fract. Eng. Mater. Struct., vol. 34, no. 4, pp. 240–249, 2011.*

[48] *I. O. De Mendibil, L. Aretxabaleta, M. Sarrionandia, M. Mateos, and J. Aurrekoetxea, "Impact behaviour of glass fibre-reinforced epoxy / aluminium fibre metal laminate manufactured by Vacuum Assisted Resin Transfer Moulding," Compos. Struct., vol. 140, pp. 118–124, 2016.*

[49] *P. Hergan, Y. Li, and L. Zaloznik, "Using (VA) RTM with a Rigid Mould to Produce Fibre Metal Laminates with Proven Impact Strength," J. Manuf. Mater. Process., vol. 2, no. 2, pp. 1–12, 2018.*

[50] *J. I. Múgica, L. Aretxabaleta, I. Ulacia, and J. Aurrekoetxea, "Impact characterization of thermoformable fibre metal laminates of 2024-T3 aluminium and AZ31B-H24 magnesium based on self-reinforced polypropylene," Compos. Part A Appl. Sci. Manuf., vol. 61, pp. 67–75, Jun. 2014.*

[51] *M. R. Abdullah and W. J. Cantwell, "The impact resistance of polypropylene-based fibre-metal laminates," Compos. Sci. Technol., vol. 66, no. 11–12, pp. 1682–1693, Sep. 2006.*

[52] *R. Santiago, W. Cantwell, and M. Alves, "Impact on thermoplastic fibre-metal laminates: Experimental observations," Composite Structures, vol. 159. Elsevier Ltd, pp. 800–817, 01-Jan-2017.*

[53] *G. S. Langdon, W. J. Cantwell, and G. N. Nurick, "The blast response of novel thermoplastic-based fibre-metal laminates - Some preliminary results and observations," Compos. Sci. Technol., vol. 65, no. 6, pp. 861–872, May 2005.*

[54] *P. Compston, W. J. Cantwell, C. Jones, and N. Jones, "Impact perforation resistance and fracture mechanisms of a thermoplastic based fiber-metal laminate," J. Mater. Sci. Lett., vol. 20, no. 7, pp. 597–599, Apr. 2001.*

[55] *Y. Chen et al., "Effect of peer ply and cooling rate on the tensile properties of Al/Gf/PP laminate prepared by hot pressing," J. Sandw. Struct. Mater., vol. 22, no. 8, pp. 2567–2581, Nov. 2020.*

[56] *V. P. Brügemann, J. Sinke, and H. de Boer, "Fracture Toughness Testing in FML," in CONFERENCE AND EXPOSITION; 25th, Structural dynamics; IMAC XXV; 2007; Orlando, FL, 2007, p. 141.*

[57] *W. Brockmann, P. L. Gei, J. Klingen, and B. Schrder, "Adhesives and Adhesive Joints: Test Methods and Properties," in Adhesive Bonding, Weinheim, Germany: Wiley-VCH Verlag GmbH & Co. KGaA, 2009, pp. 125–204.*

[58] *S. Ebnesajjad, "Surface and Material Characterization Techniques," in Surface Treatment of Materials for Adhesive Bonding, Elsevier, 2014, pp. 39–75.*

[59] *M.R.Abdullah and W.J.Cantwell, "The impact resistance of polypropylene-based fibre–metal laminates," Compos. Sci. Technol., vol. 66, no. 11–12, pp. 1682–1693, 2006.*

[60] *S. T. de Freitas and J. Sinke, "Test method to assess interface adhesion in composite bonding," Appl. Adhes. Sci., vol. 3, no. 1, pp. 1–13, Dec. 2015.*

[61] *W. Wu, D. Abliz, B. Jiang, G. Ziegmann, and D. Meiners, "A novel process for cost effective manufacturing of fiber metal laminate with textile reinforced pCBT composites and aluminum alloy," Compos. Struct., vol. 108, pp. 172–180, 2014.*

[62] *A. Zamani Zakaria, K. Shelesh-nezhad, T. Navid Chakherlou, and A. Olad, "Effects of aluminum surface treatments on the interfacial fracture toughness of carbon-fiber aluminum laminates," Eng. Fract. Mech., vol. 172, pp. 139–151, Mar. 2017.*

[63] *L. Hamill and S. Nutt, "Adhesion of metallic glass and epoxy in composite-metal bonding," Compos. Part B, vol. 134, no. 2, pp. 186–192, 2018.*

[64] *S. T. De Freitas and J. Sinke, "Adhesion properties of bonded composite-to-aluminium joints using peel tests," J. Adhes., vol. 90, no. 5–6, pp. 511–525, Jun. 2014.*

[65] *F. Khan et al., "Effect of various surface preparation techniques on the delamination properties of vacuum infused Carbon fiber reinforced aluminum laminates (CARALL): Experimentation and numerical simulation," J. Mech. Sci. Technol., vol. 31, no. 11, pp. 5265–5272, Nov. 2017.*

[66] *N. G. Gonzalez-Canche, E. A. Flores-Johnson, and J. G. Carrillo, "Mechanical characterization of fiber metal laminate based on aramid fiber reinforced polypropylene," Compos. Struct., vol. 172, pp. 259–266, Jul. 2017.*

[67] *L. Shanmugam, M. E. Kazemi, Z. Rao, L. Yang, and J. Yang, "On the metal thermoplastic composite interface of Ti alloy/UHMWPE-Elium® laminates," Compos. Part B Eng., vol. 181, p. 107578, Jan. 2020.*

[68] *N. F. Hussain, D. Sivakumar, M. A. Bin Daud, Sivaraos, and M. Z. Selamat, "Study of Interfacial Shear of aluminium / oil palm empty fruit bunch fiber reinforced polypropylene fiber metal laminates .," Appl. Mech. Mater., vol. 789–790, pp. 131–135, 2015.*

[69] *G. Wu and J. Yang, "Analytical modelling and numerical simulation of the nonlinear deformation of hybrid fibre – metal laminates," Model. Simul. Mater. Sci. Eng., vol. 13, pp. 413–425, 2005.*

[70] *P. Iaccarino, A. Langella, and G. Caprino, "A simplified model to predict the tensile and shear stress-strain behaviour of fibreglass/aluminium laminates," Compos. Sci. Technol., vol. 67, no. 9, pp. 1784–1793, 2007.*

[71] *P. Soltani, M. Keikhosravy, R. H. Oskouei, and C. Soutis, "Studying the tensile behaviour of GLARE laminates: A finite element modelling approach," Appl. Compos. Mater., vol. 18, no. 4, pp. 271–282, 2011.*

[72] *E. K. Baumert, W. S. Johnson, R. J. Cano, B. J. Jensen, and E. S. Weiser, "Mechanical evaluation of new fiber metal laminates made by the VARTM process," in ICCM-17 17th international conference on composite materials. 2009: Edinburgh,United Kingdom, 2009.*

[73] *R. C. Alderliesten and J. J. Homan, "Fatigue and damage tolerance issues of Glare in aircraft structures," Int. J. Fatigue, vol. 28, pp. 1116–1123, 2006.*

[74] *P. Cortes and W. J. Cantwell, "The tensile and fatigue properties of carbon fiber-reinforced PEEK-titanium fiber-metal laminates," J. Reinf. Plast. Compos., vol. 23, no. 15, pp. 1615–1623, 2004.*

[75] *A. Vlot and J. W. Gunnink, Eds., Fibre metal laminates an introduction. springer science & Business Media, 2001.*

[76] *H. F. . Wu, L. L. . Wu, W. J. Slagter, and J. L. Verolme, "Use of rule of mixtures and metal volume fraction for mechanical property predictions of fibre-reinforced aluminium laminates," J. Mater. Sci., vol. 29, pp. 4583–4591, 1994.*

[77] *S. E. Moussavi-torshizi, S. Dariushi, M. Sadighi, and P. Safarpour, "A study on tensile properties of a novel fiber / metal laminates," Mater. Sci. Eng. A, vol. 527, no. 18–19, pp. 4920–4925, 2010.*

[78] *W. Nam, W. Hwang, and K. Han, "Stacking Sequence Design of Fiber-Metal," J. Compos. Mater., vol. 35, no. 18, pp. 1654–1683, 2001.*

[79] *W. Asghar et al., "Investigation of fatigue crack growth rate in CARALL, ARALL and GLARE," Fatigue Fract. Eng. Mater. Struct., vol. 40, no. 7, pp. 1086–1100, 2017.*

[80] *E. C. Botelho, L. C. Pardini, and M. C. Rezende, "Hygrothermal effects on damping behavior of metal/glass fiber/epoxy hybrid composites," Mater. Sci. Eng. A, vol. 399, no. 1–2, pp. 190–198, 2005.*

[81] *R. Santiago, W. Cantwell, and M. Alves, "Impact on thermoplastic fibre-metal laminates : Experimental observations," Compos. Struct., vol. 159, pp. 800–817, 2017.*

[82] *J. G. Carrillo and W. J. Cantwell, "Mechanical properties of a novel fiber – metal laminate based on a polypropylene composite," Mech. Mater., vol. 41, no. 7, pp. 828–838, 2009.*

[83] *N. G. Gonzalez-Canche, E. A. Flores-Johnson, P. Cortes, and J. G. Carrillo, "Evaluation of surface treatments on 5052-H32 aluminum alloy for enhancing the interfacial adhesion of thermoplastic-based fiber metal laminates," Int. J. Adhes. Adhes., vol. 82, pp. 90–99, Apr. 2018.*

[84] *C. Zopp, A. Dittes, D. Nestler, I. Scharf, L. Kroll, and T. Lampke, "Quasi-static and fatigue bending behavior of a continuous fiber-reinforced thermoplastic/metal laminate," Compos. Part B Eng., vol. 174, p. 107043, Oct. 2019.*

[85] *K. Ilya, D. Andrey, H. Dmytro, V. Ekaterina, K. Vladislav, and T. Oleg, "Development thermoplastic elastomer-based fiber-metal laminate for vibration damping application," Mater. Today Proc., Jan. 2020.*

[86] *N. L. Feng and S. D. Malingam, "Monotonic and fatigue responses of fiber-reinforced metal laminates," in Mechanical and Physical Testing of Biocomposites, Fibre-Reinforced Composites and Hybrid Composites, Elsevier, 2018, pp. 307–323.*

[87] *H. Ku, H. Wang, N. Pattarachaiyakoop, and M. Trada, "Composites : Part B A review on the tensile properties of natural fiber reinforced polymer composites," Compos. Part B, vol. 42, pp. 856–873, 2011.*

[88] *H. T. N. Kuan, W. J. Cantwell, M. A. Hazizan, and C. Santulli, "The fracture properties of environmental-friendly fiber metal laminates," J. Reinf. Plast. Compos., vol. 30, no. 6, pp. 499–508, 2011.*

[89] *L. S.H., F. S.Y, Z. B.L, Z. Q.Y, and B. X.R, "Reformed bamboo and reformed bamboo/aluminium composite," J. Mater. Sci., vol. 29, pp. 5990–5996, 1994.*

[90] *S. G.X., Y. T.X., K. J.K., and Z. B.L., "Static Mechanical Behaviour of Bamboo/Aluminium Composites for Applications in Industrial Structures," in Key Engineering Materials, 1998, vol. 149, pp. 781–786.*

[91] *S. D. Malingam, N. L. Feng, M. Z. Selamat, and S. Subramonian, "Investigation on Fatigue Life Behaviour of Sustainable Bio-Based Fibre Metal Laminate Investigation on Fatigue Life Behaviour of Sustainable Bio-Based Fibre Metal Laminate," J. Mech. Eng., vol. S1 1, no. January, pp. 123–140, 2017.*

[92] *A. Thirumurugan, G. B. Bhaskar, K. Poyyathappan, R. J. Karthik, and M. K. Kumar, "Investigations on Aluminium wire mesh , Banana Fiber and Glass Fiber Reinforced*

Hybrid Composites," Indian J. Sci. Technol., vol. 9, no. November, 2016.

[93] N. L. Feng, S. Dharmalingam, K. A. Zakria, and M. Z. Selamat, "Investigation on the fatigue life characteristic of kenaf / glass woven-ply reinforced metal sandwich materials," J. Sandw. Struct. Mater., pp. 1–16, 2017.

[94] K. Subramaniam, S. D. Malingam, N. L. Feng, and O. Bapokutty, "The Effects of Stacking Configuration on the Response of Tensile and Quasi-Static Penetration to Woven Kenaf / Glass Hybrid Composite Metal Laminate," Polym. Compos., vol. 40, no. 2, pp. 568–577, 2017.

[95] S. DM, J. FA, N. LF, S. K, and A. G. AF., "Tensile and impact properties of cost- - effective hybrid fiber metal laminate sandwich structures," Adv Polym Technol, vol. 00, no. October, pp. 1–9, 2017.

[96] I. Mohammed, A. R. A. Talib, M. T. H. Sultan, M. Jawaid, A. H. Ariffin, and S. Saadon, "Mechanical properties of fibre-metal laminates made of natural / synthetic fibre composites," BioResources, vol. 13, no. 1, pp. 2022–2034, 2018.

[97] C. Muthukumar, I. MR, S. SM, L. Z, and M. Jawaid, "Tensile and flexural properties of the hybrid flax / carbon based fibre metal laminate," in 5th postgraduate seminar on Natural fiber composites 2016, 2016, no. December.

[98] N. Kali, S. Pathak, and S. Korla, "Effect on vibration characteristics of fiber metal laminates sandwiched with natural fibers," Mater. Today Proc., Jan. 2020.

[99] M. Chandrasekar, M. R. Ishak, S. M. Sapuan, Z. Leman, M. Jawaid, and R. M. Shahroze, "Effect of Freezing Temperature and Stacking Sequence on the Mechanical Properties of Hybrid Fibre Metal Laminates Made with Carbon, Flax, and Sugar Palm Fibres," BioResources, vol. 14, no. 2, pp. 3042–3056, 2019.

[100] M. Vasumathi and V. Murali, "Effect of alternate metals for use in natural fibre reinforced fibre metal laminates under bending , impact and axial loadings," Procedia Eng., vol. 64, pp. 562–570, 2013.

[101] N. K. Romli et al., "The behavior of Aluminium Carbon/Epoxy fibre metal laminate under quasi-static loading," IOP Conf. Ser. Mater. Sci. Eng., vol. 257, no. 1, 2017.

[102] N. Jones, "Note on the impact behaviour of fibre-metal laminates," Int. J. Impact Eng., vol. 108, pp. 147–152, 2017.

[103] *S. H. Song, Y. S. Byun, T. W. Ku, W. J. Song, J. Kim, and B. S. Kang, "Experimental and numerical investigation on impact performance of carbon reinforced aluminum laminates," J. Mater. Sci. Technol., vol. 26, no. 4, pp. 327–332, 2010.*

[104] *Y. Liu and B. Liaw, "Effects of Constituents and Lay-up Configuration on Drop-Weight Tests of Fiber-Metal Laminates," Appl. Compos. Mater., vol. 17, pp. 43–62, 2010.*

[105] *L. Ferrante, F. Sarasini, J. Tirillò, L. Lampani, T. Valente, and P. Gaudenzi, "Low velocity impact response of basalt-aluminium fibre metal laminates," Mater. Des., vol. 98, pp. 98–107, May 2016.*

[106] *G. B. Chai and P. Manikandan, "Low velocity impact response of fibre-metal laminates - A review," Composite Structures, vol. 107. Elsevier Ltd, pp. 363–381, 2014.*

[107] *R. Starikov, "Assessment of impact response of fiber metal laminates," Int. J. Impact Eng., vol. 59, pp. 38–45, 2013.*

[108] *G. Caprino, G. Spataro, and S. Del Luongo, "Low-velocity impact behaviour of fibreglass-aluminium laminates," Compos. Part A Appl. Sci. Manuf., vol. 35, no. 5, pp. 605–616, May 2004.*

[109] *A. P. Sharma, S. H. Khan, R. Kitey, and V. Parameswaran, "Effect of through thickness metal layer distribution on the low velocity impact response of fiber metal laminates," Polym. Test., vol. 65, pp. 301–312, Feb. 2018.*

[110] *B. Jaroslaw, S. Barbara, and J. Patryk, "The comparison of low-velocity impact resistance of aluminum/carbon and glass fiber metal laminates," Polym. Compos., vol. 37, no. 4, pp. 1056–1063, Apr. 2016.*

[111] *P. Jakubczak, J. Bieniaś, and B. Surowska, "Impact resistance and damage of fiber metal laminates," in Hybrid Polymer Composite Materials: Properties and Characterisation, Elsevier Inc., 2017, pp. 279–309.*

[112] *G. Belingardi and R. Vadori, "Low velocity impact tests of laminate glass-fiber-epoxy matrix composite material plates," Int. J. Impact Eng., vol. 27, no. 2, pp. 213–229, Feb. 2002.*

[113] *X. Li, X. Zhang, H. Zhang, J. Yang, A. B. Nia, and Gin Boay Chai, "Mechanical behaviors of Ti/CFRP/Ti laminates with different surface treatments of titanium sheets," Compos. Struct., vol. 163, pp. 21–31, 2017.*

[114] J. G. Carrillo, N. G. Gonzalez-Canche, E. A. Flores-Johnson, and P. Cortes, "Low velocity impact response of fibre metal laminates based on aramid fibre reinforced polypropylene," Compos. Struct., vol. 220, pp. 708–716, Jul. 2019.

[115] S. Krishnakumar, "Fiber Metal Laminates — The Synthesis of Metals and Composites," Mater. Manuf. Process., vol. 9, no. 2, pp. 295–354, Mar. 1994.

[116] R. Das, A. Chanda, J. Brechou, and A. Banerjee, "Impact behaviour of fibre–metal laminates," in Dynamic Deformation, Damage and Fracture in Composite Materials and Structures, Elsevier, 2016, pp. 491–542.

[117] R. C. Alderliesten and R. Benedictus, "Fiber/Metal Composite Technology for Future Primary Aircraft Structures," J. Aircr., vol. 45, no. 4, pp. 1182–1189, Jul. 2008.

[118] C. T. Lin, P. W. Kao, and F. S. Yang, "Fatigue behaviour of carbon fibre-reinforced aluminium laminates," Composites, vol. 22, no. 2, pp. 135–141, 1991.

[119] A. Vlot and W. Gunnink, Fibre Metal Laminates: an Introduction, vol. 1, no. 1. springer science & Business Media, 2001.

[120] E. Sarlin et al., "Impact properties of novel corrosion resistant hybrid structures," Compos. Struct., vol. 108, no. 1, pp. 886–893, 2014.

[121] F. D. Morinière, R. C. Alderliesten, M. Y. Tooski, and R. Benedictus, "Damage evolution in GLARE fibre-metal laminate under repeated low-velocity impact tests," Cent. Eur. J. Eng., vol. 2, no. 4, pp. 603–611, 2012.

[122] F. Bagnoli, M. Bernabei, D. Figueroa-Gordon, and P. E. Irving, "The response of aluminium/GLARE hybrid materials to impact and to in-plane fatigue," Mater. Sci. Eng. A, vol. 523, no. 1–2, pp. 118–124, Oct. 2009.

[123] F. Aymerich and P. Priolo, "Characterization of fracture modes in stitched and unstitched cross-ply laminates subjected to low-velocity impact and compression after impact loading," Int. J. Impact Eng., vol. 35, no. 7, pp. 591–608, Jul. 2008.

[124] S. Abrate and S. Abrate, "Low-Velocity Impact Damage," in Impact on Composite Structures, Cambridge University Press, 2009, pp. 135–160.

[125] E. V. González, P. Maimí, P. P. Camanho, C. S. Lopes, and N. Blanco, "Effects of ply clustering in laminated composite plates under low-velocity impact loading," Compos.

Sci. Technol., vol. 71, no. 6, pp. 805–817, Apr. 2011.

[126] T. W. Shyr and Y. H. Pan, "Impact resistance and damage characteristics of composite laminates," Compos. Struct., vol. 62, no. 2, pp. 193–203, 2003.

[127] R. Seltzer, C. González, R. Muñoz, J. Llorca, and T. Blanco-Varela, "X-ray microtomography analysis of the damage micromechanisms in 3D woven composites under low-velocity impact," Compos. Part A Appl. Sci. Manuf., vol. 45, pp. 49–60, Feb. 2013.

[128] H. Nakatani, T. Kosaka, K. Osaka, and Y. Sawada, "Damage characterization of titanium/GFRP hybrid laminates subjected to low-velocity impact," Compos. Part A Appl. Sci. Manuf., vol. 42, no. 7, pp. 772–781, Jul. 2011.

[129] F. D. Morinière, R. C. Alderliesten, and R. Benedictus, "Low-velocity impact energy partition in GLARE," Mech. Mater., vol. 66, pp. 59–68, 2013.

[130] P. Jakubczak, J. Bieniaš, K. Majerski, M. Ostapiuk, and B. Surowska, "The impact behavior of aluminum hybrid laminates," Aircr. Eng. Aerosp. Technol., vol. 86, no. 4, pp. 287–294, 2014.

[131] A. Seyed Yaghoubi, Y. Liu, and B. Liaw, "Stacking Sequence and Geometrical Effects on Low-Velocity Impact Behaviors of GLARE 5 (3/2) Fiber–Metal Laminates," J. Thermoplast. Compos. Mater., vol. 25, no. 2, pp. 223–247, Mar. 2012.

[132] T. Pärnänen, R. Alderliesten, C. Rans, T. Brander, and O. Saarela, "Applicability of AZ31B-H24 magnesium in Fibre Metal Laminates - An experimental impact research," Compos. Part A Appl. Sci. Manuf., vol. 43, no. 9, pp. 1578–1586, Sep. 2012.

[133] P. Cortés and W. J. Cantwell, "The fracture properties of a fibre-metal laminate based on magnesium alloy," Compos. Part B Eng., vol. 37, no. 2–3, pp. 163–170, Apr. 2005.

[134] P. Cortes and W. J. Cantwell, "The Tensile and Fatigue Properties of Carbon Fiber-reinforced PEEK-Titanium Fiber-metal Laminates," J. Reinf. Plast. Compos., vol. 23, no. 15, pp. 1615–1623, Oct. 2004.

[135] A. Ali, L. Pan, L. Duan, Z. Zheng, and B. Sapkota, "Characterization of seawater hygrothermal conditioning effects on the properties of titanium-based fiber-metal laminates for marine applications," Compos. Struct., vol. 158, pp. 199–207, Dec. 2016.

[136] T. de Boer, "Next Generation Fibre Metal Laminates," in Fibre Metal Laminates, Springer Netherlands, 2001, pp. 39–51.

[137] P. Cortés and W. J. Cantwell, "The Impact Properties of High-temperature Fiber-Metal Laminates," J. Compos. Mater., vol. 41, no. 5, pp. 613–632, Mar. 2007.

[138] W. S. Johnson and M. W. Hammond, "Crack growth behavior of internal titanium plies of a fiber metal laminate," Compos. Part A Appl. Sci. Manuf., vol. 39, no. 11, pp. 1705–1715, Nov. 2008.

[139] X. Li, X. Zhang, Y. Guo, V. P. W. Shim, J. Yang, and G. B. Chai, "Influence of fiber type on the impact response of titanium-based fiber-metal laminates," Int. J. Impact Eng., vol. 114, pp. 32–42, Apr. 2018.

[140] M. Sadighi, T. Pärnänen, R. C. Alderliesten, M. Sayeaftabi, and R. Benedictus, "Experimental and numerical investigation of metal type and thickness effects on the impact resistance of fiber metal laminates," Appl. Compos. Mater., vol. 19, no. 3–4, pp. 545–559, Jun. 2012.

[141] G. Wu, J. M. Yang, and H. T. Hahn, "The impact properties and damage tolerance and of bi-directionally reinforced fiber metal laminates," J. Mater. Sci., vol. 42, no. 3, pp. 948–957, Feb. 2007.

[142] S. Zhu and G. B. Chai, "Low-velocity impact response of fibre-metal laminates - Experimental and finite element analysis," Compos. Sci. Technol., vol. 72, no. 15, pp. 1793–1802, Oct. 2012.

[143] G. Reyes V. and W. J. Cantwell, "The mechanical properties of fibre-metal laminates based on glass fibre reinforced polypropylene," Compos. Sci. Technol., vol. 60, no. 7, pp. 1085–1094, May 2000.

[144] M. R. Abdullah and W. J. Cantwell, "The impact resistance of polypropylene-based fibre-metal laminates," Compos. Sci. Technol., vol. 66, no. 11–12, pp. 1682–1693, 2006.

[145] C. Y. Tan and H. Akil, "Composites : Part B Impact response of fiber metal laminate sandwich composite structure with polypropylene honeycomb core," Compos. Part B, vol. 43, no. 3, pp. 1433–1438, 2012.

[146] P. Compston, W. J. Cantwell, C. Jones, and N. Jones, "Impact perforation resistance and fracture mechanisms of a thermoplastic based fiber-metal laminate," J. Mater. Sci.

Lett., vol. 20, no. 7, pp. 597–599, 2001.

[147] A. Vlot, "Low-velocity impact loading: On fibre reinforced aluminium laminates (ARALL and GLARE) and other aircraft sheet materials," 1993.

[148] A. Vlot, "Low-velocity impact loading: On fibre reinforced aluminium laminates (ARALL and GLARE) and other aircraft sheet materials," 1993.

[149] M. S. Hoo Fatt, C. Lin, D. M. Revilock, and D. A. Hopkins, "Ballistic impact of GLARE™ fiber-metal laminates," Compos. Struct., vol. 61, no. 1–2, pp. 73–88, 2003.

[150] R. E. Farsani, S. Khalili, and V. Daghigh, "Charpy impact response of basalt fiber reinforced epoxy and basalt fiber metal laminate composites: Experimental study," Int. J. Damage Mech., vol. 23, no. 6, pp. 729–744, Aug. 2014.

[151] J. Y. Zhang, T. X. Yu, J. K. Kim, and G. X. Sui, "Static indentation and impact behaviour of reformed bamboo/aluminium laminated composites," Compos. Struct., vol. 50, no. 2, pp. 207–216, Oct. 2000.

[152] D. Sivakumar et al., "Experimental investigation on charpy impact response of kenaf bast fibre reinforced metal laminate system," APRN J. Eng. Appl. Sci., vol. 13, no. 3, pp. 822–827, 2018.

[153] H. T. N. Kuan, W. J. Cantwell, M. A. Hazizan, and C. Santulli, "The fracture properties of environmental-friendly fiber metal laminates," J. Reinf. Plast. Compos., vol. 30, no. 6, pp. 499–508, Mar. 2011.

[154] C. L. Pang, N. A. Husain, and M. R. Abdullah, "Effect of loading rate on indentation behaviour of fibre metal laminates based on kenaf / epoxy," Appl. Mech. Materails, vol. 735, pp. 26–30, 2015.

[155] S. D, K. S., M. Z. bin Selamat, M. R. Bin Said, and Sivarais, "A study on impact behaviour of a novel oil palm fibre reinforced metal laminate system," J. Eng. Appl. Sci., vol. 11, no. May, pp. 2483–2488, 2016.

[156] S. Dhar Malingam, F. A. Jumaat, L. F. Ng, K. Subramaniam, and A. F. Ab Ghani, "Tensile and impact properties of cost-effective hybrid fiber metal laminate sandwich structures," Adv. Polym. Technol., vol. 37, no. 7, pp. 2385–2393, Nov. 2018.

[157] S. Ebnesajjad and A. H. Landrock, "Material Surface Preparation Techniques," in

Adhesives Technology Handbook, Elsevier, 2015, pp. 35–66.

[158] R. Kohli, "Methods for Monitoring and Measuring Cleanliness of Surfaces," in Developments in Surface Contamination and Cleaning: Detection, Characterization, and Analysis of Contaminants, Elsevier Inc., 2012, pp. 107–178.

[159] R. G. Dillingham, "Composite bond inspection," in Structural Integrity and Durability of Advanced Composites: Innovative Modelling Methods and Intelligent Design, Elsevier, 2015, pp. 697–706.

[160] Subcommittee D30.05 on Structural Test Methods and ASTM International, "ASTM D7136 / D7136M-15, Standard Test Method for Measuring the Damage Resistance of a Fiber-Reinforced Polymer Matrix Composite to a Drop-Weight Impact Event," ASTM B. Stand. Vol. 15.03, pp. 1–16, 2015.

[161] S. P. Rodrigues, C. F. A. Alves, A. Cavaleiro, and S. Carvalho, "Water and oil wettability of anodized 6016 aluminum alloy surface," Appl. Surf. Sci., vol. 422, pp. 430–442, Nov. 2017.

[162] J. F. Watts, "Surface Characterization and its Rôle in Adhesion Science and Technology," in Handbook of Adhesion Technology, Springer Berlin Heidelberg, 2011, pp. 179–207.

[163] S. Zhu and G. B. Chai, "Low-velocity impact response of fibre-metal laminates - experimental and finite element analysis," Compos. Sci. Technol., vol. 72, no. 15, pp. 1793–1802, 2012.

[164] C. Liu et al., "Interlaminar failure behavior of GLARE laminates under short-beam three-point-bending load," Compos. Part B, vol. 97, pp. 361–367, 2016.

[165] Y. Xu, H. Li, Y. Shen, S. Liu, W. Wang, and J. Tao, "Improvement of adhesion performance between aluminum alloy sheet and epoxy based on anodizing technique," Int. J. Adhes. Adhes., vol. 70, pp. 74–80, 2016.

[166] A. Z. Zakaria, K. Shelesh-nezhad, T. N. Chakherlou, and A. Olad, "Effects of aluminum surface treatments on the interfacial fracture toughness of carbon-fiber aluminum laminates," Eng. Fract. Mech., vol. 172, no. 1, pp. 139–151, 2017.

Résumé

Dans cette étude, les propriétés mécaniques des FML renforcés de jute tissé 3D et hybrides de jute tissé 3D renforcé ont été étudiées. Le renfort tissé 3D à quatre couches a été fabriqué avec du fil de jute en utilisant quatre types de motifs imbriqués, par ex. Orthogonal Through Thickness OTT et Orthogonal Layer to Layer OLL imbriqué. La technique d'infusion sous vide a été utilisée pour la fabrication de FML avec renfort en jute tissé 3D. Après l'optimisation du renforcement tissé 3D, les FML renforcés hybrides ont été développés dans lesquels le tissu tissé OTT 3D a été pris en sandwich entre une peau tissée 2D. Quatre types de fibres différents ont été utilisés pour fabriquer une peau tissée 2D, par ex. jute, aramide, carbone et verre tandis que trois types différents de matrice ont été utilisés, par ex. époxy, PVB et PP. La presse à chaud par compression a été utilisée pour développer des FML hybrides renforcés. L'aluminium utilisé pour fabriquer tous les FML a été anodisé avant d'être utilisé pour la fabrication. Les propriétés adhésives ont été étudiées pour vérifier la qualité du traitement de surface, la liaison métal-composites et l'effet des fibres et de la matrice. Les propriétés monotones et dynamiques ont également été étudiées. Les propriétés adhésives ont été caractérisées à l'aide de tests de pelage en T et de pelage au rouleau flottant. Les propriétés monotones ont été analysées à l'aide d'essais de traction et de flexion. Les performances d'impact à faible vitesse ont été déterminées en utilisant un test d'impact à faible vitesse. Les résultats ont montré que la surface en aluminium anodisé avait une énergie libre de surface élevée, de sorte que le meilleur mouillage de l'aluminium peut être obtenu par anodisation par rapport à d'autres types de préparations de surface. Les résultats de l'analyse du collage ont montré que les propriétés de délaminage étaient principalement influencées par la nature du matériau adhésif plutôt que par le type de structures de renforcement. La nature de la matrice influence également le type de défaillance car avec l'époxy, la défaillance dominante était cohésive tandis qu'avec la matrice thermoplastique, elle s'est transformée en défaillance adhésive et intra-laminaire. La plasticité et la ductilité de la matrice ont plus influencé les propriétés finales que le type de rupture, malgré la rupture cohésive de l'époxy, la matrice thermoplastique avait plus de force de délamination. Les propriétés de traction et de flexion des FML renforcées de jute tissé OTT 3D étaient supérieures à celles des FML renforcées tissées OLL 3D en raison de la fraction de volume de métal plus élevée, ce qui était possible grâce à une construction plus serrée du tissu OTT. Les propriétés de traction et de flexion des composites hybrides renforcés et des FML ont été influencées par le type de matrice et le matériau de la peau 2D. Les propriétés globales plus élevées ont été obtenues avec une matrice

époxy suivie d'une matrice PVB. Les FML à base de PVB ont montré que leurs propriétés étaient comparables à celles de l'époxy. Le test de flexion a montré que les FML hybrides à base de PP échouaient prématurément en raison d'une délamination entre la peau synthétique et l'âme tissée 3D. L'époxy et le PVB ont montré une meilleure imprégnation du renfort contrairement au PP dans lequel seul un verrouillage mécanique a été observé. Les propriétés d'impact dynamique des composites hybrides et des FML ont montré que les caractéristiques de dissipation d'énergie étaient influencées par la matrice et l'hybridation du renforcement. En ce qui concerne le type de matrice, le PVB a montré une force d'impact globale élevée avec une tolérance élevée aux dommages. Le renfort 100% jute a montré de mauvaises caractéristiques à la fois avec l'époxy et le PP. Comme avec l'époxy, il avait une rupture fragile tandis que le PP imprégnait mal le jute, de sorte qu'il a subi une perforation. Le PVB a cependant fait un meilleur réseau avec des armatures et du métal, ce qui a donné des propriétés d'impact plus élevées. En dehors de différents types de renforcement en jute synthétique / 3D, le jute aramide / 3D a montré une meilleure résistance aux chocs avec une tolérance aux chocs et une déformation plus élevées avant la rupture. La conclusion générale qui peut être tirée de l'étude est que les FML à base de PVB peuvent remplacer les FML à base d'époxy et de PP existants pour différentes applications, plus particulièrement l'industrie automobile. Le PVB peut être utilisé avec succès avec des FML renforcés de jute pur ou hybride.

Mots Clés: Propriétés Mécaniques, Sandwiche, Tissé en 3D, Fibre Naturelle, Fibre Metal laminate

Abstract

In current study the mechanical properties of 3D woven jute reinforced and hybrid 3D woven jute reinforced FMLs were investigated. The four-layered 3D woven reinforcement was made with jute yarn using four types of interlocking patterns e.g. Orthogonal Through Thickness OTT and Orthogonal Layer to Layer OLL interlocking. The vacuum infusion technique was used for the fabrication of FMLs made with 3D woven jute reinforcement. After the optimization of 3D woven reinforcement the hybrid reinforced FMLs were developed in which OTT 3D woven fabric was sandwiched between 2D woven skin. Four different kinds of fibres were used to make 2D woven skin e.g. jute, aramid, carbon, and glass while three different kinds of matrix were employed, e.g. epoxy, PVB and PP. The compression hot press was used to develop hybrid reinforced FMLs. Aluminium used to make all FMLs was anodized before using for fabrication. The adhesive properties were investigated to check the quality of surface treatment, metal-composites bonding and effect of fibres and matrix. Both monotonic and dynamic properties were also investigated. The adhesive properties were characterized using t-peel and floating roller peel tests. The monotonic properties were analyzed using tensile and flexural tests. The low velocity impact performance was determined using drop weight low velocity impact test. The results showed that the anodized aluminium surface had high surface free energy so the better wetting of aluminium can be achieved by anodizing as compared to other type of surface preparations. The adhesive bonding analysis results showed that the delamination properties were mainly influenced by the nature of adhesive material rather than the type of structures of reinforcement. The nature of the matrix also influences the type of failure as with the epoxy the dominant failure was cohesive while with thermoplastic matrix it changed to adhesive and intra-laminar failure. The plasticity and ductility of matrix influenced the final properties more than the type of failure, in spite of cohesive failure of epoxy the thermoplastic matrix had more delamination force. The tensile and flexural properties of OTT 3D woven jute reinforced FMLs were higher than the OLL 3D woven reinforced FMLs due to the higher metal volume fraction, this was possible due to tighter construction of OTT fabric. The tensile and flexural properties of hybrid reinforced composites and FMLs were influenced by the type of matrix and material of 2D skin. The overall higher properties were achieved with an epoxy matrix followed by PVB matrix. The PVB-based FMLs showed that their properties were comparable with the epoxy. The flexural test showed that hybrid FMLs based on PP were failed prematurely due to delamination between synthetic skin and 3D woven core. Both epoxy and PVB showed better impregnation of the reinforcement unlike PP in which only mechanical

interlocking was seen. The dynamic impact properties of hybrid composites and FMLs showed that the energy dissipation characteristics were influenced by matrix and hybridization of reinforcement. As far as the type of the matrix was concerned the PVB showed overall high impact force with high damage tolerance. The 100 % jute reinforcement showed poor characteristics both with epoxy and PP. As with the epoxy it had brittle failure while PP impregnated jute poorly, so it suffered perforation. The PVB however, made better network with reinforcement and metal which resulted in higher impact properties. Out of different type of synthetic / 3D jute reinforcement the aramid / 3D jute showed better impact resistance with higher impact tolerance and deformation before failure. The overall conclusion which can be drawn from the above study that the PVB based FMLs can be a replacement of existing epoxy and PP based FMLs for different applications especially automotive. The PVB can be employed successfully with pure jute or hybrid jute reinforced FMLs.

Key Words: Mechanical Properties, 3D woven, Fibre Metal Laminate, Sandwich, Natural Fibre